VERSLAGEN EN VERHANDELINGEN

REPORTS AND TRANSACTIONS

NATIONAAL LUCHT- EN RUIMTEVAART-LABORATORIUM

NATIONAL AERO- AND ASTRONAUTICAL RESEARCH INSTITUTE

AMSTERDAM

*

XXVII - 1962

REPORTS AND TRANSACTIONS NATIONAL AERO- AND ASTRONAUTICAL RESEARCH INSTITUTE, AMSTERDAM XXVII-1962

C. C. L. Class. D 023 : D 025 : D 201

TECHNICAL REPORT G. 25

INVESTIGATIONS ON THE SUPERSONIC FLOW AROUND BODIES

BY

P. J. ZANDBERGEN

PREFACE.

The report published in this Volume of "Verslagen en Verhandelingen" ('Reports and Transactions') of the 'Nationaal Lucht- en Ruimtevaart Laboratorium', N. L. R. ('National Aero- and Astronautical Research Institute') served the author as a thesis for the degree of doctor in the Technical Sciences at the Technical University of Delft.

The greater part of the investigation was performed under contract with the 'Nederlands Instituut voor Vliegtuigontwikkeling' (N.I.V.) ('Netherlands Aircraft Development Board') The permission for publication is herewith acknowledged.

October 1962,

Amsterdam.

A. J. MARX

Director of the
'Nationaal Lucht- en Ruimtevaart -
Laboratorium'

Contents.

Page

Summary.

The supersonic flow around axially-symmetric and quasi axially-symmetric bodies is investigated with a twofold purpose. One purpose is to determine whether or not the linearized potential flow theory can give an adequate description of the flow-field around such bodies. The other purpose is to forward more reliable methods of computation for those cases where the results of the investigations lead to the conclusion that this theory is inadequate.

A consideration of the mass- and momentum flow through conveniently chosen control surfaces, proves that one can obtain a quantitative measure for the error made by using linearized theory. The usefulness of this concept is emphasized by making a direct comparison between the results of linearized theory and those of more exact theories.

For axially-symmetric bodies such a comparison can be obtained by using an exact method of characteristics. The results show that the linearized theory is of only limited value, particularly so when an interference between various parts of a configuration occurs.

This leads to the investigation of optimum shapes of axially-symmetric bodies with a given base area by using the non-linear differential equations of isentropic flow. The same mass- and momentum flow equations are used here as for the determination of the adequateness of linearized theory.

For the quasi-axially-symmetric bodies a comparison can only be obtained for the flow around an inclined cone, since it is

the only case which has been studied by using more advanced methods. Once more it is found that in most cases the linearized theory does not give reliable results. Therefore a method is presented for the calculation of the flow field around axially-symmetric bodies with axis-inclinations. This method consists, analogous to that for the cone, of superposing a perturbation on the purely axially-symmetric flow field. It is given in such a form that it is possible to perform the calculations by using a method of characteristics based on the characteristics of the axially-symmetric flow field. The analysis is restricted to terms which depend on the first order of a small deformation parameter.

1 General introduction.

The study of supersonic flow has a history of about one century. It was initiated by investigating the wave phenomena related to the propagation of sound. A now classical paper was written in 1860 by Riemann (ref.1) on the theory of waves of finite amplitude paving the way for the development of the mathematical theory of hyperbolic equations.

Although the possibility of discontinuous solutions was recognized rather early, it was not until the publication of the works of Rankine (ref.2) and Hugoniot (ref.3) that the equations for shock-waves were established as they are known today. At about the same time the first practical application of supersonic flow was made by the Swedish engineer Gustave de Laval, the discoverer of the nozzle named after him. This type of duct is and has been of fundamental importance for the development of supersonic aerodynamics, since it plays an essential role in the operation of wind tunnels.

In the beginning of this century progress into the study of plane supersonic flow was made through the important work of Prandtl and his co-workers. They discovered and elaborated the so called simple wave flow, thus making it possible to design two-dimensional de Laval nozzles that are perfect.

However, it may be stated that the great impetus to the investigation of supersonic aerodynamics was not made until about 1930. Two distinct lines of approach were then initiated.

The first approach relies on the assumption that the disturbance velocities, caused by bodies moving faster than the speed of sound, are small compared to the undisturbed velocity. It is evident that such a theory is restricted in its range of applicability, i.e. the bodies have to be slender and the Mach number not too high. On the other hand, the simplification reached by linearizing the governing differential equations opens the possibility to obtain results, which otherwise can not be found. The researches of Ackeret on plane flow (ref.4) and of von Kármán and Moore (ref.5) on axially-symmetric flow were the starting point for numerous applications of these perturbation methods.

The second approach tries to find physically acceptable solutions of the non-linear differential equations, governing supersonic flow. For plane flow several exact solutions were known. The first exact solution for an axially-symmetric supersonic flow was given by Taylor and Maccoll (ref.6). Their work on the flow around a cone, can still be considered the starting point for later investigations of more general flow fields, by the method of characteristics.

It is interesting to see how these two approaches have developed since their initiation.

Especially during the second world war and thereafter the number of problems studied and solved by using perturbation methods, leading to linearized equations, are uncountable. Attention may be drawn to examples such as the supersonic flow around inclined bodies, and the study of the optimum shape of axially-symmetric configurations with respect to wave drag. To account for such broad applications of in fact only approximate methods, various reasons may be given.

One of the most important reasons in the opinion of the author , is the fact that there was already a well-developed mathematical theory for linear partial differential equations, which together with the principle of superposition could be used to reduce many very complicated problems to a few simpler ones.

The study of exact flow fields around axially-symmetric configurations was stimulated by the publication of a comprehensive table of the flow around a cone by Kopal et.al. in 1947 (ref.7). This table was obtained by numerical integrations of the equations of Taylor and Maccoll. It is interesting to note that these computations were performed with the aid of ordinary desk computers.

A further step forward in this field was made by Stone, who determined the flow around an inclined cone,correct up to the first order in the angle of incidence(ref.8).The second order term has subsequently been determined. Extensive tables of the data obtained have also been given by Kopal (ref.9 and 10).

In the mean time several papers had appeared, exploring the applicability of the theory of characteristic surfaces and characteristic equations pertinent to hyperbolic equations, for the numerical calculation of the flow field around axially-symmetric bodies. The researches of Ferri may be mentioned here, especially since he tried to generalize the method of Stone for bodies at an angle of attack (ref.11), by using a method of characteristics. Ferri (ref.12) was also the first to point out an inconsistency in the theory of Stone who ignored the singular behaviour of the entropy at the surface of an inclined cone. This criticism, leading to the concept of a vortical layer, does not influence, however, the pressure distribution obtained by the first order theory of Stone.

A natural and important question is:"How do the results obtained by the linearized and the exact theory compare?" A direct comparison, however, is only possible if there are bodies for which the flow can be calculated by using both methods. As is evident from the foregoing discussion, this is the case for the cone. Already in 1947 this comparison was made by Kopal (ref.13). Although only valid for a cone, this work constitutes a sharp criticism against the use of the linearized theory. Already at that time it was remarked: "if we wish to progress with quantitative investigations of supersonic flow around solid bodies....., we cannot avoid the non-linear character of these problems". It is quite astonishing that this serious warning against the use of linearized theory seems to have had no effect, for since that time a tremendous number of papers on linearized methods have appeared.

However, though it is very easy to say that problems should be solved by more exact methods, such a remark has little significance when such more exact methods are not available, or if time and money are prohibitive to their application, which was certainly the case at the time they were proposed. On the other hand, quite a number of papers have appeared which have attempted to define the range of validity of the linearized theory. As an example of such a paper, the one by Miles may be mentioned (ref.14). However, all the results of these researches have the drawback that they lead to rather vague requirements, not giving a quantitative measure for the error which is made by using linearized theory.

Moreover a variety of methods have been proposed to improve the results of the first-order linearized theory. Such a procedure for instance is given by van Dyke (ref.15). This second-order theory, however, does not extend the range of validity very much, so that its practical usefulness is only limited. A comparison of the results obtained by using these improved methods has been given by Ehret (ref.16). The conclusions reached are that the range of body shapes, fineness ratios and Mach numbers for which these theories give acceptable results, is limited. It should be born in mind that this applies only to the pressure distribution along the body. Researches on the validity of the linearized theory for the determination of the whole flow field, show that the deviations between linearized and exact results become larger in the outer flow field. This makes it rather doubtful if linearized theory can be used to solve problems of interference in a reliable sense. One important representative of these problems is the search for optimum shapes with respect to wave drag. In this case a certain part of the fuselage has to interfere with all the other parts in such a way that the wave drag is as low as possible.

The point of view suggested by the results of the mentioned researches can be summarized now as follows:

Evidently the linearized potential theory is the simplest tool available for analysing supersonic flow around a certain configuration. However, in practice no measure of the quantitative error made is possible, if no comparison can be made with exact results. Up to now, there are only very few problems which can be solved by using exact methods.

On the other hand the application of exact methods for the numerical determination of a flow field, which required a large amount of time because no electronic computers were available when they were proposed for the first time, has become much simpler due to the rapid development of these devices. Therefore it seems advisable to use these exact methods wherever possible, in order to avoid the uncertainty of the values obtained by using the linearized theory. This implies the development of appropriate methods for a variety of problems.

The task set forward by these considerations can therefore be described as follows:

1. A method should be found to measure the quantitative error in the results of the linearized theory which would not require making a direct comparison between these results and the results obtained by using other more exact theories.

2. For cases where it has been shown that linearized theory cannot be applied, methods should be developed which would be both numerically applicable to, as well as based on the exact differential equations of supersonic flow.

It is the purpose of this thesis to investigate along these lines a rather small domain of the theory of supersonic flow.

Two classes of problems will be considered: In the first place the flow around axially-symmetric configurations where the axis is aligned with the direction of the undisturbed free stream; in the second place the flow around a quasi axially-symmetric body will be considered (such a body is obtained by deforming the axis of an initially axially-symmetric body. A configuration at an angle of attack is one of the most simple examples).

To achieve a systematic representation the paper has been divided into three main parts.

The first part gives a general account of the equations governing supersonic flow and shock waves, deriving thereby the frequently used equations needed in the other two parts.

The second part contains the results of investigations on the supersonic flow around axially-symmetric configurations. First a quantitative measure for the error in using the method of linearized theory is given by considering mass flow and momentum flow through conveniently chosen control surfaces. Especially for the flow around a cone simple results are obtained, but the method is equally applicable to more general axially-symmetric bodies. For greater understanding of the usefulness of this concept, a direct comparison is systematically given between the results of flow phenomena obtained by calculating with an exact method of characteristics and those results obtained by using the linearized theory. The results obtained show that linearized theory is of only limited value, especially when it is used on those problems where interference occurs.

When using the non-linear equations of supersonic flow this insight leads to the investigation of optimum shapes of axially-symmetric bodies with a given base area. The discussion will be restricted here to the case where the flow in a certain part of the flow is isentropic.

In the third part the supersonic flow around quasi axially-symmetric configurations will be investigated. Here also will be given a quantitative measure of the error made by using linearized theory. Here, however, the situation is less favourable for a direct comparison, since only the flow around a cone at an angle of attack has been solved by using more advanced methods. Therefore after having shown with momentum transport considerations, that this analysis of the flow around a cone is fully consistent, an attempt is made to forward a theory which enables the numerical calculation of the flow field around a quasi axially-symmetric body. The method proposed is, in fact, analogous to that of Stone, a perturbation theory superposed on the purely axially-symmetric flow field. The investigation is limited to the determination of the perturbations up to the first order of a small deformation parameter.

2 The basic equations.

Here a rather detailed derivation will be given of the basic equations. Subsequently the equations for a supersonic domain and for a three dimensional shock wave will be given. The equations valid for the linearized potential flow will be summarized.

2.1 The field equations.

In this section the basic equations will be given which are valid for a domain of supersonic flow not containing shock waves.

It will be assumed that the effects of viscosity, thermal conduction and diffusion can be neglected, with the medium considered an ideal gas.

A Cartesian coordinate system x_1, x_2, x_3 will be used (see fig.1.). The velocities in the directions of the respective axes are given as u_1, u_2, u_3.

Using the summation convention of Einstein the equations of motion and the equation of continuity can be written as

$$\frac{du_i}{dt} + \frac{1}{\rho}\frac{\partial p}{\partial x_i} = 0 \tag{2.1}$$

$$\frac{d\rho}{dt} + \rho\frac{\partial u_k}{\partial x_k} = 0 \tag{2.2}$$

where ρ is the density, p the pressure and t denotes time. The symbol $\frac{d}{dt}$ is the substantial derivative. The assumptions about the physical properties of the medium give rise to the equations

$$\frac{dQ}{dt} = T\frac{dS}{dt} = 0 \tag{2.3}$$

and

$$\frac{p}{\rho} = RT \tag{2.4}$$

where Q is the heat added, S the entropy and T the absolute temperature.

Use will be made of the fact that for a reversible process

$$dQ = TdS = dE - \frac{p}{\rho^2} d\rho \tag{2.5}$$

The internal energy dE for an ideal gas is given by

$$dE = c_v dT \tag{2.6}$$

where c_v is a constant, viz. the specific heat with constant volume. Introducing eq. (2.6) into (2.5) the entropy can be written as:

$$S = c_p \ln T - R \ln p \tag{2.7}$$

where c_p is the specific heat with constant pressure.

It is preferable to define a specific entropy by

$$s = \frac{S}{c_v} \tag{2.8}$$

If the values in the undisturbed stream, which is assumed to be uniform, are given by $p = p_\infty$, $\rho = \rho_\infty$ and $s = 0$, equation (2.7) can be written by using eq. (2.4) as

$$p\rho^{-\gamma} = C\, e^{+s} \tag{2.9}$$

where $C = p_\infty \rho_\infty^{-\gamma}$ and $\gamma = \frac{c_p}{c_v}$.

It should be remarked that whereas $\frac{ds}{dt} = 0$, the value of s is not in general equal to zero, because shock waves may have occurred outside the domain considered.

Differentiating eq. (2.9) and using the relation for the velocity of sound and eq. (2.3), there is obtained

$$\frac{dp}{dt} - a^2 \frac{d\rho}{dt} = 0 \tag{2.10}$$

where

$$a^2 = \left(\frac{\partial p}{\partial \rho}\right)_s = \gamma \frac{p}{\rho} \quad . \tag{2.11}$$

The analysis will be restricted to the case of steady flow hence

$$\frac{d}{dt} = u_k \frac{\partial}{\partial x_k} \tag{2.12}$$

If account is taken of eq. (2.12) equation (2.10) together with eq. (2.1) and eq. (2.2) multiplied by u_i, gives rise to the fundamental relation

$$u_k u_i \frac{\partial u_k}{\partial x_i} - a^2 \frac{\partial u_i}{\partial x_i} = 0 \quad . \tag{2.13}$$

To obtain another set of equations, use will be made of the enthalpy H. This is defined by

$$H = E + \frac{p}{\rho} \quad . \tag{2.14}$$

Using eqs. (2.3) and (2.5) and substituting eq. (2.1) times u_i into the differential equation which can be obtained from eq. (2.14), there is obtained after integration

$H + \frac{1}{2} u_i u_i$ = constant along a stream line.

Since the flow is assumed to be uniform far upstream, there holds:

$H + \frac{1}{2} u_i u_i$ = constant in the whole flow field. (2.15)

Differentiating this equation with respect to x_k and subtracting eq. (2.1) there follows:

$$u_i \left\{ \frac{\partial u_i}{\partial x_k} - \frac{\partial u_k}{\partial x_i} \right\} + \frac{\partial H}{\partial x_k} - \frac{1}{\rho} \frac{\partial p}{\partial x_k} = 0 \quad . \tag{2.16}$$

From eqs. (2.14) and (2.5) the following general relation can be obtained

$$dH - \frac{1}{\rho}\, dp = T\, d\, S \quad . \tag{2.17}$$

This means that the value of a contour integral has to be zero i.e.:

$$\oint \left\{ dH - \frac{1}{\rho}\, dp - T\, dS \right\} = 0 \, . \tag{2.18}$$

From this result, with the aid of eqs. (2.3), (2.5) and (2.14) together with the condition that the flow is uniform far upstream, it can be derived that

$$\frac{\partial H}{\partial x_k} - \frac{1}{\rho} \frac{\partial p}{\partial x_k} = T \frac{\partial S}{\partial x_k} \quad . \tag{2.19}$$

Introducing this relation into eq. (2.16) there is finally obtained

$$u_i \left\{ \frac{\partial u_i}{\partial x_k} - \frac{\partial u_k}{\partial x_i} \right\} + \frac{a^2}{\gamma(\gamma-1)} \frac{\partial S}{\partial x_k} = 0 \quad . \tag{2.20}$$

or in vector notation

$$\vec{u} \times \text{rot}\, \vec{u} = -\frac{a^2}{\gamma(\gamma-1)} \text{ grad } s \tag{2.21}$$

which equation is known as Crocco's theorem.

By using eq. (2.15) and observing that for an ideal gas the enthalpy is equal to c_pT, it follows that

$$a^2 = \left(\frac{1}{M_\infty^2} + \frac{\gamma-1}{2}\right)U_\infty^2 - \frac{\gamma-1}{2} u_i u_i \tag{2.22}$$

where M_∞ is the Mach number and U_∞ is the velocity of the uniform undisturbed flow.

Substituting eq. (2.22) into eq. (2.13) and into the system of eqs. (2.20) there is obtained a set of four non-linear differential equations for the four unknown quantities u_i and s.

This system of equations will be investigated further in the remainder of this section.

It is of advantage to use a cylindrical coordinate system x, r, ψ and associated velocity components u, v, w, because here our main interest is the study of axially-symmetric bodies (see fig.1).

The transformation formulae are given by

$$\begin{aligned} x_1 &= x \\ x_2 &= r \sin\psi \\ x_3 &= r \cos\psi \end{aligned} \tag{2.23a}$$

and

$$\begin{aligned} u_1 &= u \\ u_2 &= v \sin\psi + w \cos\psi \\ u_3 &= v \cos\psi - w \sin\psi \end{aligned} \tag{2.23b}$$

On using these equations, eq. (2.13) and eqs. (2.20) can be transformed into the following system of four equations

$$\left(1-\frac{u^2}{a^2}\right)\frac{\partial u}{\partial x} + \left(1-\frac{v^2}{a^2}\right)\frac{\partial v}{\partial r} + \frac{1}{r}\left(1-\frac{w^2}{a^2}\right)\frac{\partial w}{\partial \psi} + \frac{v}{r} +$$

$$-\frac{vu}{a^2}\left(\frac{\partial u}{\partial r} + \frac{\partial v}{\partial x}\right) - \frac{uw}{a^2}\left(\frac{\partial w}{\partial x} + \frac{1}{r}\frac{\partial u}{\partial \psi}\right) - \frac{vw}{a^2}\left(\frac{1}{r}\frac{\partial v}{\partial \psi} + \frac{\partial w}{\partial r}\right) = 0 \tag{2.24a}$$

$$v\left(\frac{\partial v}{\partial x} - \frac{\partial u}{\partial r}\right) + w\left(\frac{\partial w}{\partial x} - \frac{1}{r}\frac{\partial u}{\partial \phi}\right) + \frac{a^2}{\gamma(\gamma-1}\frac{\partial s}{\partial x} = 0 \qquad (2.24)b$$

$$-w\left(\frac{1}{r}\frac{\partial v}{\partial \phi} - \frac{\partial w}{\partial r} - \frac{w}{r}\right) - u\left\{\frac{\partial v}{\partial x} - \frac{\partial u}{\partial r}\right\} + \frac{a^2}{\gamma(\gamma-1)}\frac{\partial s}{\partial r} = 0 \qquad (2.24)c$$

$$v\left(\frac{1}{r}\frac{\partial v}{\partial \phi} - \frac{\partial w}{\partial r} - \frac{w}{r}\right) - u\left\{\frac{\partial w}{\partial x} - \frac{1}{r}\frac{\partial u}{\partial \phi}\right\} + \frac{a^2}{\gamma(\gamma-1)}\frac{1}{r}\frac{\partial s}{\partial \phi} = 0 \quad . \qquad (2.24)d$$

This system will now be brought into the form of a set of relations valid along characteristic surfaces.

These surfaces are thus defined that the relations that are valid along them contain only derivatives along the surface.

Hence, it is not possible to construct a solution for the flow field starting from quantities given along such a characteristic surface.

To find the characteristic surfaces it will be assumed that such a surface can be written as

$$r = f(x,\phi)$$

The derivatives along this surface or the so called "inner" derivatives are given then by

$$\frac{\delta}{\delta x} = \frac{\partial}{\partial x} + \sigma_1 \frac{\partial}{\partial r} \qquad \text{where } \sigma_1 = \frac{\partial f}{\partial x} \qquad (2.26)a$$

$$\frac{1}{r}\frac{\delta}{\delta \phi} = \frac{1}{r}\frac{\partial}{\partial \phi} + \sigma_2 \frac{\partial}{\partial r} \qquad \text{where } \sigma_2 = \frac{1}{r}\frac{\partial f}{\partial \phi} \qquad (2.26)b$$

Substituting these equations into the system (2.24), the result can be written as:

$$a_{ij}\frac{\partial \omega_j}{\partial r} = b_i \qquad (2.27)$$

This set of equations has been given in full on the following page.

This is a system of equations from which the quantities $\frac{\partial \omega_j}{\partial r}$ can be solved, provided that the surface and the flow quantities ω_j along the surface are given. In that case the right hand side is known, together with the coefficients of the unknown derivatives.

Now as has already been remarked, the requirement for $r = f(x,\phi)$ to be a characteristic surface, is that it is not possible to continue the solution starting from quantities given along the surface. This

$$\begin{bmatrix} (1-\frac{u^2}{a^2})\sigma_1 - \frac{uw}{a^2}\sigma_2 + \frac{uv}{a^2} , & -\frac{vu}{a^2}\sigma_1 - \frac{vw}{a^2}\sigma_2 - (1-\frac{v^2}{a^2}) , & -\frac{uw}{a^2}\sigma_1 + (1-\frac{w^2}{a^2})\sigma_2 + \frac{vw}{a^2} , & 0 \\ -w\sigma_2 + v , & v\sigma_1 , & w\sigma_1 , & \frac{a^2}{\gamma(\gamma-1)}\sigma_1 \\ -u , & -u\sigma_1 - w\sigma_2 , & -w , & \frac{-a^2}{\gamma(\gamma-1)} \\ u\sigma_2 , & v\sigma_2 , & -u\sigma_1 + v , & \frac{a^2}{\gamma(\gamma-1)}\sigma_2 \end{bmatrix} \begin{bmatrix} \frac{\partial u}{\partial r} \\ \frac{\partial v}{\partial r} \\ \frac{\partial w}{\partial r} \\ \frac{\partial s}{\partial r} \end{bmatrix}$$

$$\begin{bmatrix} (1-\frac{u^2}{a^2})\frac{\delta u}{\delta x} - \frac{uv}{a^2}\frac{1}{r}\frac{\delta u}{\delta \psi} - \frac{vu}{a^2}\frac{\delta v}{\delta x} - \frac{vw}{a^2}\frac{1}{r}\frac{\delta v}{\delta \psi} - \frac{uw}{a^2}\frac{\delta w}{\delta x} + (1-\frac{w^2}{a^2})\frac{1}{r}\frac{\delta w}{\delta \psi} + \frac{v}{r} \\ -w\frac{1}{r}\frac{\delta u}{\delta \psi} + v\frac{\delta v}{\delta x} + w\frac{\delta w}{\delta x} + \frac{a^2}{\gamma(\gamma-1)}\frac{\delta s}{\delta x} \\ -u\frac{\delta v}{\delta x} - w\frac{1}{r}\frac{\delta v}{\delta \psi} + \frac{w^2}{r} \\ u\frac{1}{r}\frac{\delta u}{\delta \psi} + v\frac{1}{r}\frac{\delta v}{\delta \psi} - u\frac{\delta w}{\delta x} + \frac{a^2}{\gamma(\gamma-1)}\frac{1}{r}\frac{\delta s}{\delta \psi} - \frac{vw}{r} \end{bmatrix}$$

The matrix equation $a_{ij}\frac{\partial \omega_j}{\partial r} = b_i$ (2.27) written in full. (2.27)a means that there cannot be found unique solutions for the quantities $\frac{\partial \omega_j}{\partial r}$.

The system should be either incompatible or dependent. Then there holds

$$\text{Det. } a_{ij} = \left| a_{ij} \right| = 0 \tag{2.28}$$

This requirement leads to an equation for the unknown quantities σ_1 and σ_2.

Now the only physically possible case is that the equations are dependent. This means that for each associated pair of values for σ_1, and σ_2 obtained from eq. (2.28) an "annuling vector" can be found such that

$$\nu_i \, a_{ij} = 0 \quad . \tag{2.29}$$

This is only possible if at the same time the following relation is satisfied.

$$\nu_i b_i = 0 \tag{2.30}$$

This equation is the compatibility equation, for it is valid if equation (2.29) is valid. Now b_i is an expression containing only the functions and the inner derivatives along the surface $r = f(x,\phi)$, and thus eq. (2.30) is a relation which satisfies the requirements for f to be a characteristic surface.

The characteristic directions can be found by applying eq. (2.28). If the operation of determining the determinant of a_{ij} is performed, the result obtained is:

$$(v-u\sigma_1-w\sigma_2)^2 \left\{ \sigma_1^{\,2} + \sigma_2^{\,2} + 1 - \frac{1}{a^2}\,(v-u\sigma_1-w\sigma_2)^2 \right\} = 0 \tag{2.31}$$

Now the vector $(\sigma_1, -1, \sigma_2)$ is proportional to the unit normal vector (n_1, n_2, n_3) of the surface $r = f(x,\phi)$.

Equation (2.31) gives as characteristic directions therefore

$$v-u\sigma_1-w\sigma_2 = un_1 + vn_2 + wn_3 = 0 \tag{2.32)a}$$

and $$v-u\sigma_1-w\sigma_2 = \pm a\sqrt{\sigma_1^{\,2} + \sigma_2^{\,2} + 1}$$

or

$$un_1 + vn_2 + wn_3 = \mp a \tag{2.32)b}$$

It should be observed that the relation (2.32)a has to be counted twice according to eq. (2.31). The interpretation of the eqs. (2.32)a and (2.32)b is in fact quite simple. Equation (2.32)a states that the normal vector in a certain point P of the surface $r = f(x,\psi)$ should be perpendicular to the vector (u, v, w). The set of characteristic surfaces obtained in this case is therefore the set of stream surfaces. The streamline can be considered as a characteristic line in this case.

Equation (2.32)b states that the velocity normal to the characteristic surface is equal to the local velocity of sound. This means that this surface is locally a cone with a half top angle μ with respect to the vector u, v, w, where μ is defined by

$$\tan \mu = \frac{1}{\beta} = \pm \frac{1}{\sqrt{M^2-1}} \qquad (2.33)$$

where M is the local Mach number.

To find the relations (2.30) which are valid along the characteristic surfaces, first the annuling vectors ν_i have to be determined.

If eq. (2.32)a is valid, the matrix a_{ij} of eq. (2.27) reduces to

$$\begin{Vmatrix} \sigma_1 & -1 & \sigma_2 & 0 \\ u\sigma_1 & v\sigma_1 & w\sigma_1 & c\sigma_1 \\ -u & -v & -w & -c \\ u\sigma_2 & v\sigma_2 & w\sigma_2 & c\sigma_2 \end{Vmatrix} \qquad (2.34)$$

where $c = \frac{a^2}{\gamma(\gamma-1)}$

It can be seen immediately that the annuling vector has to satisfy the the relations

$$\sigma_1\nu_2 - \nu_3 + \sigma_2\nu_4 = 0 \qquad \nu_1 = 0 \qquad (2.35)$$

If the components ν_2, ν_3 and ν_4 are considered to be the components of a vector $\vec{\nu}$, equation (2.35) can be written analogous to eq. (2.32)a as

$$\vec{n}.\vec{\nu} = 0 \qquad (2.36)$$

This equation has the two independent solutions

$$\vec{\nu} = \vec{u} \tag{2.37)a}$$

and

$$\vec{\nu} = \vec{u} \times \vec{n} \tag{2.37)b}$$

as follows by using eq. (2.32)a.

The two annuling vectors for this case are therefore given by

$$\nu_i = \left\{ o,\ u,\ v,\ w \right\} \tag{2.38)a}$$

and

$$\nu_1 = \left\{ o,\ v\sigma_2 + w,\ w\sigma_1 - u\sigma_2,\ -u-v\sigma_1 \right\} \tag{2.38)b}$$

The compatibility equation for the annuling vector (2.38)a is given by

$$u \frac{\delta s}{\delta x} + w \frac{1}{r} \frac{\delta s}{\delta \varphi} = 0 \tag{2.39}$$

From this equation, by using the eqs. (2.26)a and (2.26)b it follows, that

$$u \frac{\partial s}{\partial x} + v \frac{\partial s}{\partial r} + \frac{w}{r} \frac{\partial s}{\partial \varphi} = 0 \quad \text{or} \quad \frac{ds}{dt} = 0 \tag{2.40}$$

Thus the result is found that the entropy has to be constant along a streamline. This cannot be too surprising, since in fact this is a direct consequence of the assumption made about the physical behaviour of the medium. Equation (2.40) is the same as eq. (2.3) as it ought to be

The compatibility equation for the annuling vector (2.38)b is given by

$$\frac{u}{r} \frac{\delta u}{\delta \varphi} - u\sigma_2 \frac{\delta v}{\delta x} + u\sigma_1 \frac{1}{r} \frac{\delta v}{\delta \varphi} - u \frac{\delta w}{\delta x} - \frac{uw}{r} \sigma_1 + \frac{a^2}{\gamma(\gamma-1)} \frac{1}{r} \frac{\delta s}{\delta \varphi} = 0 \tag{2.41}$$

where use has been made of eq. (2.39).

It can be shown that this equation expresses the fact that the component of the rotation vector, normal to a stream surface for which the entropy is constant, vanishes.

Now the annuling vectors and the compatibility equations will be determined in case that eq. (2.32)b holds.

In that case the matrix a_{ij} of eq. (2.27) reduces to

$$\left\| \begin{matrix} \sigma_1 \pm \frac{u}{a}\sqrt{\sigma_1^2+\sigma_2^2+1}, & -1 \pm \frac{v}{a}\sqrt{\sigma_1^2+\sigma_2^2+1}, & \sigma_2 \pm \frac{w}{a}\sqrt{\sigma_1^2+\sigma_2^2+1}, & 0 \\ u\sigma_1 \pm a\sqrt{\sigma_1^2+\sigma_2^2+1}, & v\sigma_1, & w\sigma_1, & c\sigma_1 \\ -u, & -v\pm a\sqrt{\sigma_1^2+\sigma_2^2+1}, & -w, & -c \\ u\sigma_2, & v\sigma_2, & w\sigma_2 \pm a\sqrt{\sigma_1^2+\sigma_2^2+1}, & c\sigma_2 \end{matrix} \right\| \quad (2.42)$$

where the + sign refers to $v-u\sigma_1-w\sigma_2 = a\sqrt{\sigma_1^2+\sigma_2^2+1}$ and the - sign to $v-u\sigma_1-w\sigma_2 = -a\sqrt{\sigma_1^2+\sigma_2^2+1}$.

Again the components ν_2, ν_3 and ν_4 *of the annuling vector have to* satisfy the relation

$$\sigma_1 \nu_2 - \nu_3 + \sigma_2 \nu_4 = 0$$

or

$$\vec{n}.\vec{\nu} = 0 \quad .$$

Now according to eq. (2.32)b there holds

$$\vec{n}.\vec{u} = \mp a \quad .$$

These two equations together with eq. (2.42) give

$$\vec{\nu} = \frac{\vec{u}}{a^2} \pm \frac{\vec{n}}{a} \qquad \nu_1 = -1 \quad . \tag{2.43}$$

The complete expressions for the annuling vectors are then given by:

$$\nu = \left\{ -1,\ \frac{u}{a^2} + \frac{\sigma_1}{a\sqrt{\sigma_1^2+\sigma_2^2+1}},\ \frac{v}{a^2} - \frac{1}{a\sqrt{\sigma_1^2+\sigma_2^2+1}},\ \frac{w}{a^2} + \frac{\sigma_2}{a\sqrt{\sigma_1^2+\sigma_2^2+1}} \right\}$$

(2.44)a

and

$$\nu = \left\{ -1,\ \frac{u}{a^2} - \frac{\sigma_1}{a\sqrt{\sigma_1^2+\sigma_2^2+1}},\ \frac{v}{a^2} + \frac{1}{a\sqrt{\sigma_1^2+\sigma_2^2+1}},\ \frac{w}{a^2} - \frac{\sigma_2}{a\sqrt{\sigma_1^2+\sigma_2^2+1}} \right\} \quad (2.44)\text{b}$$

The compatibility equation for the annuling vector (2.44)a is given by

$$(u\sigma_2-w\sigma_1)\frac{1}{r}\frac{\delta u}{\delta\psi}+(u+v\sigma_1)\frac{\delta v}{\delta x}+(w+v\sigma_2)\frac{1}{r}\frac{\delta v}{\delta\psi}+(w\sigma_1-u\sigma_2)\frac{\delta w}{\delta x}+$$

$$+\frac{v-u\sigma_1-w\sigma_2}{\gamma(\gamma-1)}\left\{u\frac{\delta s}{\delta x}+\frac{w}{r}\frac{\delta s}{\delta\psi}\right\}+\frac{a^2}{\gamma(\gamma-1)}\left\{\sigma_1\frac{\delta s}{\delta x}+\sigma_2\frac{1}{r}\frac{\delta s}{\delta\psi}\right\}+$$

$$-(v-u\sigma_1-w\sigma_2)\left\{(1-\frac{u^2}{a^2})\frac{\delta u}{\delta x}-\frac{uw}{a^2}\frac{1}{r}\frac{\delta u}{\delta\psi}-\frac{vu}{a^2}\frac{\delta v}{\delta x}-\frac{vw}{a^2}\frac{1}{r}\frac{\delta v}{\delta\psi}-\frac{uw}{a^2}\frac{\delta w}{\delta x}+\right.$$

$$\left.+(1-\frac{w^2}{a^2})\frac{1}{r}\frac{\delta w}{\delta\psi}+\frac{v}{r}\right\}=0 \qquad (2.45)$$

As can be seen, the characteristic equation (2.45) in this form is equally valid for the annuling vector (2.44)b. The equation thus is valid along the two different surfaces given by eq. (2.32)b. The difference lies in the fact that the quantities σ_1 and σ_2 are related by a different formula in the two cases.

Thus the original set of four partial differential equations has been transformed into a system of four characteristic equations given by eqs. (2.40), (2.41) and (2.45) together with the characteristic directions given by the eqs. (2.32)a and (2.32)b. It is this set of relations which will play an important role in the following investigations.

2.2 The equations for shock transition.

Since in the following paragraphs the notion of a shock wave will be used frequently, here an account will be given of the equations valid for the transition. In fact a shock wave is a surface where the flow quantities can be considered to change discontinuously. In reality it is in general a domain of the flow with a thickness of a few mean free molecular pathes, where due to viscosity and thermal conduction rapid changes occur.

In the treatment given here, it will be assumed as before that the gas is ideal, and that outside the shock the effects of viscosity and thermal conduction are negligible. The general conditions for shock transition are given by

1° conservation of mass

2° conservation of momentum

3° conservation of energy.

Moreover the transition should be such that the entropy cannot diminish in accordance with the second fundamental law of thermodynamics.

With the assumptions made here, the resulting equations get a rather simple form. To derive these equations it will be assumed that in a certain arbitrary point of the shock surface the normal vector $\vec{n}$ and two tangent vectors $\vec{t}_1$ and $\vec{t}_2$ are given. The component of the velocity $\vec{q}$ in the direction of these vectors will be denoted by u_n, u_{t_1} and u_{t_2} respectively.

The shock wave itself is assumed to have zero velocity.

If the index f refers to the state in front of the shock and the index a to the state aft of the shock the relations can be written as:

$$\rho_f u_{f_n} = \rho_a u_{a_n} \tag{2.46a}$$

$$p_f + \rho_f u_{f_n}^2 = p_a + \rho_a u_{a_n}^2 \tag{2.46b}$$

$$\rho_f u_{f_n} u_{f_{t_1}} = \rho_a u_{a_n} u_{a_{t_1}} \tag{2.46c}$$

$$\rho_f u_{f_n} u_{f_{t_2}} = \rho_a u_{a_n} u_{a_{t_2}} \tag{2.46d}$$

$$H_f + \frac{1}{2}(u_{f_n}^2 + u_{f_{t_1}}^2 + u_{f_{t_2}}^2) = H_a + \frac{1}{2}(u_{a_n}^2 + u_{a_{t_1}}^2 + u_{a_{t_2}}^2) \tag{2.46e}$$

$$S_a - S_f = \Delta S \geqslant 0 \tag{2.46f}$$

These equations together with the equation of state (2.4) and the equation for the change in entropy (2.9) suffice to determine all the quantities aft of the shock wave, if those in front of it are given. It must be noticed that equation (2.46)e has already been derived (see eq.(2.15)).

The system (2.46) can be greatly simplified by observing that from eqs. (2.46)c and (2.46)d follows by using eq. (2.46)a

$$u_{f_{t_1}} = u_{a_{t_1}} \tag{2.47a}$$

and

$$u_{f_{t_2}} = u_{a_{t_2}} \tag{2.47b}$$

If now the Mach number M_n is introduced by

$$M_n = \frac{u_{f_n}}{a_f} \tag{2.48}$$

the system gives, by eliminating ρ_a and p_a, rise to the following equation

$$\frac{\gamma+1}{2} u_{a_n}^2 M_n^2 - u_{a_n} u_{f_n} \left\{ 1 + \gamma M_n^2 \right\} + u_{f_n}^2 - \left\{ 1 + \frac{\gamma-1}{2} M_n^2 \right\} = 0$$

or

$$\frac{u_{a_n}}{u_{f_n}} = \frac{1}{\gamma+1} \; \frac{1+\gamma M_n^2 \pm (1-M_n^2)}{M_n^2} \tag{2.49}$$

As can be shown the condition (2.46)f allows only the + sign in eq. (2.49). The final result is therefore:

$$\frac{u_{a_n}}{u_{f_n}} = \frac{1}{\gamma+1} \frac{(\gamma-1)M_n^2+2}{M_n^2} \tag{2.50}$$

From this equation it is readily derived that

$$\frac{\rho_a}{\rho_f} = \frac{(\gamma+1)M_n^2}{(\gamma-1)M_n^2+2} \tag{2.51)a$$

and

$$\frac{p_a}{p_f} = 1 + \frac{2\gamma}{\gamma+1} (M_n^2 - 1) \tag{2.51)b$$

Equation (2.9) gives then:

$$\Delta S = \ln \left(\frac{p_a}{p_f}\right)\left(\frac{\rho_a}{\rho_f}\right)^{-\gamma}$$

or

$$\Delta S = \ln \left\{ \left[1 + \frac{2\gamma}{\gamma+1} (M_n^2 - 1) \right] \left[\frac{(\gamma+1)M_n^2}{(\gamma-1)M_n^2+2} \right]^{-\gamma} \right\} \tag{2.52}$$

The general shock conditions for an ideal gas and a shock velocity zero are thus derived. The equations that are important for the following investigations are the four relations (2.47)a, (2.47)b, (2.50) and (2.52).

2.3 The equations for linearized potential flow.

Here a short derivation will be given of the equations valid for a linearized potential flow. To that end it will be assumed that the perturbation velocities are small as compared with the velocity U_∞ of the free stream.

Hence
$$u = 0\ (U_\infty) \tag{2.53)a}$$
$$v \ll U_\infty \tag{2.53)b}$$
$$w \ll U_\infty \tag{2.53)c}$$

Furthermore it will be assumed that the effects of entropy production can be neglected. According to the interpretation given of eq. (2.41) this means that the rotation vector is identically zero in the whole flow field. Thus there holds:

$$\frac{1}{r}\frac{\partial v}{\partial \psi} - \frac{1}{r}\frac{\partial wr}{\partial r} = 0 \tag{2.54)a}$$

$$\frac{1}{r}\frac{\partial wr}{\partial x} - \frac{1}{r}\frac{\partial u}{\partial \psi} = 0 \tag{2.54)b}$$

$$\frac{\partial u}{\partial r} - \frac{\partial v}{\partial x} = 0 \tag{2.54)c}$$

From eq. (2.24)a together with eqs. (2.53) there follows by neglecting products of small quantities

$$-\beta_\infty^2 \frac{\partial u}{\partial x} + \frac{\partial v}{\partial r} + \frac{1}{r}\frac{\partial w}{\partial \psi} + \frac{v}{r} = 0 \tag{2.55}$$

where $\beta_\infty = \sqrt{M_\infty^2 - 1}$

The eqs. (2.54) allow the introduction of a velocity potential φ by

$$u = \frac{\partial \varphi}{\partial x} \tag{2.56)a}$$

$$v = \frac{\partial \varphi}{\partial r} \tag{2.56)b}$$

$$w = \frac{1}{r}\frac{\partial \varphi}{\partial \psi} \tag{2.56)c}$$

The flow is then governed by one linear partial differential equation of the second order. This equation follows by inserting eqs. (2.56) into eq. (2.55). The result is

$$\beta_{\infty}^{2}\varphi_{xx}-\frac{1}{r}\varphi_{r}-\varphi_{rr}-\frac{1}{r^{2}}\varphi_{\psi\psi}=0 \tag{2.57}$$

This is the well-known linearized potential equation for supersonic flow. It should be observed that eqs. (2.56) are valid in every flow domain where the entropy is a constant throughout this domain.

3 Studies on supersonic flow around axially symmetric bodies.

To study the characteristics of supersonic flow past a certain configuration, in most of the cases use has been made of the linearized potential theory. However, as has been already indicated in the introduction, this theory has the disadvantage of being only approximate, the approximation being poorer if the configuration is less slender and the Mach number is higher.

No direct estimates, however, are known about the limits of applicability of this theory, other than by comparison with the results of exact theory. This is only possible in very few cases, for instance in the case of flow around cones.

In this chapter, the validity of linearized theory as applied to the study of supersonic flow around axially symmetric configurations will first be investigated. It will be shown that the linearized theory is inadequate in predicting the flow field around bodies of practical importance for nearly every Mach number. Especially in the case of interference no other result can be expected than the correct order of magnitude, since on the basis of the present investigations, it appears to be that the flow quantities at a certain distance from the configuration are more in error than those nearer to the body.

According to these arguments, the determination of optimum body shapes by using linearized methods should be suspected. Therefore it seemed wanted to devise a method using the non-linear equations for deriving optimum conditions. In the second part of this chapter such a method will be discussed for a body with a prescribed value of the base area and for a given Mach number. The method of analysis is closely related to the study of linearized flow since in both cases use will be made of the notion of a control surface.

3.1 On the validity of linearized theory for axially symmetric flow.

The present investigation, whose aim it is to give a quantitative value of the error made by using linearized theory, was undertaken after certain inconsistencies were discovered by applying the theory of ref.17.

There a method is given, based on linearized theory, which aims at constructing axially symmetric configurations of optimum shape with a given base area, by prescribing the value of the disturbance velocities on the forward characteristic emanating from the base (see fig.2).

The method of characteristics was used to construct these bodies and due to the properties of the configuration investigated, the first part of the body contour could be chosen freely. It then proved, however, to be impossible to reach the proper value of the radius of the base area, and moreover the drag as found by integrating along the body contour was not equal to the prescribed value. The differences were rather large and this seemed very surprising since the prescribed disturbance velocities were such as to give the correct mass- and momentum transport.

It was found along the lines outlined below, that this difference was due to the use of the linearized theory, in particular because of the rather thick nose of the configuration and the interference of flow between various parts of the configuration.

A method to study the validity of linearized theory, can be found by observing that the body area at a certain distance from the nose of the body and the drag on that part of the body can be expressed as integrals of functions of the disturbance velocities over a control surface.

This surface emanates from the section considered and intersects the shock wave from the nose of the body (see fig.3). In most of the cases it is convenient to take as a control surface the forward directed characteristic surface.

The method of comparison between these integrals and body area, and integrated drag offered itself as a natural tool to study the applicability of linearized theory.

The order of magnitude of the average error in the flow quantities can be predicted correctly on the basis of this comparison. It should be remarked that this method of estimation of error is independent of the use of more exact theory.

Here, the case of an axially-symmetric body will be considered, where the free stream is in alignment with the axis of the body. The simplest case of such a body is a cone, and much attention will be focussed upon this configuration.

To give more insight, a detailed comparison of flow fields and pressure distributions is presented for certain configurations.

The investigation will start with a derivation of integral expressions for body area and drag.

3.1.1. Integral expressions for body area and drag.

In this section a derivation will be given for certain integral expressions which are suitable to discuss the validity of linearized theory. The derivation will be given first without making any assumptions about the order of magnitude of the quantities occurring.

There after a simplified version will be given, by making the same assumptions used for deriving the linearized potential equation. In particular it is this latter version which will be used to discuss the validity of the results obtained by using linearized theory.

To derive the integral expressions use will be made of the concept of a control surface. This is a surface which envelops a certain volume, in which a part of the body is imbedded. The control surface which will be used here consists of two opposing parts, one of the two being part of the shockwave, the other emanating from the body section which is considered to intersect the shockwave in a circle with a certain radius.

The integral expression for the body area is found by observing that the ingoing mass has to be equal to the outgoing mass. This can be written as

$$\oint\!\!\oint \rho_n V_n \, dO = 0 \qquad (3.1)$$

where V_n is the outward directed component of the velocity along a normal to the surface and dO is an element of the control surface.

In fact, eq. (3.1) is the macroscopic form of the continuity equation.

If the part of the shock wave belonging to the control surface is denoted by O_1, and the rest of the control surface by O_2, eq. (3.1) can be written as

$$\oiint_{O_1} \rho_1 V_{n_1} dO_1 + \oiint_{O_2} \rho_2 V_{n_2} dO_2 = 0 \quad . \tag{3.2}$$

If now ϑ_1 is the angle between the tangent to the first part of the control surface and the axis of the body at a point at the radial distance r and ϑ_2 the supplement of the corresponding angle for the aft part of the control surface (see fig.3), eq. (3.2) can be written as

$$2\pi\rho_\infty U_\infty \int_0^{R_c} r\,dr = 2\pi U_\infty \int_{R_B}^{R_c} \rho_2 \left\{ u_2 \sin\vartheta_2 + v_2 \cos\vartheta_2 \right\} \frac{r dr}{\sin\vartheta_2} \tag{3.3}$$

where R_B is the radius of the body section considered and R_c is the radius of intersection of the two parts of the control surface (see fig.3). It should be observed that the velocities u and v are made dimensionless with respect to the free stream velocity U_∞ .

Equation (3.3) can be brought in a more elegant form by choosing for the aft part of the control surface a characteristic surface. It will be shown later that in this case there holds (according to eq. (2.32)b)

$$\tan\vartheta_2 = - \frac{v_2\beta_2 - u_2}{u_2\beta_2 + v_2} \quad . \tag{3.4}$$

Moreover from equations (2.9) and (2.22) there follows

$$\rho_2 = \rho_\infty \left(a_2^2 M_\infty^2\right)^{\frac{1}{\gamma-1}} P \tag{3.5}$$

Here "a" is the velocity of sound, made dimensionless with respect to U_∞. The function P, which is in fact the ratio of the stagnation pressures of the disturbed and the undisturbed flow, is given by

$$P = e^{-\frac{s}{\gamma-1}} \quad . \tag{3.6}$$

Substituting eqs. (3.4) and (3.5) into eq. (3.3) there is obtained

$$R_B^2 = 2 \int_{R_B}^{R_c} \left\{ \left(a^2 M_\infty^2\right)^{\frac{1}{\gamma-1}} \frac{q^2}{u - v\beta} P - 1 \right\} r\,dr \tag{3.7}$$

where $q^2 = u^2 + v^2$, and where the subscripts 2 have been dropped. This is the required equation, expressing the body area as an integral of a function of the velocities and the entropy only.

Now this equation will be simplified by using the assumptions that the disturbances are small and that the effects of entropy are negligible. In this case eqs. (2.53)a-b are valid while $P = 1$.

As can be seen immediately eq. (3.4) can be written then as

$$\tan \vartheta_2 = \frac{1}{\beta_\infty} \tag{3.8}$$

indicating that in this case the characteristics are straight parallel lines, which is in accordance with eq. (2.57).

Moreover, as can be found by expanding eq. (3.5), the density can be written as

$$\rho_2 = \rho_\infty \left\{ 1 - M_\infty^2 u' \right\} \tag{3.9}$$

where u' is the perturbation velocity defined by

$$u' = u - 1 \quad . \tag{3.10}$$

Inserting these equations into equation (3.3) gives

$$R_B{}^2 = 2 \int_{R_B}^{R_c} \left\{ -\beta_\infty^2 u' + \beta_\infty v' \right\} r dr \tag{3.11}$$

where v' has been written instead of v.

Equation (3.11) can be considered as a first order expression for the body area, and thus should be consistent with the use of linearized theory.

The second integral expression can be obtained by applying the momentum equation in an axial direction to the air within the control volume. If D is the drag force exerted by the air on the body and if it is assumed that the pressure p of the undisturbed stream is acting on the base of the body the momentum equation can be written as

$$D + \pi p_\infty R_B{}^2 + \iint_{O_2} p_2 \sin \vartheta_2 dO_2 - \iint_{O_1} p_1 \sin \vartheta_1 dO_1 =$$

$$= - \iint_{O_1} \rho_1 V_{n_1} U_1 dO_1 - \iint_{O_2} \rho_2 V_{n_2} U_2 dO_2 \tag{3.12}$$

Since U_1 is equal to the free stream velocity U_∞, eq. (3.12) can be simplified by using the mass flow relation (3.2). The result obtained is

$$\frac{D}{\rho_\infty U_\infty^2} = \iint\limits_{O_2} \frac{p_\infty - p_2}{\rho_\infty U_\infty^2} \sin\vartheta_2 dO_2 - \iint\limits_{O_2} \frac{\rho_2 V_{n_2}(U_2 - U_\infty)}{\rho_\infty U_\infty^2} dO_2 \qquad (3.13)$$

Now this equation will be brought into a form where the integrand is dependent on the velocities only. To this end it is observed that by using eq. (3.5) together with eq. (2.9) there follows

$$p_2 = p_\infty (a_2^2 M_\infty^2)^{\frac{\gamma}{\gamma-1}} P \quad . \qquad (3.14)$$

Introducing this equation into eq. (3.13) and using eqs. (3.5) and (3.10) there is found

$$\frac{D}{\rho_\infty U_\infty^2} = \iint\limits_{O_2} \frac{p_\infty}{\rho_\infty U_\infty^2} \left[1 - (a_2^2 M_\infty^2)^{\frac{\gamma}{\gamma-1}} P\right] \sin\vartheta_2 dO_2 +$$

$$- \iint\limits_{O_2} (a_2^2 M_\infty^2)^{\frac{1}{\gamma-1}} P(u_2 - 1)(u_2 \sin\vartheta_2 + v_2 \cos\vartheta_2) dO_2 \quad . \qquad (3.15)$$

Taking again for the aft part of the control surface a characteristic surface, the final result can be obtained by using eq.(3.4) together with the following evident relation

$$\frac{p_\infty}{\rho_\infty U_\infty^2} = \frac{1}{\gamma M_\infty^2} \quad . \qquad (3.16)$$

If the subscripts 2 are omitted, the integral expression can be written then as

$$\frac{D}{\rho_\infty U_\infty^2} = 2\pi \int_{R_B}^{R_c} \frac{1}{\gamma M_\infty^2} \left[1 - (a^2 M_\infty^2)^{\frac{\gamma}{\gamma-1}} P\right] r dr - 2\pi \int_{R_B}^{R_c} (u-1)(a^2 M_\infty^2)^{\frac{1}{\gamma-1}} P \frac{q^2}{u - v\beta} r dr$$

$$(3.17)$$

If the flow field is calculated correctly this equation has to give the same value of the drag as found by integrating the axial components of the pressure forces working on the body.

Also here, the first order form of this equation will be given. To do this, the Taylor-expansion of eq. (3.14) will be given. It turns out that up to the squares of the disturbance velocities

$$p_2 - p_\infty = \rho_\infty U_\infty^2 \left\{ -u' - \frac{1}{2} v'^2 + \frac{1}{2} \beta_\infty^2 u'^2 \right\} \tag{3.18}$$

Substituting this equation together with eqs. (3.8), (3.9) and (3.10) into eq. (3.13) there is found

$$\frac{D}{\rho_\infty U_\infty^2} = \pi \int_{R_B}^{R_c} (\beta_\infty u' - v')^2 \, r dr \tag{3.19}$$

One of the interesting features of this simple expression is the fact that the integrand is quadratic, thus leading to the result that the drag is at least zero. A far more important remark must, however, be made. The usual approximation for the pressure coefficient is given by the first term of eq. (3.18), while eq. (3.19) has been derived by using also the quadratic terms. In fact the drag would be identically zero if only the first term of eq. (3.18) had been used. This result indicates the necessity of using the form for the pressure coefficient given by eq. (3.18). This statement will be further commented on.

The integral expressions (3.7), (3.11), (3.13) and (3.19) are the basic tools which will be used in the following investigations on the supersonic axially symmetric flow.

3.1.2 The linearized flow around a cone.

In this section a study will be made of the supersonic flow around a cone with the aid of linearized theory. By using the already derived integral expressions, the validity of this theory for a cone will be investigated.

According to eq. (2.57) the linearized potential equation for supersonic flow in the case of a cylindrical coordinate system, is given by

$$-\beta_\infty^2 \varphi_{xx} + \varphi_{rr} + \frac{1}{r} \varphi_r + \frac{1}{r^2} \varphi_{\phi\phi} = 0 \tag{3.20}$$

Here, φ is defined in such a way, that the disturbance velocities, made dimensionless with respect to the free stream velocity U_∞ are given by

$$u' = \frac{\partial\varphi}{\partial x} \tag{3.21a}$$

$$v' = \frac{\partial\varphi}{\partial r} \tag{3.21b}$$

and

$$w' = \frac{1}{r}\frac{\partial\varphi}{\partial\psi} \tag{3.21c}$$

Since the flow is conical, the disturbance velocities are constant along rays through the origin. Introducing

$$t = \frac{x}{r} \tag{3.22a}$$

and $$\varphi = rtG(t) \tag{3.22b}$$

equation (3.20) can be written, after observing that $\varphi_{\psi\psi}$ vanishes due to the axially symmetrical character of the flow, as

$$t(t^2-\beta_\infty^2)\frac{d^2G}{dt^2} + \left\{2(t^2-\beta_\infty^2)-t^2\right\}\frac{dG}{dt} = 0 \ . \tag{3.23}$$

Solving this equation there is obtained

$$G = -K\frac{\sqrt{t^2-\beta_\infty^2}}{t} + K\cosh^{-1}\frac{t_o}{\beta_\infty} + Q \ . \tag{3.24}$$

The disturbance velocities are given by

$$u' = G + t\frac{dG}{dt} \tag{3.25a}$$

$$v' = \quad -t^2\frac{dG}{dt} \tag{.325b}$$

Since along the first characteristic $t = \beta_\infty$ the quantity $\beta_\infty u'+v'$ has to be equal to zero, it follows that $Q = 0$.

Equations (3.25)a and (3.25)b can then be written as

$$u' = K\cosh^{-1}\frac{t}{\beta_\infty} \tag{3.26a}$$

$$v' = -K\sqrt{t^2-\beta_\infty^2} \tag{3.26b}$$

The integration constant can be determined from the condition that the body has to be a stream surface, or if $\frac{dr}{dx}$ is the tangent to the body contour:

$$(1+u')\frac{dr}{dx} = v' \quad . \tag{3.27}$$

It should be observed that here the exact form of the boundary condition will be used.

If the semi-top angle of the conical body is denoted by ϑ_s, it can be shown that

$$K = \frac{-1}{t_o\sqrt{t_o^2-\beta_\infty^2}+\cosh^{-1}\frac{t_o}{\beta_\infty}} \tag{3.28}$$

where $t_o = \cot\vartheta_s$.

The equations (3.26)a-b and (3.28) thus give the flow field, around a cone according to linearized theory.

The question that will be raised now, is :

"What is the range of Mach-numbers M_∞ and semi-top angles ϑ_s for which this result is approximately valid?"

This question will be answered by using the integral expressions derived in the foregoing section.

First use will be made of the expression for the square of the radius of the body cross section eq. (3.11). The integral at the right hand side of this equation can be calculated by using the expressions for the perturbation velocities u' and v'. The result is

$$2\int_{R_B}^{R_c}\left\{-\beta_\infty^2 u'+\beta_\infty v'\right\}rdr = R_B^2\left[1-\frac{M_\infty^2\cosh^{-1}\frac{t_o}{\beta_\infty}}{t_o\sqrt{t_o^2-\beta_\infty^2}+\cosh^{-1}\frac{t_o}{\beta_\infty}}\right] \tag{3.29}$$

It is evident from eq. (3.29) that eq. (3.11) is not satisfied. This could be expected since only an approximate theory is used. The important point concerning these two equations, however, is that eq. (3.29) gives the possibility to obtain a judgement on the validity of the linearized theory. Due to the form of the integrand of eq. (3.11), the difference between the left-hand side and the right-hand side of this equation gives a measure of the average error in the flow quantities.

If a difference of $\varkappa$ percent between the left-hand side and the right-hand side is considered as permissible, there can be calculated limits of applicability of the linearized theory for a cone by solving the following equation

$$M_\infty^2 \cosh^{-1} \frac{t_o}{\beta_\infty} = \frac{K}{100} \left\{ t_o \sqrt{t_o^{\,2} - \beta_\infty^2} + \cosh^{-1} \frac{t_o}{\beta_\infty} \right\} \tag{3.30}$$

In fig.4 the limits for $K = 5$ and $K = 10$ have been given. As can be seen from these curves the region of applicability is very small. If the flow field has to be known accurately, the lower bound has to be applied. This indicates that only the flow around very slender cones can be calculated by using linearized theory. For a practical semi-angle, say 10^o, linearized theory is unable to give the flow field accurately.

One important aspect of the curves given in fig.4 is, that for M_∞ very near to unity, the value of ϑ_s which is allowed decreases rapidly, showing that linearized theory is invalid around $M_\infty = 1$. This fact about the linearized theory, long since known, can thus be shown to be true in a very simple way.

If K is calculated as a function of Mach number M_∞ and of semi-top angle ϑ_s it appears that with increasing Mach number and increasing semi-angle the average error in the flow field characterized by K increases rapidly, as is shown in table 1a.

To substantiate these results an analogous investigation will be performed by using eq. (3.19). The right-hand side of this equation proves to be

$$\pi \int_{R_B}^{R_c} (\beta_\infty u' - v')^2 r dr = \pi K^2 R_B^{\,2} \left\{ -\frac{1}{2}(t_o^2 - \beta_\infty^2) + \cosh^{-1} \frac{t_o}{\beta_\infty} \left[t_o \sqrt{t_o^2 - \beta_\infty^2} - \frac{1}{2} \beta_\infty^2 \cosh^{-1} \frac{t_o}{\beta_\infty} \right] \right\} \tag{3.31}$$

The right-hand side of eq. (3.19) can be obtained, as has already been remarked, by integrating the axial component of the pressure force acting on the body. Thus it is found that

$$\frac{D}{\rho_\infty U_\infty^2} = \pi \int_0^{R_B} c_p r dr \tag{3.32}$$

where c_p is the pressure coefficient, which is given by

$$c_p = \frac{p - p_\infty}{\frac{1}{2} \rho_\infty U_\infty^2} \tag{3.33}$$

Now, different expressions can be obtained for D, according to the different approximations, used for the pressure coefficient. Here use will be made of the formula given in eq. (3.18), which was used also when deriving eq. (3.19). Performing the integration indicated in eq. (3.32) there follows

$$\frac{D}{\rho_\infty U_\infty^2} = \pi K^2 R_B{}^2 \left\{ -\frac{1}{2}(t_o^2-\beta_\infty^2)+\cosh^{-1}\frac{t_o}{\beta_\infty}\left[t_o\sqrt{t_o{}^2-\beta_\infty^2}+(\frac{1}{2}\beta_\infty^2+1)\cosh^{-1}\frac{t_o}{\beta_\infty}\right]\right\} \quad (3.34)$$

Again there is an apparent difference between the two expressions for the drag, eqs. (3.31) and (3.34). It should be observed that both are calculated by using approximate values for the perturbation velocities. If both the drag according to the integral expression and that found by direct integration of the axial forces along the fuselage are equal, then no other conclusion can be reached than that both contain an error of equal order. But they are not equal, and therefore, this difference must be a measure for the consistency of linearized theory. Thus again limits of applicability can be calculated by solving the equation

$$\frac{\mathcal{K}_1}{100}\cosh^{-1}\frac{t_o}{\beta_\infty}\left\{(\frac{1}{2}\beta_\infty^2+1)\cosh^{-1}\frac{t_o}{\beta_\infty}+t_o\sqrt{t_o^2-\beta_\infty^2}\right\}-\frac{1}{2}(t_o^2-\beta_\infty^2)= M_\infty^2\left(\cosh^{-1}\frac{t_o}{\beta_\infty}\right)^2 \quad (3.35)$$

where $\mathcal{K}_1$ is the difference in percents between the expressions (3.31) and (3.34). In table 1 b the quantity $\mathcal{K}_1$ has been given as a function of M_∞ and ϑ_s. The results are in complete agreement with those of table 1 a, leading thus to the same conclusions about the validity of linearized theory.

A detailed comparison between the flow fields as determined by linearized theory and exact methods respectively shows how large the actual error is at each point. This will be done in section 3.1.4. However, first the flow field around pointed axially symmetric bodies will be studied along the same lines as given here, to see if the conclusions reached for a cone have to be altered with more general configurations.

3.1.3 The linearized flow around a body.

To obtain the flow field around a general axially-symmetric configuration in the linearized approximation, a solution of eq. (2.57) must be obtained which fulfills the boundary condition along the body contour as given by eq. (3.27).

This problem can be solved, by means of an analytical method, such as a distribution of sources along the axis, or by a numerical method.

An excellent numerical method for the solution of hyperbolic differential equations is the method of characteristics, where the flow field is calculated step by step by using the characteristic equations along characteristic surfaces. A detailed description of the derivation of such equations has been given in chapter 2. It can be shown by using the results of this chapter that in the linearized approximation these equations take the following form

$$\frac{du'}{dr} + \frac{1}{\beta_\infty}\frac{dv'}{dr} + \frac{1}{\beta_\infty}\frac{v'}{r} = 0 \tag{3.36)a}$$

along the characteristic with $\frac{dr}{dx} = -\frac{1}{\beta_\infty}$ and

$$\frac{du'}{dr} - \frac{1}{\beta_\infty}\frac{dv'}{dr} - \frac{1}{\beta_\infty}\frac{v'}{r} = 0 \tag{3.36)b}$$

along the characteristic with $\frac{dr}{dx} = \frac{1}{\beta_\infty}$.

The flow field can be determined by using these relations if beside the boundary, the flow around the nose of the body is also given. The shape of a pointed nose can always be considered as conical. This gives the possibility to use the results of the preceding section. In that case the flow quantities are known along the last characteristic of the conical region (see fig.5). The method of characteristics to be used here is straightforward and the most advisable for quantitative results if the flow field has to be known.

For the study of the applicability of linearized theory the flow field around two bodies is calculated for different Mach numbers. In fact each body represents a whole family, since the base can be selected at arbitrary values of the axial coordinate x between the nose and the base, because the flow is supersonic. This means that the flow aft of a given value of x cannot influence the flow field before the backward directed characteristic emanating from the cross section at x.

The two bodies chosen have a conical nose over 0.025 of the length and are followed by a parabolic shape which is symmetric with respect to the line x = 0.5125. The base lies at x = 1.0. The conical nose of the first body has a semi-top angle $\vartheta_s = 7.5^\circ$ and that of the second body has $\vartheta_s = 12.5^\circ$. If the slenderness is given by

$$s = \frac{\ell}{2\, r_{max}} \tag{3.37}$$

the bodies have $s = 13.7$ and $s = 8.4$ respectively. The flow field around the body with $\vartheta_s = 7.5^\circ$ and $s = 13.7$ has been determined for the Mach numbers $M_\infty = 2$ and $M_\infty = 5$. The flow field around the body with $\vartheta_s = 12.5^\circ$ and $s = 8.4$ has been determined for the Mach numbers $M_\infty = 2$ and $M_\infty = 4$.

Along several characteristics for different values of x, the right-hand side of the integral expression for the mass flow eq.(3.11) has been calculated. The results found thus have to be compared with the function R_B^2 as prescribed by the body contours. The results for the various cases, have therefore been given in figs 6 (a-d) together with the prescribed distribution of the cross sectional area of the bodies.

The deviation between the two curves gives, just as for the cone, a measure of the average error in the flow field. It is found that the differences are relatively the largest at the nose and at the end of the body. The curves indicate that for bodies which have a positive slope over most of the length, the error decreases with increasing slenderness. However, if a negative slope is present over an appreciable length of the body the deviation grows rapidly with increasing negative slope.

From the figures 6 (a-d) it can be seen that the general trend of increasing deviations with decreasing slenderness is very striking. The great importance of these figures, however, is that they give a quantitative answer to the question of the validity of linearized theory for the calculation of the flow field around these particular configurations. Seen in this light, although in general the deviations for bodies are less pronounced than for cones, the only case that may be given a reliable numerical value, is the case where $\vartheta_s = 7.5^\circ$ and $M_\infty = 2$. The differences for the other cases are so large that linearized theory determines apparently only the order of magnitude of the flow quantities.

As was done for the cone, a comparison will also be made of the drag as found by integrating the axial pressure forces working on the body, and the drag as found by calculating the loss of momentum through a suitably chosen control surface. The respective expressions are given by eqs. (3.32) and (3.19).

In the figs 6(a–d) the quantities $\frac{D}{\rho_\infty U_\infty^2}$ are given as a function of x, and are calculated by using both the above mentioned expressions. The difference apparent here underlines the conclusions based already on the investigation of the expression for the mass flow.

One important remark to be made is that the drag of the body is apparently generated for the largest part by the nose and the end of the body, which is evident from figs 6 where the drag does not increase midway between the ends. In those terminal parts, however, the largest errors are present in the flow field according to the results already obtained. Thus it may be concluded that the drag on rather slender bodies is not predicted more accurately, than for cones which have a slope of the order of the slope at the nose of the body.

From the fact that the curves which are compared at the end of the body for instance are closer to each other than at the nose, no other conclusion can be drawn, than that the error in eq. (3.19) is nearly the same as that in eq. (3.32).

Only if eq. (3.11) for the mass-flow is satisfied and at the same time eq. (3.19) gives the same result as eq. (3.32) can it be concluded that linearized theory is able to give a quantitative answer. In the given examples this occurs only for the case where $\vartheta_s = 7{,}5^\circ$ and $M_\infty = 2$.

Thus the conclusions reached at in this section are as follows: Linearized theory is only able to describe the flow field around a body if the shape is slender and the slope is small and moreover the Mach numbers are low. For higher Mach numbers, less slender shapes and rather large slopes, only the order of magnitude of the flow quantities can be predicted. The methods given here enable the calculation of the average error present in the flow field. As is shown in figs. 7a–b where κ, being the percentual difference between the left-hand side and the right-hand side of the mass flow equation, is given as a function of the axial distance x for two of the cases considered, the error is, even in parts where the slope is very small, rather large.

For practical applications the range of validity is evidently so small, if accurate results are required, that the question can be raised whether it is advisable to use linearized theory for the calculation of the flow field around axially-symmetric configurations.

3.1.4 The exact flow around a cone.

One of the first exact solutions for the inviscid supersonic axially-symmetric flow was given in 1933 by Taylor and Maccoll for the flow around a cone. Assuming that the flow quantities are constant along rays through the vertex of the cone, the governing differential equations take a simple form

$$\frac{d\bar{v}}{d\vartheta} + \bar{u} = \frac{a^2(\bar{u}+\bar{v}\cot\vartheta)}{\bar{v}^2-a^2} \qquad (3.38)a$$

$$\frac{d\bar{u}}{d\vartheta} - \bar{v} = 0 \qquad (3.38)b$$

where $\bar{u}$ is the velocity along the cone with semi-top angle ϑ and $\bar{v}$ is the velocity orthogonal with respect to $\bar{u}$ in a meridional plane, "a" is as usual the velocity of sound. The system (3.38) is a set of two first order differential equations which can be derived from the general expressions given in chapter 2. The second equation states in fact that the flow is irrotational, since the entropy rise across the shock wave, which is itself conical, is a constant.

A comprehensive compilation of numerical data,solutions to the non-linear differential equations (3.38) for flow around a cone, has been given in ref.7 for various semi-top angles ϑ_s and Mach numbers M_∞.

If the flow around a cone has to be known for a particular case it is best in general to interpolate the results in ref.7. Especially accurate calculations of flow fields require then a large amount of work.

However, with present day electronic computers, numerical integration of particular equations can be easily handled.

Because all the calculations are performed in a cylindrical coordinate system, it is easier to work with the axial and radial velocities u and v than with other velocity components. These are given by

$$\bar{u} = u\cos\vartheta + v\sin\vartheta \qquad (3.39)a$$

$$\bar{v} = -u\sin\vartheta + v\cos\vartheta \qquad (3.39)b$$

Substituting these equations into the system (3.38) there is obtained

$$\frac{du}{d\vartheta} = \frac{-a^2 v}{(v\cos\vartheta - u\sin\vartheta)^2 - a^2} \qquad (3.40)a$$

$$\frac{dv}{d\vartheta} = -\cot\vartheta \frac{du}{d\vartheta} \qquad (3.40)b$$

The boundary condition at the cone surface, according to eq.(3.27), is given by

$$u = v\cot\vartheta_s \qquad \text{for} \quad \vartheta = \vartheta_s \qquad (3.41)$$

The conditions on the as yet unknown shock wave $\vartheta = \vartheta_w$ are given by:

$$u - 1 = -v\tan\vartheta_w \qquad (3.42)a$$

and

$$M_\infty^2 = \frac{1}{\frac{\gamma+1}{2}(u-1) + \sin^2\vartheta_w} \qquad (3.42)b$$

The derivation of these two equations will be given with some details in section 4.24 of the following chapter. They are based on the general results for shock transition given in chapter 2.

The method of solution of the equations (3.40) with the boundary conditions (3.41) and (3.42) is analogous to that of Kopal, and need not therefore to be discussed here. The rise of entropy across the shock wave is given by

$$P = e^{-\frac{s}{\gamma-1}} = \left[\frac{(\gamma+1)M_\infty^2\sin^2\vartheta_w}{(\gamma-1)M_\infty^2\sin^2\vartheta_w + 2}\right]^{\frac{\gamma}{\gamma-1}} \left[1 + \frac{2\gamma}{\gamma+1}(M_\infty^2\sin^2\vartheta_w - 1)\right]^{\frac{-1}{\gamma-1}} \qquad (3.43)$$

For a flow which is determined exactly the integral expressions (3.7) and (3.17) have to be identities; the deviations will give an insight in the numerical accuracy obtained. As a test case the flow around two cones with $\vartheta_s = 7.5^\circ$ and $\vartheta_s = 12.5^\circ$ have been used, for the Mach numbers $M_\infty = 2$, $M_\infty = 5$ and $M_\infty = 2$, $M_\infty = 4$ respectively. In table 2, the two sides of equation (3.7) have been given together with the drag as calculated by using eq. (3.17) and eq. (3.32). The agreement obtained shows that the numerical accuracy is very good.

3.1.5 The exact flow around a body.

The solution of the problem to determine the flow field around an axially-symmetric body, can be obtained by using the exact inviscid flow equations and then to transform these equations into characteristic equations according to the treatment given in chapter 2. By using a numerical method of solution, based on these equations, the flow field can be constructed. This construction is greatly aided by the use of electronic computers.

The governing differential equations are according to eqs. (2.24) a-d, for an axially-symmetric flow given by

$$\left(1-\frac{u^2}{a^2}\right)\frac{\partial u}{\partial x}+\left(1-\frac{v^2}{a^2}\right)\frac{\partial v}{\partial x}+\frac{v}{r}-\frac{uv}{a^2}\left\{\frac{\partial u}{\partial r}+\frac{\partial v}{\partial r}\right\}=0 \qquad (3.44)\text{a}$$

$$v\left\{\frac{\partial v}{\partial x}-\frac{\partial u}{\partial r}\right\}+\frac{a^2}{\gamma(\gamma-1)}\frac{\partial s}{\partial x}=0 \qquad (3.44)\text{b}$$

$$u\left\{\frac{\partial u}{\partial r}-\frac{\partial v}{\partial x}\right\}+\frac{a^2}{\gamma(\gamma-1)}\frac{\partial s}{\partial r}=0 \qquad (3.44)\text{c}$$

where it is understood that all the velocities are made dimensionless with respect to the free stream velocity U_∞ ; hence the speed of sound "a" is given by

$$a^2=\frac{1}{M_\infty^2}+\frac{\gamma-1}{2}-\frac{\gamma-1}{2}\left(u^2+v^2\right) \quad .$$

Instead of working with the specific entropy s, use will be made of the ratio of the stagnation pressures P, as defined by eq.(3.6).

From the system of characteristic equations (2.40), (2.41) and (2.45) it can be derived that for axially-symmetric flow the following characteristic equations are valid:

$$P = \text{constant}^{*)} \qquad (3.45)\text{a}$$

along lines with a slope $\frac{dr}{dx}=\frac{v}{u}$ (i.e. streamlines).

*) It should be observed that this constant can be different for each streamline.

$$(u\beta+v)\,\frac{du}{dr} - (u-\beta v)\,\frac{dv}{dr} - \frac{v}{r}\,\frac{q^2}{u+\beta v} - \frac{a^2\beta}{\gamma P}\,\frac{dP}{dr} = 0 \qquad (3.45)b$$

along a line with the slope $\frac{dr}{dx} = \frac{u+\beta v}{\beta u-v}$

and

$$(u\beta-v)\frac{du}{dr} + (u+\beta v)\frac{dv}{dr} + \frac{v}{r}\,\frac{q^2}{u-\beta v} - \frac{a^2\beta}{\gamma P}\,\frac{dP}{dr} = 0 \qquad (3.45)c$$

along a line with the slope $\frac{dr}{dx} = -\frac{u-\beta v}{\beta u+v}$.

From these equations it is evident that the influence of the quantity P on the velocity components u and v is determined by the gradient $\frac{dP}{dr}$ along the characteristic surfaces. If $\frac{dP}{dr}$ is identically zero in the whole domain of the flow considered, u and v can be calculated without any knowledge of P. This is the case for a conical body. In those cases where $\frac{dP}{dr}$ is small along both the families of characteristic surfaces, the last terms in eqs. (3.45)b–c can be neglected, thus in fact neglecting the influence of the curvature of the shock waves on the flow field.

This will be a valid assumption if the curvature of the shock wave is small. Since according to eq. (2.52) the entropy rise across a shock wave can be calculated as soon as the shape of the shock is known, it is possible to check the assumption of having a small $\frac{dP}{dr}$ by calculating the quantity P as a function of r along the shock wave.

To establish the accuracy of the linearized theory it will be useful to complement the results obtained in section 3.1.3 by a direct comparison of the flow fields, as calculated by using linearized and exact theory respectively.

For that purpose the flow field around the same bodies as considered in that section will be determined by using exact methods. However, an assumption will be made, viz. that $\frac{dP}{dr}$ is negligible along both families of characteristic surfaces. This means that eq. (3.45)a will not be used in the actual computations. The influence of this assumption will be measured by using the integral expressions for drag and body area.

To start the flow field construction by using the characteristic equations, the flow around the conical nose has to be known just as in the linearized case. The solution for this problem has already been given in the preceding section.

The boundary condition along the fuselage is given by eq. (3.27), while the boundary conditions along the shock wave are very analogous to those for the cone, i.e.

$$(u-1) = \frac{2}{\gamma+1} \; \frac{1-M_\infty^2 \sin^2\vartheta^*}{M_\infty^2} \tag{3.46a}$$

$$v = -(u-1)\cot\vartheta^* \tag{3.46b}$$

where now ϑ^* is the angle between the shock wave and the x-axis, and is in general dependent on the radial coordinate. The third shock condition is given by eq. (3.43) when ϑ_w is replaced by ϑ^*. Because no use is made of eq. (3.45)a, this condition need not be used in the actual calculation, but will serve to determine the entropy rise along the shock wave afterwards.

The pressure coefficient is given by the following formula (see eq. (3.33) and eq. (3.14))

$$C_p = \frac{2}{\gamma M_\infty^2} \left\{ (a^2 M_\infty^2)^{\frac{\gamma}{\gamma-1}} . P-1 \right\} \tag{3.47}$$

After determining the flow field around the two bodies, a check on the results has been applied by calculating the right hand side of the mass flow equation (3.7) and by comparing the drag as found by integration along the control surface and along the body.

Since, as has already been remarked, the gradient of the entropy has been neglected, it can not be expected that a perfect agreement will be obtained. By applying the mass flow- and drag equations, it should be observed that there are two reasons for a deviation. In the first place the velocities calculated are incorrect due to the neglection of $\frac{dP}{dr}$. However, as has been argued the influence of this approximation is indeed negligible if the gradient is small. In the second place a deviation will be caused by the fact that the entropy rise across shock waves is neglected, which means that the quantity P occurring in the expressions considered is unknown. It is immediately clear (for instance by comparison with a cone) that this latter reason is the most important for small $\frac{dP}{dr}$.

To see if this reasoning is acceptable the integral expressions have been calculated with various assumptions on the function P.

In the first place, it is assumed that there is no rise in entropy or $P = 1$, thus physically no shock wave is present.

A second choice is that P has the value prescribed by the conical part of the shock wave.

However, the best result should be obtained by adjusting to every field point a value of P in an approximate way. It should be remembered that the entropy has to be constant along axially-symmetric stream surfaces. If now the assumption is made that the density and the disturbance velocity are constant along a characteristic surface, the shape of a stream surface can be constructed in an approximate way. Since along the shock wave the function P can be calculated, this assumption together with the mass flow equation suffices to calculate the function P in an arbitrary point of the flow field in the following way. If D is a point on the shock wave and E the field point then

$$P_{(R_E)} = P_{(R_D)} \tag{3.48)a}$$

provided that R_E and R_D are related by the following expression

$$\frac{R_c^{\,2} - R_D^{\,2}}{R_D^{\,2} - R_A^{\,2}} = \frac{R_c^{\,2} - R_E^{\,2}}{R_E^{\,2} - R_B^{\,2}} \quad , \tag{3.48)b}$$

where the various quantities occurring are indicated in fig.8.

In table 3 the results of the calculations for body radius and drag are given with the various assumptions for P, mentioned above. For each of the four bodies considered these quantities have been compared for two different cross sections.

It is evident from these results that the assumptions of a constant entropy rise across the shock wave give rise to appreciable differences, while the third method, as prescribed above, gives an agreement which is remarkably good. This suggests that the influence of the neglect of the gradient of the entropy $(\frac{dP}{dr})$ on the field quantities u and v is indeed very small.

Thus, here again, the importance of the integral expressions found by using a control surface for estimating the quantitative error when certain factors are neglected, is shown.

In the four last sections enough results have been obtained to give a detailed comparison between the results of the linearized and the exact theories. This comparison will be given in the following sections.

3.1.6 Comparison of the pressure distributions.

In this section a more detailed analysis will be made of the pressure distribution along a fuselage as calculated by using linearized and exact methods.

Although already in ref.13 a rather comprehensive analysis is given for the case of the cone, part of this analysis will be repeated here, in order to give the connection with what has been already said.

In the sections 3.1.2 and 3.1.3 it is proved that the mean error in flow quantities increases rapidly with higher Mach numbers, and not slender bodies. A question now arises, being one which has been asked by many investigators before, whether or not the pressure distribution over the body is as much in error as the quantities in the outer flow field.

As will be shown the answer to this question depends largely on the approximation which is made in the formula for the pressure coefficient.

First the pressure distribution on the surface of a cone will be considered.

In the figures 9 a-d the pressure coefficient is given as a function of the Mach number M_{∞} for several values of the semi-top angle ϑ_s.

In each case four different curves are given for the pressure coefficient. The correct one is calculated with eq. (3.47) by using the theory of Taylor and Maccoll as set forward in section 3.1.4. If the same formula (3.47) is used with $P \equiv 1$, and the flow quantities according to the linearized theory, the approximation according to Kármán-Moore is found. If the expression for the pressure coefficient is expanded by using the binomial theorem and if only linear and quadratic terms are retained, the formula (3.18) results. One step further is to omit the quadratic terms and to put the formula for c_p in the usual form for thin wings

$$c_p = -2u' \tag{3.49}$$

It might be expected that the error would increase with increasing approximation of the formula for the pressure distribution, This, however, is not true. From fig.9 it is evident that the absolute best approximation is obtained with the most simple form for c_p, i.e. eq. (3.49).

The approximation which can be considered the most valuable is given by the expression (3.18). Although absolutely more in error than eq.(3.49) it gives the same trend for all Mach numbers and semi-top angles as the correct solution. The approximation according to Kármán-Moore gives the greatest deviations, the error in that case being about two times larger than that found on using eq. (3.18). This indicates that the values of the flow quantities differ appreciably from those of the correct ones, and that by using an approximate formula for the pressure coefficient part of this error can be corrected for. This result cannot be based on a rigorous analytical investigation. It must be considered as rather arbitrarily.

To see how the deviation between the pressure-coefficients, according to the linearized approximation and the exact ones is related to the mean error in the flow as given in table 1, table 4 is given indicating this deviation as a function of Mach number M_∞ and semi-top angle ϑ_s. It has been defined by the quantity $\overline{K}$ in the following way

$$\overline{K} = 100 \, \frac{c_{p_{(T.M)}} - c_{p_{(gu)}}}{c_{p_{(T.M)}}} \tag{3.50}$$

In fact this $\overline{K}$ is the percentage by which the pressure coefficient according to eq. (3.18) differs from the exact one.

Comparing table 4 with table 3 it is remarkable that the error in the pressure-coefficient as calculated by using eq. (3.18) is not as strongly dependent on the Mach number as the mean error K is. On the other hand the amount that linearized theory differs from the exact theory, does not allow quantitative meaning be given to the linearized theory for practical shapes.

To see how these conclusions have to be modified for more realistic configurations, the pressure distributions for the four different cases already studied in the sections 3.1.3 and 3.1.5 have been given in figs. 10 a-d. In each case three different curves are given, based respectively on eq. (3.47) which gave the exact value of c_p and of the two approximations to the formula for the pressure coefficient, based on eqs.(3.18) and (3.49) for the linearized theory.

One property which the figures have in common is, that the slope of the exact curve is larger than those of the linear curves over the forward part of the configurations, while this situation is reversed at the aft-part. This indicates that the curves based on the linearized theory, in all cases, do not give the actual trend of the exact curve. If a choice has to be made upon which of the two versions of the linearized pressure coefficient is preferable, it will be seen that this question is hard to answer. In some cases, over certain parts of the configuration eq.(3.49) will give a better result than eq. (3.18), while on other parts this situation is reversed.

The curve based on eq. (3.18), however, can in all cases be related to the exact curve in a unique way. This curve shows in all cases a steady increase in deviation with increasing Mach number or decreasing slenderness.

It is remarkable that the deviations are larger on the aft part of the fuselage than on the forward part. Even in the case $\vartheta_s = 7.5^{\circ}$, $M_{\infty} = 2$ these deviations are very large.

In figs 11 a-d the results obtained have been shown in another way by calculating the percentual difference between the exact c_p and the pressure coefficient as given by eq. (3.18). Here more clearly the indeed large differences are shown. In conclusion, it can be said that the remarks already made for cones, apply as well for bodies. The deviation in the pressure coefficient, at least along the parts of the contour with a positive slope, is always smaller than the mean error in the flow field based on the mass-flow and momentum considerations. The conclusion for a part with negative slope, however, must be, that in each case the result of the linearized theory for the pressure coefficient is highly questionable, apart from those pieces of the contour where the use of linearized theory is admitted by a very low mean error in the field quantities.

As has been said above the error in c_p is for some parts of the body far less than the mean error. This indicates that the flow field at a certain distance from the body is more in error than the flow field closely surrounding this body. In the following section, it will be investigated if this suggestion is true.

3.1.7 Comparison of the flow fields.

Until now the comparison between the results of the exact and the linearized theory have been restricted to global results based on the control surface approach, which gave a kind of mean error of the flow quantities and to a direct comparison of the pressure distribution. In many problems, however, not only the value of the flow quantities on the body is important, but also the values in the outer flow field. A simple example, where this is important, is the interference between the body and another configuration.

Again the conical body presents the most simple example for discussing the differences between the exact- and the linearized theory in the outer flow field.

To this end, in fig.12 a-d, the disturbance velocities u' and v' caused by a cone, are given as a function of the spherical coordinate ϑ. In each figure the results, as derived by using the exact theory of Taylor and Maccoll and according to the linearized theory of section 3.1.2, are given. This has been done for the Mach numbers $M_\infty = 2.1469$ and $M_\infty = 4$.

From these figures it is evident that linearized theory, at least for a cone, gives results that best approximate the exact values at the fuselage, while the deviation between the two theories increases very rapidly in the outer flow field. It is clear that the region of disturbed flow, caused by the body, even for rather low Mach numbers, is much larger according to the exact theory than with the linearized theory. Moreover another serious drawback of the linearized theory for a cone, which must be noted, is that it is not able to give a shock wave. This means that in the outer parts of the flow completely different phenomena are predicted by linearized theory than occur in reality. The limits of applicability are therefore even more severe than those given in the table 1 (where the mean error in the flow quantities is given), if interference effects are important.

In figs 13 a-d and 14 a-d a trial is made to indicate the differences between linearized theory and exact theory for bodies with respect to the flow field. The alreay earlier investigated body with a semi-top angle of 12.5^o has been studied for the Mach numbers $M_\infty = 2$ and $M_\infty = 4$. In each case the velocity distribution along a forward directed characteristic surface has been given. The characteristics start from about the cross sections at $\frac{x}{\ell} = 0.4$ and $\frac{x}{\ell} = 0.8$. The results must be treated with some care, for it was not possible to select the same position of $\frac{x}{\ell}$ for the linearized and the exact case. They were taken, however, as near to each other as could be accomplished. These figures display the same features which are already evident in those for the cone. The larger region of disturbance given by the exact theory together with the existence of a shock wave give rise to very large differences between the results of the two theories for the outer flow field. This trend is strongly dependent on the Mach number. The results obtained in this section thus give rise to the statement, that the linearized theory is very inadequate, which is particularly true when the theory has to be used in cases where the flow phenomena in the outer flow field are important.

3.1.8 Concluding remarks.

In the foregoing sections the validity of linearized theory for the study of the flow around axially-symmetric configurations has been investigated. Use has been made of integral expressions for the body area and the drag, derived by using suitably chosen control surfaces.

It has been shown that by using these integral expressions a quantitative estimate can be given of the error made by applying the linearized theory. The results, which are given in terms of the so called mean error, indicate that only in those cases where this mean error is very small, the differences between the linearized and the exact theory can be considered as negligible.

It occurs that this is only the case for shapes, which are impractical.

Furthermore it has been shown by a detailed comparison that the linearized theory gives results which are more in error at some distance from the body, than near to the body itself. This statement is related to the fact that the linearized theory for pointed bodies is unable to give the existence of a shock wave. Such facts should lead to total misleading impressions of the phenomena occurring in reality, in cases where the effects of interference are important. Some of such cases are indeed known in the literature.

The above given reasons lead to the necessity of giving the utmost care to the study of the axially-symmetric optimum configurations. In all cases the condition for an optimum shape can be given by a prescribed velocity distribution on a closed surface, surrounding the body. To determine now the shape of such a body, the flow field has to be calculated. However, if use is made of linearized theory, the same large errors are present in the flow field as in the flow field around given shapes, depending of course on slenderness and Mach number. Therefore the shape constructed by using such a theory has little chance to be the actual shape of the derived optimum configuration.

For this reason it is necessary to have resort to more exact methods of investigation for the flow field of an axially-symmetric configuration. Since already methods are known for constructing the flow field if sufficient conditions are given, the only remaining problem is to find these conditions.

In the following part of this section the important problem of the necessary conditions for an optimum shape with given base area, will therefore be solved by using the exact equations for isentropic, inviscid flow.

3.2 On the determination of optimum axially-symmetric shapes.

In the first part of this chapter a variety of reasons were given to suspect optimum-shape configurations as determined by the linearized theory. To remedy this situation a more exact description of the properties of supersonic flow must be given. This means that the non-linear differential equations as given in chapter 2 have to be used.

The problem which will be studied, is the determination of an optimum shape with a given base area at a given Mach number M_∞ of the free stream.

It is to be understood that an optimum shape is such a configuration for which the wave drag is as low as possible under certain restraints.

This problem has been solved already in 1935 with the aid of linearized theory by von Kármàn [x)] (ref.18).

However, the method used there can not be generalized for a treatment where non-linear differential equations are used. A scheme which permits such a generalization is given in ref.17.

There, use has been made of a control surface approach. As has been set forth in section 3.1.1, the drag and the body area can be written as

x) with the accessory condition of given length integrals of functions of the velocities along the control surface. It will be assumed that the body whose shape has to be determined, is in the volume enclosed by the control surface. This control surface will consist of two parts; namely the surface separating the regions of undisturbed and disturbed flow, and the forward facing characteristic surface emanating from the base. In this case, the whole flow field inside the control surface is governed by the velocity distribution along the aft-characteristic surface. The problem reduces, therefore, to the determination of such a velocity distribution along this surface, that the drag has the smallest value possible, and that the base area has a given value.

To solve this problem use will be made of variational theory; with the differential equation thereby derived, together with the appropriate characteristic equation and the boundary conditions, the optimum velocity distribution along the aft-characteristic surface can be determined.

To make the problem as simple as possible, it will be assumed that the flow is isentropic in the volume enclosed by the control surface. This has the consequence that the flow is also irrotational in that domain.

A remark should be made about the isoperimetric conditions in the optimization procedure. If the exact flow equations are used, the characteristic surfaces have a slope which varies from point to point in a meridian plane, since it depends on the velocities. Thus the shape of the aft-characteristic surface is not known beforehand, but follows as a result of the solution of the problem.

This makes it hard to prescribe a given length, as is usual in the linearized treatment of this problem. Instead therefore it will be assumed that the base area of the body as well as the radius of the intersecting circle of front- and aft part of the control surface is given.

Another, very important point is the following: Far behind the body, the drag of the configuration that is considered is accompanied with a rise in entropy. This may seem quite amazing since it has been assumed that the flow is isentropic. However, it must be emphasized that this is only true inside the control surface. Somewhere in the outer flow field, a shock wave will be formed which gives the expected rise of entropy. This shock wave will be formed at the point of convergence of the compression fan which has to be generated by the nose of the optimum body, in order to fulfill the condition of isentropic flow inside the control surface. The point of convergence together with the optimum distribution will now be determined in the following sections. These sections contain a revised version of the subject matter of ref.19.

3.2.1 The requirements for minimum drag.

In this part a summary will be given of the equations which have to be used for deriving the optimum conditions along the aft characteristic surface. All these equations have already been derived but for the sake of the clearness they will be given here in the proper order, together with the fundamental assumptions underlying this analysis.

In the first place it has been assumed that the aft part of the control surface consists of a characteristic surface. Due to the analysis being restricted to rotationally symmetric flow fields, this surface itself is axially-symmetric.

According to eq. (3.4) the slope of this surface is given by

$$\frac{dr}{dx} = -\frac{u-v\beta}{v+u\beta} \quad . \tag{3.51}$$

The base area and the drag of the configuration imbedded in the volume enclosed by the control surface are given, if eq. (3.51) is valid, by the equations (3.7) and (3.17). Since it is assumed that the flow inside the control surface is isentropic, the function P of eq. (3.6) is in this case equal to 1.

The equation for the mass flow (3.7) can be written then as

$$R_c^{\,2} = 2\int_{R_B}^{R_c} (a^2M_\infty^2)^{\frac{1}{\gamma-1}} \frac{q^2}{u-\beta v}\, r\,dr \tag{3.52}$$

The equation for the drag is according to eq. (3.17) given by

$$\frac{D}{\rho_\infty U_\infty^2} = 2\pi\int_{R_B}^{R_c} \frac{1}{\gamma M_\infty^2}\left[1-(a^2M_\infty^2)^{\frac{\gamma}{\gamma-1}}\right] r\,dr - 2\pi\int_{R_B}^{R_c} (u-1)(a^2M_\infty^2)^{\frac{1}{\gamma-1}} \frac{q^2}{u-\beta v}\, r\,dr \tag{3.53}$$

In these expressions R_B is the radius of the base area, while R_c is the radius of the intersecting circle of the fore and aft part of the control surface. As before, all velocities are made dimensionless with the aid of the velocity U_∞ . The quantities R_B, R_c and M_∞ have certain prescribed values.

The problem to be solved, therefore, is to minimize the expression for the drag given by eq. (3.53), while at the same time satisfying eq. (3.52). Moreover it is necessary for the quantities u and v to satisfy the characteristic equation for axially-symmetric flow which is valid along the aft-characteristic surface. This equation can be found from eq. (3.45)c, if it is remembered that $\frac{dP}{dr} = 0$ in this case.
Then there is found:

$$(u\beta - v)\frac{du}{dr} + (u+\beta v)\frac{dv}{dr} + \frac{v}{r}\frac{q^2}{u-\beta v} = 0 \quad . \tag{3.54}$$

The expressions (3.52), (3.53) and (3.54) enable the formulation of the problem. This problem is to find such a distribution of the velocities u and v as a function of the radial distance r, that the drag D has its minimum value at a given value of R_c^2 in eq. (3.52), while the characteristic eq. (3.54) has to be satisfied for every value of r inside the interval $R_E \leq r \leq R_c$. This problem is stated in such a form that it is particularly suited for application of the variational theory. Before this theory will be applied, something should be said about the boundary conditions which have to be imposed at the boundary points B and C. At the rim of the base of the configuration no physical boundary condition is present; therefore the variational procedure itself must yield a so called "natural" boundary condition at this point. About the boundary condition at the intersection of the fore and aft part of the control surface nothing further will be said at this moment other than that it must be such that a physically realizable transformation occurs from the undisturbed to the disturbed flow.

First, the differential equations valid for the velocity distribution along the aft characteristic surface, will be derived by using variational theory.

3.2.2 Application of variational theory.

In the foregoing section a problem has been formulated which in fact comes down to the determination of the extremum of eq. (3.53) under the conditions (3.52) and (3.54). The variational problem presented here is a particular case of a more general problem, known as the problem of

Bolza (ref.20). This problem can be solved by applying the method of multipliers, a method given in essence by Lagrange. To do so, the following expression has to be considered

$$F=\left\{\frac{1}{\gamma M_\infty^2}\left[1-(a^2M_\infty^2)^{\frac{\gamma}{\gamma-1}}\right]-(u-1)(a^2M_\infty^2)^{\frac{1}{\gamma-1}}\frac{q^2}{u-v\beta}\right\}r+\lambda(a^2M_\infty^2)^{\frac{1}{\gamma-1}}\frac{q^2r}{u-v\beta}+$$

$$+\mu(r)\left\{(\beta u-v)\frac{du}{dr}+(u+\beta v)\frac{dv}{dr}+\frac{v}{r}\frac{q^2}{u-\beta v}\right\} \tag{3.55}$$

where λ and μ are the multipliers. The essential difference between the two multipliers is that λ is a constant, while μ is a function of r. This difference is caused by the fact that λ is the multiplier of an integrand, while μ is the multiplier of a relation that has to be satisfied in every point of the interval considered.

The necessary conditions for a minimum are found by considering the variation of the integral over the function F and to require that this variation is zero, or

$$\delta\int_{R_B}^{R_C}F(r,u,v,\frac{du}{dr},\frac{dv}{dr},\mu,\lambda)\,dr=0 \tag{3.56}$$

If the variations of u and v are denoted by ρ and η and differentiations with respect to r are indicated by a prime these equations can be written as

$$\int_{R_B}^{R_C}\left\{\frac{\partial F}{\partial u}\rho+\frac{\partial F}{\partial v}\eta+\frac{\partial F}{\partial u'}\rho'+\frac{\partial F}{\partial v'}\eta'\right\}dr=0\quad. \tag{3.57}$$

Partial integration then gives

$$\int_{R_B}^{R_C}\left[\rho\left\{\frac{\partial F}{\partial u}-\frac{d}{dr}\left(\frac{\partial F}{\partial u'}\right)\right\}+\eta\left\{\frac{\partial F}{\partial v}-\frac{d}{dr}\left(\frac{\partial F}{\partial v'}\right)\right\}\right]dr+\rho\frac{\partial F}{\partial u'}\Big/_{R_B}^{R_C}+\eta\frac{\partial F}{\partial v'}\Big/_{R_B}^{R_C}=0 \tag{3.58}$$

Since ρ and η are arbitrary along the characteristic surface, the integrand has to be identically zero. This gives rise to a system of differential equations, known as Euler's equations, viz.:

$$\frac{d}{dr}\left(\frac{\partial F}{\partial u'}\right) - \frac{\partial F}{\partial u} = 0 \tag{3.59a}$$

$$\frac{d}{dr}\left(\frac{\partial F}{\partial v'}\right) - \frac{\partial F}{\partial v} = 0 \quad . \tag{3.59b}$$

According to equation (3.58) the boundary conditions required by the variational problem are

$$\rho \frac{\partial F}{\partial u'} + \eta \frac{\partial F}{\partial v'} = 0 \qquad \text{in } r = R_B \text{ and } r = R_c \tag{3.60}$$

Performing the operations indicated in eqs. (3.59) the following result is found

$$r \frac{\partial(A+\lambda B)}{\partial u} + \mu\left\{2v' + \frac{1}{r}\frac{\partial}{\partial u}(v\alpha_2)\right\} = (u\beta - v)\frac{d\mu}{dr} \tag{3.61)a}$$

$$r \frac{\partial(A+\lambda B)}{\partial v} + \mu\left\{-2u' + \frac{1}{r}\frac{\partial}{\partial v}(v\alpha_2)\right\} = (u+\beta v)\frac{d\mu}{dr} \tag{3.61)b}$$

The quantities A and B are given by

$$A = \frac{1}{\gamma M_\infty^2}\left[1-\alpha_1^{\gamma}\right] - (u-1)\alpha_1\alpha_2 \tag{3.62)a}$$

$$B = \alpha_1\alpha_2 \tag{3.62)b}$$

where $\alpha_1 = (a^2M_\infty^2)^{\frac{1}{\gamma-1}}$ (3.63)a

and $\alpha_2 = \frac{q^2}{u-v\beta}$ (3.63)b

By using the following operations the system of differential equations (3.61) can be brought in a more convenient form.

Multiplying eq. (3.61)a by u' and eq. (3.61)b by v' and adding the result together, the following equation can be derived by using the characteristic equation (3.54)

$$r \frac{d}{dr}(A+\lambda B) + \frac{1}{r}\frac{d}{dr}(\mu v\alpha_2) = 0 \tag{3.64}$$

The second relation can be derived by multiplying eq. (3.61)a by $(u+v\beta)$ and (3.61)b by $(u\beta-v)$ and subtracting the results. By using the characteristic equation (3.54) one obtains

$$\alpha_1\left[-2\beta v-(u-1-\lambda)\left\{(1-\beta^2)-\alpha_2\left[\frac{u\beta a^2-vb}{\beta a^4}\right]\right\}\right]+\mu\,\frac{\alpha_2}{r^2}\;\frac{v^2b-\beta^2a^4}{\beta a^4}=0 \qquad (3.65)$$

where $\quad b=\dfrac{1}{M_\infty^2}+\dfrac{\gamma-1}{2}$.

It is important to remark, that eq. (3.65) is not a differential equation, but a functional relation between the unknown functions u, v and μ. This peculiar feature of the system makes it possible to eliminate the multiplier function μ, which in itself is not interesting. This elimination gives rise to the following result.

$$\left[uZ+\beta^2a^4\left\{-u-\beta v+(u-1-\lambda)\right\}\right]\frac{du}{dr}+\left[vZ+\beta^2a^4\left\{4v-\beta(u-1-\lambda)-2vb\,\frac{X}{Y}\right\}\right]\frac{dv}{dr}+$$

$$-2\,\frac{v}{r}\,\beta a^4\left[-2\beta v-(u-1-\lambda)\left\{(1-\beta^2)-\alpha_2\left[\frac{u\beta a^2-vb}{\beta a^4}\right]\right\}\right]=0 \qquad (3.66)$$

In this equation the quantities X, Y and Z are given by

$$X=2v^2+(u-1-\lambda)(u-\beta v) \qquad (3.67)a$$

$$Y=v^2b-\beta^2a^4 \qquad (3.67)b$$

$$Z=Y+a^2\,\frac{X}{Y}\left\{v^2b(\gamma+1-\gamma\beta^2)+\beta^4a^4\right\}-(u-1-\lambda)\beta vb \qquad (3.67)c$$

The system of equations (3.54) and (3.66) is a set of non-linear first order differential equations for the functions u and v. Such a system has a unique solution if two boundary conditions are given, and λ is a given quantity.

In order to obtain the boundary conditions, first the rim of the base $r=R_B$ will be considered. As has been said already no physical condition is present there. This means that the variations ρ and η are arbitrary.

From eq. (3.60) there follows then

$$\frac{\partial F}{\partial u'}=\frac{\partial F}{\partial v'}=0 \qquad \text{for } r=R_B \qquad (3.68)$$

These equations are satisfied by the condition $\mu(R_B)=0$, which according to eq. (3.65) gives rise to the following boundary condition

$$-2\beta v-(u-1-\lambda)\left\{(1-\beta^2)-\alpha_2\left[\frac{u\beta a^2-vb}{\beta a^4}\right]\right\}=0 \qquad (3.69)$$

Since only two boundary conditions are permitted, at the point $r = R_c$ only one boundary condition can be present if a solution exists. In the first place this condition has to satisfy the natural boundary condition given by eq. (3.60); on the other hand it also has to be such that a physically realizable transformation from the undisturbed to the disturbed flow is presented.

The condition (3.60) is given by

$$(\beta u-v)\rho + (\beta v+u)\eta = 0 \quad . \qquad (3.70)$$

To find the function $G(u,v) = 0$ which satisfies this equation, the differential equation synonymous with eq. (3.70) has to be considered. This equation is

$$(\beta u-v)\,du + (\beta v+u)dv = 0 \quad . \qquad (3.71)$$

But this equation is the well-known differential equation of two-dimensional theory, for the Prandtl-Meyer compression fan. This relation between u and v is given by

$$\sqrt{\frac{\gamma+1}{\gamma-1}}\ \tan^{-1}\frac{\sqrt{\frac{\gamma-1}{\gamma+1}}\,(\beta-\beta_\infty)}{1+\frac{\gamma-1}{\gamma+1}\,\beta\,\beta_\infty} - \tan^{-1}\frac{\beta-\beta_\infty}{1+\beta\ \beta_\infty} + \tan^{-1}\frac{v}{u} = 0 \quad . \qquad (3.72)$$

This result can be interpreted as follows. To satisfy eq. (3.70) at the point $r = R_c$, the relation (3.72) has to be valid. This point is thus the place where a compression generated by the nose of the body converges. From this point on a shock wave will be formed in the outer flow field, giving the rise of entropy which is responsible for the wave drag.

However, it should be remarked that the flow conditions at the point $r = R_c$, where the compression fan converges and the shock wave starts, are in general such, that a reflection occurs, satisfying the relations of equal pressure and slope at this point. This reflection is either a shock wave or an expansion fan (see fig.15). The strength of this reflection is always very much smaller than that of the outgoing shock wave. In the case that this reflection is an expansion fan, the aft characteristic is the first characteristic of this fan and thus, according to the assumptions, the flow inside the control surface is isentropic. As calculations have shown, this situation occurs, roughly speaking, above a Mach number $M_\infty = 2.3$. Below this number, the reflection is a shock wave penetrating into the region inside the control surface. The theory as given here should therefore not be applicable to this case.

However, such an objection is purely theoretical, since in general the strength of this shock wave is so small, that it is actually negligible.

As a solution of the variational problem, we have found now the system of differential equations (3.54) and (3.66) together with the boundary conditions (3.69) and (3.72). Moreover the mass flow equation (3.52) has to be satisfied.

This is a set of three equations for the unknown functions u and v and the unknown multiplier λ . As will be shown in the following section, it is possible to solve this system by numerical methods.

3.2.3 Determination of the optimum velocity distribution.

It will be clear at first sight that it is not possible to find easily an analytical solution of the differential equations (3.54) and (3.66). It would be possible to integrate the differential equations numerically by a variety of methods if both the quantity λ and the velocities u and v either at $r = R_c$ or $r = R_B$ were given. But here, one condition is given in $r = R_B$ and another one in $r = R_c$, whilst λ is unknown and must be determined by using the mass flow relation (3.52). For given values of $r = R_B$, $r = R_c$ and M_∞ this problem can only be solved by a double iteration. This can be done by the following method.

At the point $r = R_B$ the values of λ and u are chosen arbitrary. With the aid of equation (3.69) the velocity v can now be calculated. As has been remarked above, it is possible then to integrate the differential equations, thus determining the values of u and v as a function of r. In general, the values found in this way at the point

$r = R_c$ will not satisfy eq. (3.72), while moreover also both sides of the mass flow equation will not be equal.

By keeping the value of λ constant an iteration with respect to u is performed such that finally the boundary condition at the point $r = R_c$ is satisfied.

However, a further value of λ has to be determined for which the mass flow relation is an identity. This can be done by performing the above explained iteration with respect to u for different values of λ and then to perform an iteration with respect to λ. It is clear that this is a very complex programme, even when using a digital computer. Therefore a different approach was used, where only one iteration step was necessary, thus reducing the computer time by an order of magnitude.

This has been achieved by not prescribing the value of R_c, but by determining this quantity from computations.

In this approach, the values of u and λ at $r = R_B$ are chosen, just as before. However, now the solution is continued until eq. (3.72) is satisfied. The value of r for which this occurs can be considered as a value for $r = R_c$. By using the mass flow relation an iteration with respect to λ can be performed, until a solution is obtained which satisfies all the equations.

This scheme for the solution proved to be very satisfactory. The actual integration of the differential equations was performed by using the version of Gill (ref.21) of the Runge-Kutta method. To save computation time, the iteration with respect to λ was performed, by using first a large step Δr and, if λ was already sufficiently close approximated, by choosing the final step width. To start the computations an estimate of the values of u and λ, necessary for a certain R_c, can be obtained by using the linearized theory of ref.17.

The computations were performed on the medium sized digital computer Z.E.B.R.A.

As soon as the velocity distribution is found, it is possible to calculate, the hitherto unknown shape of the characteristic surface by using eq. (3.51). The total length of the body is then given by

$$\ell = \beta_\infty R_c + \int_{R_B}^{R_c} \frac{v+u\beta}{u-v\beta}\, dr \qquad (3.73)$$

The optimum velocity distribution has been calculated for several Mach numbers, for a given value of R_B. The attempt has been to obtain body lengths that were not too different. In the tables 5 a–c the quantities u and v have been given together with the shape of the aft characteristic surface for the Mach numbers $M_\infty = 2.5$, 3.5 and 4.5. In addition the values of R_B, R_c and the length ℓ of the body are given.

In the figs 16 a–c the results of a comparison of the present theory with the linearized theory of ref.1 has been given. This theory is based on the first order relations for mass flow and drag as derived in section 3.1.1.

It will be seen that even for the very slender bodies considered, the differences are significant and are rapidly growing with increasing Mach number. However, as will be clear, the importance of the method as given here, consists in the fact, that it enables the calculation of the optimum conditions in those cases where the linearized theory fails to give reliable results. As has been shown, this is the case for non-slender bodies and higher Mach numbers.

After the determination of the aft characteristic surface and the velocity distribution along it the problem of calculating the shape of the optimum body has to be solved. This will be prescribed in the following section.

3.2.4 Determination of the optimum shape.

The actual shape of the optimum body can be determined by calculating the flow field inside the control surface.

The body itself is given by the differential equation

$$\frac{dr}{dx} = \frac{v}{u} \qquad (3.74)$$

with the boundary conditions

$$r = 0 \qquad \text{for } x = 0 \qquad (3.75)\text{a}$$

and

$$r = R_c \qquad \text{for } x = \ell \qquad (3.75)\text{b}$$

One of these conditions is sufficient to determine the contour, but the other has to be satisfied because of the relation for the mass flow.

Since the flow is isentropic, there is no shock wave present inside the control surface. This means that the backward characteristic surface from the nose of the body to the point of convergence of the compression fan is a simple circular Mach cone, along which the disturbance velocities are zero. This fact has already been used in deriving eq. (3.73). Thus, the field between two characteristic surfaces has to be found. This is a so-called problem of Gourçat. It must be remembered, however, that the point R_c is a multivalued point for the velocity and that a fan of characteristics converges here. Therefore, first the compression fan will be calculated by using the system of characteristic equations (3.45). Since along the first characteristic $u = 1$ and $v = 0$, according to eq. (3.74), the slope of the contour at the nose is equal to zero.

This gives rise to the occurrence of a cusped nose. The construction of such a nose can cause large difficulties due to the singular behaviour of the functions u and v for r approaching the axis. By observing that the cusped nose has to be parabolic over some distance and by choosing a suitable mesh length, these difficulties can be removed. As soon as the compression fan has been calculated, the construction of the field between the last characteristic of this fan and the aft characteristic is an ordinary problem of Gourçat and can be performed by standard routine.

The results of the computations made for $M_\infty = 2.5$ and $M_\infty = 4.5$ have been given in figs 17 a-b together with the slope of the contour $\frac{dr}{dx}$. The pressure coefficient which is given by

$$c_p = \frac{2}{\gamma M_\infty^2}\left\{(a^2 M_\infty^2)^{\frac{\gamma}{\gamma-1}} - 1\right\} \tag{3.76}$$

and the distribution of the axial force $\frac{\ell}{\frac{1}{2}\rho_\infty U_\infty^2 \pi R_B^2} \frac{dD_o}{dx}$,

$$\text{where} \quad \frac{dD_o}{dx} = 2\pi c_p r \frac{dr}{dx}, \tag{3.77}$$

have been given in figs. 18 a-b.

A check on the numerical accuracy of the results is provided by the radius of the base area as found by determining the body contour, and by a comparison of the drag as found by integrating $\frac{dD_o}{dx}$ along the fuselage and the prescribed minimum drag. The results obtained indicate that the differences are of the order of one percent, showing that the accuracy of the calculations is quite satisfactory.

In conclusion a few words will be said about the differences between the overall results of the method prescribed here and the results of the linearized theory. One very remarkable point is the cusped nose, which is in sharp contrast with the nose shape found with linearized theories, where $\frac{dr}{dx} \rightarrow \infty$ for $x \rightarrow 0$.

For low Mach numbers this cusped nose is only a very small part of the fuselage length, but for higher Mach numbers the length of this cusped nose grows rapidly. Since apparently the largest differences occur at the nose, this leads to the following result.

If the shapes are slender and the Mach number is low the differences at the nose are not able to influence the overall result very much and the results of linearized theory will compare reasonably with those of the present theory over most of the body length.

However, for less slender shapes and higher Mach numbers the results will show rapidly increasing differences making linearized theory a tool of very limited value. These general observations are fully in accordance with all the results already found.

4 Studies on quasi axially-symmetric flow.

Since one of the main interests to the aerodynamicist is the study of the lifting properties of flight-vehicles it is not surprising that there are many methods devised for making such studies. This is especially true for the subsonic regime, where a variety of theories exists for calculating the lift distribution on a wing. All these methods are based on the linearized theory, which gives good results as long as the Mach number is not too near to unity. The influence of the body on the lift is due to its interference with the wing, a body alone not giving a net lift.

This situation is radically changed if the body, which is for instance axially-symmetric, is moving faster than the speed of sound. It then can develop lift, provided its axis is curved or not aligned with the direction of motion. Thus the study of the lifting properties of such bodies can have some merits on its own.

Rather early, some research in this direction was made, especially with respect to the motion of ballistic projectiles. In 1938, Tsien published a method to calculate the supersonic flow over an inclined body of revolution (ref.22). This method, which is in fact a generalization of the treatment given by Kármán and Moore, is based on the assumption of small disturbances and thus use can be made of the linearized potential flow equation. As in the case of purely axially-symmetric flow, this linearized theory can be expected to be valid only if the Mach-number is not much greater than unity and if the body is sufficiently slender.

In the first part of this chapter therefore a method will be given to obtain quantitative results on the limits of the applicability of the linearized theory for the calculation of the flow-field around inclined bodies. It appears also that for the field determined in this way, the same conclusions are valid reached in the foregoing chapter. However, in this case there is no opportunity to obtain more exact results. Only for the cone a theory has been given for calculating, by a perturbation method applied to the axially-symmetric flow field, the flow field due to inclination of the axis, correct up to the first (and second) order of the angle of incidence. The results on the validity of linearized theory for more general body shapes indicate that it would be worthwhile to devise such a more exact method for general quasi axially-symmetric shapes. The second part of this chapter is devoted therefore to the presentation and discussion of such a method.

4.1 On the validity of linearized theory for quasi axially-symmetric flow.

As a corollary to the study of the validity of the linearized theory for axially-symmetric flow, a treatment will be given here, aimed at giving a quantitative value of the error made, when using the linearized theory for the determination of the flow field around an inclined body of revolution. Also in this case, the motive for the investigation was given by the striking differences between the prescribed value of the lift and the lift as found by integrating the pressure along the fuselage when constructing an optimum body for a given lift. It will be clear, that the comparison between the lift as integrated along the body and as determined by a control surface approach, is the most simple and effective method to measure the validity of the theory. Although in principle a second comparison coud have been obtained by considering the induced drag, no use of this quantity has been made here.

Also, very much attention has been paid here to the consideration of the flow around an inclined cone. Due to the fact that more exact solutions are also known a detailed comparison has been possible. It will be shown by using the subsequently derived integral expression for the lift, that the first-order solution of Stone is a formally fully consistent method for constructing these more exact solutions; a fact which will be of much importance for the second part of this chapter.

4.1.1 Integral expression for the lift as found by using linearized theory.

In this section the same body will be considered as in section 3.1.1. It will be assumed now, however, that there is a small cross-flow component of the velocity εU_∞ where ε is small compared with unity. This means, that in fact a body with an angle of attack ε is considered. The lift on this body can be determined by using the same control surface as before and considering the momentum transport in the z-direction.

If the lift L is the force perpendicular to the axis of the body, the following relation is obtained:

$$L + \iint_{O_1} p_1' \cos\mu \cos\psi \, dO_1 + \iint_{O_1} \rho_1 V_{n_1} W_1 dO_1 + \iint_{O_2} p_2 \cos\mu \cos\psi \, dO_2 +$$

$$+ \iint_{O_2} \rho_2 V_{n_2} W_2 dO_2 = 0 \tag{4.1}$$

where W_1 and W_2 are the velocity components in z-direction and the angle μ, being the semi-top angle of the characteristic cone is given by

$$\sin\mu = \frac{1}{M_\infty} \tag{4.2}$$

The velocities in the field of an inclined body can be given as

$$u = U_\infty \left\{ 1 + u' + \varepsilon\, u'' \cos\psi \right\} \tag{4.3a}$$

$$v = U_\infty \left\{ v' + \varepsilon\, v'' \cos\psi \right\} \tag{4.3b}$$

$$w = U_\infty \varepsilon\, w'' \sin\psi \tag{4.3c}$$

The functions u", v" and w" here are the amplitude of the cross flow disturbance velocities. The occurrence of the trigonometrical functions $\cos\psi$ and $\sin\psi$ is required by the boundary condition on the body.

Using eqs. (4.3) the following relations can be derived:

$$\frac{V_{n_1}}{U_\infty} = -\sin\mu + \varepsilon\,\beta_\infty \sin\mu\cos\psi \tag{4.4a}$$

$$\frac{W_1}{U_\infty} = \varepsilon \tag{4.4b}$$

$$\frac{V_{n_2}}{U_\infty} = (1+u'+\varepsilon u''\cos\psi)\sin\mu+\beta_\infty(v'+\varepsilon v''\cos\psi)\sin\mu \tag{4.4c}$$

$$\frac{W_2}{U_\infty} = (v'+\varepsilon v''\cos\psi)\cos\psi - \varepsilon w''\sin^2\psi \tag{4.4d}$$

The pressure and the density follow by a Taylor expansion of eqs.(3.5) and (3.6). (See also eq.(3.9) and eq. (3.18)).
It is found that

$$\rho_2 = \rho_\infty\left\{1-M_\infty^2(u'+\varepsilon u''\cos\psi)\right\} \tag{4.5a}$$

$$p_2-p_\infty = -\rho_\infty U_\infty^2\left[(1+u'+\varepsilon u''\cos\psi)-\frac{1}{2}\beta_\infty^2(1+u'+\varepsilon u''\cos\psi)^2 + \right. \\ \left. +\frac{1}{2}(v'+\varepsilon v''\cos\psi)^2+\frac{1}{2}\varepsilon^2 w''^2\cos^2\psi\right] \tag{4.5b}$$

where again quadratic terms are retained in the pressure.

Substituting the equations (4.4) and (4.5) into the expression for the lift L and performing the integration with respect to ψ the following is obtained:

$$\frac{L}{\rho_\infty U_\infty^2\pi\varepsilon} = \int_{R_B}^{R_c}\beta_\infty\left\{u''-\beta_\infty^2 u'u''+v'v''\right\}rdr + \\ + 2\int_{R_B}^{R_c}\left\{1-\beta_\infty^2 u'+\beta_\infty v'-M_\infty^2 u'^2-\beta_\infty M_\infty^2 u'v'\right\}rdr + \\ \int_{R_B}^{R_c}\left\{v''-w''-\beta_\infty^2 v'u''-\beta_\infty^2 u'v''+2\beta_\infty v'v''+\beta_\infty^2 u'w''-\beta_\infty v'w''\right\}rdr \tag{4.6}$$

Since u' and v' are considered small quantities, the terms $M_\infty^2 u'^2$ and $\beta_\infty M_\infty^2 u'v'$ can be neglected compared with unity. It should be observed that thus only terms of the order ε and $\varepsilon\delta$ are retained where δ is of the order of the axially-symmetric perturbation velocities. Quantities of the order ε^2 do not occur. By rearranging the terms, the following result is obtained:

$$\frac{L}{\rho_\infty U_\infty^2} = \pi\varepsilon \int_{R_B}^{R_C} \left\{\beta_\infty u''-v''+w''+2\right\}\left\{1-\beta_\infty^2 u'+\beta_\infty v'\right\} r dr \tag{4.7}$$

In this expression, a certain coupling between the thickness field and the lift field is present. However, in the linearized theory, the lift field is considered as a perturbation of the undisturbed free stream. This means that the disturbance velocities u' and v' vanish in this case. Equation (4.7) takes then the following form :

$$\frac{L}{\rho_\infty U_\infty^2} = \pi\varepsilon \int_{R_B}^{R_C} \left\{ \beta_\infty u''-v''+w''+2 \right\} r dr \tag{4.8}$$

By using eqs. (4.7) or (4.8) the lift can be calculated by an independent method, giving the opportunity of checking the consistency of the linearized theory after calculation of the flow field. In the following sections these expressions will be used therefore to study the applicability of this theory.

4.1.2 Linearized theory for an inclined cone.

Consider the flow around a cone which has a small cross-flow component εU_∞. If ε is sufficiently small, the configuration sufficiently slender and the Mach-number sufficiently low, then the linearized theory can be applied. However, it is very important to know what is meant by sufficiently. The investigation of the answer to this question will form the subject of this section.

The differential equation, which has to be satisfied, has already been given several times, viz. eqs. (2.57) and (3.20). For the sake of completeness it will be repeated here once more

$$-\beta_\infty^2 \varphi_{xx} + \varphi_{rr} + \frac{1}{r}\varphi_r + \frac{1}{r^2}\varphi_{\psi\psi} = 0 \tag{4.9}$$

As has already been remarked, the perturbation due to the inclination is considered as based on an undisturbed free stream. According to the remarks made when introducing the eqs. (4.3) the potential for the cross flow can be written as

$$\varphi = \bar{\varphi} \cos\psi \tag{4.10}$$

The amplitudes u", v", w" of the disturbance velocities are then given by

$$u'' = \frac{\partial\bar{\varphi}}{\partial x} \qquad (4.11)a$$

$$v'' = \frac{\partial\bar{\varphi}}{\partial r} \qquad (4.11)b$$

$$w'' = \frac{1}{r}\frac{\partial\bar{\varphi}}{\partial\psi} \qquad (4.11)c$$

Since the flow is conical these quantities are constant along rays through the vertex of the cone.

Introduce therefore, as before

$$t = \frac{x}{r} \qquad (4.12)a$$

and

$$\bar{\varphi} = rF(t) \qquad (4.12)b$$

On substituting the expressions (4.10) and (4.12) into eq. (4.9) there is obtained the following differential equation for the function F(t):

$$(t^2-\beta_\infty^2)\frac{d^2F}{dt^2} - t\frac{dF}{dt} = 0 \tag{4.13}$$

while the disturbance velocities are given by

$$u'' = \frac{dF}{dt} \qquad (4.14)a$$

$$v'' = -t\frac{dF}{dt} + F \qquad (4.14)b$$

$$w'' = \qquad - F \qquad (4.14)c$$

The boundary condition on the surface, viz. $\vartheta = \vartheta_s$, is given by

$$v'' = u'' \frac{dr}{dx} = \frac{u''}{t_o} \tag{4.15}$$

The boundary conditions on the Mach-cone through the vertex of the cone, i.e. $t = \beta_\infty$ are given by

$$v'' = -w'' = 1 \tag{4.16}$$

The solution of eq. (4.13) can be written as

$$F = \frac{Ct\sqrt{t^2-\beta_\infty^2}}{2} - \frac{C\beta_\infty^2}{2}\cosh^{-1}\frac{t_o}{\beta_\infty} + D \tag{4.17}$$

Application of eq. (4.16) gives

$$D = 1 \tag{4.18a}$$

and of eq. (4.15)

$$C = \frac{1}{\frac{\sqrt{t_o^2-\beta_\infty^2}}{t_o} + \frac{1}{2}t_o\sqrt{t_o^2-\beta_\infty^2} + \frac{1}{2}\beta_\infty^2\cosh^{-1}\frac{t_o}{\beta_\infty}} \tag{4.18b}$$

while u'', v'' and w'' are given by

$$u'' = C\sqrt{t^2-\beta_\infty^2} \tag{4.19a}$$

$$v'' = -\frac{1}{2}Ct\sqrt{t^2-\beta_\infty^2} - \frac{1}{2}C\beta_\infty\cosh^{-1}\frac{t_o}{\beta_\infty} + 1 \tag{4.19b}$$

$$w'' = -\frac{1}{2}Ct\sqrt{t^2-\beta_\infty^2} - \frac{1}{2}C\beta_\infty^2\cosh^{-1}\frac{t_o}{\beta_\infty} - 1 \tag{4.19c}$$

In order to obtain quantitative limits of applicability of the above equations use will be made of eq. (4.8). According to eq. (4.5)b, the pressure coefficient can be given by

$$c_p = c_{p_o} + c_p'' \cos\psi \tag{4.20a}$$

where

$$c_p'' = 2\varepsilon\left\{-u'' + \beta_\infty^2 u'u'' - v'v''\right\} \tag{4.20b}$$

However, since the cross-coupling between the thickness- and the lift field is neglected, the last two terms in eq. (4.20)b have to be omitted. The lift on a cone with length ℓ is then given by

$$L = -\frac{1}{2}\int_0^{2\pi}\int_0^{\frac{\ell}{t_o}} c_p'' \cos^2\phi \; r \frac{dx}{dr}\, dr\, d\phi = \frac{\pi\varepsilon}{2} c \ell^2 \sqrt{1-\left(\frac{\beta_\infty}{t_o}\right)^2}\, \rho_\infty U_\infty^2 \qquad (4.21)$$

If now the quantities u", v" and w" are substituted into eq. (4.8) and the integration is performed, the result is

$$L = \pi\varepsilon\, \rho_\infty U_\infty^2\, c \left\{ \frac{1}{2}\ell^2 \sqrt{1-\left(\frac{\beta_\infty}{t_o}\right)^2} - \frac{1}{2}\left(\frac{\ell}{t_o}\right)^2 \beta_\infty^2 \cosh^{-1}\frac{t_o}{\beta_\infty} \right\} \qquad (4.22)$$

Comparison of the eqs. (4.22) and (4.21) shows that the lift as calculated by integrating the pressure along the fuselage, is higher than the lift calculated by using the integral expression along a characteristic. What now is the conclusion which can be drawn from this part?

If the difference between the two expressions is small, it could be concluded that either the average error in the integrands of the expressions (4.21) and (4.8) is the same or that there are no errors in the integrands; if, however, a deviation is present the conclusion must be that the error in the field quantities is greater or smaller than those in the pressure distribution along the fuselage. If this deviation is large the theory used is inconsistent and thus not valid.

The question which now has to be answered is : Can linearized theory be considered to be valid if the deviation is very small? From the eqs. (4.21) and (4.22) follows that the deviation is small if $\frac{t_o}{\beta_\infty}$ is large. This is true if t_o is large or β_∞ is small. The first case means that the cone is very slender and certainly linearized theory should be applicable in that case. The latter case means that the Mach-number is very near to one, it should then be permissible to have far less slender cones. This possibility will be considered further on. First the deviation between the two expressions will be discussed.

If a deviation of χ percent is thought to be permissible, it can be derived that

$$\frac{t_o}{\beta_\infty} < \cosh\left\{\frac{K}{100}\left(\frac{t_o}{\beta_\infty}\right)^2\sqrt{1-\left(\frac{\beta_\infty}{t_o}\right)^2}\right\} \qquad (4.23)$$

If $\quad K \leqslant 5 \qquad \frac{\beta_\infty}{t_o} = \leqslant 0.135$

and $\quad K \leqslant 10 \qquad \frac{\beta_\infty}{t_o} \leqslant 0.21$.

The limit lines are given in fig.19. By comparison with fig.4 it can be seen that for higher Mach-numbers the curves coincide, showing that the limits of applicability are the same for axially-symmetric flow and the flow with a small cross component. It is interesting to remark that the treatment given in section 3.1.2 leads to eq. (4.23) if use had been made of the linearized boundary condition

$$v' = \frac{dr}{dx} \qquad (4.24)$$

Apparently the use of the exact boundary condition leads to the restriction in the vicinity of $M_\infty = 1$.

In this case, however, it seems that linearized theory is able to describe the flow around an inclined cone very well for M_∞ very near to one. However, in the derivation it has been assumed that the cross coupling between the thickness field and the cross flow field is negligible. Thus the results obtained have a meaning only if K as derived from eq. (4.23), is small, and also at the same time the perturbation velocities of the thickness field are very small compared with the free stream velocity U_∞ .

Now it is obvious that this is fulfilled for very slender cones. An idea about the influence of the cross coupling can then be obtained by using eq. (4.7) instead of eq. (4.8). It turns out, though not more than the order of magnitude of the influence is given, that this can be quite large even for very small values of K. This means that for not so slender cones the influence of the thickness field will be quite large. Thus very near to the Mach number unity the results of eq. (4.23), which indicate that $\vartheta_s \rightarrow \frac{\pi}{2}$ without making a large error, are invalidated by the fact that no account had been taken of this cross coupling.

The conclusions reached here can be summarized as follows. In order to calculate the flow field around a cone at an angle of attack, linearized theory can be used only for very slender cones. For higher Mach-numbers ($M_\infty > 2$) the situation is the same as for the axially-symmetric case. For $M_\infty < 2$ the requirements on ϑ_s are strongly dependent on the Mach-number, due to the influence of the cross coupling of the flow fields.

The conclusions given above are independent of the value of ε. Besides the requirements given here for the applicability of linearized theory, it is necessary that $\varepsilon u''$, $\varepsilon v''$ and $\varepsilon w''$ are small against unity.

4.1.3 Linearized theory for the flow around an inclined body.

As it has been done in the case of axially-symmetric flow, here too a study will be made of the flow around an axially-symmetric body at an angle of attack to see if the conclusions reached in the foregoing section have to be changed.

In the first place the lift generated by a body with a parabolic shape has been investigated along several lines. The shape is given by

$$r = 0.22182\,x - 0.19471\,x^2 \qquad o \leq x \leq 1 \qquad (4.25)$$

With the aid of the linearized method of characteristics (ref. 23) the flow field has been calculated for $M_\infty = 2.476$. Thereafter the lift has been calculated by using eq. (4.7) and eq. (4.8), thus using momentum flow considerations, and by integrating the pressure distribution along the fuselage using eq. (4.20) and its more usual form

$$c_p'' = -2\,\varepsilon u'' \qquad (4.26)$$

As it has been already observed the use of the eqs. (4.7) and (4.20) is in fact not in accordance with the assumptions of the linearized theory for cross flow, but on the other hand should these assumptions be valid, no large differences between the results of eqs. (4.7) and (4.8) and (4.20) and (4.26) should be present. The four curves for the lift are given in fig.20. The results indicate that the influence of the axially-symmetric flow field is so large, that it apparently cannot be neglected. However, this leads to the conclusion that a theory based on the linearized equation (4.9) is unable to describe the flow field for this particular case. Thus not one of the curves presented has a quantitative meaning. At the most they indicate the order of magnitude of the lift generated.

Also an investigation has been made of the flow field around the two bodies already considered in section 3.1.3. The lift has been calculated by using eq. (4.8) for the momentum flow approach, while eq. (4.26) has been used for the integration of the lift along the fuselage. The results have been given in figs. 21.a-b.

The theory is, according to the results given here, rather accurate for the case $\vartheta_s = 7.5^\circ$ and $M_\infty = 2$, while for $\vartheta_s = 12.5^\circ$ and $M_\infty = 2$ the results seem to have a quantitative value.

For $\vartheta_s = 7.5^\circ$ and $M_\infty = 5$ and $\vartheta_s = 12.5^\circ$, $M_\infty = 4$ only the order of magnitude of the lift is indicated by the results.

In general therefore the conclusion has to be the same as for the axially-symmetric case.

If linearized theory is used to predict the flow field around an axially-symmetric configuration under incidence, the results have only a quantitative value if the shape is very slender and the Mach number low. The average error to be expected can be predicted by using the methods given here, together with the results obtained for the purely axially-symmetric case.

It is a pity that these results cannot be substantiated in the same way as in the case of the axially-symmetric flow by a direct comparison with exact results. Only for the cone such a treatment has been given by considering the cross flow field as a perturbation on the exact thickness field. This theory will be discussed in the next section.

4.1.4 The first order theory of Stone for the flow around an inclined cone.

If a more reliable solution of the flow around an inclined cone is wanted, we must resort to a more exact treatment of the governing differential equations. Stone (ref.8) has given a method to calculate the flow field around a cone at an angle of attack ε, where ε is small. In ref. 24 he extends his method by taking account of the square of ε. In fact he thus has tried to calculate the quantities $\frac{dc_\ell}{d\varepsilon}$ and $\frac{d^2c_\ell}{d\varepsilon^2}$ for $\varepsilon \to 0$, where c_ℓ is the lift coefficient. The first order theory of ref. 8 will be treated here for several reasons.

First, it offers the possibility of obtaining a direct comparison with the results of the foregoing sections, while by the application of the control surface approach which is now well known several interesting results can be obtained. On the other hand the description of the method will give an easy access to the contents of the second part of this chapter, where this first order theory is generalized for more general configurations. The second order theory will not be treated. Its mathematical correctness is questionable, at least at the surface of the cone and moreover it is a very complex theory, which does not give much hope to extend it to the determination of the flow field around more general configurations.

The following analysis presents only the formula which are appropriate for the above mentioned investigations. For the details of the method and the derivation of the equations used, the reader is referred to the papers by Stone, refs. 8 and 24.

Introducing a spherical coordinate system r, ϑ and ψ as given in fig.22, the equation of a cone inclined at an angle ε with respect to the main flow direction is given by

$$r \cos \vartheta \cos \varepsilon - r \sin \vartheta \sin \varepsilon \cos \psi = r \cos \vartheta_s \quad (4.27)$$

It can be shown that correct up to first order terms in ε, the following expressions are valid for the velocities, the pressure and the density

$$u = \bar{u} - \varepsilon x \cos \psi \quad (4.28)a$$

$$v = \bar{v} - \varepsilon y \cos \psi \quad (4.28)b$$

$$w = - \varepsilon z \sin \psi \quad (4.28)c$$

$$p = \bar{p} - \varepsilon \eta \cos \psi \quad (4.28)d$$

$$\rho = \bar{\rho} - \varepsilon \xi \cos \psi \quad (4.28)e$$

The dashed symbols are the quantities as calculated by the theory of Taylor and Maccoll for the axially-symmetric case. If the eqs. (4.28) are substituted into the governing aerodynamic differential equations, a system of differential equations is obtained for the quantities $x, y,$ z, ξ and η. In order to solve the system the boundary conditions have to be known. The first boundary condition is that the solid surface of the cone has to be a stream surface. Moreover certain conditions should be satisfied at the shock surface.

Correct up to the first order in ε, the body contour is given by

$$\vartheta = \vartheta_s - \varepsilon \cos\psi \tag{4.29a}$$

This can be checked by substitution into eq. (4.27).
The shock wave surface can be written as

$$\vartheta = \vartheta_w - \varepsilon\alpha \cos\psi \tag{4.29b}$$

where α is an unknown constant, which has to be determined.

Stone now solves the problem by transforming the boundary conditions along the cone surface and along the shock wave to conditions along $\vartheta = \vartheta_s$ and $\vartheta = \vartheta_w$ respectively. In fact he thus transforms the problem to one for the same domain as in the axially-symmetric case. It is in this transformed field that the equations (4.28) are considered to be valid.

This transformation is based on the following formulae, which are given in ref. 24

$$\vartheta = \theta - \varepsilon \cos\phi + \frac{1}{2}\varepsilon^2 \cot\theta \sin^2\phi + \dots\dots \tag{4.30a}$$

$$\psi = \phi + \varepsilon \cot\theta \sin\phi + \frac{1}{2}\varepsilon^2 \sin\phi \cos\phi\,(2\cot^2\theta + 1) + \dots\dots \tag{4.30b}$$

where θ and ϕ are spherical coordinates referred to the axis of the body. The equations apply for the case of the transformation of the boundary conditions on the fuselage. Only the terms in ε are actually taken into account.

One very important remark should be made, however, regarding the eqs. (4.30). Apparently the transformation is based on the fact that ε is small and that the squares of ε can be neglected therefore, but in order that this be true the defining parameter $\varepsilon \cot\theta$ has to be small. Since $\varepsilon \cot\theta$ is the largest on $\theta = \theta_s$, the requirement is that $\varepsilon \cot\theta_s$ is small against unity or that approximately

$$\frac{\varepsilon}{\theta_s} < 1 \tag{4.31}$$

It should be noted that in the outer flow field transformations similar to that of eq. (4.30) are more rapid convergent.

As soon as $\frac{\varepsilon}{\vartheta_s} \gtrsim 1$, the higher order terms are as important as the lower order terms and the method breaks down.

Even a second order theory along these lines is, mathematically speaking, invalid, at least in the surrounding of the cone surface. The conclusion to be drawn from these arguments is thus, that for less slender cones, i.e. having larger semi-top angles ϑ_s, higher values of ε are permissible when using this theory.

If the theory gives the correct answer for the first order term, then the lift as calculated by integrating the pressure along the cone surface, should be equal to the lift as calculated by the momentum transport through a control surface. This comparison and the derivation of the necessary expressions will be given in the following section.

4.1.5 The lift on a cone according to Stone's first order theory.

If a cone is considered at an angle of attack ε and if ζ is the direction perpendicular to the free stream velocity U_∞ (see fig.23), the force acting on the cone in the ζ-direction can be written as :

$$L + \iint_{O_1} p_\infty \cos(n,\zeta) dO_1 + \iint_{O_1} \rho_1 V_{n_1} W_1 dO_1 + \iint_{O_2} p_2 \cos(n,\zeta) dO_2 +$$

$$+ \iint_{O_2} \rho_2 V_{n_2} W_2 dO_2 - p_\infty \varepsilon \pi R_B^2 = 0 \quad . \tag{4.32}$$

The last term results from the fact that it is assumed that the free stream pressure is acting on the base of the cone.

Now, as has already been indicated, Stone transforms the problem to one which has the same domain as the axially-symmetric solution of Taylor and Maccoll. The results found are thus valid in this so called transformed flow field. However, in deriving the lift from the momentum equation the real flow field has to be used and a reverse transformation has to be applied therefore to the results of Stone.

In order to obtain the values on the true cone surface it is most convenient to use a spherical coordinate system based on the body-axis; to do the same for the real shock wave a coordinate system based on the axis of the inclined shock wave will be the natural one to choose. According to eq. (4.29)b the angle of inclination is $\delta = \alpha\varepsilon$.

The flow quantities in these local coordinate systems are obtained by using Taylor-series expansions to account for the required displacements.

The difficult question which arises now is :"What method has to be used to calculate the value of the flow quantities in a point between the cone surface and the shock wave in the real flow field? "

With the aid of fig.24 this question will be answered.

A local coordinate system is defined, the axis of which makes an angle $\lambda\varepsilon$ with the free stream direction in the vertical plane and where λ is dependent on ϑ as measured in the axially symmetric system used by Stone.

It is assumed that the flow quantities on a cone with semi-top angle ϑ, when referred to the local coordinate system of fig.24, can be correlated to the results of Stone for the same angle ϑ in the axially-symmetric system by using Taylor-series expansions. The flow quantities in the local coordinate system on this cone can be derived by establishing the relations between the velocities in the two coordinate systems, and using the transformation formula (4.30) by replacing ε by $\varepsilon\lambda$. The result is (see also ref.25)

$$u = \bar{u} - (x + \lambda\bar{u}')\varepsilon \cos \varphi_\ell \tag{4.33a}$$

$$v = \bar{v} - (y + \lambda\bar{v}')\varepsilon \cos \varphi_\ell \tag{4.33b}$$

$$w = (-z + \bar{v}\lambda \operatorname{cosec} \vartheta)\varepsilon \sin \varphi_\ell \tag{4.33c}$$

$$p = \bar{p} - (\eta + \lambda\bar{p}')\varepsilon \cos \varphi_\ell \tag{4.33d}$$

$$\rho = \bar{\rho} - (\xi + \lambda\bar{\rho}')\varepsilon \cos \varphi_\ell \tag{4.33e}$$

where a prime means differentiation with respect to ϑ . The function λ varies from α to 1, and it will be assumed that this variation is linearly dependent on ϑ as measured in the axially-symmetric system. This gives

$$\lambda = \frac{\alpha(\vartheta - \vartheta_s) + \vartheta_w - \vartheta}{\vartheta_w - \vartheta_s} \tag{4.34}$$

By using the eqs. (4.33) and (4.34) and the local coordinate system, the flow quantities at any point of the real flow field are defined.

The particular choice of control surface made to derive the force L from eq. (4.32) consists of a part of the shock wave and a sphere with radius R (see fig.24).

The quantities occurring in eq. (4.32) are given, correct up to first order terms in ε by

$$\cos(n,\mathfrak{z}) = \cos\vartheta_w \cos\varphi_\ell + \alpha\varepsilon \sin\vartheta_w \quad \text{on } O_1 \tag{4.35a}$$

$$W_1 = 0 \tag{4.35b}$$

$$\cos(n,\mathfrak{z}) = \sin\vartheta \cos\varphi_\ell - \lambda\varepsilon \cos\vartheta \quad \text{on } O_2 \tag{4.35c}$$

$$V_{n_2} = u \tag{4.35d}$$

$$\begin{aligned} W_2 &= (u \sin\vartheta + v \cos\vartheta)\cos\varphi_\ell - w \sin\varphi_\ell + \\ &\quad - \lambda\varepsilon(u \cos\vartheta - v \sin\vartheta) \end{aligned} \tag{4.35e}$$

In order to derive the expression for the surface element of the sphere, as a function of ϑ and φ_ℓ , consider the local coordinate systems characterized by λ and $\lambda + d\lambda$. They define the quantities on the cones

$$\vartheta_1 = \vartheta - \lambda\varepsilon \cos\varphi_\ell \tag{4.36a}$$

$$\vartheta_1 + d\vartheta_1 = \vartheta + d\vartheta - (\lambda + d\lambda)\varepsilon \cos\varphi_\ell \tag{4.36b}$$

where ϑ_1 is the angle as measured in the wind axis system. These cones cut out a slice of the sphere considered with the surface element (see fig.25)

$$dO = R\, d\vartheta_1\, R \sin\vartheta\, d\varphi_\ell$$

On applying eqs. (4.36)a and b this can be written as

$$dO = R^2 \left\{ 1 - \varepsilon \frac{d\lambda}{d\vartheta} \cos\varphi_\ell \right\} \sin\vartheta\, d\vartheta\, d\varphi_\ell \tag{4.37}$$

With the aid of eqs. (4.33), (4.35) and (4.37) the integrals occurring in eq. (4.32) can be written as follows :

$$\iint_{O_2} p_2 \cos(n,\zeta)\, dO_2 = \pi\varepsilon\, R^2 \int_{\vartheta_s}^{\vartheta_w} \left\{ -2\lambda \bar{p} \cos\vartheta - \bar{p}\frac{d\lambda}{d\vartheta}\sin\vartheta - (\eta + \lambda \frac{d\bar{p}}{d\vartheta})\sin\vartheta \right\} \sin\vartheta\, d\vartheta \qquad (4.38)a$$

$$\iint_{O_2} p_2\, V_{n_2} W_2\, dO_2 = \pi\varepsilon\, R^2 \int_{\vartheta_s}^{\vartheta_w} \Big[-\bar{\rho}\,\bar{u} \left\{ x \sin\vartheta + y \cos\vartheta - z \right\} +$$

$$- \bar{\rho}\,\bar{u}\lambda \left\{ \bar{u}' \sin\vartheta + \bar{v}'\cos\vartheta + \frac{\bar{v}}{\sin\vartheta} \right\} - 2\,\bar{\rho}\,\bar{u}\lambda\,(\bar{u}\cos\vartheta - \bar{v}\sin\vartheta) +$$

$$+ \left\{ -\bar{\rho}\,\bar{u}\frac{d\lambda}{d\vartheta} - \bar{\rho}(x + \lambda \bar{u}') \right\} (\bar{u}\sin\vartheta + \bar{v}\cos\vartheta) \Big] \sin\vartheta\, d\vartheta \qquad (4.38)b$$

$$\iint_{O_1} p_1 \cos(n,\zeta)\, dO_1 = \pi\alpha\varepsilon\, p_\infty R^2 \sin^2\vartheta_w \qquad (4.38)c$$

$$\iint \rho_\infty V_{n_1} W_1\, dO_1 = 0 \qquad (4.38)d$$

These equations can now be integrated by using eq. (4.34) together with the following expressions for the derivatives of the flow quantities (ref.24 and 25)

$$\bar{u}' = \bar{v} \qquad (4.39)a$$

$$\bar{v}' = -\frac{a^2(\bar{u} + \bar{v}\cot\vartheta)}{a^2 - \bar{v}^2} - \bar{u} \qquad (4.39)b$$

$$\bar{\rho}' = \frac{\bar{\rho}\,\bar{v}(\bar{u} + \bar{v}\cot\vartheta)}{a^2 - \bar{v}^2} \qquad (4.39)c$$

$$\bar{p}' = \frac{a^2\bar{\rho}\,\bar{v}(\bar{u} + \bar{v}\cot\vartheta)}{a^2 - \bar{v}^2} \qquad (4.39)d$$

If further use is made of eqs. (3.5) and (3.14) to express the density and the pressure as a function of the velocities, the integral proves to be after some tedious algebraic calculations as follows:

$$\frac{L}{\pi\varepsilon R^2 \rho_\infty U_\infty^2} = \frac{\sin^2\vartheta_s - \alpha \sin^2\vartheta_w}{\gamma M_\infty^2} +$$

$$
-\frac{p}{\gamma M_\infty^2}\int_{\vartheta_s}^{\vartheta_w}(a^2M_\infty^2)^{\frac{\gamma}{\gamma-1}}\left\{-2\lambda\cos\vartheta+\left(\frac{1-\alpha}{\vartheta_w-\vartheta_s}+\frac{d}{\gamma-1}\right)\sin\vartheta+\gamma\,\frac{\bar{u}x+\bar{v}y}{a^2}\sin\vartheta+\right.
$$

$$
\left.+\lambda\gamma\,\bar{v}\,\frac{\bar{u}\sin\vartheta+\bar{v}\cos\vartheta}{a^2-\bar{v}^2}\right\}\sin\vartheta\,d\vartheta\,+
$$

$$
-p\int_{\vartheta_s}^{\vartheta_w}(a^2M_\infty^2)^{\frac{1}{\gamma-1}}\left[-\bar{u}(x\sin\vartheta+y\cos\vartheta-z)+\bar{u}\left(\frac{1-\alpha}{\vartheta_w-\vartheta_s}+\frac{d}{\gamma-1}\right)(\bar{u}\sin\vartheta+\bar{v}\cos\vartheta)+\right.
$$

$$
\left.+\left(\bar{u}\,\frac{\bar{u}x+\bar{v}y}{a^2}-x\right)(\bar{u}\sin\vartheta+\bar{v}\cos\vartheta)-\lambda\bar{v}\left(\frac{\bar{u}^2}{a^2-\bar{v}^2}+1\right)(\bar{u}\sin\vartheta+\bar{v}\cos\vartheta)\right]\sin\vartheta\,d\vartheta \tag{4.40}
$$

It is to be understood that all the velocities are non-dimensionalized with U_∞, while d is a constant dependent on α (see Stone ref.8).

When considering the derivation of eq. (4.40) it is obvious that a quite complex and not very satisfying result is obtained, since the quantity λ has been assumed to be linearly dependent on ϑ. Therefore, at first sight it would seem that the result will be influenced by the particular choice being made for the function λ.

However, as it will be shown now, the lift correct up to first order is indeed independent of the function λ*. To this end a more thorough investigation is made of the eqs. (4.38) a and b. As it can be seen, the first of these equations gives

$$
\iint_{O_2} p_2\cos(n,z)\,dO_2=\pi\varepsilon R^2\int_{\vartheta_s}^{\vartheta_w}\left\{-2\lambda\bar{p}\cos\vartheta\sin\vartheta-\eta\sin^2\vartheta-\frac{d(\bar{p}\lambda)}{d\vartheta}\sin^2\vartheta\right\}d\vartheta \tag{4.41}
$$

By integrating there is obtained

$$
\iint_{O_2} p_2\cos(n,z)\,dO_2=\pi\varepsilon R^2\left[-\bar{p}\lambda\sin^2\vartheta\Big|_{\vartheta_s}^{\vartheta_w}-\int_{\vartheta_s}^{\vartheta_w}\eta\sin^2\vartheta\,d\vartheta\right] \tag{4.42}
$$

* provided that this function takes the values 1 and α at $\vartheta=\vartheta_s$ and $\vartheta=\vartheta_w$ respectively.

In the same way it can be derived that eq. (4.38)b reduces to

$$\iint_{O_2} \rho_2 V_{n_2} W_2 dO_2 = \pi\varepsilon\, R^2 \left[-\bar{\rho}\lambda\,\bar{u}(\bar{u}\,\sin\vartheta + \bar{v}\,\cos\vartheta)\sin\vartheta \Big/_{\vartheta_s}^{\vartheta_w} + \right.$$

$$\left. + \int_{\vartheta_s}^{\vartheta_w} \left[-\bar{\rho}\,\bar{u}\left\{ x\,\sin\vartheta + y\,\cos\vartheta - z \right\} - \left\{ \bar{u}\,\xi + \bar{\rho}\,x \right\} (\bar{u}\,\sin\vartheta + \bar{v}\,\cos\vartheta) \right] \sin\vartheta\, d\vartheta \right] \qquad (4.43)$$

The lift can now be written as

$$\frac{L}{\pi\varepsilon R^2} = p_\infty \left\{ \sin^2\vartheta_s - \alpha\,\sin^2\vartheta_w \right\} + p_w\alpha\,\sin^2\vartheta_w - p_s\,\sin^2\vartheta_s +$$

$$+ \bar{\rho}_w\alpha\,\bar{u}_w(\bar{u}_w\,\sin\vartheta_w + \bar{v}_w\cos\vartheta_w)\sin\vartheta_w - \bar{\rho}_s\bar{u}_s(\bar{u}_s\,\sin\vartheta_s + v_s\cos\vartheta_s)\sin\vartheta_s +$$

$$+ \int_{\vartheta_s}^{\vartheta_w} \left[\eta\,\sin^2\vartheta + \bar{\rho}\,\bar{u}\left\{ x\,\sin\vartheta + y\,\cos\vartheta - z \right\} \sin\vartheta + (u\xi + \bar{\rho}x)(\bar{u}\,\sin\vartheta + \bar{v}\,\cos\vartheta)\sin\vartheta \right] d\vartheta \qquad (4.44)$$

where s refers to the cone surface and w to the shock wave.

Inspection of eq. (4.44) gives the affirmation that the function λ has vanished from the integrand, only the known quantity α is occurring. Moreover the complicated derivatives of the axially-symmetric flow quantities have vanished. As before the expression can be written in terms of the velocities only, this, however, will not be undertaken here.

The starting point for the investigation presented in this section was the question whether or not the lift as found by momentum transport considerations was equal to the lift as found by integrating the pressure along the body surface. Since the quantity η, as can be found by using the results of Stone and expanding eq. (3.14), proves to be equal to

$$\eta = \bar{p}\left\{ -\frac{d}{\gamma-1} - \gamma\,\frac{\bar{u}x + \bar{v}y}{a^2} \right\} \qquad (4.45)$$

the lift along the fuselage can be calculated to be

$$\frac{L}{\pi\varepsilon R^2 \rho_\infty U_\infty^2} = \frac{1}{\gamma M_\infty^2}\left[-\frac{1}{2}\sin\vartheta_s \cos\vartheta_s (a^2 M_\infty^2)^{\frac{\gamma}{\gamma-1}} P\left(\frac{d}{\gamma-1} + \gamma\,\frac{\overline{ux+vy}}{a^2}\right) + \right.$$
$$\left. - \left\{(a^2 M_\infty^2)^{\frac{\gamma}{\gamma-1}} P - 1\right\} \sin^2\vartheta_s \right] \qquad (4.46)$$

where the values of the quantities are those for $\vartheta = \vartheta_s$.

For a number of cases the lift has been calculated according to eq. (4.46) and eq. (4.40). The results are given in table 6, together with the quantities P and α giving an idea about the entropy rise and the angle of yaw of the shock wave respectively. The agreement is within the numerical accuracy of the results. The conclusions which can be based upon these considerations are therefore that the first order theory of Stone is a valuable tool to calculate the quantity $\frac{dc_\ell}{d\varepsilon}$ for $\varepsilon \to 0$. It has to be remarked that this agreement was obtained by using the assumption for λ given by eq. (4.34). In fact this led to the derivation of eq. (4.44), affirming the statement that this agreement was not dependent on the particular choice made for the function λ .

This leads to a very important conclusion, for, from the above mentioned results it must be clear that the first order theory is not able to give the actual flow field. Only the values at the shock wave and at the body surface are given correctly.

However, it may be expected that the linear dependence of λ on ϑ gives a fairly accurate picture of the true flow field. In each case it is as good as any other assumption, while it is moreover the most simple one to make.

Before finishing the discussion presented in this section, some words should be said about the induced drag. This drag is of the order ε^2 and is only found partially by applying the theory presented here. This is so, because the change of the axially-symmetric flow field due to the angle of attack, which is of the order ε^2 as follows from ref.24, is not taken into account. Thus only the component of the lift in the direction of the free stream is found as induced drag. Hence, the theory is not able to predict the quantitative value of the drag, although it is found in most of the cases that the component of the lift is the largest part.

In the following sections a direct comparison of the results of this theory with the results of the linearized theory will be given.

4.1.6 Comparison of the pressure distribution as obtained by different theories for an inclined cone.

The results thus far obtained concerning the validity of the linearized theory for the prediction of the flow field around an axially-symmetric configuration at an angle of attack are, what may be called, global. A mean error is given, but no indication about the distribution of the error in the flow field.

One of the main interests of the aerodynamicist is the pressure distribution over a certain configuration. In order to check the validity of the linearized theory with respect to this quantity, a comparison has to be made with the results of an exact theory. This is only possible for a cone, because this is a configuration for which, as has been shown, a more exact theory is available.

In figs. 26 a-d the pressure coefficient according to the linearized theory and according to the first order theory of Stone is given.

For the linearized pressure coefficient the two versions of this formula, viz. eqs. (4.20) and (4.26), have been used. The value of the pressure coefficient according to the first order theory of Stone is given by

$$c_p'' = -\varepsilon \frac{\eta}{\frac{1}{2}\rho_\infty U_\infty^2} = -2\varepsilon \left\{ \frac{1}{\gamma M_\infty^2} + \frac{c_{p_o}}{2} \right\} \frac{\eta}{p} \qquad (4.47)$$

(In the figures the quantities $\frac{c_p''}{\varepsilon}$ are used).

It should be emphasized again that the second and third term in eq. (4.20) are terms giving the influence of the thickness distribution on the field with an angle of attack, while in the derivation this coupling between the two fields is neglected. This is an inconsistency which is worthwhile to think over. Seen from a purely formal point of view the use of eq. (4.20) instead of eq. (4.26) is not allowed.

Now, if looking at fig. 26, the remarkable fact is noted that the curve according to eq. (4.20) gives a far better agreement with eq. (4.47) than the application of eq. (4.26). The error is even decreasing with increasing Mach-number. The approximation given by eq. (4.26), however, shows a very large deviation, rapidly increasing with the Mach-number and the half-top angle. Thus it would seem that the approximation given by eq. (4.20) is the best one which can be obtained.

However, its validity being not more than empirical, it is shown that the results according to this approximation, give rather good agreement with the exact results, at least for a cone. But a more rigorous investigation reveals that this astonishing behaviour is obtained by the introduction of the second and third term in eq. (4.20) containing the flow quantities of the thickness field, which are largely in error according to the foregoing discussions, certainly at the higher Mach-numbers.

Moreover the theory used to determine the flow field around an inclined cone is only valid if the thickness field can be neglected, that means, when the second and third term in eq. (4.20) are small as compared to the first one. As follows from figs. 26 a-d, this is not true for the higher Mach-numbers. Thus the conclusion has to be drawn that the approximation according to eq. (4.20) **gives** a good agreement by chance, but that it has no theoretical justification. Thus it would seem dangerous to use such a formula, because of the possibility that it will be applied to more general configurations, where the validity of its application is not affirmed.

On the other hand the results given by eq. (4.26) show that linearized theory in this case is not very valuable for obtaining quantitative results. The investigations to be performed in the following section will learn how the situation is in the actual flow field, with respect to the validity of using linearized theory.

4.1.7 Comparison of the flow fields for inclined cones.

In order to obtain an insight into the validity of the linearized theory, for instance in the case of interference problems, it is worthwhile to make a comparison between the flow fields as calculated by the linearized theory and by the first order theory of Stone. This comparison is, as is evident, only possible for a cone.

Using eqs. (4.18)b and (4.19) the flow field according to linearized theory, can be calculated as a function of the spherical variable ϑ .

The flow quantities, as derived by using the first order theory of Stone, can be obtained from section 4.1.5 by using eqs. (4.33).

However, some care has to be exercized, since these quantities are referred to the so called body-axis coordinates.

In figs. 27 a–c, the quantities u", v" and w" as measured in a wind axis system are given for a cone with a semi-top angle of 7.5° and for the Mach-numbers 2.0108 and 5.1033.

In figs. 28 a–c the same quantities are given for the flow field around a cone with a semi-top angle of 12.5 degrees for the Mach-numbers $M_{\infty} = 2.1496$ and $M_{\infty} = 4.3002$.

From the figures it is evident that even for low Mach-numbers and small top angles the agreement between linearized and "exact" results is very poor. The deviations in this case again are increasing with increasing distance from the fuselage.

A detailed analysis reveals that the curves for u" have the same trend at least for the lower Mach-numbers, although they show an appreciably error for each case. The curves for v" show a rather good agreement in the vicinity of the fuselage. This is due to the boundary conditions valid at the surface of the cone. In the outer flow field, however, the curves become more and more deviating. The curves for w" show a complete disagreement near to the surface of the body. Only at the shock wave the values are close to each other, which is again due to the conditions to be fulfilled at this place.

From these curves another fact can be noted. The value of u" according to the linearized theory, seems to be in each case appreciably lower than according to the exact theory. Now equation 4.22 indicates that the lift as calculated by momentum transport considerations, in its turn is lower than the lift as calculated by integrating the pressure along the fuselage, which, since it is proportional to u", is lower than the exact value. This agreement leads to the conclusion that the mean error for the lift case will be much larger then given in table 1. This fact seems to be confirmed by the figs. 27 and 28.

It is clear that in calculating interference effects with the aid of linearized theory, the results obtained are expected to be very suspect, if not to say quite misleading.

4.1.8 Concluding remarks on the flow over inclined bodies.

In this part of the present chapter the investigations on the flow around axially-symmetric bodies have been supplemented by those pertaining to the flow field of inclined bodies of revolution. Therefore use is again made of a comparison of the same quantity as derived by different methods. The quantity used is the lift as derived from momentum transport considerations and as integrated along the fuselage. It is shown by the results of this comparison that the conclusions of the first part of the third chapter are also valid in this case. This means that the results obtained by application of the linearized theory in practically every case do not give more than the correct order of magnitude of integrated values, such as lift. In large parts of the flow field itself the errors are enormously large, at least for a cone, the only case for which a more refined theory is available.

These rather discouraging results about the validity of linearized theory make the search for more advanced methods of calculation for the flow around inclined bodies essential, if reliable results about the flow quantities itself are wanted.

Since, even nowadays, the application of truly three dimensional methods is prohibitive, because of the large time of calculation which is required (there may be hoped that this statement will be disproved within the following five years), a more simple method should be used, if possible.

Such a method, which gives the correct value of the quantity $\frac{dc_\ell}{d\varepsilon}$ for $\varepsilon \to 0$ will be set forth in the following part of this chapter. Its principle goal is to present a theory which does not have the disadvantages of the linearized one, while the cost and time of calculation are within reasonable limits.

4.2 A first order perturbation theory for the calculation of the inviscid supersonic flow around axially-symmetric configurations with arbitrary axis inclinations.

As has been shown in the first part of this chapter, the linearized method for calculating the flow around an inclined body - in essence being due to Tsien - does not give much hope to obtain reliable results.

Although already at several places in this paper something has been said about the available, more exact methods, it seems worthwhile, as an introduction to the general method set forth here, to remind the reader of the progresses made and the insight obtained thereby.

After the publication of the paper by Tsien (ref.22), a more refined method was given by Sauer in 1942 (ref.26). He does not linearize the equations, but calculates the shape of a body which gives a rotationally symmetric shock wave, which is inclined to the free stream. The effects of the entropy rise and the non-rotationality of the flow are neglected. Since in practical problems almost always the body is given beforehand and not the shock wave, this second method, although theoretically less restricted, has a great disadvantage. In fact it is only usable for a cone at a constant angle of attack.

In 1947 a table (ref.9) appeared which gives the numerical values of the flow quantities around a cone inclined with respect to the free stream. The calculations were based on the theory devised by Stone (ref.8). As has been discussed in section 4.1.4, this theory assumes that the flow quantities can be given as the sum of the axially-symmetric term and a term which depends on the circumferential variable ψ. The boundary conditions on the shock wave and the fuselage are transformed to the positions of these surfaces in the axially-symmetric flow field.

In fact it is assumed that the flow quantities can be given as a power series in the angle of attack ε, and in ref.8 only the term linear in ε is considered, while in a later publication (ref.24) also the term in ε^2 is determined.

Thus it seems that the slope and the curvature of the lift curve for $\varepsilon \rightarrow 0$ can be determined exactly. In this approximation the induced drag consists of a part due to the streamwise component of the lift (ε term) and a part due to the disturbance of the axially-symmetric flow field by the inclination (ε^2 term).

However, the theory given for the determination of the term in ε^2 lacks mathematical soundness, at least in the neighbourhood of the surface of the cone.

Moreover, in 1951 Ferri pointed out a fundamental inconsistency in the assumptions on which the theory for the term in ε was based (ref. 12). In ref. 8 it is assumed namely that the entropy in the inclined flow field can be given as the sum of the axially-symmetric term and also a term which depends on the cosine of the circumferential angle ϕ . This would mean that the entropy is not constant along the surface of the cone, which is the case in the real situation. In fact there should be a discontinuity in the entropy along the surface of the cone. This means that the cone is a singular surface for the entropy distribution and that the assumption of ref.8 is, therefore, invalid. However, it can be shown that the region in which this so called "vortical layer" influences the solution of Stone is very small and does not influence the pressure up to the term in ε^2, although the velocity components are changed. An analysis of these facts has been given by Willett (ref.27).

Therefore it follows that with the exact first order theory of ref.8, exact results can be obtained for the lift on a cone at a small angle of attack, in spite of the fact that no account is taken of the vortical layer.

There has been some criticism against the method of Stone, because the flow quantities are given in a transformed space and not in the real space. However, the method given in section 4.1.5 for calculating the real flow field from the results of Stone is fully successful, as has been proved by consideration of the momentum transport through a surface surrounding the cone.

After what has been said about the possibilities of using truly three-dimensional methods, it will not be very surprising that an generalization of the method of Stone seems the only acceptable possibility to obtain a more reliable calculation method for the flow field around inclined bodies.

A first try in this direction has been made by Ferri, in ref.11. The treatment given is not very lucid, and is not quite analogous to the method of Stone. Two methods are given by Ferri, one that is mostly graphical and a second one for a complete numerical treatment. Due to the fact that in the second method the perturbation terms have been considered as the only unknowns, this method yields the same characteristics as the axially-symmetric flow field. The reasoning by which this result is obtained is somewhat dubious, although the result itself is probably correct. It seems advisable to use a more systematic approach, where, for instance, first the full equations for the characteristic surfaces should have been derived, and thereafter these equations should have been linearized, thus avoiding the possibility of an incorrect treatment of the cross coupling terms.

It must be remarked here, that such an error does not have any influence in the linearized potential theory, because it is assumed beforehand that there is no coupling between the flow field in the axially-symmetric case and the flow field in the inclined case. However, it does lead to false results if this coupling is not neglected. The difference in this respect between truly linearized theories and the first order theories considered here, can also be explained in this way, that linearized theory considers the lifting flow field as a first order perturbation of the undisturbed flow field, whereas the first order theories consider it as a first order perturbation of the exact thickness flow field.

Because of the fact that the first method of ref.11 gives rise to a new characteristic network it is not very well adapted to numerical calculations, while moreover both methods are not applicable to bodies with axis curvature.

From this review it will be clear now, that the search has been for developing a method which is manageable from the numerical point of view, which is applicable to bodies with arbitrary axial inclinations and which gives exact results for the lift if the inclination is small.

The method developed in this paper, is essentially a generalization of the method of Stone. Because of the fact that only the first order term of the inclination will be taken into account, a consideration of the influence of the vortical layer can be left out of the analysis, according to the remarks already made with respect to this subject.

The analysis is based on a transformation from the real flow field to the axially-symmetric field. This is done by transforming the boundary conditions that have to be fulfilled on the fuselage and on the shock wave in the real field, to the position of these surfaces, in the axially-symmetric case. This transformation can be obtained by using a Taylor-series expansion to connect the flow quantities in the real field with those in the transformed field.

The calculation of the transformed flow field is performed along the axially-symmetric characteristics. Though these are not the characteristics of the inclined transformed field, the relations along these latter lines can be given in terms of the quantities occurring along the axially-symmetric characteristics, by using again the concept of the Taylor-series transformation.

To have the opportunity to calculate the real flow field, the connection between the quantities in this field and in the transformed field will be discussed. Moreover an expression will be derived for the lift as calculated from the momentum transport through a control surface. This gives a means to check the calculations, since it should yield the same value for the lift as derived by integrating the pressure along the fuselage surface.

To start the calculations the conditions at the nose of the body have to be known. By assuming that this nose is conical the results of Stone can be used as a starting point.

The analysis consists of five main parts.

First, the calculation of the quantities at a point of the inside field is considered. The equations valid along the characteristics of the axially-symmetric field in the transformed field are given. The derivation of these equations is given in full, starting from the results obtained in chapter 2.

In the second place, a detailed derivation of the boundary condition on the fuselage is given.

In the third place, the conditions which have to be fulfilled at the shock wave are derived from the general shock wave equations given in chapter 2.

These three parts contain the material necessary to construct the calculation procedure, which is also discussed to some extent.

Finally the method for calculating the real flow field from the transformed one is outlined. By applying it to the calculation of the lift as an integral over a control surface, it is found that it is not possible to determine this real flow field in a unique way.

4.2.1 Outline of the method.

In this section an outline will be given of the fundamental ideas underlying the present method. It is assumed that the shape of an axially-symmetric configuration, together with its rotationally symmetric flow field including the shock wave are given. Such a flow field can be calculated by applying the method of characteristics as explained in chapter 3. Since it is the only method available to calculate the flow field by exact methods, it will be assumed that actually this method is used for the determination of the axially-symmetric flow field.

Now the configuration is given a small deformation by deforming its axis by an amount $\varepsilon\lambda(x)$ where ε is a small parameter and $\frac{d\lambda(x)}{dx}$ is of the order unity (fig.29). It is assumed that the cross sections remain perpendicular to the axis. A special case of such a deformation is a body with a constant angle of attack ε. It is obtained by rotating the axis through the vertex of the configuration. Up to the first order in ε the function $\lambda(x)$ is determined by x in this case.

As has already been said it would be possible to construct the flow field by using the method of characteristics into three space coordinates. Hewever, up to now, the numerical application of such methods is scarcely known and the actual computation remains a tremendous task, even for high speed computers.

Therefore, in this paper, a method is derived where the flow quantities generated by the deformation are considered as perturbations on the already known, axially-symmetric flow field. It is assumed that the total value of the flow quantities can be written as a power series in the small quantity ε. Here, we will restrict ourselves to the term that is linear in ε.

To make the method applicable from the numerical point of view, it wpuld be desirable to be able to calculate simultaneously the axially-symmetric flow field and the flow field due to the deformation. However, at first sight, this may seem a rather strange desire. For this would be possible only if the boundaries of the flow fields were the same for the two fields to be calculated, whereas it is obvious that this is not true.

One of the main points of the method therefore is the transformation of the conditions valid on the deformed surface of the body and on the deformed shock wave to conditions along the axially-symmetric boundaries of the flow field, just as this has been explained for the case of the cone in the foregoing sections.

Now the deformation of the body is a known function of the coordinates.

As will be shown in section 4.2.3 it proves to be of the form

$$dx = 0\ (\varepsilon\ \cos\psi) \qquad (4.48)a$$

$$dr = 0\ (\varepsilon\ \cos\psi) \qquad (4.48)b$$

The deformation of the shock wave is a still unknown function of the coordinates. By making an assumption about the relation between the axially-symmetric and the deformed shock wave, an unknown function $\alpha(r)$ is introduced which enables one to present the deformation as follows:

$$dx = 0\ (\varepsilon\alpha\ \cos\psi) \qquad (4.49)a$$

$$dr = 0\ (\varepsilon\alpha\ \cos\psi) \qquad (4.49)b$$

The equations (4.48) and (4.49) now strongly suggest that the total velocities can be written as the sum of an axially-symmetric term and a perturbation term depending upon $\cos\psi$ and $\sin\psi$. It is therefore assumed that the flow quantities in the transformed field, i.e. in the field where the boundary conditions are given along the axially-symmetric boundaries, have the following form:

$$u_1 = u + \varepsilon u''\ \cos\psi \qquad (4.50)a$$

$$v_1 = v + \varepsilon v''\ \cos\psi \qquad (4.50)b$$

$$w_1 = \varepsilon w''\ \sin\psi \qquad (4.50)c$$

$$p_1 = p + \varepsilon p''\ \cos\psi \qquad (4.50)d$$

$$\rho_1 = \rho + \varepsilon\rho''\ \cos\psi \qquad (4.50)e$$

$$s_1 = s +\ s''\ \cos\psi \qquad (4.50)f$$

where the first terms in the right-hand side refer to the already known quantities in the axially-symmetric flow field.

By inserting these expressions into the governing differential equations, this proves to be a formally consistent assumption, i.e. all the terms of the order ε have the same trigonometric form.

From the eqs. (4.50) the boundary conditions in the real flow field can be written in terms of the quantities occurring in the transformed flow field by observing that up to the first order in ε the quantities in the real flow field are given by, for instance,

$$u_1 = u + \frac{\partial u}{\partial x}\,dx + \frac{\partial u}{\partial r}\,dr + \varepsilon u'' \cos\phi \tag{4.51}$$

It can be noticed that due to eqs. (4.48) and (4.49) the displacement terms are, as they should be, also of the order $\varepsilon \cos\phi$.

There is only one point which is troublesome. As has already been pointed out in the introduction, the model given here is not consistent with the requirement of constant entropy along the body. It can be shown, however, that this does not influence the pressure up to the first order in ε. Only the velocities have to be corrected in a small layer near to the surface. These difficulties, which will be neglected here, can be important for boundary value problems (ref.27).

The problem is now posed in such a way that the axially-symmetric flow field and the flow field generated by the deformation of the body can be calculated simultaneously. The domain of the calculation is the same for both flow fields.

As has been remarked the actual calculations are performed by using the method of characteristics. This gives no difficulty for the axially-symmetric flow field. But since the characteristics of the transformed field are not the same as those for the axially-symmetric field, there is reason to fear a rather complex calculation scheme.

This difficulty can be removed by deriving expressions for the transformed field, which are valid along the characteristics of the axially-symmetric field. This is one of the main advantages of this method.

After the determination of the flow fields, the quantities occurring along the contour of the body can be determined. Moreover, the shape of the real shock can be constructed. However, it is impossible to construct the real flow field itself. Although a reasonable assumption can be made, there are no theoretical means to determine this field. This is in accordance with the results obtained earlier for the flow around a cone. Just as in that case, the pressure distribution along the fuselage and thus the lift, are correct up to the first order in ε. This can be assured by applying a momentum transport theorem to a control surface. The value of the lift as found by these two different methods has to be the same. Along the lines sketched above, a detailed derivation and discussion of the method will be presented in the following sections.

4.2.2 The calculation of the transformed flow field.

In this section it will be explained how the quantities u, v, s, u", v", w" and s" can be calculated in the transformed field. For this purpose it will be assumed that this set of quantities is given along an arbitrary surface which does not coincide with a characteristic surface. It is important to remark that p, ρ, p" and ρ" are derived quantities, thus they can be calculated once the set of values given above is known at a certain point.

If it is assumed that the effects of viscosity, thermal conduction and diffusion can be neglected and that the gas can be considered as ideal, the set of governing relations consists of the continuity equation together with the three equations of motion, while a thermodynamic relation gives the expression for the entropy as a function of the temperature and the pressure.

By eliminating all quantities except the components of the velocity and the entropy, a system of four equations can be derived composed of the well-known "potential flow" equation together with the three components of Crocco's theorem. It must be remarked that the occurrence of an entropy gradient makes it impossible to define a potential function in this case. The equations are derived in chapter 2 and are given by the system (2.24).

Since we are dealing with supersonic flow, the problem is hyperbolic and thus there exist real characteristic surfaces. With a view to the suggested way of solution of the problem, it is convenient therefore to write the system of governing equations in the characteristic form.

First the direction cosines of the characteristic surface through a certain point have to be determined. As is proved in chapter 2, through each point three different characteristic surfaces can be traced (in fact there are four). It turns out that they are given by the stream surfaces counted twice and a circular cone with the stream line through the point considered as an axis. The semi-top angle of this cone is such that the component of the local velocity normal to the cone surface is precisely equal to the local velocity of sound.

By the techniques explained in chapter 2 it is possible to derive the equations which are valid along the characteristic surfaces. They contain derivatives along these surfaces only, making them extremely useful for a numerical calculation of the field. The four characteristic equations have been derived and are given by equations (2.40), (2.41) and (2.45).

Until now only the general case of a wholly three-dimensional flow has been considered. But the purpose was to derive the equations for the transformed flow field. Therefore the expressions for the flow quantities as given in eqs. (4.50) are substituted into the equations so far obtained in chapter two. From the analysis as given here, not only the equations valid for the transformed field are derived, but also the equations valid for the truly axially-symmetric flow, equations which have been used already several times. To obtain a systematic presentation of the material, first the equations for the characteristic surfaces will be derived in terms of the set of quantities mentioned in the beginning of this section. Thereafter these equations will be used to obtain the appropriate relations along the axially-symmetric characteristic surfaces.

Consider a characteristic surface through the circle $x = x_0$, $r = r_0$ where (x_0, r_0) is an arbitrary point of the domain considered. In that case the characteristic directions σ_1 and σ_2 in a point of the circle as introduced in chapter 2, can be written correctly up to the first order in ε as

$$\sigma_1 = \frac{\partial f}{\partial x} = \sigma + \varepsilon\sigma'' \cos\psi \tag{4.52a}$$

$$\sigma_2 = \frac{1}{r}\frac{\partial f}{\partial \psi} = 0 \tag{4.52b}$$

Here the quantity σ is the characteristic direction for the axially-symmetric flow field.

The characteristic directions are given by the eqs. (2.32)a and (2.32)b.

At first equation (2.32)a will be considered

$$v_1 - u_1\sigma_1 - w_1\sigma_2 = 0 \tag{4.53}$$

Using eqs. (4.50) and (4.52) and neglecting second order terms in ε^2 the result can be written as

$$v - u\sigma + \varepsilon\left\{v'' - u\sigma'' - \sigma u''\right\}\cos\psi = 0$$

From this equation the well-known result for the quantity σ can be derived together with the expression for the unknown quantity σ''.

$$\sigma = \frac{v}{u} \qquad (4.54)\text{a}$$

and $$\sigma'' = \frac{uv''-vu''}{u^2} \qquad (4.54)\text{b}$$

These equations give the directions of the stream surface. The equations for the other characteristic directions are given by eq. (2.32)b

$$v_1 - u_1\sigma_1 - w_1\sigma_2 = \pm a_1\sqrt{\sigma_1^2+\sigma_2^2+1}$$

To evaluate this equation, at first the expression for the velocity of sound a_1 has to be derived correct up to the first order in ε. Applying eq. (2.23) there is found

$$a_1 = a\left\{1 - \frac{\gamma-1}{2}\varepsilon\,\frac{uu''+vv''}{a^2}\cos\psi\right\} \qquad (4.55)$$

Together with the eqs. (4.50) and (4.52) the equation for the characteristic directions obtains the following form

$$v - u\sigma + \varepsilon\left\{v'' - u''\sigma - u\sigma''\right\}\cos\psi =$$
$$= \pm a\sqrt{\sigma^2+1}\left\{1 + \varepsilon\,\frac{\sigma''}{\sigma^2+1}\cos\psi - \frac{\gamma-1}{2}\varepsilon\,\frac{uu''+vv''}{a^2}\cos\psi\right\} \qquad (4.56)$$

If the minus sign on the right-hand side of eq. (4.56) is taken, so called "backward running" characteristics (in a plane ψ is constant) are obtained. They are characterized by a positive slope $\frac{dr}{dx} > 0$. The expression for the axially-symmetric slope is given by the part undependent of ε and reads

$$\sigma = \frac{u+\beta v}{\beta u-v} \qquad (4.57)\text{a}$$

Together with eq. (4.57)a an expression for the perturbation term σ'' can be derived from eq. (4.56). After some calculations the result can be written as

$$\sigma'' = \frac{M^2}{\beta(\beta u-v)^2}\left\{\beta(uv''-vu'') - (1+\frac{\gamma-1}{2}M^2)(uu''+vv'')\right\} \tag{4.57)b}$$

where M is, as before, the local Mach-number of the axially-symmetric flow.

If the positive sign on the right-hand side of eq. (2.32)b is taken, the "forward running" characteristics ($\frac{dr}{dx}<0$) are obtained. The results in this case are given by

$$\sigma = \frac{v\beta-u}{\beta u+v} \tag{4.58)a}$$

and
$$\sigma'' = \frac{M^2}{\beta(\beta u+v)^2}\left\{\beta(uv''-vu'') + (1+\frac{\gamma-1}{2}M^2)(uu''+vv'')\right\} \tag{4.58)b}$$

The equations (4.57)a and (4.58)a giving the characteristic directions for purely axially-symmetric flow have been used in several sections of chapter 3. It turns out, from the analysis given, that the characteristic directions in the transformed field are different from those in the axially-symmetric field. Along these lines the characteristic equations (2.40), (2.41) and (2.45) are valid and thus the flow field could be constructed by using this set of characteristics. However, it is very important from a numerical point of view, to be able to construct the flow field for the axially-symmetric as well as for the transformed field, along the same set of lines.

The natural set of lines for the construction of the axially-symmetric flow field are the axially-symmetric characteristics.

Therefore, it is desired, if possible, to replace the characteristic equations by differential relations which are valid along the axially-symmetric characteristics.

To do so, the differential quotients $\frac{\delta u_i}{\delta x}$ and $\frac{1}{r}\frac{\delta u_i}{\delta\psi}$ along the characteristics of the transformed field, have to be expressed in differential relations along the axially-symmetric characteristics. If it is assumed, as before, that $\sigma_2 = 0$ and thus that a characteristic surface is considered that passes through the circle $x = x_o$, $r = r_o$, the relations $\frac{1}{r}\frac{\delta u_i}{\delta\psi}$ offer no difficulty and can be obtained by differentiating the expressions (4.50) with respect to the angular variable ψ .

To obtain the correct expressions for $\frac{\delta u_i}{\delta x}$ more care is needed. The differentiation along a certain direction can be given by

$$\frac{\delta}{\delta x} = \frac{\partial}{\partial x} + \mu\frac{\partial}{\partial r} \tag{4.59}$$

where μ is the slope of the direction considered.

Applying eq. (4.59) to the present case gives for instance

$$\frac{\delta u_1}{\delta x} = \frac{\partial}{\partial x}(u + \varepsilon u''\cos\psi) + (\sigma + \varepsilon\sigma''\cos\psi)\frac{\partial}{\partial r}(u + \varepsilon u''\cos\psi)$$

If higher order terms in ε are neglected this relation can be written as

$$\frac{\delta u_1}{\delta x} = \frac{\partial u}{\partial x} + \sigma\frac{\partial u}{\partial r} + \left\{\frac{\partial u''}{\partial x} + \sigma\frac{\partial u''}{\partial r} + \sigma''\frac{\partial u}{\partial r}\right\}\varepsilon\cos\psi \tag{4.60}$$

This can be simplified further by observing that along the axially-symmetric characteristics there holds

$$\frac{\delta}{\delta\bar{x}} = \frac{\partial}{\partial x} + \sigma\frac{\partial}{\partial r} \tag{4.61}$$

where $\bar{x}$ is measured along the axially-symmetric characteristic.

Applying this equation to eq. (4.60) it follows that

$$\frac{\delta u_1}{\delta x} = \frac{\delta u}{\delta\bar{x}} + \varepsilon\left(\frac{\delta u''}{\delta\bar{x}} + \sigma''\frac{\partial u}{\partial r}\right)\cos\psi \tag{4.62}$$

This relation is the desired expression. It expresses the differentiation along the characteristics of the transformed field into a relation along the characteristics of the axially-symmetric field. This may seem surprising since the term $\frac{\partial u}{\partial r}$ is present, but by using eq. (4.61) along the two different axially-symmetric characteristics, this term can be expressed as a function of the differential quotients along these characteristics. Along a backward running characteristic there holds

$$\left(\frac{\delta u}{\delta\bar{x}}\right)_b = \frac{\partial u}{\partial x} + \sigma_b\frac{\partial u}{\partial r}$$

Along a forward running characteristic there holds

$$\left(\frac{\delta u}{\delta \bar{u}}\right)_f = \frac{\partial u}{\partial x} + \sigma_f \frac{\partial u}{\partial r}$$

From these two equations the quantity $\frac{\partial u}{\partial r}$ can be found, viz.

$$\frac{\partial u}{\partial r} = \frac{\left(\frac{\delta u}{\delta \bar{x}}\right)_b - \left(\frac{\delta u}{\delta \bar{x}}\right)_f}{\sigma_b - \sigma_f} \tag{4.63}$$

Now sufficient knowledge is available for deriving the final expressions that are valid for the transformed field along the axially-symmetric characteristics.

Along a stream surface there holds, according to eqs. (2.39) and (4.62)

$$(u+\varepsilon u'' \cos\psi)\left\{\frac{\delta s}{\delta \bar{x}} + \left(\frac{\delta s''}{\delta \bar{x}} + \sigma'' \frac{\partial s}{\partial r}\right)\varepsilon \cos\psi\right\} - \frac{\varepsilon^2}{r} s'' w'' \sin^2\psi = 0$$

The terms independent of ε give the equation valid for the axially-symmetric flow field, or

$$\frac{\delta s}{\delta \bar{x}} = 0 \tag{4.64)a}$$

The equation valid for the transformed field is given by

$$\frac{\delta s''}{\delta \bar{x}} = -\sigma'' \frac{\partial s}{\partial r}$$

Using eq. (4.63) together with (4.54)a,(4.57)a and (4.58)a, the final result can be written after some algebraic operations as

$$\frac{2\beta u^2}{1-\frac{u^2}{a^2}} \frac{\delta s''}{\delta \bar{x}} = (uv''-vu'')\left\{\left(\frac{\delta s}{\delta \bar{x}}\right)_b - \left(\frac{\delta s}{\delta \bar{x}}\right)_f\right\} \tag{4.64)b}$$

where the indices b and f refer to backward and forward running characteristics respectively.

This equation thus is valid along an axially-symmetric stream surface. The second relation valid along such a surface is given by eq. (2.41). The result obtained reads as follows:

$$-\frac{1}{r}\left(uu'' + u\sigma v'' + u\sigma w'' + \frac{a^2}{\gamma(\gamma-1)}s''\right) - u\frac{\delta w''}{\delta\bar{x}} = 0$$

On introducing the relation given by eq. (4.54)a for σ, this equation can be written as

$$u\frac{\delta w''}{\delta\bar{x}} + \frac{1}{r}\left\{uu'' + v(v'' + w'') + \frac{a^2}{\gamma(\gamma-1)}\;s''\right\} = 0 \qquad (4.64)\text{a}$$

The two other equations, valid along the axially-symmetric characteristics given by eqs. (4.57)a and (4.58)a, can be derived by using equation (2.45). First of all this equation will be simplified by neglecting all the second order terms in ε. The equation is then given by

$$(u_1 + \sigma_1 v_1)\frac{\delta v_1}{\delta x} - \frac{v_1 - u_1\sigma_1}{\gamma(\gamma-1)}u_1\frac{\delta s_1}{\delta x} + \frac{a_1^2}{\gamma(\gamma-1)}\sigma_1\frac{\delta s_1}{\delta x} +$$
$$-(v_1 - u_1\sigma_1)\left\{\left(1 - \frac{u_1^2}{a_1^2}\right)\frac{\delta u_1}{\delta x} - \frac{v_1 u_1}{a^2}\frac{\delta v_1}{\delta x} + \frac{1}{r}\frac{\delta w_1}{\delta\psi} + \frac{v_1}{r}\right\} = 0 \qquad (4.65)$$

The derivation of the relation along the axially-symmetric characteristics will be given in a fairly complete form in order to show how the final and rather simple result is obtained. Using eqs. (4.50) together with eq. (4.63) and eq. (4.55) there results for the various terms occurring in this equation

$$(u_1+\sigma_1 v_1)\frac{\delta v_1}{\delta x} = (u+\sigma v)\frac{\delta v}{\delta\bar{x}} + (u''+\sigma''v+\sigma v'')\frac{\delta v}{\delta\bar{x}}\varepsilon\cos\psi +$$
$$+ (u+\sigma v)\left(\frac{\delta v''}{\delta\bar{x}} + \sigma''\frac{\partial v}{\partial r}\right)\varepsilon\cos\psi \qquad (4.66)\text{a}$$

$$(v_1-u_1\sigma_1)u_1\frac{\delta s_1}{\delta x} = (v-u\sigma)\,u\frac{\delta s}{\delta\bar{x}} +$$
$$+\left[(v-u\sigma)u'' + (v''-u\sigma''-u''\sigma)u\right]\frac{\delta s}{\delta\bar{x}}\varepsilon\cos\psi +$$
$$+ (v-u\sigma)u\left[\frac{\delta s''}{\delta\bar{x}} + \sigma''\frac{\delta s}{\delta r}\right]\varepsilon\cos\psi \qquad (4.66)\text{b}$$

$$a_1^2\sigma_1\frac{\delta s_1}{\delta x} = a^2\sigma\frac{\delta s}{\delta\bar{x}} - (\gamma-1)(uu''+vv'')\sigma\frac{\delta s}{\delta\bar{x}}\varepsilon\cos\psi +$$

$$+ a^2\left\{\sigma''\frac{\delta s}{\delta\bar{x}} + \sigma\left(\frac{\delta s''}{\delta\bar{x}} + \sigma''\frac{\delta s}{\delta r}\right)\right\}\varepsilon\cos\psi \qquad (4.66)c$$

$$(v_1-u_1\sigma_1)\left[\left(1-\frac{u_1^2}{a_1^2}\right)\frac{\delta u_1}{\delta x} - \frac{v_1u_1}{a_1^2}\frac{\delta v_1}{\delta x} + \frac{1}{r}\frac{\delta w_1}{\delta\psi} + \frac{v_1}{r}\right] =$$

$$= (v-u\sigma)\left[\left(1-\frac{u^2}{a^2}\right)\frac{\delta u}{\delta\bar{x}} - \frac{vu}{a^2}\frac{\delta v}{\delta\bar{x}} + \frac{v}{r}\right] +$$

$$+ (v''-u\sigma''-u''\sigma)\left[\left(1-\frac{u^2}{a^2}\right)\frac{\delta u}{\delta\bar{x}} - \frac{vu}{a^2}\frac{\delta v}{\delta\bar{x}} + \frac{v}{r}\right]\varepsilon\cos\psi +$$

$$+(v-u\sigma)\left\{\left(1-\frac{u^2}{a^2}\right)\left(\frac{\delta u''}{\delta\bar{x}} + \sigma''\frac{\partial u}{\partial r}\right) - \frac{(\gamma-1)\frac{u^2}{a^2}(uu''+vv'')+2uu''}{a^2}\frac{\delta u}{\delta\bar{x}}\right\}\varepsilon\cos\psi$$

$$+(v-u\sigma)\left\{\frac{v''}{r} + \frac{w''}{r} - \frac{vu}{a^2}\left(\frac{\delta v''}{\delta\bar{x}} + \sigma''\frac{\partial v}{\partial r}\right) - \frac{uv''+vu''+(\gamma-1)(uu''+vv'')\frac{uv}{a^2}}{a^2}\frac{\delta v}{\delta\bar{x}}\right\}\varepsilon\cos\psi$$

$$(4.66)d$$

By taking together the terms that are independent of ε, the characteristic equations for the axially-symmetric flow field are obtained

$$(u + v\sigma)\frac{\delta v}{\delta\bar{x}} - (v - u\sigma)\left[\left(1-\frac{u^2}{a^2}\right)\frac{\delta u}{\delta\bar{x}} - \frac{vu}{a^2}\frac{\delta v}{\delta\bar{x}} + \frac{v}{r}\right] +$$

$$+ \frac{1}{\gamma(\gamma-1)}\frac{\delta s}{\delta\bar{x}}\left\{(v-u\sigma)u + a^2\sigma\right\} = 0 \qquad (4.67)$$

When use is made of the following relations

$$(v - u\sigma)^2 = a^2(1+\sigma^2) \qquad (4.68)a$$

and $$u + v\sigma = \frac{v-u\sigma}{\sigma}\left\{-\left(1-\frac{v^2}{a^2}\right) - \frac{uv}{a^2}\sigma\right\} \qquad (4.68)b$$

the equations can be simplified considerably. Equation (4.67) takes the form

$$(1-\frac{u^2}{a^2})\frac{\delta u}{\delta \bar{x}}+\frac{1}{\sigma}(1-\frac{v^2}{a^2})\frac{\delta v}{\delta \bar{x}}+\frac{v}{r}-\frac{1}{\gamma(\gamma-1)}\frac{\delta s}{\delta \bar{x}}\frac{u+v\sigma}{1+\sigma^2}=0 \qquad (4.69)$$

By using the eqs. (4.67) and (4.68) the equation for the transformed field can be written as

$$\left\{\frac{u''v-v''u}{a^2}+\frac{\sigma''M^2}{1+\sigma^2}\right\}\frac{\delta v}{\delta \bar{x}}-(1-\frac{u^2}{a^2})(\frac{\delta u''}{\delta \bar{x}}+\sigma''\frac{\delta u}{\delta r})-\frac{w''}{r}-\frac{v''}{r}+$$

$$-\frac{1}{\sigma}(1-\frac{v^2}{a^2})(\frac{\delta v''}{\delta \bar{x}}+\sigma''\frac{\partial v}{\partial r})+(\gamma-1)\frac{uu''+vv''}{a^2}\left[\frac{uv}{a^2}\frac{\delta v}{\delta \bar{x}}+\frac{u^2}{a^2}\frac{\delta u}{\delta \bar{x}}\right]+$$

$$+2\frac{uu''}{a^2}\frac{\delta u}{\delta \bar{x}}+\frac{uv''+vu''}{a^2}\frac{\delta v}{\delta \bar{x}}+\frac{1}{\gamma(\gamma-1)}\frac{u+v\sigma}{1+\sigma^2}\left[\frac{\delta s''}{\delta \bar{x}}+\sigma''\frac{\partial s}{\partial r}\right]+$$

$$+\frac{1}{\gamma(\gamma-1)}\left[u''-(v''-u''\sigma)\frac{\sigma}{1+\sigma^2}+\frac{\sigma''v}{1+\sigma^2}-\frac{uu''+vv''}{a^2(1+\sigma^2)}(\gamma-1)\sigma(v-u\sigma)\right]\frac{\delta s}{\delta \bar{x}}=0 \qquad (4.70)$$

The equations (4.69) and (4.7o) will now be simplified further by using the expressions derived for the characteristic directions, i.e. eqs. (4.57) and (4.58) and the equation for the radial derivative (4.63). When again the indices b and f are used to indicate the backward and forward running characteristics the following results can be obtained. Along the backward running characteristics the equation for the axially-symmetric flow is

$$(\beta u+v)\frac{\delta u}{\delta \bar{x}}+(\beta v-u)\frac{\delta v}{\delta \bar{x}}-\frac{v}{r}\frac{q^2}{\beta u-v}+\frac{a^2\beta}{\gamma(\gamma-1)}\frac{\delta s}{\delta \bar{x}}=0 \qquad (4.71)a$$

The equation for the transformed field, which is obtained after some tedious algebraic calculations reads:

$$\frac{\delta u''}{\delta \bar{x}}+\frac{v\beta-u}{u\beta-v}\frac{\delta v''}{\delta \bar{x}}+\frac{w''+v''}{r(1-\frac{u^2}{a^2})}+\frac{1}{\gamma(\gamma-1)}\frac{a^2\beta}{\beta u+v}\frac{\delta s''}{\delta \bar{x}}+$$

$$+\sigma_f''\left(\frac{\delta v}{\delta \bar{x}}\right)_b+\sigma_b''\left(\frac{\delta v}{\delta \bar{x}}\right)_f+\frac{1}{\gamma(\gamma-1)}\frac{v}{M^2}\left\{\sigma_f''\left(\frac{\delta s}{\delta \bar{x}}\right)_b+\sigma_b''\left(\frac{\delta s}{\delta \bar{x}}\right)_f\right\}+$$

$$+\frac{2vu}{r(a^2-u^2)^2}\left[\frac{\gamma-1}{2}v(uv''-vu'')+\frac{1+\frac{\gamma-1}{2}M_\infty^2}{M_\infty^2}u''\right]+$$

$$+\frac{M^2}{\beta u+v}\left\{\beta(uu''+vv'')\left[1+(\gamma-1)M^2\right]+(uv''-vu'')\right\}\frac{1}{\gamma(\gamma-1)}\frac{\delta s}{\delta\bar{x}}=0 \qquad (4.71)\text{b}$$

Along the same lines the result for the forward running characteristics can be derived. The equation for the axially-symmetric flow proves to be in this case

$$(\beta u-v)\frac{\delta u}{\delta\bar{x}}+(u+\beta v)\frac{\delta v}{\delta\bar{x}}-\frac{v}{r}\frac{q^2}{\beta u+v}+\frac{a^2\beta}{\gamma(\gamma-1)}\frac{\delta s}{\delta\bar{x}}=0 \qquad (4.72)\text{a}$$

The equation for the transformed field along such a characteristic is given by:

$$\frac{\delta u''}{\delta\bar{x}}+\frac{u+\beta v}{\beta u-v}\frac{\delta v''}{\delta\bar{x}}+\frac{w''+v''}{r(1-\frac{u^2}{a^2})}+\frac{1}{\gamma(\gamma-1)}\frac{a^2\beta}{\beta u-v}\frac{\delta s''}{\delta\bar{x}}+$$

$$+\sigma_f''\left(\frac{\delta v}{\delta\bar{x}}\right)_b+\sigma_b''\left(\frac{\delta v}{\delta\bar{x}}\right)_f+\frac{1}{\gamma(\gamma-1)}\frac{v}{M^2}\left\{\sigma_f''\left(\frac{\delta s}{\delta\bar{x}}\right)_b+\sigma_b''\left(\frac{\delta s}{\delta\bar{x}}\right)_f\right\}+$$

$$+\frac{2vu}{r(a^2-u^2)^2}\left[\frac{\gamma-1}{2}v(uv''-vu'')+\frac{1+\frac{\gamma-1}{2}M_\infty^2}{M_\infty^2}u''\right]+$$

$$+\frac{M^2}{\beta u+v}\left\{\beta(uu''+vv'')\left[1+(\gamma-1)M^2\right]+(uv''-vu'')\right\}\frac{1}{\gamma(\gamma-1)}\frac{\delta s}{\delta\bar{x}}=0 \qquad (4.72)\text{b}$$

Thus complete sets of equations are derived, that are valid along the axially-symmetric characteristics. They give the equations necessary for the calculation of the flow quantities for the axially-symmetric field as well as for the transformed field. The set of equation for the axially-symmetric flow field is given by the equations (4.64)a, (4.17)a and (4.72)a. These are three equations to calculate the flow quantities u, v and s. These equations have been used already at several places in chapter 3, to study the flow around axially-symmetric bodies. The derivation of these equations has been postponed until this chapter, because the transformed field depends on the knowledge of the axially-symmetric field.As soon namely as the quantities u, v and s are known the four unknown quantities u",v",w" and s" of the transformed field can be calculated by using the set of four relations given by eqs. (4.64)b, (4.64)c, (4.71)b and (4.72)b. In one of the following sections it will be shown how the transformed field can be constructed by using these equations. Before this, a derivation will be given of the conditions which have to be satisfied on the body surface and at the shock wave. First, however, a version will be given of the equations which have been derived, that are valid for the case of isentropic flow.

An interesting simplification of the equations follows if the region of interest is separated from the undisturbed stream by a conical or near-conical shock of vanishing strength, such as it will occur for small values of the top angle of the nose and for low Mach-numbers.

In that case it is permitted to neglect the entropy terms in the flow equations. The set is then reduced to a system of three equations.

In this case, according to eq. (4.64)c, there holds along a streamline

$$u\frac{\delta w''}{\delta x} + \frac{1}{r}\left\{uu'' + v(v'' + w'')\right\} = 0 \qquad (4.73)$$

Along a backward running characteristic there is obtained, according to eq. (4.71)b

$$\frac{\delta u''}{\delta \bar{x}} + \frac{v\beta-u}{u\beta+v}\frac{\delta v''}{\delta \bar{x}} + \frac{w''+v''}{r(1-\frac{u^2}{a^2})} + \sigma_f''\left(\frac{\delta v}{\delta \bar{x}}\right)_b + \sigma_b''\left(\frac{\delta v}{\delta \bar{x}}\right)_f +$$

$$+ \frac{2vu}{r(a^2-u^2)^2}\left[\frac{\gamma-1}{2}\, v(uv''-vu'') + \frac{1+\frac{\gamma-1}{2}M_\infty^2}{M_\infty^2}\, u''\right] = 0 \qquad (4.74)\text{a}$$

and along a forward characteristic one has

$$\frac{\delta u''}{\delta \bar{x}} + \frac{v\beta+u}{u\beta-v}\frac{\delta v''}{\delta \bar{x}} + \frac{w''+v''}{r(1-\frac{u^2}{a^2})} + \sigma_f''\left(\frac{\delta v}{\delta \bar{x}}\right)_b + \sigma_b''\left(\frac{\delta v}{\delta \bar{x}}\right)_f +$$

$$+ \frac{2vu}{r(a^2-u^2)^2}\left[\frac{\gamma-1}{2}\, v(uv''-vu'') + \frac{1+\frac{\gamma-1}{2}M_\infty^2}{M_\infty^2}\, u''\right] = 0 \qquad (4.74)\text{b}$$

This system is considerably simpler than the complete system, moreover it can be simplified even further, since eq. (4.73) in this case can be replaced by an equation valid along every surface in the flow field. This will be proved as the final step in this investigation of the flow equations. It may be recalled that for an isentropic flow field, the usual zero vorticity relations are valid. These relations are given by the equations (2.54). Along an arbitrary surface with direction numbers $(\sigma_1, -1, \sigma_2)$ the equations (2.26) are valid. Using these equations it can be proved that the system (2.54) can be combined to give along an arbitrary surface

$$\frac{1}{r}\,\frac{\delta u_1}{\delta \psi} - \sigma_2\,\frac{\delta v_1}{\delta x} + \frac{\sigma_1}{r}\,\frac{\delta v_1}{\delta \phi} - \frac{\delta w_1}{\delta x} - \frac{\sigma_1}{r}\,w_1 = 0 \qquad (4.75)$$

as follows by taking $\vec{n}.\mathrm{rot}\,\vec{u} = 0$.

Choosing a point on this surface for which $\sigma_2 = 0$ and on using the eqs. (4.50) and (4.52) there is obtained

$$r\,\frac{\delta w''}{\delta x} + u'' + \sigma\,(v'' + w'') = 0 \qquad (4.76)$$

This equation holds along an arbitrary surface and hence also along a characteristis surface. The advantage thus is, that it is not necessary to use stream surfaces, but that only the use of the backward and forward running characteristics is needed.

It should be observed that for a conical shock of finite strength such a simplification is not possible, due to the fact that s_1 is a function of the circumferential variable ϕ . Although eqs. (4.74) are valid in this case, use has to be made of eq. (4.64)c. The only simplification results from the fact that s" is a constant then.

4.2.3 The boundary condition on the body.

The boundary condition on any solid body submerged into a gas flow is that no particle can cross the boundary. Or stated in other words: The velocity component normal to the boundary has to be zero. This is the only condition which has to be fulfilled at the boundary of the solid body if the effects of viscosity are neglected.

In a cartesian coordinate system with correspondingly defined components of the velocity, this condition can be written as

$$u_1 \cos(n,x) + u_2 \cos(n,y) + u_3 \cos(n,z) = 0 \tag{4.77}$$

where n is the normal to the surface.

Before this equation can be applied two problems must be solved. First the geometry of the deformed body has to be known. In the second place it should be observed that equation (4.77) is valid for the real flow field, whereas the boundary condition for the transformed field has to be derived. In the following exposition first the geometry will be considered and thereafter the derivation of the boundary condition itself.

As has been discussed in section 4.2.1 it is assumed that the quasi-axially-symmetric body can be obtained by deforming an originally axially-symmetric body.

To this end it is assumed that the axis of the body in the deformed state lies in the x, z plane and that its shape can be given by the equation

$$z = -\varepsilon\lambda(x) \qquad \text{with } \lambda(x) = 0 \quad \text{for} \quad x = 0 \tag{4.78}$$

The cross sections remain perpendicular to the axis and attached to the same point. This means that the distance from the nose of the body along the deformed axis to a certain cross section is the same as the original axial distance of this section. This situation is given in fig.30. It may be remarked that this shape can be obtained by bending the axis of the original axially-symmetric body.

If a cylindrical coordinate system is used the shape of the undeformed body can be given by

$$x = x^*(r) \tag{4.79a}$$

$$y = r \sin\varphi \tag{4.79b}$$

$$z = r \cos\varphi \tag{4.79c}$$

If the distance along the deformed axis is denoted by s, at a certain position x^*, this distance is given by

$$s = \int_0^{x^*} \sqrt{1+\varepsilon^2\left(\frac{d\lambda}{d\xi}\right)^2}\, d\xi \tag{4.80}$$

At this point the radius of the circle, as measured in the plane perpendicular to the axis, is therefore

$$r = r\left(\int_0^{x^*} \sqrt{1+\varepsilon^2\left(\frac{d\lambda}{d\xi}\right)^2}\, d\xi\right) \tag{4.81}$$

Now the problem is to derive the coordinates of such a circle in the coordinate system (x, r, ϕ). To show the procedure in some detail, terms to the second degree of ε will be retained. Equations (4.80) and (4.81) can then be written as

$$s = x^* + \frac{1}{2}\varepsilon^2 \int_0^{x^*} \left(\frac{d\lambda}{d\xi}\right)^2 d\xi \tag{4.82)a}$$

$$r = r(x^*) + \frac{1}{2}\varepsilon^2 \frac{dr}{dx^*} \int_0^{x^*} \left(\frac{d\lambda}{d\xi}\right)^2 d\xi \tag{4.82)b}$$

If now a local coordinate system (x', y', z') is introduced which has its origin in the point where the tangent to the deformed axis cuts the x-axis (fig.31), the equation of the circle in this system is given by

$$y' = \left\{r(x^*) + \frac{1}{2}\varepsilon^2 \frac{dr}{dx^*} \int_0^{x} \left(\frac{d\lambda}{d\xi}\right)^2 d\xi\right\} \sin\varphi \tag{4.83)a}$$

$$z' = \left\{r(x^*) + \frac{1}{2}\varepsilon^2 \frac{dr}{dx^*} \int_0^{x} \left(\frac{d\lambda}{d\xi}\right)^2 d\xi\right\} \cos\varphi \tag{4.83)b}$$

where φ is the circumferential variable as measured in the local coordinate system.

If now this local system is rotated through an angle γ given by

$$\tan\gamma = \varepsilon \frac{d\lambda}{dx} \tag{4.84}$$

it coincides with the original coordinate system, except that the origin has been shifted by amount $x^* - \dfrac{\lambda}{\frac{d\lambda}{dx}}$.

The coordinates of the circle in the original system are therefore given by

$$y = \left\{ r(x^*) + \frac{1}{2}\,\varepsilon^2 \,\frac{dr}{dx^*} \int_0^{x^*} \left(\frac{d\lambda}{d\xi}\right)^2 d\xi \right\} \sin\varphi \tag{4.85a}$$

$$z = \left\{ r(x^*) + \frac{1}{2}\,\varepsilon^2 \,\frac{dr}{dx^*} \int_0^{x^*} \left(\frac{d\lambda}{d\xi}\right)^2 d\xi \right\} \left\{ 1 - \frac{1}{2}\,\varepsilon^2 \left(\frac{d\lambda}{dx^*}\right)^2 \right\} \cos\varphi - \varepsilon\lambda \tag{4.85b}$$

$$x = x^* + \varepsilon \left\{ r(x^*) + \frac{1}{2}\,\varepsilon^2 \,\frac{dr}{dx^*} \int_0^{x^*} \left(\frac{d\lambda}{d\xi}\right)^2 d\xi \right\} \left\{ 1 - \frac{1}{2}\,\varepsilon^2 \left(\frac{d\lambda}{dx}\right)^2 \right\} \frac{d\lambda}{dx} \cos\varphi \tag{4.85c}$$

whereuse has been made of the values for $\sin\gamma$ and $\cos\gamma$. To obtain the final result it is necessary to settle the relation between φ and ψ. From eqs. (4.85)a and (4.85)b there follows

$$\tan\psi = \frac{\sin\varphi}{\left\{ 1 - \frac{1}{2}\,\varepsilon^2 \left(\frac{d\lambda}{dx}\right)^2 \right\} \cos\varphi - \frac{\varepsilon\lambda}{r(x^*)} \left\{ 1 - \frac{1}{2}\,\varepsilon^2 \,\frac{1}{r(x^*)}\,\frac{dr}{dx^*} \int_0^{x^*} \left(\frac{d\lambda}{d\xi}\right)^2 d\xi \right\}} \tag{4.86}$$

If it is assumed now that φ can be given as

$$\varphi = \psi + \varepsilon\, h + \varepsilon^2\, k$$

the quantities h and k can be calculated by using eq. (4.86). To the first order in ε there results

$$\varphi = \psi - \varepsilon \,\frac{\lambda}{r(x^*)} \sin\psi \tag{4.87}$$

Inserting this result into the system (4.85) the final expressions for the circle considered can be obtained.

Correct up to the first order in ε they prove to be

$$y = r \sin\psi - \varepsilon\,\lambda \sin\psi\cos\psi \tag{4.88a}$$

$$z = r\cos\psi - \varepsilon\,\lambda\cos^2\psi \tag{4.88b}$$

$$x = x^* \qquad + \varepsilon\,\frac{d\lambda}{dx}\, r\cos\psi \tag{4.88c}$$

If it should be necessary to give these formulae correct up to the second order in ε this should be equally possible along the same lines. It will be evident that the equations (4.88) are valid for the whole surface by considering x^*, and thus r, as running coordinates.

According to eq. (4.77) the expressions for the direction cosines in an arbitrary point of the surface have to be known.

These expressions will be derived by using the results obtained in the appendix for the geometry of an arbitrary surface. Therefore the equations (4.88) have to be differentiated with respect to r and ψ. On using eq.A(11) the result reads correct, up to terms in ε,

$$a_{11} = 1 + \left(\frac{dx^*}{dr}\right)^2 + 2\varepsilon\left\{\frac{d\lambda}{dx} + r\frac{d^2\lambda}{dx^2}\frac{dx^*}{dr}\right\}\cos\psi - 2\varepsilon\frac{d\lambda}{dx}\frac{dx^*}{dr}\cos\psi$$

$$a_{22} = r^2 - 2\varepsilon\lambda\, r\cos\psi$$

$$a_{12} = O(\varepsilon)$$

$$\sqrt{a} = r\sqrt{1+\left(\frac{dx^*}{dr}\right)^2}\left\{1-\varepsilon\frac{\lambda}{r}\cos\psi + \varepsilon\frac{\frac{d\lambda}{dx} + r\frac{d^2\lambda}{dx^2}\frac{dx^*}{dr} - \frac{d\lambda}{dx}\frac{dx^*}{dr}}{1+\left(\frac{dx^*}{dr}\right)^2}\cos\psi\right\} \quad (4.89)$$

Using eqs. A(7) and A(13) there follows

$$\cos(n,x) = \frac{1}{\sqrt{a}}\left\{-r + \varepsilon\lambda\cos\psi + \varepsilon r\frac{d\lambda}{dx}\frac{dx^*}{dr}\cos\psi\right\} \quad (4.90)a$$

$$\cos(n,y) = \frac{1}{\sqrt{a}}\left\{r\sin\psi\frac{dx^*}{dr} + \varepsilon r^2\frac{d^2\lambda}{dx^2}\frac{dx^*}{dr}\cos\psi\sin\psi + \right.$$

$$\left. -2\varepsilon\lambda\frac{dx^*}{dr}\sin\psi\cos\psi\right\} \quad (4.90)b$$

$$\cos(n,z) = \frac{1}{\sqrt{a}}\left\{r\cos\psi\frac{dx^*}{dr} + \varepsilon r\frac{d\lambda}{dx} + \varepsilon r^2\frac{d^2\lambda}{dx^2}\frac{dx^*}{dr}\cos^2\psi + \right.$$

$$\left. -\varepsilon\lambda\frac{dx^*}{dr}(\cos^2\psi - \sin^2\psi)\right\} \quad (4.90)c$$

The equations (4.88), (4.89) and (4.90) give the required geometrical relations, which will be used when applying the boundary condition given by eq. (4.77).

As has been remarked, the boundary condition valid in the transformed field has to be derived. To this end it is necessary to express the quantities u_1, v_1 and w_1 occurring in eq. (4.77) in terms of the velocity components in the transformed field. Now, according to eqs. (4.50) in this field the following equations are valid

$$u_1 = u + \varepsilon\ u'' \cos\psi \tag{4.91a}$$

$$v_1 = v + \varepsilon\ v'' \cos\psi \tag{4.91b}$$

$$w_1 = \varepsilon\ w'' \sin\psi \tag{4.91c}$$

The velocities at the surface of the deformed body are then given by (see eq. (4.51))

$$u_s = u + \frac{\partial u}{\partial x}\ dx + \frac{\partial u}{\partial r}\ dr + \varepsilon u'' \cos\psi \tag{4.92a}$$

$$v_s = v + \frac{\partial v}{\partial x}\ dx + \frac{\partial v}{\partial r}\ dr + \varepsilon v'' \cos\psi \tag{4.92b}$$

$$w_s = \varepsilon w'' \sin\psi \tag{4.92c}$$

where the index s refers to the surface.

Herein dx and dr are the axial and radial distances between corresponding points of the deformed and undeformed surface. These distances can be obtained by comparing eqs. (4.88) with (4.79). The results are :

$$dx = \varepsilon \frac{d\lambda}{dx}\ r \cos\psi \tag{4.94a}$$

$$dr = -\varepsilon\lambda \cos\psi \tag{4.94b}$$

Herewith the eqs. (4.92) can be rewritten as

$$u_s = u + \varepsilon \left\{ r \frac{d\lambda}{dx}\ \frac{\partial u}{\partial x} - \lambda \frac{\partial u}{\partial r} + u'' \right\} \cos\psi \tag{4.95a}$$

$$v_s = v + \varepsilon \left\{ r \frac{d\lambda}{dx}\ \frac{\partial v}{\partial x} - \lambda \frac{\partial v}{\partial r} + v'' \right\} \cos\psi \tag{4.95b}$$

$$w_s = \varepsilon\ w'' \sin\psi \tag{4.95c}$$

These expressions give the velocities at the surface of the deformed body, correct up to terms in ε.

The problem at hand is to translate the boundary condition for the real flow field at the surface of the deformed body into one for the transformed flow field at the surface of the undeformed body. With the aid of the results already obtained, this will be possible.

To apply eq. (4.77) it is necessary to express u_2 and u_3 in terms of v_s and w_s. The results are:

$$u_2 = v_s \sin\psi + w_s \cos\psi = v \sin\psi + \varepsilon w'' \cos\psi \sin\psi +$$

$$+ \varepsilon\left\{r \frac{d\lambda}{dx}\frac{\partial v}{\partial x} - \lambda \frac{\partial v}{\partial r} + v''\right\} \cos\psi \sin\psi \qquad (4.96)a$$

$$u_3 = v_s \cos\psi - w_s \sin\psi = v \cos\psi - \varepsilon w'' \sin^2\psi +$$

$$+ \varepsilon\left\{r \frac{d\lambda}{dx}\frac{\partial v}{\partial x} - \lambda \frac{\partial v}{\partial r} + v''\right\} \cos^2\psi \qquad (4.96)b$$

On using eqs. (4.95)a, (4.96) and (4.90), the boundary condition can now be written, correct up to first order terms in ε, as :

$$-ru + rv\frac{dx^*}{dr}\sin^2\psi + rv\frac{dx}{dr}\cos^2\psi +$$

$$+ \varepsilon\cos\psi\left\{u(\lambda + r\frac{d\lambda}{dx}\frac{dx^*}{dr}) - r(\frac{\partial u}{\partial x}r\frac{d\lambda}{dx} - \lambda\frac{\partial u}{\partial r} + u'')\right\} +$$

$$+ \varepsilon\cos\psi\left\{v(r\frac{d\lambda}{dx} + r^2\frac{d^2\lambda}{dx^2}\frac{dx^*}{dr} - \lambda\frac{dx^*}{dr}) + \right.$$

$$\left. + r\frac{dx^*}{dr}(r\frac{\partial v}{\partial x}\frac{d\lambda}{dx} - \lambda\frac{\partial v}{\partial r} + v'')\right\} = 0 \qquad (4.97)$$

The first part of this equation which is independent of ε gives the boundary condition for the purely axially symmetric field, or

$$v = u\frac{dr}{dx} \qquad (4.98)$$

The second part of eq. (4.97) gives the boundary condition for the transformed field, since all the quantities occurring in it are referring to this field. Using eq. (4.98) the condition can be written as

$$u\frac{d\lambda}{dx} - \left\{r\frac{\partial u}{\partial x}\frac{d\lambda}{dx} - \lambda\frac{\partial u}{\partial r} + u''\right\}\frac{dr}{dx^*} + v\left\{r\frac{d^2\lambda}{dx^2} + \frac{d\lambda}{dx}\frac{dr}{dx^*}\right\} +$$

$$+ \left\{r\frac{\partial v}{\partial x}\frac{d\lambda}{dx} - \lambda\frac{\partial v}{\partial r} + v''\right\} = 0 \qquad (4.99)$$

This equation although giving the correct boundary condition is, however, not very useful for numerical calculations since it contains the partial derivatives of u and v.

However, these can be written in terms of derivatives along the fuselage by using the continuity condition and equation (4.98). On using the following relations that are valid along the fuselage:

$$\frac{du}{dx} = \frac{\partial u}{\partial x} + \frac{\partial u}{\partial r}\frac{dr}{dx} \tag{4.100a}$$

and

$$\frac{dv}{dx} = \frac{\partial v}{\partial x} + \frac{\partial v}{\partial r}\frac{dr}{dx} \tag{4.100b}$$

equation (4.99) can be transformed into :

$$u\frac{d\lambda}{dx} - \left\{\frac{du}{dx}\frac{dr}{dx} - \frac{dv}{dx}\right\} r\frac{d\lambda}{dx} + \left\{\frac{\partial u}{\partial r}\frac{dr}{dx} - \frac{\partial v}{\partial r}\right\}\left\{\lambda + r\frac{d\lambda}{dx}\frac{dr}{dx}\right\}$$

$$-u''\frac{dr}{dx} + v'' + v\left\{r\frac{d^2\lambda}{dx^2} + \frac{d\lambda}{dx}\frac{dr}{dx}\right\} = 0 \tag{4.101}$$

The term $\frac{\partial u}{\partial r}\frac{dr}{dx} - \frac{\partial v}{\partial r}$ will now be brought into a more suitable form by using the continuity equation for axially-symmetric flow (3.44)a. Together with the condition (4.98) the following equation, valid along the surface of the body is obtained

$$\frac{\partial u}{\partial x} - \frac{u^2}{a^2}\frac{du}{dx} + \frac{\partial v}{\partial r} + \frac{v}{r} - \frac{vu}{a^2}\frac{dv}{dx} = 0 \tag{4.102}$$

Using eq. (4.100)a it follows that

$$\frac{\partial u}{\partial r}\frac{dr}{dx} - \frac{\partial v}{\partial r} = \frac{du}{dx}\left(1 - \frac{u^2}{a^2}\right) + \frac{v}{r} - \frac{vu}{a^2}\frac{dv}{dx} \tag{4.103}$$

Moreover $\frac{dv}{dx}$ can be expressed in terms of u and $\frac{du}{dx}$ by differentiating eq. (4.98). The result is

$$\frac{dv}{dx} = u\frac{d^2r}{dx^2} + \frac{du}{dx}\frac{dr}{dx} \tag{4.104}$$

Introducing eqs. (4.103) and (4.104) into the boundary condition (4.101) the resulting expression is

$$(1+u')\frac{d\lambda}{dx}+(1+u')r\,\frac{d\lambda}{dx}\,\frac{d^2r}{dx^2}-u''\,\frac{dr}{dx}+v''+(1+u')\,\frac{dr}{dx}\,\left(r\,\frac{d^2\lambda}{dx^2}+\frac{d\lambda}{dx}\,\frac{dr}{dx}\right)+$$

$$+\left\{(1-\frac{u^2}{a^2})\,\frac{du}{dx}+\frac{v}{r}-\frac{vu}{a^2}\,\left(u\,\frac{d^2r}{dx^2}+\frac{dr}{dx}\,\frac{du}{dx}\right)\right\}\left\{\lambda+r\,\frac{d\lambda}{dx}\,\frac{dr}{dx}\right\}=0$$

Taking together some terms the final result is

$$v''-u''\,\frac{dr}{dx}+(1+u')\left\{\left[1+\left(\frac{dr}{dx}\right)^2\right]\frac{d\lambda}{dx}+r\left(\frac{d^2r}{dx^2}\,\frac{d\lambda}{dx}+\frac{d^2\lambda}{dx^2}\,\frac{dr}{dx}\right)\right\}+$$

$$+\left\{r\,\frac{d\lambda}{dx}\,\frac{dr}{dx}+\lambda\right\}\left[\frac{1+u'}{r}\,\frac{dr}{dx}-\frac{(1+u')^3}{a^2}\,\frac{dr}{dx}\,\frac{d^2r}{dx^2}-\beta^2\,\frac{du}{dx}\right]=0 \qquad (4.105)$$

This expression is the required formulation of the boundary condition along the fuselage in the transformed field. It should be remarked that only the first two terms contain the unknown functions v" and u", while the complicated rest of the equation can be calculated as soon as the axially-symmetric field and the function λ are known.

As an example the boundary condition for a cone with semi-top angle ϑ_s will be derived. If the angle of attack is equal to ε the function λ is given by

$$\lambda = x$$

The equation of the cone reads

$$r = x \cot\vartheta_s$$

The boundary condition for a cone proves to be then,

$$v'' - u''\,\tan\vartheta_s + \frac{2}{\cos^2\vartheta_s}\,(1+u') = 0 \qquad (4.106)$$

where use is made of the fact that along the cone surface $\frac{du}{dx} = 0$.

It can be shown that this equation is identical with the boundary condition derived by Stone in ref.8.

To finish the derivation of the equations necessary to construct the transformed field, in the following section, the conditions valid at the shock wave will be derived by applying the general equations obtained in chapter 2.

4.2.4 The boundary conditions at the shock wave.

One of the most important phenomena that occur is the change in the shape of the shock wave due to the flow around the deformed body. To determine this flow field in a unique way certain conditions have to be satisfied at the shock wave. Since the problem has been reduced to the determination of the transformed flow field, the boundary conditions at the real shock have to be given as conditions for the transformed field at the position of the shock for the undeformed body.

First of all, the geometry of the shock wave has to be determined. As indicated in fig.32 the shape of the deformed shock wave has been derived by rotating the cone tangent to the axially-symmetric shock wave, at the point under consideration, through an angle $\varepsilon\alpha$ around the vertex of this cone in the xz plane. This assumption is, as will be shown, in accordance with the analysis up to terms of the order ε. The function α depends on the radial variable r and is, as yet, an unknown quantity.

The velocities at the point P' of the deformed shock can be derived by using equations similar to eq. (4.51). The geometry of the deformed shock surface can be derived analogous to the investigation given in the preceding section. It is given by

$$y = r \sin\psi - \varepsilon\alpha\, r \cot\vartheta_W \sin\psi \cos\psi \qquad (4.107)\text{a}$$

$$z = r \cos\psi - \varepsilon\alpha\, r \cot\vartheta_w \cos^2\psi \qquad (4.107)\text{b}$$

$$x = x^*(r) + \varepsilon r\, \alpha \cos\psi \qquad (4.107)\text{c}$$

where ϑ_w denotes the semi-top angle of the local tangent cone to the axially-symmetric shock surface.

From these equations is readily derived that the local deformations are given by

$$dx = \varepsilon\, r\, \alpha \cos\psi \qquad (4.108)\text{a}$$

$$dr = -\varepsilon\, r\, \alpha \cot\vartheta_w \cos\psi \qquad (4.108)\text{b}$$

Herewith the equations for the velocities prove to be

$$u_1 = u + \varepsilon\alpha r \left\{\frac{\partial u}{\partial x} - \frac{\partial u}{\partial r}\cot\vartheta_w\right\}\cos\psi + \varepsilon u'' \cos\psi \qquad (4.109)\text{a}$$

$$v_1 = v + \varepsilon\alpha r \left\{\frac{\partial v}{\partial x} - \frac{\partial v}{\partial r}\cot\vartheta_w\right\}\cos\psi + \varepsilon v'' \cos\psi \qquad (4.109)\text{b}$$

$$w_1 = \varepsilon w'' \sin\psi \qquad (4.109)\text{c}$$

From a numerical point of view the occurrence of the partial derivatives is undesirable. Just as before they can be eliminated by using the derivatives along more suitable lines. In this case use will be made of the derivative along the shock wave and along a characteristic.

Along a backward running characteristic one has

$$\left(\frac{du}{dx}\right)_b = \frac{\partial u}{\partial x} + \sigma_b \frac{\partial u}{\partial r} \tag{4.110a}$$

and along the shock wave

$$\left(\frac{du}{dx}\right)_w = \frac{\partial u}{\partial x} + \tan\vartheta_w \frac{\partial u}{\partial r} \tag{4.110b}$$

Solving for $\frac{\partial u}{\partial x}$ and $\frac{\partial u}{\partial r}$ from these equations it follows that

$$\frac{\partial u}{\partial r} = \frac{1}{\sigma_b - \tan\vartheta_w}\left\{\left(\frac{du}{dx}\right)_b - \left(\frac{du}{dx}\right)_w\right\} \tag{4.111a}$$

$$\frac{\partial u}{\partial x} = \frac{-1}{\sigma_b - \tan\vartheta_w}\left\{\left(\frac{du}{dx}\right)_b \tan\vartheta_w - \left(\frac{du}{dx}\right)_w \sigma_b\right\} \tag{4.111b}$$

Similar expressions can be derived for $\frac{\partial v}{\partial r}$ and $\frac{\partial v}{\partial x}$. Substituting these expressions into eqs. (4.109) the following relations are obtained for the first two equations:

$$u_1 = u + \frac{\varepsilon\alpha r}{\sigma_b - \tan\vartheta_w}\left\{\left(\frac{du}{dx}\right)_w (\sigma_b + \cot\vartheta_w) - \frac{1}{\sin\vartheta_w \cos\vartheta_w}\left(\frac{du}{dx}\right)_b\right\}\cos\psi + \\ + \varepsilon u'' \cos\psi \tag{4.112a}$$

$$v_1 = v + \frac{\varepsilon\alpha r}{\sigma_b - \tan\vartheta_w}\left\{\left(\frac{dv}{dx}\right)_w (\sigma_b + \cot\vartheta_w) - \frac{1}{\sin\vartheta_w \cos\vartheta_w}\left(\frac{du}{dx}\right)_b\right\}\cos\psi + \\ + \varepsilon v'' \cos\psi \tag{4.112b}$$

The third equation remains unchanged.

The conditions which exist at the shock wave can be given in the easiest way by decomposing the uniform velocity before the shock into three components, one normal to the shock wave, while the other two are tangent to the shock. The relations valid for these components behind the shock as a function of those in front of it have been derived in chapter 2. First the equations for the tangential components will be considered. They are, according to eqs. (2.47), given by

$$u_{f_{t_1}} = u_{a_{t_1}} \tag{2.47a}$$

$$u_{f_{t_2}} = u_{a_{t_2}} \tag{2.47b}$$

If the relations given in the Appendix are used, the direction numbers of the vectors tangent to the shock wave are given by

$$\left\{t_1\right\} = \left\{\frac{\partial x}{\partial r}, \frac{\partial y}{\partial r}, \frac{\partial z}{\partial r}\right\} \tag{4.113a}$$

$$\left\{t_2\right\} = \left\{\frac{\partial x}{\partial \psi}, \frac{\partial y}{\partial \psi}, \frac{\partial z}{\partial \psi}\right\} \tag{4.113b}$$

Observing that cot ϑ_w can be written as $\frac{dx^*}{dr}$, and remembering the relations between the euclidean and cylindrical velocity components, the eqs. (2.47) give rise to the following system of equations

$$v_1 = -(u_1-1)\left\{\frac{dx^*}{dr} + \varepsilon(\alpha + r\frac{d\alpha}{dr})\cos\psi\right\}\left\{1+\varepsilon(\alpha\frac{dx^*}{dr} + r\frac{d\alpha}{dr}\frac{dx^*}{dr} + r\alpha\frac{d^2x^*}{dr^2})\cos\psi\right\} \tag{4.114a}$$

and

$$-\varepsilon r\alpha(u_1-1)\sin\psi + v_1\varepsilon\alpha r\frac{dx^*}{dr}\sin\psi + w_1\left\{r - \varepsilon\alpha r\frac{dx^*}{dr}\cos\psi\right\} = 0 \tag{4.114b}$$

To obtain the third relation between u_1, v_1 and w_1 use will be made of eq. (2.50)

$$\frac{u_{a_n}}{u_{f_n}} = \frac{1}{\gamma+1}\,\frac{(\gamma-1)M_n^2+2}{M_n^2} \tag{2.50}$$

Now it is easily verified that the component u_{f_n} is given by

$$u_{f_n} = \cos\,(n,x) \tag{4.115}$$

Then M_n^2 is given by

$$M_n^2 = M_\infty^2\,\cos\,(n,x)^2 \tag{4.116}$$

To apply the eqs. (2.50) and (4.116) the expressions for the direction cosines have to be derived. According to eq. A(7) they are given by

$$\frac{\cos(n,x)}{X} = -r\left\{1-\varepsilon\left(\alpha\frac{dx^*}{dr} + r\frac{d\alpha}{dr}\frac{dx^*}{dr} + r\alpha\frac{d^2x^*}{dr^2}\right)\cos\psi + -\varepsilon\alpha\frac{dx^*}{dr}\cos\psi\right\} \qquad (4.117)a$$

$$\frac{\cos(n,y)}{X} = r\left\{\sin\psi\frac{dx^*}{dr} + r\varepsilon\frac{d\alpha}{dr}\cos\psi\sin\psi + -\varepsilon\alpha\left(\frac{dx^*}{dr}\right)^2\sin 2\psi\right\} \qquad (4.117)b$$

$$\frac{\cos(n,z)}{X} = r\left\{\cos\psi\frac{dx^*}{dr} + \varepsilon\alpha + r\varepsilon\frac{d\alpha}{dr}\cos^2\psi - \varepsilon\alpha\left(\frac{dx^*}{dr}\right)^2\cos 2\psi\right\} \qquad (4.117)c$$

From these equations there follows for the Mach-number M_n

$$M_n^2 = M_\infty^2\sin^2\vartheta_w\left\{1-2\varepsilon\left(\alpha\frac{dx^*}{dr} + r\frac{d\alpha}{dr}\frac{dx^*}{dr} + r\alpha\frac{d^2x^*}{dr^2}\right)\cos\psi + + 2\varepsilon r\alpha\frac{d^2x^*}{dr^2}\sin^2\vartheta\cos\psi\right\} \qquad (4.118)$$

Now eq. (2.50) can be written into the following form :

$$\cos(n,x) = \frac{(\gamma+1)M_n^2}{(\gamma-1)M_n^2+2}\left\{u_1\cos(n,x)+(v_1\sin\psi + w_1\cos\psi)\cos(n,y) + +(v_1\cos\psi - w_1\sin\psi)\cos(n,z)\right\} \qquad (4.119)$$

By using eq. (4.115) together with eqs. (4.117) and (4.118) this equation can be written as follows:

$$-r\left\{1-\varepsilon\left(\alpha\frac{dx^*}{dr} + r\frac{d\alpha}{dr}\frac{dx^*}{dr} + r\alpha\frac{d^2x^*}{dr^2}\right)\cos\psi - \varepsilon\alpha\frac{dx^*}{dr}\right\}\cdot$$

$$\left[-2M_\infty^2\sin^2\vartheta_w\left\{1-2\varepsilon\left(\alpha\frac{dx^*}{dr} + r\frac{d\alpha}{dr}\frac{dx^*}{dr} + r\alpha\frac{d^2x^*}{dr^2}\right)\cos\psi + 2\varepsilon r\alpha\frac{d^2x^*}{dr^2}\sin^2\vartheta\cos\psi\right\}+2\right] =$$

$$=(\gamma+1)M_\infty^2\sin^2\vartheta_w\left\{1-2\varepsilon\left(\alpha\frac{dx^*}{dr}+r\frac{d\alpha}{dr}\frac{dx^*}{dr}+r\alpha\frac{d^2x^*}{dr^2}\right)\cos\psi+\right.$$

$$\left.+2\varepsilon r\alpha\frac{d^2x^*}{dr^2}\sin^2\vartheta\cos\psi\right\}.$$

$$\left[-(u_1-1)\left\{1-\varepsilon\left(\alpha\frac{dx^*}{dr}+r\frac{d\alpha}{dr}\frac{dx^*}{dr}+r\alpha\frac{dx^*}{dr^2}\right)\cos\psi-\varepsilon\alpha\frac{dx^*}{dr}\cos\psi\right\}+\right.$$

$$+v_1\left\{r\frac{dx^*}{dr}+\varepsilon r\alpha\cos\psi+r^2\varepsilon\frac{d\alpha}{dr}\cos\psi-\varepsilon\alpha r\left(\frac{dx^*}{dr}\right)^2\cos\psi\right\}+$$

$$\left.+w_1.O(\varepsilon)\right] \qquad (4.120)$$

Since only terms up to the order ε are included and since w_1 is of the order ε according to eq. (4.109)c, the term containing w_1 can be dropped from eq. (4.120). Moreover the term v_1 can be eliminated by using eq. (4.114)a. Performing these operations and rearranging the resulting equation for (u_1-1) the following is obtained:

$$(u_1-1)=\frac{2}{\gamma+1}\frac{1-M_\infty^2\sin^2\vartheta_w}{M_\infty^2}+\frac{4\varepsilon}{\gamma+1}\sin^2\vartheta_w\left(\alpha\frac{dx^*}{dr}+r\frac{d\alpha}{dr}\frac{dx^*}{dr}+r\alpha\frac{d^2x^*}{dr^2}\cos^2\vartheta_w\right)\cos\psi \qquad (4.121)$$

This equation gives together with eq. (4.112)a the conditions for u' and u'' which have to be satisfied at the shock. For the axially-symmetric flow the familiar result is derived

$$u'=\frac{2}{\gamma+1}\frac{1-M_\infty^2\sin^2\vartheta_w}{M_\infty^2} \qquad (4.122)\text{a}$$

and for the transformed field one has

$$u''=-\frac{\alpha r}{\sigma_b-\tan\vartheta_w}\left\{\left(\frac{du}{dx}\right)_w(\sigma_b+\cot\vartheta_w)-\frac{1}{\sin\vartheta_w\cos\vartheta_w}\left(\frac{du}{dx}\right)_b\right\}\cos\psi+$$

$$+\frac{4}{\gamma+1}\sin^2\vartheta_w\left(\alpha\frac{dx^*}{dr}+r\frac{d\alpha}{dr}\frac{dx^*}{dr}+r\alpha\frac{d^2x^*}{dr^2}\cos^2\vartheta_w\right) \qquad (4.122)\text{b}$$

To find the values of v' and v'' use will be made of eqs. (4.112)b and (4.114)a, together with eq. (4.121). For the axially-symmetric flow the following condition is found

$$v' = -u' \frac{dx^*}{dr} = -u' \cot \vartheta_w \tag{4.123)a}$$

while for the transformed flow the condition is given by

$$v'' = -\frac{\alpha r}{\sigma_b - \tan\vartheta_w} \left\{ \left(\frac{dv}{dx}\right)_w (\sigma_b + \cot \vartheta_w) - \frac{1}{\sin\vartheta_w \cos\vartheta_w} \left(\frac{dv}{dx}\right)_b \right\} +$$
$$- \frac{4}{\gamma+1} \sin\vartheta_w \cos\vartheta_w \left\{ \left(\alpha + r \frac{d\alpha}{dr}\right) \frac{dx^*}{dr} + r\alpha \frac{d^2x^*}{dr^2} \cos^2\vartheta_w \right\} +$$
$$- u' \left\{ \frac{1}{\sin^2\vartheta_w} \left(\alpha + r \frac{d\alpha}{dr}\right) + r\alpha \frac{dx^*}{dr} \frac{d^2x^*}{dr^2} \right\} \tag{4.123)b}$$

From eq. (4.114)b together with eqs. (4.114)a and (4.121) the condition for the quantity w" can be derived. It takes the following simple form :

$$w'' = \frac{\alpha u'}{\sin^2\vartheta_w} \tag{4.124}$$

So far the velocity components of the transformed field u", v" and w" are expressed as functions of the axially-symmetric velocity components u', v' and the geometry of the shock wave together with the deformation function α.

To complete the discussion of the boundary conditions at the shock the rise in entropy given by eq. (2.52) has to be analyzed. The entropy rise behind the deformed shock can be written in analogy with eqs. (4.109)a and (4.109)b as

$$s_1 = s + \varepsilon\alpha r \left\{ \frac{\partial s}{\partial x} - \frac{\partial s}{\partial r} \cot \vartheta_w \right\} \cos\psi + \varepsilon s'' \cos\psi \tag{4.125}$$

To eliminate the partial derivatives use will be made of the characteristic equation along a streamline and of the derivative along the shock wave. Thus the following relations are valid:

$$u \frac{\partial s}{\partial x} + v \frac{\partial s}{\partial r} = 0$$

and

$$\left(\frac{ds}{dx}\right)_w = \frac{\partial s}{\partial x} + \tan\vartheta_w \frac{\partial s}{\partial r}$$

Solving for $\frac{\partial s}{\partial x}$ and $\frac{\partial s}{\partial r}$ and substituting into eq. (4.125) gives

$$s_1 = s + \varepsilon\alpha r \frac{v+u\cot\vartheta_w}{v-u\tan\vartheta_w} \left(\frac{ds}{dx}\right)_w \cos\psi + \varepsilon s'' \cos\psi \qquad (4.126)$$

By using eq. (4.118), which gives the quantity M_n and retaining only the terms in ε the entropy rise can be written as follows:

$$s_1 = \ln\left\{\left[1+\frac{2\gamma}{\gamma+1}(M_\infty^2\sin^2\vartheta_w-1)\right]\left[\frac{(\gamma+1)M_\infty^2\sin^2\vartheta_w}{(\gamma-1)M_\infty^2\sin^2\vartheta_w+2}\right]^{-\gamma}\right\}+$$

$$+4\varepsilon\left\{\frac{\gamma}{(\gamma-1)M_\infty^2\sin^2\vartheta_w+2} - \frac{\gamma M_\infty^2\sin^2\vartheta_w}{(\gamma+1)\left\{1+\frac{2\gamma}{\gamma+1}(M_\infty^2\sin^2\vartheta_w-1)\right\}}\right\}\cdot$$

$$\left[\left(\alpha+r\frac{d\alpha}{dr}\right)\frac{dx^*}{dr} + r\alpha\frac{d^2x^*}{dr^2}\cos^2\vartheta_w\right]\cos\psi \qquad (4.127)$$

where use is made of the fact that to the first order in ε one has

$$\ln(1+\varepsilon x) = \varepsilon x$$

Comparing eq. (4.127) with eq. (4.126) the quantities s and s" can be obtained. For the axially-symmetric flow the following already used relation is found:

$$s = \ln\left\{\left[1+\frac{2\gamma}{\gamma+1}(M_\infty^2\sin^2\vartheta_w-1)\right]\left[\frac{(\gamma+1)M_\infty^2\sin^2\vartheta_w}{(\gamma-1)M_\infty^2\sin^2\vartheta_w+2}\right]^{-\gamma}\right\} \qquad (4.128)a$$

For the transformed field one has

$$s'' = -\frac{v+u\cot\vartheta_w}{v-u\tan\vartheta_w}\left(\frac{ds}{dx}\right)_w +$$

$$+4\gamma\left\{\frac{1}{(\gamma-1)M_\infty^2\sin^2\vartheta_w+2} - \frac{M_\infty^2\sin^2\vartheta_w}{(\gamma+1)\left\{1+\frac{2\gamma}{\gamma+1}(M_\infty^2\sin^2\vartheta_w-1)\right\}}\right\}\cdot$$

$$\left[\left(\alpha+r\,\frac{d\alpha}{dr}\right)\frac{dx^*}{dr} + r\alpha\,\frac{d^2x^*}{dr^2}\quad \cos^2\vartheta_w\right] \tag{4.128b}$$

The conditions given by the four equations (4.122)b, (4.123)b, (4.124) and (4.128)b constitute quite a complicated system, which can impede the numerical computations considerably. This is mainly due to the occurrence of the derivatives of u, v, and $\frac{dx^*}{dr}$. In this connection it should be observed that elimination of the partial derivatives of u and v is not unique and that another scheme of elimination might lead to more usable forms in some cases.

In the following section a scheme will be given by which the actual computation can be performed in principle.

4.2.5 The calculation procedure.

In the preceding sections the equations for the flow around a deformed axially-symmetric body have been derived in such a way that the calculation of the axially-symmetric flow field and the transformed flow field can be performed simultaneously. The principal features of such a calculation scheme will be discussed here.

The method described relies on a step-by-step computation. The flow quantities in a certain point are derived by using the known quantities in some other point. To start the computation, the flow quantities for the axially symmetric and the transformed field along a certain surface, not coinciding with a characteristic surface, have to be known.

However, the situation encountered here is different. Certain conditions are given along two surfaces, namely the body and the shock wave. To construct the flow field it is necessary that in this case the flow quantities are known along a characteristic surface connecting shock wave and body. Since the analysis has been restricted to bodies with a pointed nose, it is possible to consider this nose over some distance as conical. Then the flow over the nose will be known, since use can be made of the results of Stone, Taylor and Maccoll as discussed before.

As is indicated in fig.33 the quantities are hence known along the backward running characteristic which emanates from the end of the conical region. This characteristic will be called the "first characteristic".

The numerical method, which in fact reduces the governing differential equations into difference equations can be splitted into three essential parts, namely the calculation of a boundary point, a field point and a point on the shock wave. These will be analyzed subsequently. It will be assumed that the computation of the axially-symmetric flow field is a known technique.

The calculation of the quantities u", v", w" and s" in a boundary proceeds as follows. Assume that the points P_1 and P_2 are lying on a backward running characteristic (in the meridional plane) and that P_1 is itself a boundary point. Now the quantities u", v" and s" have to be determined in the point P_3 lying on the boundary and on the forward running characteristic through P_2, provided that these quantities are given in the points P_1 and P_2 (fig.34). Along the boundary the eqs. (4.64)b and (4.64)c are valid. Along the forward running characteristic eq. (4.72)b is valid. In the point P_3 itself the boundary condition, eq. (4.605), has to be satisfied. If the equations are written as difference equations a system of four equations for the four unknown quantities is obtained. This system can in general be solved, giving the required result.

To calculate the flow quantities in a field point, it will be assumed that they are already known in three points of the field (see fig.35). These points are denoted by Q_1, Q_2 and Q_3. They are chosen such that the backward running characteristic through Q_1, the forward running characteristic through Q_3 and the stream line through the point Q_2 are cutting each other in the point Q_4. In this point the four unknown quantities u", v", w" and s" have to be calculated.

Again a system of four equations can be derived, since along Q_3 Q_4 eq. (4.72) is valid and along Q_1 Q_4 eq. (4.71)b is valid, while along the stream line Q_2 Q_4 the eqs. (4.64)b and (4.64)c have to be satisfied. Thus the flow quantities in a field point can be determined in a unique way. Once a new boundary point has been determined, the characteristic can be constructed in the manner described here, until the shock wave. There, use has to be made of the conditions derived for the flow quantities behind the shock wave by applying the procedure sketched below.

Assuming that the flow quantities are given in the point R_1 in the flow field and in the point R_2 on the shock wave, the problem is to compute the velocities in the point R_3 on the shock wave and on the backward running characteristics through R_1 (fig.36).

However, not only the velocities and the rise in entropy, but also the quantity α, determining the deformation of the shock wave, have to be calculated. Thus five unknown quantities u", v", w", s" and α have to be determined. From the last section it follows that in the point R_3 four equations have to be satisfied, viz. eqs. (4.122)b, (4.123)b, (4.124) and (4.128)b. Moreover along R_1R_3 the characteristic equation (4.71)b has to be satisfied. This gives rise to a system of five equations. Thus the required values can be determined. The point R_2 is needed in this case to give a measure of the value of the quantity $\frac{d\alpha}{dr}$.

It will be evident that the above sketched solution is not the only way to calculate the flow field. In fact, in the above given scheme the calculation is performed along backward running characteristics. This can be changed at will to a calculation procedure along forward running characteristics. There is no essential difference. It is perhaps needless to say, that the whole calculation is performed in the plane $\psi = 0$, and that the quantities in an arbitrary point $\psi = \psi_0$ can be obtained by multiplying the obtained results with the appropriate trigonometric quantity, viz. cos ψ_0 or sin ψ_0.

The numerical calculation, although only dependent on two variables, forms a programme of great complexity. No essential difficulties are present, however.

Since all of the calculations are performed in the transformed field, in the following section something will be said about the calculation of the real flow field and on the determination of the lift by using the now known momentum transport method.

4.2.6 On the calculation of the real flow field and the lift.

To calculate the real flow field from the transformed field use has to be made of eq. (4.51). In order to be able to use this formula, the quantities dx and dr have to be known.

However, these quantities are so far only known on the fuselage and on the shock wave. In the flow field itself no method is available to determine these quantities. This is analogous to the statement made about the first order theory of Stone for the flow round an inclined cone in paragraph 4.1. A check on this conclusion and on the whole procedure given here can be obtained by the calculation of the lift as the deficiency of the momentum transport through a control surface. This will be set forth below.

The lifting force working on a configuration moving through a gaseous medium can be derived by two different methods. The usual one is to integrate the pressure along the fuselage. However, the result can also be obtained by considering the momentum flow through a suitably chosen control surface. From the point of view of the accuracy of the numerical calculations it is very desirable to calculate the same quantity using two essentially different expressions. In this case, where care is taken that the flow quantities are correct up to the first order in the small parameter ε, these two expressions should be identical. A special case of such an investigation has already been given in paragraph 4.1 where for the case of a cone, complete agreement between the two expressions for the lift was found.

Moreover it is desirable to have the expression for the lift as an integral over a control surface with a view on the application to optimum problems. To derive such an expression first the control surface has to be chosen. The most convenient choice seems to be to take a part of the shock wave together with an arbitrary closing surface (fig.37), although in most cases it will be of advantage to consider this closing surface as generated by an axially-symmetric characteristic surface.

The part of the shock wave considered is denoted by O_1 and the closing surface by O_2. The coordinate system is defined such that the x-axis lies in the direction of the uniform stream velocity U_∞ through the vertex of the body.

The force L exerted by the body on the air is then given by an equation which is nearly identical to eq. (4.32) :

$$L + \int_{O_1} p_\infty \cos(n,z)dO_1 + \int_{O_1} \rho_1 V_{n_1} W_1 \, dO_1 + \int_{O_2} p_2 \cos(n,z)dO_2 +$$

$$+ \int_{O_2} \rho_2 V_{n_2} W_2 \, dO_2 - p_\infty \pi R_B^2 \varepsilon \alpha^* = 0 \qquad (4.129)$$

Herein the index 1 refers to the shock wave and the index 2 to the closing surface. V_n is the velocity component normal to the surface, whereas W is the velocity in the positive z-direction. The quantity $\varepsilon\alpha^*$ gives the angle between the tangent to the deformed axis and the x-axis at the point where the closing surface is attached to it. Since the solution of the problem has been obtained in the transformed field which is axially-symmetric, the connection between this field and the real flow field should be given.

It may be recalled that the real shock wave can be obtained from the axially-symmetric one by applying a transformation, which is in fact a small rotation of the tangent cone. Also the deformed fuselage is obtained by a given transformation. The assumption is made now that the closing surface is generated by the transformation of an axially-symmetric surface in the transformed field. To this end it is assumed that a certain cone with semi-top angle ϑ_m is rotated through an angle $\varepsilon\alpha_m$ as indicated in fig.38. Here ϑ_m and α_m are functions of the radial coordinate r as measured along the transformed closing surface. It must be stressed that ϑ_m and α_m are unknown quantities in the flow field. Only at the shock wave and the fuselage these quantities are known. At the moment no further assumption about ϑ_m and α_m will be made.

First of all, the geometry of the two parts of the control surface will be analyzed. The geometry of the shock wave has been given in section 4.2.4. The geometry of the closing surface can be given along the same lines as

$$z = r\cos\psi - r\alpha_m\,\varepsilon\cot\vartheta_m\cos^2\psi \qquad (4.130)a$$

$$y = r\sin\psi - r\alpha_m\,\varepsilon\cot\vartheta_m\cos\psi\sin\psi \qquad (4.130)b$$

$$x = x^* + r\alpha_m\,\varepsilon\cos\psi \qquad (4.130)c$$

The quantity x^* is the axial distance of the transformed closing surface, x^*, α_m and ϑ_m are functions of r. From eqs. (4.130) there follows, by applying the results obtained in the Appendix, for the direction cosines of the closing surface

$$\cos(n,x) = \frac{1}{\sqrt{a}}\left[r - \varepsilon r \frac{d}{dr}(r\alpha_m \cot\vartheta_m)\cos\psi - \varepsilon r\, \alpha_m \cot\vartheta_m \cos\psi\right] \tag{4.131a}$$

$$\cos(n,y) = \frac{1}{\sqrt{a}}\left[-r \sin\psi \frac{dx^*}{dr} - \varepsilon r \frac{d}{dr}(\alpha_m r)\cos\psi \sin\psi + \right.$$

$$\left. + 2\varepsilon r\alpha_m \cot\vartheta_m \frac{dx^*}{dr}\cos\psi \sin\psi + \varepsilon r\alpha_m \sin\psi \cos\psi\right] \tag{4.131b}$$

$$\cos(n,z) = \frac{1}{\sqrt{a}}\left[-r\cos\psi \frac{dx^*}{dr} - \varepsilon r \frac{d}{dr}(\alpha_m r)\cos^2\psi + \right.$$

$$\left. + \varepsilon r\alpha_m \cot\vartheta_m \frac{dx^*}{dr}(\cos^2\psi - \sin^2\psi) - \varepsilon r\alpha_m \sin^2\psi\right] \tag{4.131c}$$

The terms of eq. (4.129) will now be calculated one by one. The first integral of this equation can be found by applying the expressions derived in section (4.2.4) for the geometry of the shock wave. It follows that

$$\int_{O_1} p_\infty \cos(n,z)dO_1 = p_\infty \int_0^{2\pi}\int_0^{R_c}\left\{\frac{dx^*}{dr}\cos\psi + \varepsilon\alpha + r\varepsilon\frac{d\alpha}{dr} - \varepsilon\alpha\left(\frac{dx^*}{dr}\right)^2\cos 2\psi\right\} r\,dr\,d\psi$$

or

$$\int_{O_1} p_\infty \cos(n,z)dO_1 = \pi\varepsilon\, p_\infty \int_0^{R_c}\left(2\alpha + r\frac{d\alpha}{dr}\right)r\,dr = \pi\varepsilon\, p_\infty r^2\alpha \Big|_0^{R_c}$$

Thus the first term gives

$$\int_{O_1} p_\infty \cos(n,z)dO_1 = \pi\varepsilon\, p_\infty \alpha_w R_c^2 \tag{4.132}$$

where α_w is the quantity α in the point $r = R_c$ on the shock wave. The second term of eq. (4.129) is very easy, W_1 being equal to zero, because in front of the shock wave the stream is uniform and directed along the x-axis.

Hence

$$\int_{O_1} \rho_1 V_{n_1} W_1\, dO_1 = 0 \tag{4.133}$$

The third term will give some more trouble. First the quantity p_2 has to be evaluated. According to the techniques known now, the following can be written :

$$p_2 = p + \left\{ \frac{\partial p}{\partial x} \; dx + \frac{\partial p}{\partial r} dr \right\} + \varepsilon p'' \cos \psi$$

Using eq. (4.130)a this becomes

$$p_2 = p + \varepsilon \; \alpha_m r \left\{ \frac{\partial p}{\partial x} - \cot \vartheta_m \frac{\partial p}{\partial r} \right\} \cos \psi + \varepsilon \; p'' \cos \psi \tag{4.134}$$

The third term of eq. (4.129) can be found by applying eq. (4.134) together with eq. (4.131)c. It then takes the form

$$I_3 = \int_{O_2} p_2 \cos(n,z) dO_2 = \int_0^{2\pi} \int_0^{R_c} \left\{ p + \varepsilon \alpha_m r \left(\frac{\partial p}{\partial x} - \cot \vartheta_m \frac{\partial p}{\partial r} \right) + \varepsilon p'' \cos \psi \right\} .$$

$$\left\{ -r \cos \psi \frac{dx^*}{dr} - \varepsilon r \frac{d}{dr} (\alpha_m r) \cos^2 \psi + \varepsilon r \alpha_m \cot \vartheta_m \frac{dx^*}{dr} \cos 2\psi + \right.$$

$$\left. - \varepsilon r \alpha_m \sin^2 \psi \right\} dr \, d\psi$$

Integrating with respect to ψ gives

$$I_3 = \varepsilon \pi \int_{R_B}^{R_c} \left[-pr \frac{d}{dr} (\alpha_m r) - pr \alpha_m - r^2 \alpha_m \left(\frac{\partial p}{\partial x} - \cot \vartheta_m \frac{\partial p}{\partial r} \right) \frac{dx^*}{dr} - r \frac{dx^*}{dr} p'' \right] dr$$

By integrating the first term on the right-hand side partially, the following is obtained.

$$I_3 = -\pi \varepsilon p r^2 \alpha_m \Big/_{R_B}^{R_c} + \varepsilon \pi \int_{R_B}^{R_c} \left[r^2 \alpha_m \frac{dp}{dr} - r^2 \alpha_m \left(\frac{\partial p}{\partial x} - \cot \vartheta_m \frac{\partial p}{\partial r} \right) \frac{dx^*}{dr} + \right.$$

$$\left. - r \frac{dx^*}{dr} \; p'' \right] dr$$

Observe now that $\frac{dp}{dr}$ can be written in terms of $\frac{\partial p}{\partial r}$ and $\frac{\partial p}{\partial x}$ as

$$\frac{dp}{dr} = \frac{\partial p}{\partial r} + \frac{\partial p}{\partial x} \frac{dx^*}{dr} \tag{4.135}$$

Substituting this into the expression for I_3 the final result is

$$\int_{O_2} p_2 \cos(n,z)dO_2 = -\pi\varepsilon\left[p_w\alpha_w R_c{}^2 - p_s R_B{}^2\alpha^*\right] +$$

$$-\pi\varepsilon\int_{R_B}^{R_c} r\,\frac{dx^*}{dr}\,p''dr + \pi\varepsilon\int_{R_B}^{R_c} r^2\alpha_m\,\frac{\partial p}{\partial r}\left(1+\cot\vartheta_m\,\frac{dx^*}{dr}\right)dr \qquad (4.136)$$

Finally the fourth integral of eq. (4.129) has to be analyzed. This is the most complicated term occurring in this expression. First of all the expression for the factors occurring in the integrand will be given, viz. :

$$\rho_2 = \rho + \varepsilon\alpha_m r\left\{\frac{\partial\rho}{\partial x} - \cot\vartheta_m\,\frac{\partial\rho}{\partial r}\right\}\cos\psi + \varepsilon\rho''\cos\psi \qquad (4.137)a$$

$$V_{n_2} = \left[1+u'+\alpha_m r\varepsilon\left\{\frac{\partial u}{\partial x} - \cot\vartheta_m\,\frac{\partial u}{\partial r}\right\}\cos\psi + \varepsilon u''\cos\psi\right].$$

$$\left[r-\varepsilon r\,\frac{d}{dr}\,(r\alpha_m\cot\vartheta_m)\cos\psi - \varepsilon r\alpha_m\cot\vartheta_m\cos\psi\right] +$$

$$+\left[v+\varepsilon r\alpha_m\left\{\frac{\partial v}{\partial x} - \cot\vartheta_m\,\frac{\partial v}{\partial r}\right\}\cos\psi + \varepsilon\,v''\cos\psi\right].$$

$$\left[-r\,\frac{dx^*}{dr} - r\,\frac{d}{dr}\,(\alpha_m r)\varepsilon\cos\psi + \varepsilon r\alpha_m\cot\vartheta_m\,\frac{dx^*}{dr}\cos\psi\right] + O(\varepsilon^2) \qquad (4.137)b$$

$$W_2 = v\cos\psi - w\sin\psi =$$

$$= v\cos\psi + \varepsilon r\alpha_m\left\{\frac{\partial v}{\partial x} - \cot\vartheta_m\,\frac{\partial v}{\partial r}\right\}\cos^2\psi + \varepsilon v''\cos^2\psi - \varepsilon w''\sin^2\psi \qquad (4.137)c$$

Multiplying the various quantities with each other and integrating with respect to ψ gives

$$\int_{O_2} \rho_2\,V_{n_2}\,W_2\,dO_2 =$$

$$= \pi\varepsilon\int_{R_B}^{R_c}\left\{\rho''\left[1+u'-v\,\frac{dx^*}{dr}\right]v + \rho v\left[u''-v''\,\frac{dx^*}{dr}\right] + \rho\left[1+u'-v\,\frac{dx^*}{dr}\right](v''-w'')\right\}rdr+$$

$$+\pi\varepsilon \int_{R_B}^{R_c} \alpha_m r^2 \left[1+u'-v\,\frac{dx^*}{dr}\right]\left\{v\left(\frac{\partial\rho}{\partial x} -\cot\ \vartheta_m\,\frac{\partial\rho}{\partial r}\right)+\rho\left(\frac{\partial v}{\partial x} -\cot\ \vartheta_m\,\frac{\partial v}{\partial r}\right)\right\} dr+$$

$$+\pi\varepsilon \int_{R_B}^{R_c} \rho v \left[-(1+u')\left\{r\,\frac{d}{dr}\,(r\alpha_m\cot\vartheta_m)+r\alpha\,\cot\vartheta_m\right\}+\alpha_m r^2\left(\frac{\partial u}{\partial x} -\cot\ \vartheta_m\,\frac{\partial u}{\partial r}\right)\right]dr\ +$$

$$+\pi\varepsilon \int_{R_B}^{R_c} \rho v\left[-v\left\{r\,\frac{d}{dr}\,(\alpha_m r)-r\alpha\cot\vartheta_m\,\frac{dx^*}{dr}\right\}-r^2\alpha_m\,\frac{dx^*}{dr}\,\left(\frac{\partial v}{\partial x} -\cot\vartheta_m\,\frac{\partial v}{\partial r}\right)\right] dr$$

(4.138)

To simplify this complicated expression, first the terms containing derivatives of α_m will be considered. It should be observed that presumably the unknown functions α_m and ϑ_m can be eliminated, just as the function λ in the case of the cone.

$$\pi\varepsilon \int_{R_B}^{R_c} \rho v\left[-(1+u')\left\{r\,\frac{d}{dr}\,(r\alpha_m\cot\vartheta_m)+r\alpha\,\cot\vartheta_m\right\}+\right.$$

$$\left.-v\left\{r\,\frac{d}{dr}\,(\alpha_m r)-r\alpha\,\cot\vartheta_m\,\frac{dx^*}{dr}\right\}\right]\,dr\ =$$

$$= -\pi\varepsilon\rho v r^2\alpha_m\left\{(1+u')\cot\vartheta_m + v\right\}\Bigg/_{R_B}^{R_c} \quad +$$

$$+\ \pi\varepsilon \int_{R_B}^{R_c} r^2\alpha_m\cot\vartheta_m\left\{\rho v\,\frac{du}{dr} + \rho(1+u')\,\frac{dv}{dr} +v(1+u')\,\frac{d\rho}{dr}\right\}dr\ +$$

$$+\ \pi\varepsilon \int_{R_B}^{R_c} \rho v^2\alpha_m r\left\{1+\cot\ \vartheta_m\,\frac{dx^*}{dr}\right\}+\pi\varepsilon \int_{R_B}^{R_c}\alpha_m r^2\left\{2\rho v\,\frac{dv}{dr} + v^2\,\frac{d\rho}{dr}\right\}$$

(4.139)

If now $\frac{d\rho}{dr}$, $\frac{du}{dr}$ and $\frac{dv}{dr}$ are replaced by the expressions corresponding to eq. (4.135), the following result is obtained

$$\int_{O_2} \rho_2 V_{n_2} W_2 dO_2 = -\pi\varepsilon\rho_w v_w R_c{}^2\alpha \left\{(1+u')_w \cot \vartheta_w + v_w\right\} +$$

$$+ \pi\varepsilon\rho_s v_s R_B{}^2\alpha^* \left\{(1+u')_s \cot\vartheta_s + v_s\right\} +$$

$$+\pi\varepsilon \int_{R_B}^{R_c} \left\{\rho'\left[(1+u')-v \frac{dx^*}{dr}\right] v+\rho v \left[u''-v'' \frac{dx^*}{dr}\right] +\rho\left[(1+u')-v \frac{dx^*}{dr}\right] (v''-w'')\right\} r dr$$

$$+\pi\varepsilon \int_{R_B}^{R_c} \alpha_m r^2 \left\{1+\cot\vartheta_m \frac{dx^*}{dr}\right\}\left[(1+u')v \frac{\partial\rho}{\partial x} +v^2 \frac{\partial\rho}{\partial r} + \rho \frac{v^2}{r} + \rho v \frac{\partial u}{\partial x} +\right.$$

$$\left. + \rho(1+u') \frac{\partial v}{\partial x} + 2 \rho v \frac{\partial v}{\partial r} \right] dr \qquad (4.140)$$

Taking all terms together in eq. (4.129) gives the desired result. However, first of all the terms containing the unknown quantity α_m in the integrand will be taken together. The result is obtained by using eq. (4.136) and eq. (4.140). It reads

$$I_\alpha = \pi\varepsilon \int_{R_B}^{R_c} \alpha_m r^2 \left\{1+\cot\vartheta_m \frac{dx^*}{dr}\right\} \left[(1+u')v \frac{\partial\rho}{\partial x} +v^2 \frac{\partial\rho}{\partial r} +\rho \frac{v^2}{r} +\rho v \frac{\partial u}{\partial x} +\rho v \frac{\partial v}{\partial r}\right] dr+$$

$$+\pi\varepsilon \int_{R_B}^{R_c} \alpha_m r^2 \left\{1+\cot\vartheta_m \frac{dx^*}{dr}\right\}\left[\rho(1+u') \frac{\partial v}{\partial x} + \rho v \frac{\partial v}{\partial r} + \frac{\partial p}{\partial r}\right] dr \qquad (4.141)$$

This equation is written in such a way that the important features can be easily seen. They become apparent when the continuity equation and the equation of motion in radial direction for an axially-symmetric flow are written down.
They are:

$$\frac{\partial}{\partial x} \left\{r\rho(1+u')\right\} + \frac{\partial}{\partial r}\left\{r\rho v\right\} = 0 \qquad (4.142)a$$

and $$\rho\left\{(1+u') \frac{\partial v}{\partial x} + v \frac{\partial v}{\partial r}\right\} + \frac{\partial p}{\partial r} = 0 \qquad (4.142)b$$

Inserting these equations into eq. (4.141) it follows that

$$I_\alpha = 0 \tag{4.143}$$

Due to this very important and interesting result, the expression for the lift becomes

$$L = \pi\varepsilon\ R_c^{\,2}\alpha(p_w - p_\infty) - \pi\varepsilon\ R_B^{\,2}\alpha^*\ (p_s - p_\infty) +$$
$$+\pi\varepsilon\ R_c^{\,2}\alpha\rho_w v_w\left\{u_w \cot\vartheta_w + v_w\right\} - \pi\varepsilon\ R_B^{\,2}\alpha^*\rho_s v_s\left\{u_s \cot\vartheta_s + v_s\right\} +$$
$$+\pi\varepsilon \int_{R_B}^{R_c}\left\{p''\frac{dx^*}{dr} - \left(u - v\frac{dx^*}{dr}\right)\left[\rho'' v + \rho(v'' - w'')\right] - \rho v\left(u'' - v''\frac{dx^*}{dr}\right)\right\} r\,dr \tag{4.144}$$

In the case of a cone this result is in accordance with eq. (4.44)

The equation for the lift is thus relatively simple and contains only known quantities, whereas the total expression was derived by using the unknown quantities α_m and ϑ_m.

These quantities are only known on the shock wave and on the fuselage and, indeed, only these occur in the expression. As can be seen this remarkable result is due to the fact that I_α is equal to zero, which in its turn is effected by the occurrence of two of the governing differential equations for the axially-symmetric flow. This leads to the following important conclusion.

Although it is <u>possible</u> by the techniques given here to calculate the pressure distribution along the contour of a given fuselage, it is <u>not possible</u> to calculate the real flow field. Only if an assumption is made about the functions α_m and ϑ_m such a calculation is possible. There are, however, no means to determine such functions.

These statements generalize the result already obtained for the cone.

4.2.7 Summary of the investigation of the flow around a deformed axially-symmetric configuration.

In the second paragraph of this chapter a method has been given to obtain the lifting properties of a deformed axially-symmetric body.

This deformation is caused by rotating the axis. The analysis is exact up to the first order in ε, which is a small parameter defining the deformation.

The influence of the vortical layer is left out from consideration because of not disturbing the pressure distribution in an approximation of this order.

The calculation is set up in such a way that the determination of the axially-symmetric flow field and of the deformed flow field can be done together. To this end the calculation of the deformed field is made in the so-called transformed field. This field is obtained by transforming the boundary conditions on the fuselage and at the shock wave to conditions on the boundaries for the axially-symmetric field.

The equations governing the flow in the transformed field are written in such a way that they become characteristic equations for the transformed field along the axially-symmetric characteristics.

A full account of the derivations necessary to use this method has been given, including the determination of the lift by momentum transport considerations.

The equations are given in such a form that they can be reduced immediately to difference equations for use in numerical calculations. As a start for such calculations the already known results for the flow around a cone will be used.

5 References.

1 Riemann, B. — Ueber die Fortpflanzung ebener Luftwellen von endlicher Schwingungsweite. Gesammelte Werke 1876, p.144.

2 Rankine, J.W.M. — On the thermodynamic theory of waves of finite longitudinal disturbance. Transactions of the Royal Society of London 160 (1870) p. 277-286.

3 Hugoniot, H. — Sur la propogation du mouvement dans les corps et spécialement dans les gaz parfaits. Journal de l'Ecole Polytechnique 58 (1889) 1-125.

4 Ackeret, J. — Ueber Luftkräfte bei sehr grossen Geschwindigkeiten, insbesonders bei ebener Strömungen. Helvetica Physica Acta 1 (1928) 301-322.

5 Kármân, Th. von and N.B. Moore — Resistance of slender bodies moving with supersonic velocities, with special reference to projectiles. American Society of Mechanical Engineers, Transactions 54 (1932) 303-310

6 Taylor, G.I. and J.W. Maccoll — The air pressure on a cone moving at high speeds. Proceedings of the Royal Society (A) 139 (1933) 278-310.

7 Kopal, Z. — Tables of supersonic flow around cones. M.I.T. Technical Report no.1, 1947.

8 Stone, A.H. — On supersonic flow past a slightly yawing cone. Journal of Mathematics and Physics 27 (1948) april.

9 Kopal, Z. — Tables of supersonic flow around yawing cones. M.I.T. Technical Report no.3, 1947.

10 Kopal, Z. — Tables of supersonic flow around cones of large yaw. M.I.T. Technical Report no.5, 1949.

11 Ferri, A. — The method of characteristics for the determination of supersonic flow over bodies of revolution at small angles of attack. NACA report 1044, 1951.

12 Ferri, A. — Supersonic flow around circular cones at angles of attack. NACA report 1045, 1951.

13 Kopal, Z. — A few remarks on the limitations of linearized theory in supersonic flow. M.I.T. Technical report no.2, 1947.

14	Miles, J.W.	Unsteady supersonic flow past slender pointed bodies. NAVORD report 2031, may 1953.
15	Van Dyke, M.D.	Practical calculation of second-order supersonic flow past non-lifting bodies of revolution. NACA TN 2744, 1952.
16	Ehret, D.M.	Accuracy of approximate methods for predicting pressures on pointed non-lifting bodies of revolution in supersonic flow. NACA TN 2764, 1952.
17	Van der Walle, F. and P.J.Zandbergen	Determination of optimum shapes for minimum drag for a given lift and base area in linearized supersonic flow. NLL-report TR-G.10, 1958.
18	Kármàn, Th.von	The problem of resistance in compressible fluids. Proc. Fifth Volta Congress, 1935.
19	Zandbergen P.J. and F.van der Walle	Determination of optimum axially-symmetric shapes with the exact theory of isentropic supersonic flow. NLL-report TR-G.12 (restricted), 1959.
20	Bliss, G.A.	Lectures on the calculus of variations. The University of Chicago Press. Chicago, Ill., 1946.
21	Gill, S.	Proceedings of the Cambridge Philosophical Society, 47, 1951, 96-108.
22	Tsien, H.S.	Supersonic flow over an inclined body of revolution. Journal of the Aeronautical Sciences 5 (1938) 480-483.
23	Erdmann, S.F. and K. Oswatitsch	Schnell arbeitende, lineare Charakteristiken-Verfahren für axiale und schräge Ueberschall-Anströmung um Rotations-Körper mit Ringflächer. Zeitschrift für Flugwissenschaften 2 (1954) 201-215
24	Stone, A.H.	On supersonic flow past a slightly yawing cone.II. Journ. of Math. and Physics. 30 (1952) no.4.
25	Roberts, R.C. and J.D. Riley	A guide to the use of the M.I.T. cone tables. Journal of the Aeronautical Sciences. 21 (1954) 336-342.
26	Sauer, R.	Ueberschallströmung um beliebig geformte Geschoss-spitze unter kleinem Anstellwinkel. Luftfahrtforschung 19 (1942) 148-152.

27 Willett, J.E. — Supersonic flow at the surface of a circular cone at angle of attack. Journ. of Aerospace Sci. 27 (1960) no.12.

28 Sokolnikoff, I.S. — Tensor analysis, Theory and applications. New York, 1951.

Appendix A

On certain geometric relations of an arbitrary surface

In this thesis at several places the geometry has to be known of a so-called deformed surface, the equation of which is given by referring to the variables as measured on the undeformed axially-symmetric body. In general the direction cosines and the element of surface area are the quantities which are of the greatest interest. It seemed advantageous to present the derivation of these quantities here together.

If the arbitrary surface is given by the following equations, with r and ψ considered as surface coordinates

$$x = f\ (r, \psi) \qquad A(1.a)$$

$$y = g\ (r, \psi) \qquad A(1.b)$$

$$z = h\ (r, \psi) \qquad A(1.c)$$

the radius vector can be written as

$$\vec{\rho} = x.\vec{i} + y.\vec{j} + z.\vec{k} \qquad A(2)$$

where $\vec{i}$, $\vec{j}$ and $\vec{k}$ are the unit vectors along the coordinate axes.

If now the change in the vector $\vec{\rho}$ is considered by holding r constant and giving an increment $d\psi$ to ψ and vice versa, the following is obtained

$$\vec{d\rho}_{r=c} = \left\{\frac{\partial x}{\partial \psi}\ \vec{i} + \frac{\partial y}{\partial \psi}\vec{j} + \frac{\partial z}{\partial \psi}\ \vec{k}\right\} d\psi \quad \text{for } r = \text{constant} \qquad A(3.a)$$

$$\vec{d\rho}_{\psi=c} = \left\{\frac{\partial x}{\partial r}\ \vec{i} + \frac{\partial y}{\partial r}\vec{j} + \frac{\partial z}{\partial r}\ \vec{k}\right\} dr \quad \text{for } \psi = \text{constant} \qquad A(3.b)$$

As will be immediately clear, the vector $\vec{d\rho}$ of eq. A(3.a) is tangent to the curve r = constant, whereas eq. A(3.b) gives a vector which is tangent to the curve ψ = constant.

The plane through these two vectors is thus the plane tangent to the surface in the point considered.

The two following vectors tangent to the surface are now introduced.

$$\vec{a}_1 = \frac{\partial x}{\partial r}\ \vec{i} + \frac{\partial y}{\partial r}\vec{j} + \frac{\partial z}{\partial r}\ \vec{k} \qquad (A(4.a)$$

and

$$\vec{a}_2 = \frac{\partial x}{\partial \psi}\vec{i} + \frac{\partial y}{\partial \psi}\vec{j} + \frac{\partial z}{\partial \psi}\vec{k} \qquad A(4.b)$$

Now a vector normal to the surface in the point considered can be found by taking the vector product of $\vec{a}_1$ and $\vec{a}_2$.

This gives

$$\vec{n} = \vec{a}_1 \times \vec{a}_2 \qquad A(5)$$

It is not possible to say in this general case when this vector is pointing inwards or outwards. This depends on the orientation of $\vec{a}_1$ with respect to $\vec{a}_2$. Performing the operation indicated in eq.A(5) gives :

$$\vec{n} = \left\{\frac{\partial y}{\partial r}\frac{\partial z}{\partial \psi} - \frac{\partial z}{\partial r}\frac{\partial y}{\partial \psi}\right\}\vec{i} + \left\{\frac{\partial z}{\partial r}\frac{\partial x}{\partial \psi} - \frac{\partial x}{\partial r}\frac{\partial z}{\partial \psi}\right\}\vec{j} + \left\{\frac{\partial x}{\partial r}\frac{\partial y}{\partial \psi} - \frac{\partial y}{\partial r}\frac{\partial x}{\partial \psi}\right\}\vec{k} \qquad A(6)$$

To obtain the direction cosines it is sufficient to remark that according to eq. A(6) it can be written

$$\cos(n,x) = \left\{\frac{\partial y}{\partial r}\frac{\partial z}{\partial \psi} - \frac{\partial z}{\partial r}\frac{\partial y}{\partial \psi}\right\}\chi \qquad A(7)a$$

$$\cos(n,y) = \left\{\frac{\partial z}{\partial r}\frac{\partial x}{\partial \psi} - \frac{\partial x}{\partial r}\frac{\partial z}{\partial \psi}\right\}\chi \qquad A(7b)$$

$$\cos(n,z) = \left\{\frac{\partial x}{\partial r}\frac{\partial y}{\partial \psi} - \frac{\partial y}{\partial r}\frac{\partial x}{\partial \psi}\right\}\chi \qquad A(7)c$$

Using the relation

$$\cos^2(n,x) + \cos^2(n,y) + \cos^2(n,z) = 1$$

it follows that

$$\chi = \frac{1}{\sqrt{\left\{\frac{\partial y}{\partial r}\frac{\partial z}{\partial \psi} - \frac{\partial z}{\partial r}\frac{\partial y}{\partial \psi}\right\}^2 + \left\{\frac{\partial z}{\partial r}\frac{\partial x}{\partial \psi} - \frac{\partial x}{\partial r}\frac{\partial z}{\partial \psi}\right\}^2 + \left\{\frac{\partial x}{\partial r}\frac{\partial y}{\partial \psi} - \frac{\partial y}{\partial r}\frac{\partial x}{\partial \psi}\right\}^2}} \qquad A(8)$$

Thus the form of the direction cosines is now completely determined. The element of the surface area is now immediately obtained by remarking that it must be equal to the absolute value of the vector product of eqs.A(3)a and A(3)b. It follows by applying eq.A(8) that

$$d\sigma = \frac{1}{\chi}\, dr\, d\psi \qquad A(9)$$

It is perhaps illustrative to show the relation between this result and the first fundamental tensor of the surface. According to eqs.A(2) and A(3) the first fundamental tensor is given by (see f.i. ref.28)

$$ds^2 = (\vec{d\rho}_{\psi=c} + \vec{d\rho}_{r=c})^2 = a_{\alpha\beta}\, du^\alpha du^\beta \qquad A(10)$$

where $a_{\alpha\beta}$ is the first fundamental tensor and $du^\alpha = dr$ and $du^\beta = d\psi$

It follows from eq.A(10) that

$$a_{11} = \vec{a}_1.\vec{a}_1 = \left(\frac{\partial x}{\partial r}\right)^2 + \left(\frac{\partial y}{\partial r}\right)^2 + \left(\frac{\partial z}{\partial r}\right)^2 \qquad A(11)a$$

$$a_{12} = a_{21} = \vec{a}_1.\vec{a}_2 = \frac{\partial x}{\partial r}\frac{\partial x}{\partial \psi} + \frac{\partial y}{\partial r}\frac{\partial y}{\partial \psi} + \frac{\partial z}{\partial r}\frac{\partial z}{\partial \psi} \qquad A(11)b$$

$$a_{22} = \vec{a}_2.\vec{a}_2 = \left(\frac{\partial x}{\partial \psi}\right)^2 + \left(\frac{\partial y}{\partial \psi}\right)^2 + \left(\frac{\partial z}{\partial \psi}\right)^2 \qquad A(11)c$$

Now it is known that

$$d\sigma = \sqrt{a}\, dr\, d\psi = \sqrt{a_{11}a_{22}-a_{12}^{\;2}}\, dr\, d\psi \qquad A(12)$$

From this it can be concluded that

$$\chi = \frac{1}{\sqrt{a}} \qquad A(13)$$

Herewith the required relations for the geometry of the surface are obtained.

Summary in Dutch.

In dit proefschrift is het resultaat van een aantal onderzoekingen betreffende de supersone stroming van een gasvormig medium over axiaal-symmetrische- en daarvan afgeleide - lichamen neergelegd. Bij de bestudering van dergelijke stromingen maakt men vrijwel steeds gebruik van de zogenaamde gelineariseerde potentiaaltheorie, hoewel reeds vrij vroeg gebleken is dat het gebruik van deze theorie in bepaalde gevallen tot grote fouten kan leiden. Men beschikt echter in de meeste gevallen niet over een betere methode van berekening, omdat dit bijna altijd leidt tot de behandeling van de oplossing van niet-lineaire differentiaalvergelijkingen waarvoor slechts in een incidenteel geval een practisch bruikbare berekeningsmethode bestaat.

Het doel van de hier vermelde onderzoekingen is daarom tweeledig. Enerzijds is het van belang, indien mogelijk, een quantitatieve bepaling te geven van de fout die in een bepaald geval ontstaat door het toepassen van de gelineariseerde theorie en zodoende tot een uitspraak te komen over de mogelijke toepasbaarheid van deze theorie. Anderzijds is het gewenst in die gevallen, waarin het blijkt dat het gebruik van de gelineariseerde theorie tot onjuiste resultaten voert, zo mogelijk methodes te ontwikkelen die tot een juister resultaat voeren. Daarbij zal het gewenst zijn deze in een zodanige vorm te presenteren, dat zij gemakkelijk toegankelijk zijn voor een numerieke berekening.

Door de massa- en de impulsstroom te beschouwen met behulp van geschikt gekozen controle-oppervlakken kan men op eenvoudige wijze een quantitatieve waarde voor de gemiddelde fout verkrijgen die door het gegebruik van de gelineariseerde theorie ontstaat. Ter toelichting van de waarde en de bruikbaarheid van deze methode wordt een gedetailleerde vergelijking tussen de resultaten van deze theorie en die van andere, minder benaderende theorieën gegeven.

Voor axiaal-symmetrische lichamen, die volgens hun asrichting worden aangestroomd kan men zulk een vergelijking verkrijgen door gebruik te maken van een exakte karakteristiekenmethode. De resultaten tonen aan dat in het beschouwde geval de waarde van de gelineariseerde theorie sterk beperkt is, vooral wanneer interferentieverschijnselen belangrijk zijn.

Dit inzicht leidt tot het onderzoek van vormen die een zo klein mogelijke golfweerstand bezitten. Hierbij wordt gebruik gemaakt van de niet-lineaire differentiaalvergelijkingen voor isentrope stroming. Door uit te gaan van dezelfde massa- en impulsstroom-vergelijkingen, als gebruikt voor de studie van de toepasbaarheid van de gelineariseerde theorie, kan men met behulp van de variatierekening een oplossing verkrijgen. Voor het geval dat de oppervlakte van de basis van het lichaam is gegeven zijn enige voorbeelden voor verschillende Machgetallen berekend.

Bij de bestudering van de stroming om axiaal-symmetrische lichamen onder invalshoek of met askromming is slechts in het geval van de kegel onder invalshoek een vergelijking mogelijk tussen de gelineariseerde theorie en een minder benaderende theorie. Ook hier blijkt dat de gelineariseerde theorie in de meeste gevallen slechts de orde van grootte van de stromingsgrootheden kan geven, doch dat men voor een meer nauwkeurige berekening van deze grootheden gebruik zal moeten maken van andere, betere theorieën.

Tot dat doel wordt hier een methode afgeleid waarbij men uitgaat van de volledige vergelijkingen voor een supersone stroming. Het veld om een quasi axiaal-symmetrisch lichaam denkt men daarbij te bestaan uit het oorspronkelijke axiaal-symmetrische veld en een daarop gesuperponeerde verstoring, overeenkomstig de door Stone opgestelde theorie voor de stroming om een kegel onder invalshoek. Het onderzoek blijft beperkt tot termen van de eerste orde van een kleine vervormingsparameter. Er zij opgemerkt dat reeds Ferri een poging heeft gedaan tot een dergelijke theorie te komen. Het hier beschouwde geval is echter iets algemener van opzet en sluit meer aan bij de door Stone gegeven afleiding. Speciale aandacht wordt besteed aan het afleiden van de voorwaarden op de romp en ter plaatse van de schokgolf, terwijl met behulp van de reeds eerder genoemde impulsstroom-vergelijking wordt aangetoond dat het in feite niet mogelijk is een uitspraak te doen over het echte stromingsveld. De methode, die het mogelijk maakt de berekening als een karakteristiekenmethode gebaseerd op de axiaal-symmetrische karakteristieken, uit te voeren, is in een zodanige vorm gegeven dat men haar zonder verdere bewerking voor de numerieke behandeling kan gebruiken.

Table 1.a The quantity K as a function of Mach number M_∞ and semi-angle ϑ_s.

ϑ_s \ M_∞	1.5	2.0	3.0	4.0	5.0
5.0°	5.10	7.82	14.51	22.40	31.18
7.5°	9.82	11.80	26.82	40.66	55.78
10.0°	15.34	22.84	40.68	60.91	82.70
12.5°	21.40	31.60	55.56	82.40	-
15.0°	27.83	40.82	71.10	-	-
20.0°	41.25	60.09	-	-	-
25.0°	54.96	79.92	-	-	-

Table 1.b The quantity K_1 as a function of Mach number M_∞ and semi-angle ϑ_s.

ϑ_s \ M_∞	1.5	2.0	3.0	4.0	5.0
5.0°	5.98	9.30	17.38	26.69	36.67
7.5°	11.61	17.65	31.72	46.92	62.22
10.0°	18.16	27.08	46.91	67.11	86.36
12.5°	25.24	36.97	61.97	86.10	-
15.0°	32.57	46.95	76.41	-	-
20.0°	47.22	66.26	-	-	-
25.0°	61.17	84.01	-	-	-

Table 2 Comparison of body radius and drag as obtained by different methods for cones.

Cones		R_B^2 as given	R_B^2 acc. to eq. (3.7)	$\frac{D_o}{\rho_\infty U_\infty^2}$ acc. to eq. (3.32)	$\frac{D_o}{\rho_\infty U_\infty^2}$ acc. to eq. (3.17)
$\vartheta_s = 7.5°$	$M_\infty = 2$	1.0000	0.99998	0.10303	0.10303
	$M_\infty = 5$	1.0000	1.00012	0.07139	0.07140
$\vartheta_s = 12.5°$	$M_\infty = 2$	1.0000	0.99999	0.23577	0.23576
	$M_\infty = 4$	1.0000	1.00021	0.18334	0.18337

Table 3 The comparison of the body radius and the drag calculated by different methods.

	Characteristic from x/ℓ =	R_B^2	R_B^2 along characteristic	$D/\rho_\infty U_\infty^2$ along fuselage	$D/\rho_\infty U_\infty^2$ along characteristic
$\vartheta=7.5^\circ$ $M_\infty=2$	0.4466	0.00121	0.00122	$0.4070.10^{-4}$	$0.4086.10^{-4}$
P=1.0	0.8399	0.00044	0.00045	$0.8421.10^{-4}$	$0.8421.10^{-4}$
$\vartheta=7.5^\circ$ $M_\infty=2$	0.4466	0.00121	0.00122	$0.4070.10^{-4}$	$0.4092.10^{-4}$
P=0.999997	0.8399	0.00044	0.00045	$0.8421.10^{-4}$	$0.8435.10^{-4}$
$\vartheta=7.5^\circ$ $M_\infty=2$	0.4666	0.00121	0.00122	$0.4070.10^{-4}$	$0.4092.10^{-4}$
P variable	0.8399	0.00044	0.00045	$0.8421.10^{-4}$	$0.8435.10^{-4}$
$\vartheta=12.5^\circ$ $M_\infty=2$	0.3966	0.00321	0.00322	$0.3003.10^{-3}$	$0.2974.10^{-3}$
P=1.0	0.7184	0.00249	0.00251	$0.4040.10^{-3}$	$0.3966.10^{-3}$
$\vartheta=12.5^\circ$ $M_\infty=2$	0.3966	0.00321	0.00321	$0.2994.10^{-3}$	$0.3013.10^{-3}$
P=0.999606	0.7184	0.00249	0.00248	$0.4033.10^{-3}$	$0.4090.10^{-3}$
$\vartheta=12.5^\circ$ $M_\infty=2$	0.3966	0.00321	0.00321	$0.2994.10^{-3}$	$0.3008.10^{-3}$
P variable	0.7184	0.00249	0.00249	$0.4033.10^{-3}$	$0.4050.10^{-3}$
$\vartheta=7.5^\circ$ $M_\infty=5$	0.3975	0.00113	0.00115	$0.3481.10^{-4}$	$0.3345.10^{-4}$
P=1	0.7275	0.00085	0.00089	$0.4430.10^{-4}$	$0.4194.10^{-4}$
$\vartheta=7.5^\circ$ $M_\infty=5$	0.3975	0.00113	0.00112	$0.3399.10^{-4}$	$0.3453.10^{-4}$
P=0.993965	0.7275	0.00085	0.00083	$0.4357.10^{-4}$	$0.4608.10^{-4}$
$\vartheta=7.5^\circ$ $M_\infty=5$	0.3975	0.00113	0.00113	$0.3399.10^{-4}$	$0.3424.10^{-4}$
P variable	0.7275	0.00085	0.00086	$0.4357.10^{-4}$	$0.4416.10^{-4}$
$\vartheta=12.5^\circ$ $M_\infty=4$	0.3946	0.00318	0.00333	$0.2674.10^{-3}$	$0.2480.10^{-3}$
P=1	0.7704	0.00198	0.00226	$0.3528.10^{-3}$	$0.3184.10^{-3}$
$\vartheta=12.5$ $M_\infty=4$	0.3946	0.00318	0.00312	$0.2465.10^{-3}$	$0.2572.10^{-3}$
P=0.970768	0.7704	0.00198	0.00171	$0.3344.10^{-3}$	$0.3776.10^{-3}$
$\vartheta=12.5$ $M_\infty=4$	0.3946	0.00318	0.00319	$0.2465.10^{-3}$	$0.2547.10^{-3}$
P variable	0.7704	0.00198	0.00204	$0.3344.10^{-3}$	$0.3463.10^{-3}$

Table 4 The quantity $\bar{X}$ as a function of Mach number M_∞ and semi-angle ϑ_s.

ϑ_s \ M_∞	1.5	2.0	3.0	4.0
10°	7.26	7.31	10.50	13.50
15°	11.72	13.02	15.52	-
20°	17.53	16.56	-	-
30°	32.85	-	-	-

Table 5a Velocity distribution along the aft characteristic surface, and the shape of this surface for $M_\infty = 2.5$
$R_B = 0.0845$ $R_C = 0.7541$ $\ell = 3.2773$

u-1	v	x	r
-0.0012055	0.0027474	1.72794	0.75413
-0.0011896	0.0027842	1.77312	0.7345
-0.0011727	0.0028233	1.81915	0.7145
-0.0011550	0.0028641	1.86519	0.6945
-0.0011366	0.0029068	1.91124	0.6745
-0.0011174	0.0029513	1.95730	0.6545
-0.0010973	0.0029980	2.00336	0.6345
-0.0010761	0.0030469	2.04943	0.6145
-0.0010539	0.0030983	2.09551	0.5945
-0.0010306	0.0031524	2.14161	0.5745
-0.0010060	0.0032094	2.18771	0.5545
-0.0009800	0.0032696	2.23382	0.5345
-0.0009526	0.0033332	2.27994	0.5145
-0.0009235	0.0034008	2.32607	0.4945
-0.0008925	0.0034726	2.37222	0.4745
-0.0008595	0.0035491	2.41838	0.4545
-0.0008243	0.0036309	2.46456	0.4345
-0.0007865	0.0037186	2.51074	0.4145
-0.0007459	0.0038129	2.55695	0.3945
-0.0007021	0.0039147	2.60317	0.3745
-0.0006545	0.0040251	2.64942	0.3545
-0.0006028	0.0041453	2.69568	0.3345
-0.0005462	0.0042769	2.74197	0.3145
-0.0004839	0.0044218	2.78828	0.2945
-0.0004148	0.0045823	2.83462	0.2745
-0.0003378	0.0047615	2.88099	0.2545
-0.0002510	0.0049634	2.92739	0.2345
-0.0001522	0.0051931	2.97384	0.2145
-0.0000386	0.0054576	3.02033	0.1945
0.0000943	0.0056667	3.06687	0.1745
0.0002524	0.0061345	3.11347	0.1545
0.0004448	0.0065820	3.16015	0.1345
0.0006861	0.0071428	3.20692	0.1145
0.0010014	0.0078742	3.25381	0.0945
0.0012000	0.0083342	3.27731	0.0845

Table 5b. Velocity distribution along the aft characteristic surface, and the shape of this surface for $M_{\infty} = 3.5$

$R_B = 0.0845$ $R_C = 0.4982$ $\ell = 3.0867$

u-1	v	x	r
-0.0013026	0.0043242	1.67103	0.4982
-0.0013017	0.0043274	1.67342	0.4975
-0.0012831	0.0043909	1.72090	0.4835
-0.0012637	0.0044572	1.76840	0.4695
-0.0012435	0.0045266	1.81592	0.4555
-0.0012222	0.0045993	1.86345	0.4415
-0.0011999	0.0046757	1.91100	0.4275
-0.0011765	0.0047559	1.95856	0.4135
-0.0011519	0.0048403	2.00615	0.3995
-0.0011259	0.0049294	2.05375	0.3855
-0.0010985	0.0050235	2.10138	0.3715
-0.0010694	0.0051231	2.14903	0.3575
-0.0010386	0.0052289	2.19670	0.3435
-0.0010058	0.0053414	2.24440	0.3295
-0.0009708	0.0054614	2.29212	0.3155
-0.0009335	0.0055898	2.33988	0.3015
-0.0008933	0.0057276	2.38766	0.2875
-0.0008502	0.0058759	2.43547	0.2735
-0.0008035	0.0060363	2.48333	0.2595
-0.0007529	0.0062104	2.53122	0.2455
-0.0006976	0.0064002	2.57915	0.2315
-0.0006371	0.0066083	2.62713	0.2175
-0.0005704	0.0068378	2.67516	0.2035
-0.0004963	0.0070927	2.72325	0.1895
-0.0004134	0.0073778	2.77140	0.1755
-0.0003198	0.0076997	2.81962	0.1615
-0.0002130	0.0080670	2.86792	0.1475
-0.0000895	0.0084913	2.91631	0.1335
0.0000555	0.008989	2.96482	0.1195
0.0002290	0.0095838	3.01345	0.1055
0.0004418	0.0103115	3.06224	0.0915
0.0005680	0.0107420	3.08671	0.0845

Table 5c Velocity distribution along the aft characteristic surface, and the shape of this surface for $M_\infty = 4.5$
$R_B = 0.0845$ $R_C = 0.3886$ $\ell = 3.0816$

u-1	v	x	r
-0.0012669	0.0054712	1.70497	0.3886
-0.0012603	0.0055012	1.72330	0.3845
-0.0012436	0.0055765	1.76803	0.3745
-0.0012263	0.0056549	1.81277	0.3645
-0.0012082	0.0057367	1.85754	0.3545
-0.0011894	0.0058221	1.90233	0.3445
-0.0011697	0.0059114	1.94714	0.3345
-0.0011491	0.0060048	1.99198	0.3245
-0.0011274	0.0061028	2.03684	0.3145
-0.0011048	0.0062056	2.08173	0.3045
-0.0010809	0.0063137	2.12664	0.2945
-0.0010558	0.0064275	2.17159	0.2845
-0.0010294	0.0065477	2.21657	0.2745
-0.0010014	0.0066747	2.26158	0.2645
-0.0009717	0.0068092	2.30662	0.2545
-0.0009403	0.0069521	2.35171	0.2445
-0.0009068	0.0071043	2.39683	0.2345
-0.0008710	0.0072666	2.44199	0.2245
-0.0008328	0.0074404	2.48720	0.2145
-0.0007917	0.0076270	2.53246	0.2045
-0.0007474	0.0078282	2.57778	0.1945
-0.0006996	0.0080457	2.62314	0.1845
-0.0006476	0.0082821	2.66857	0.1745
-0.0005908	0.0085400	2.71407	0.1645
-0.0005285	0.0088231	2.75964	0.1545
-0.0004596	0.0091356	2.80530	0.1445
-0.0003831	0.0094830	2.85104	0.1345
-0.0002973	0.0098721	2.89689	0.1245
-0.0002001	0.0103119	2.94285	0.1145
-0.0000889	0.0108144	2.98894	0.1045
0.0000400	0.0113958	3.03519	0.0945
0.0001920	0.0120788	3.08162	0.0845

Table 6 Comparison between the lift on a cone as integrated along the cone surface and determined from momentum transport considerations according to the first order theory of Stone.

ϑ_s	M_∞	P	α	$\frac{L}{\pi R_s^2 \varepsilon \rho_\infty U_\infty^2}$ (along body)	$\frac{L}{\pi R_B^2 \varepsilon \rho_\infty U_\infty^2}$ (momentum)
5°	1.1554	1.0000	0.0000	0.007188	0.007177
12.5°	1.6530	0.9999	0.2155	0.03761	0.03762
12.5°	1.8810	0.9997	0.2688	0.03791	0.03792
12.5°	2.1496	0.9993	0.3322	0.03821	0.03819
12.5°	2.4760	0.9982	0.4059	0.03853	0.03851
12.5°	2.8907	0.9950	0.4900	0.03896	0.03895
12.5°	3.4532	0.9861	0.5834	0.03947	0.03948
12.5°	4.3002	0.9590	0.6891	0.04014	0.04014
30°	3.8497	0.5712	0.9714	0.11476	0.11471

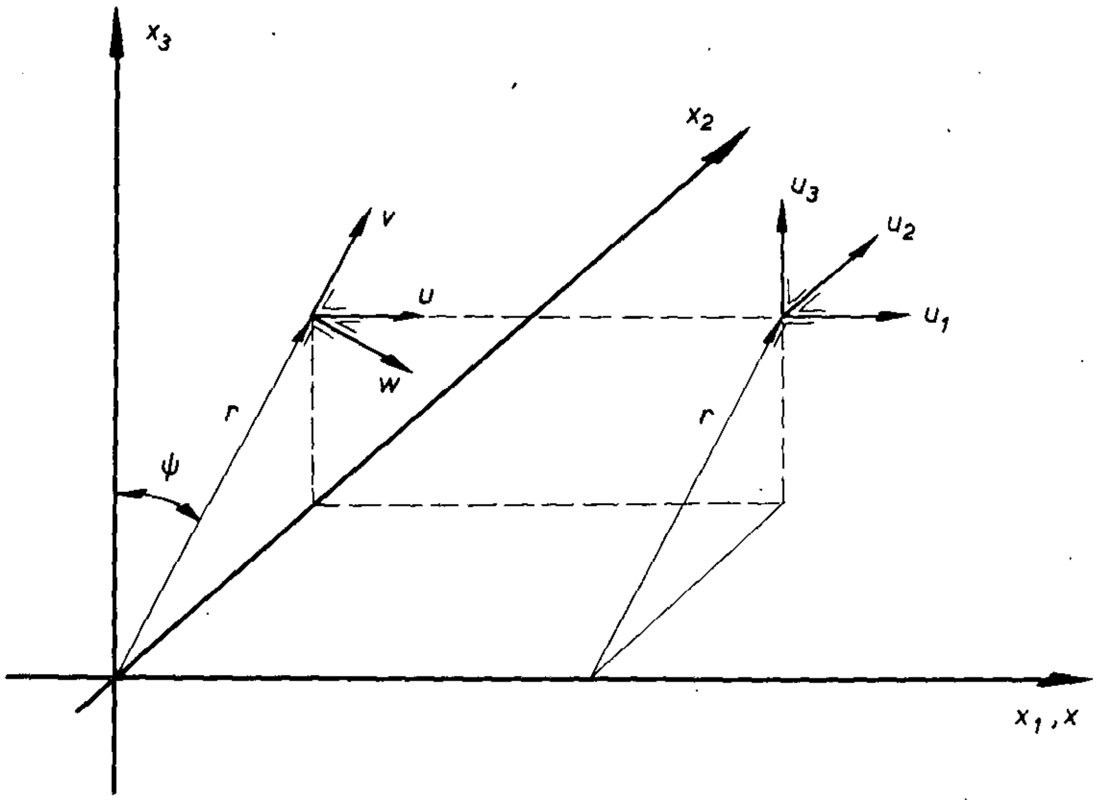

FIG. 1 THE CARTESIAN AND THE CYLINDRICAL COORDINATE SYSTEMS WITH THE ASSOCIATED VELOCITY COMPONENTS.

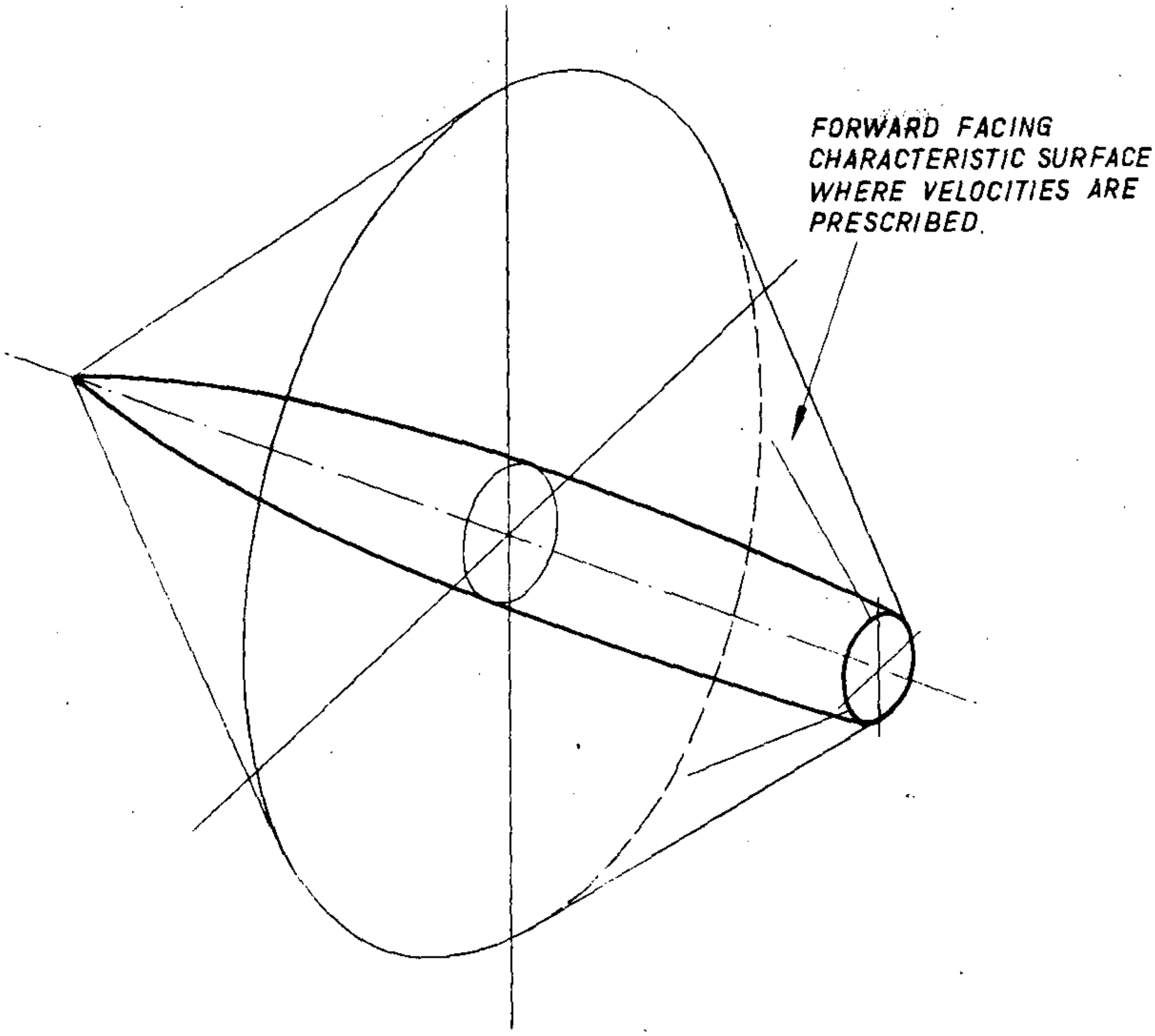

FIG. 2 THE FORWARD FACING CHARACTERISTIC SURFACE, EMANATING FROM THE BASE.

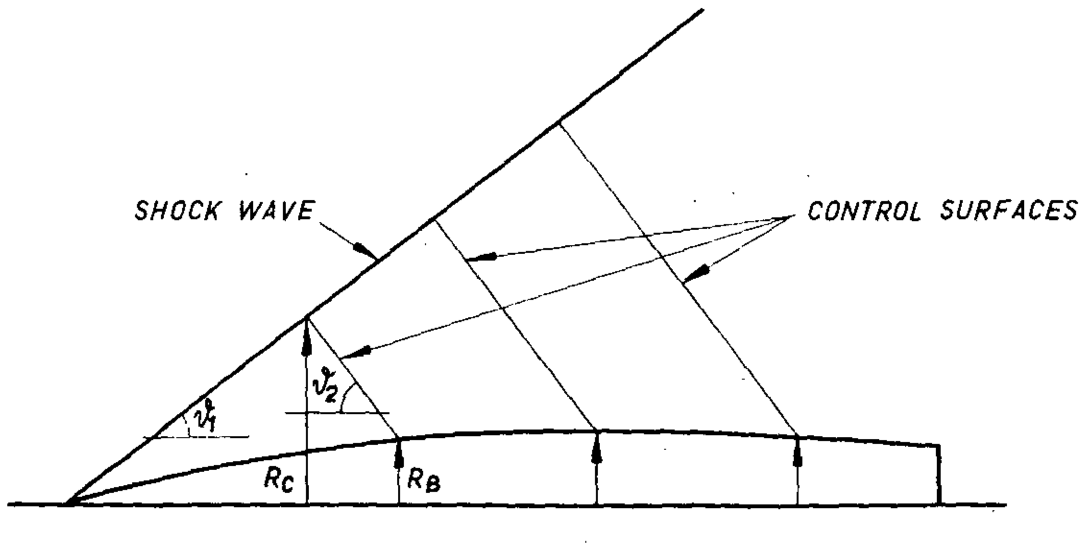

FIG. 3 MERIDIONAL SECTION OF BODY AND CONTROL SURFACES.

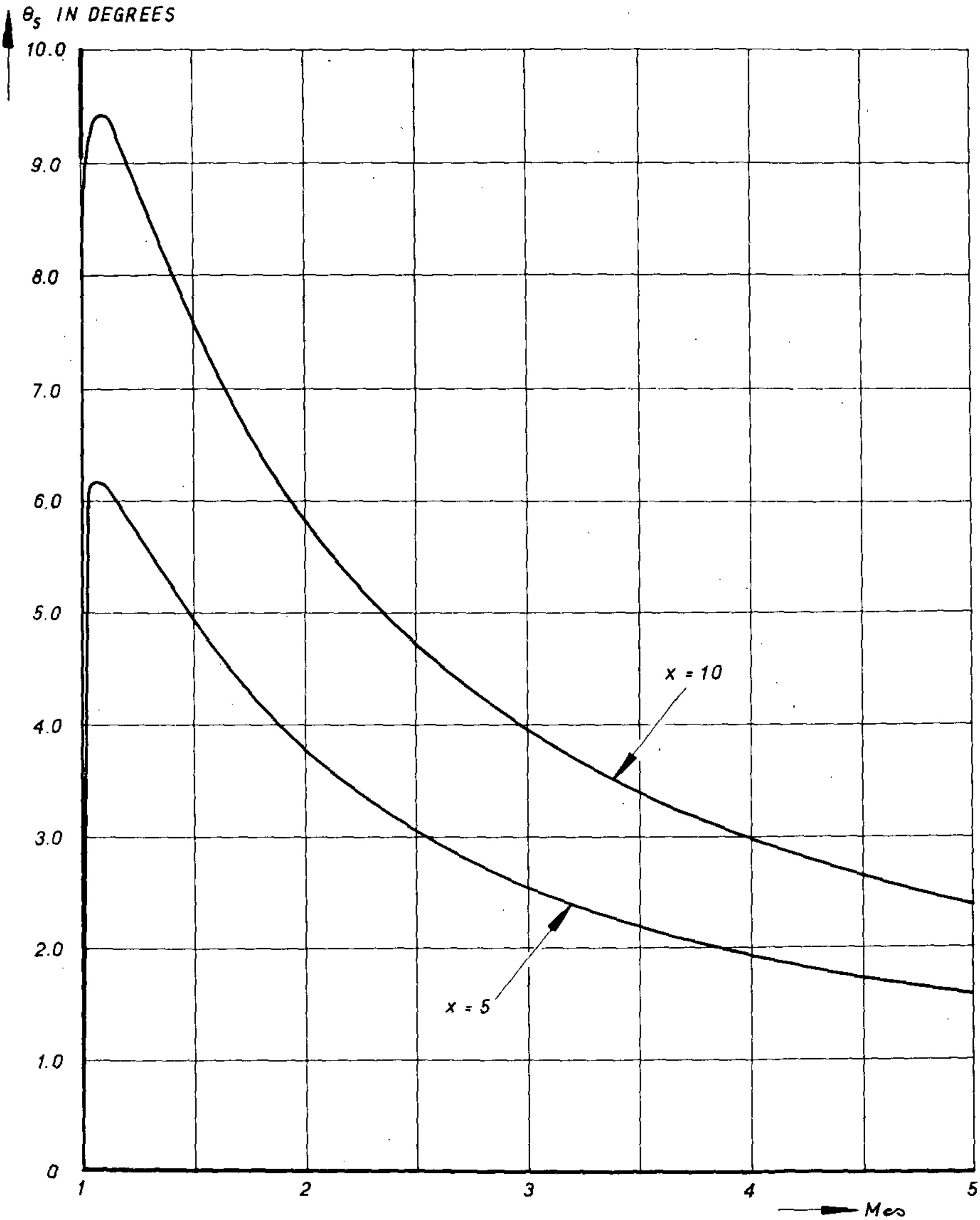

FIG. 4 LIMITS OF THE APPLICABILITY OF LINEARIZED THEORY FOR THE FLOW AROUND A CONE.

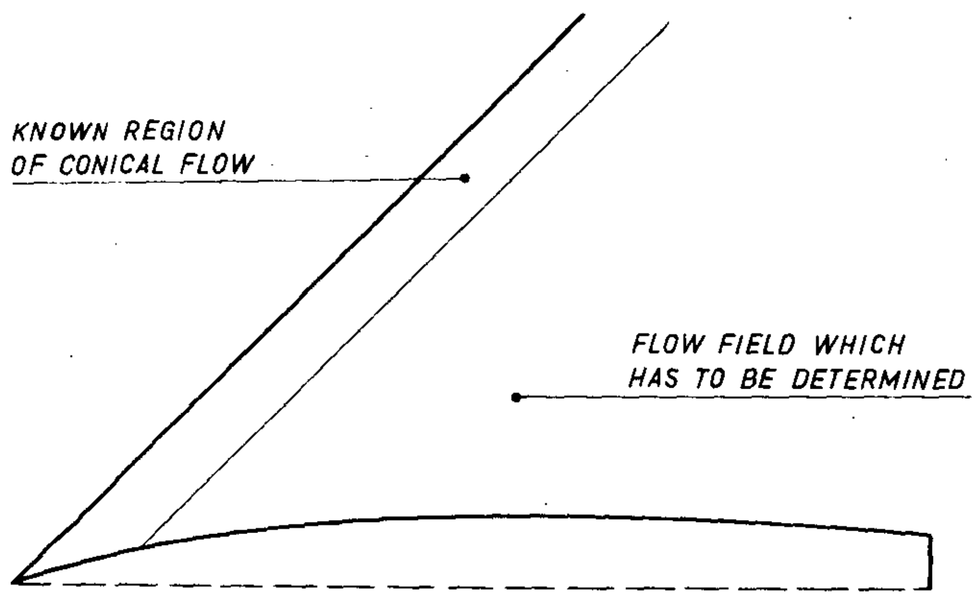

FIG. 5 ARBITRARY AXIALLY SYMMETRIC BODY WITH CONICAL NOSE REGION.

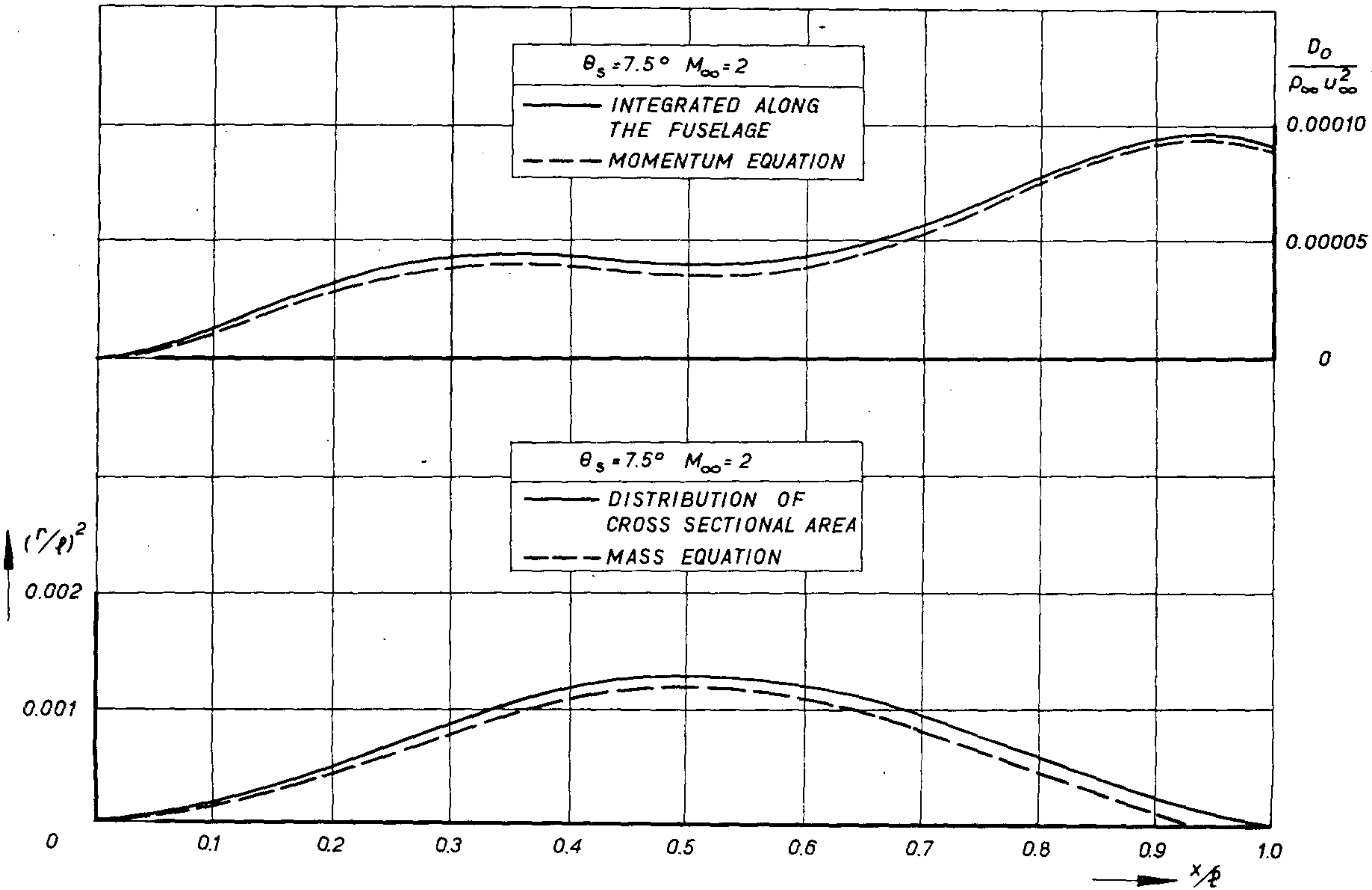

FIG. 6a COMPARISON OF THE TWO SIDES OF THE MASS FLOW AND MOMENTUM EQUATION FOR THE BODY WITH $s = 13.7$ AND $M_\infty = 2$.

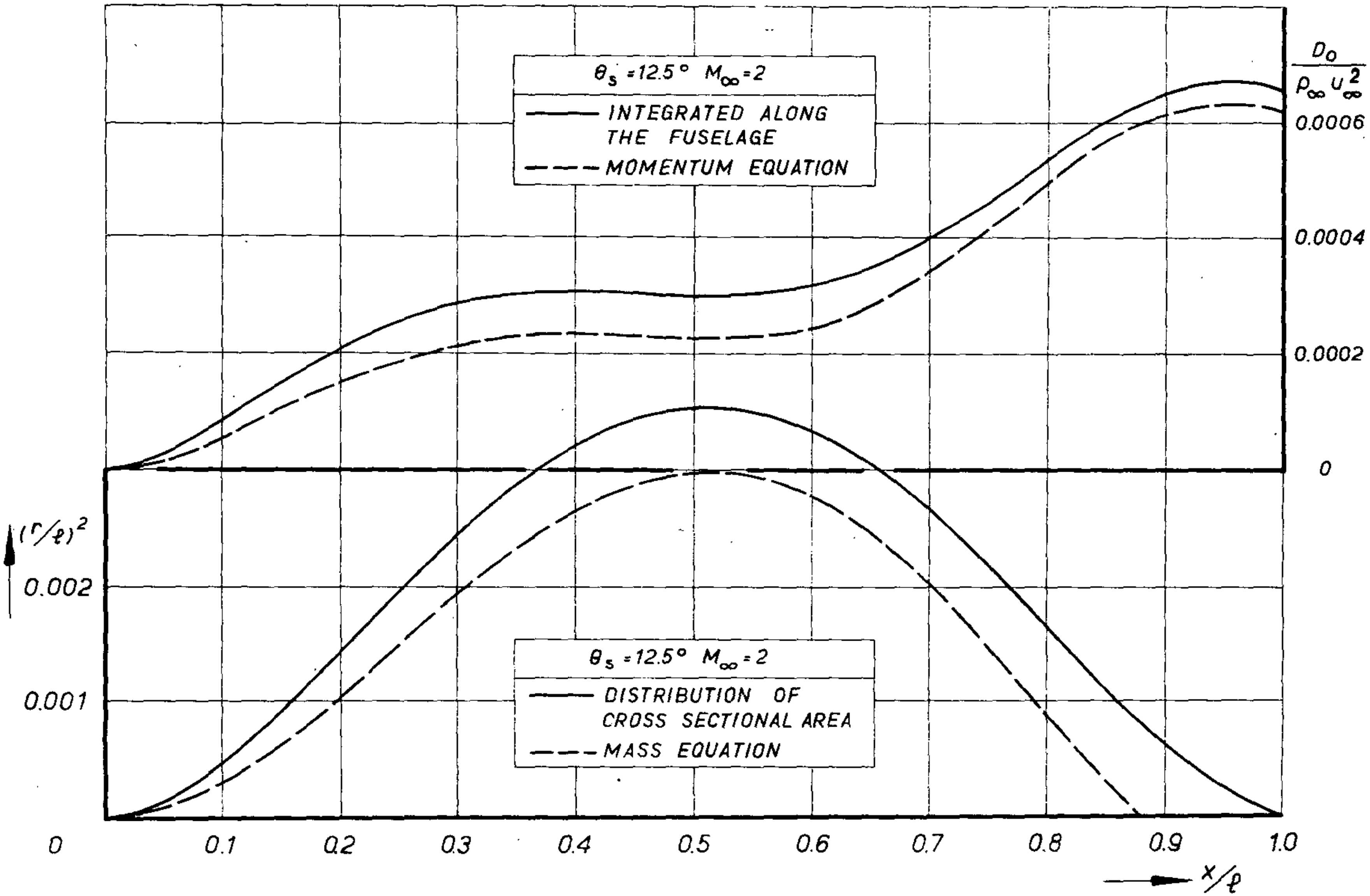

FIG. 6b COMPARISON OF THE TWO SIDES OF THE MASS FLOW AND MOMENTUM EQUATION FOR THE BODY WITH s = 2.4 AND $M_\infty = 2$.

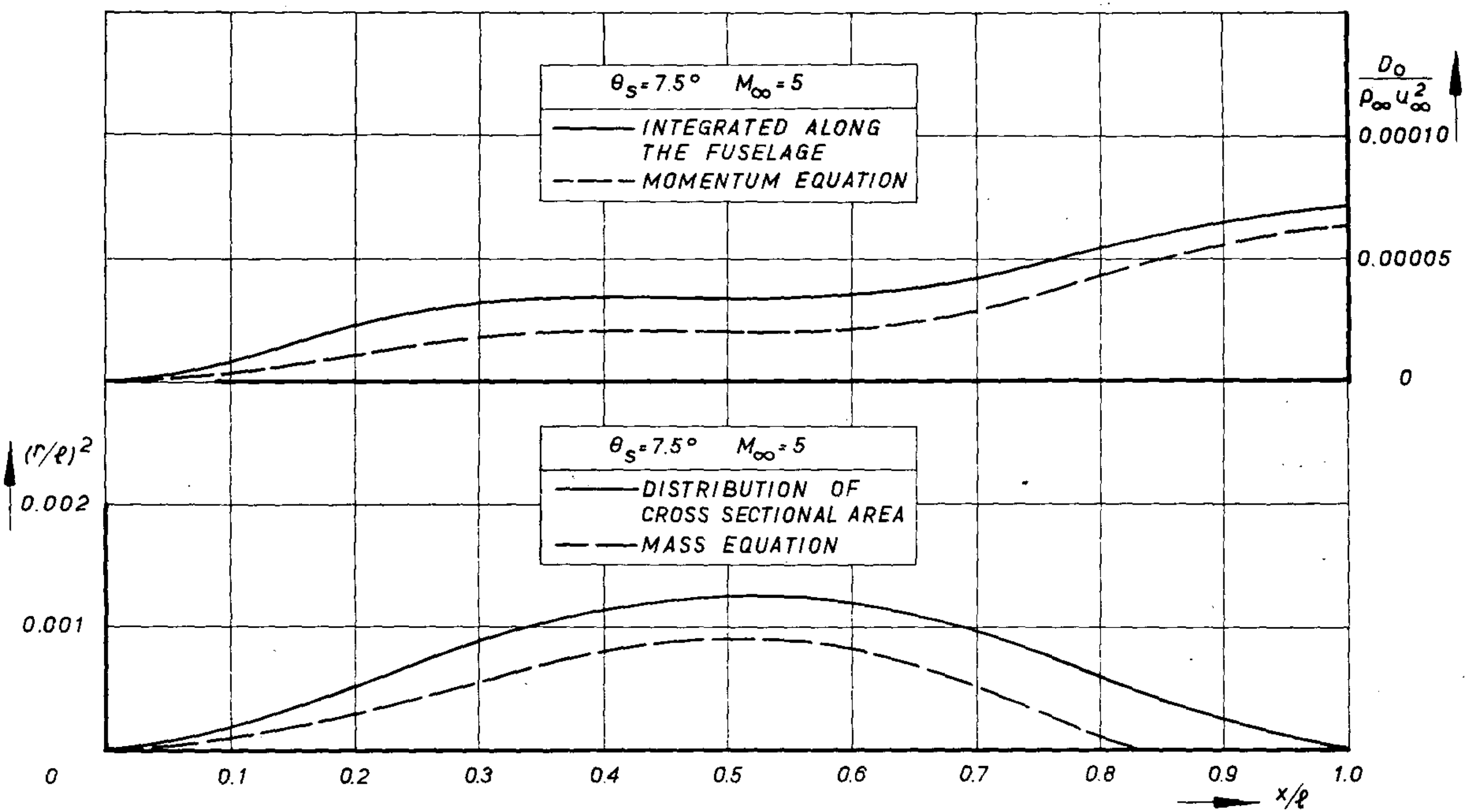

FIG. 6c COMPARISON OF THE TWO SIDES OF THE MASS FLOW AND MOMENTUM EQUATION FOR THE BODY WITH $s = 13.7$ AND $M_\infty = 5$.

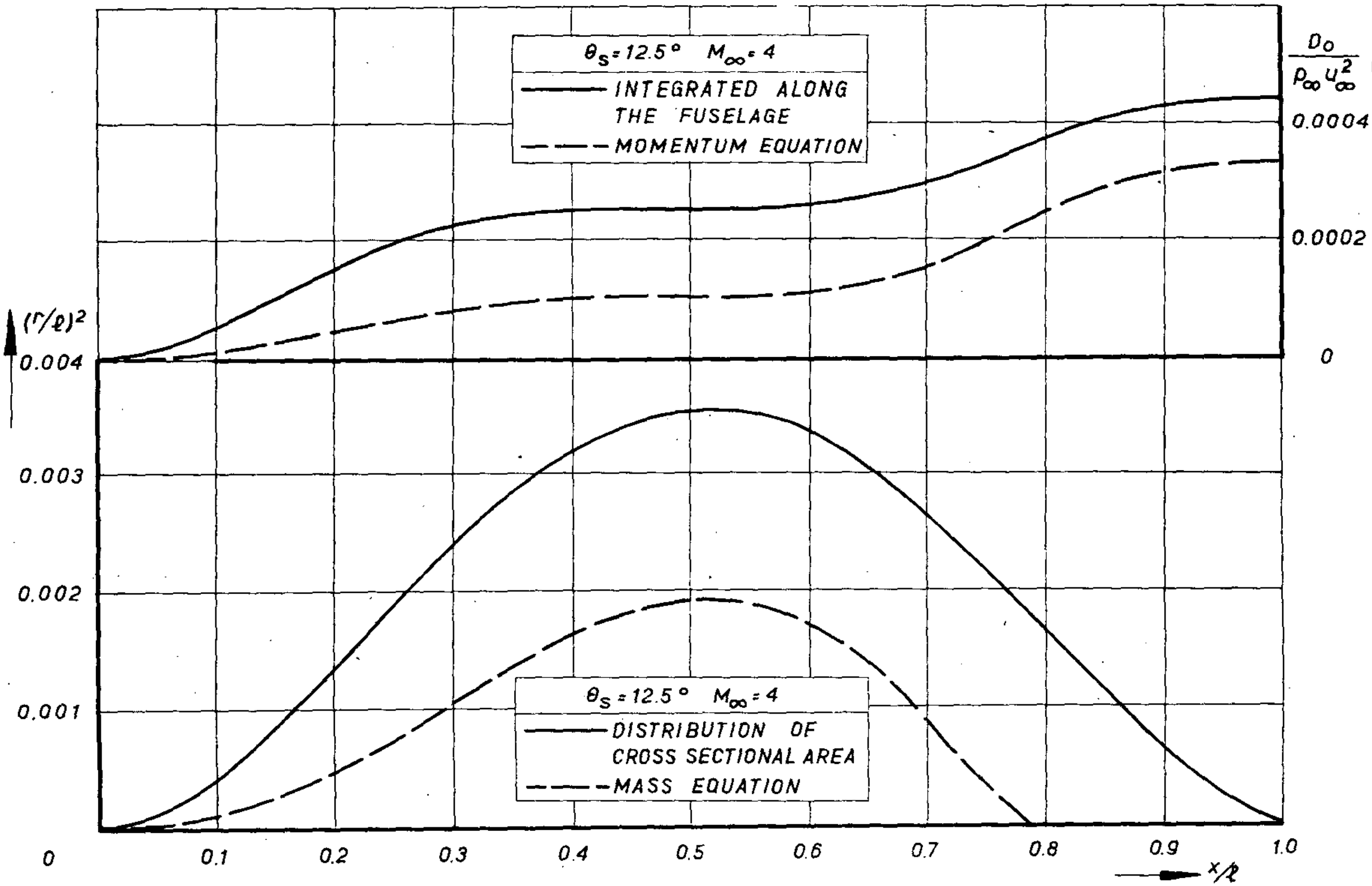

FIG. 6d COMPARISON OF THE TWO SIDES OF THE MASS FLOW AND MOMENTUM EQUATION FOR THE BODY WITH s=8.4 AND $M_\infty = 4$.

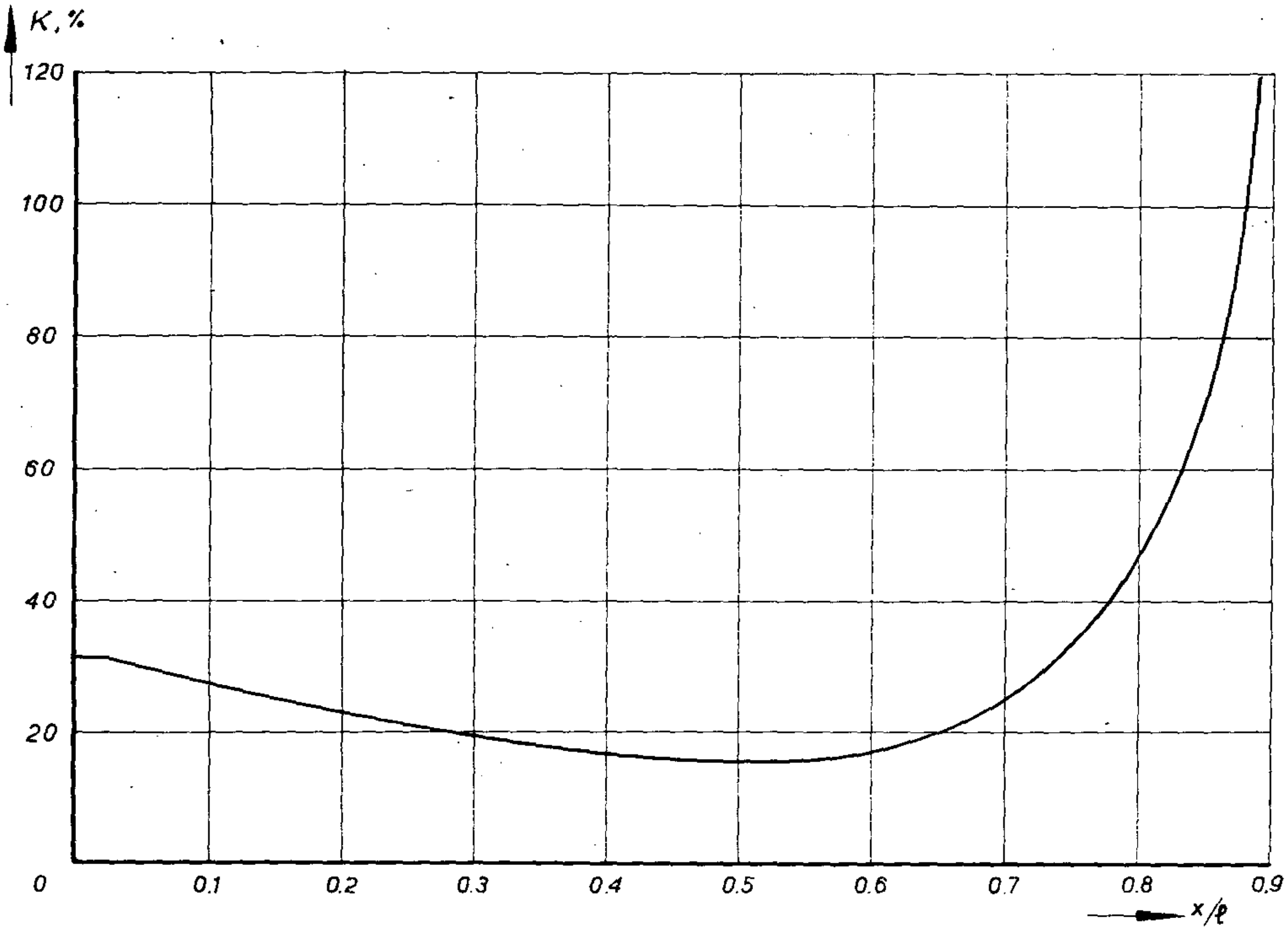

FIG. 7a THE PERCENTUAL DIFFERENCE K OF THE LEFT-HAND SIDE AND THE RIGHT-HAND SIDE OF THE MASS-FLOW EQUATION FOR THE CASE $\theta_s = 12.5°$, $M_\infty = 2$.

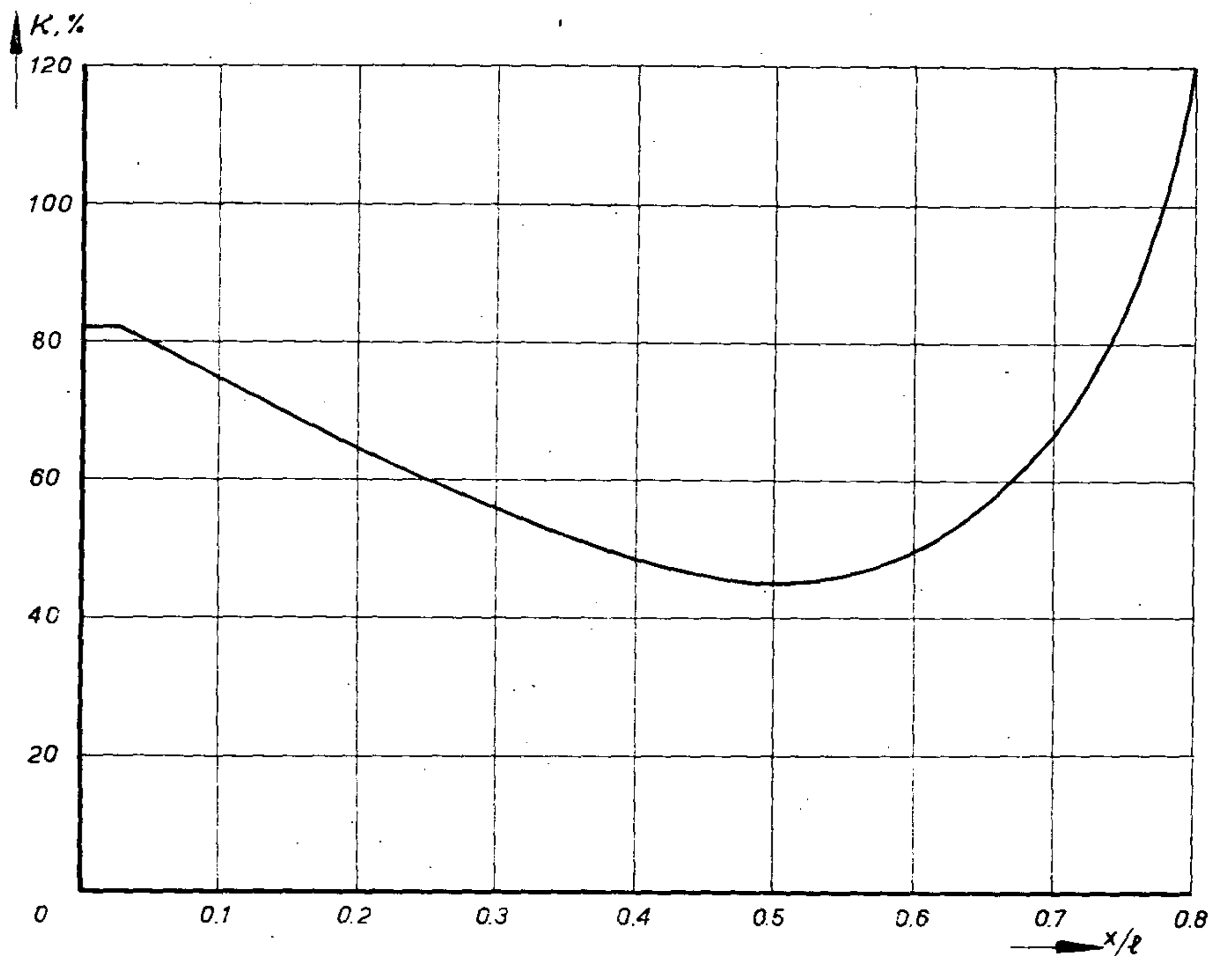

FIG. 7b THE PERCENTUAL DIFFERENCE K OF THE LEFT-HAND SIDE AND THE RIGHT-HAND SIDE OF THE MASS-FLOW EQUATION FOR THE CASE $\theta_s = 12.5°$, $M_\infty = 4$.

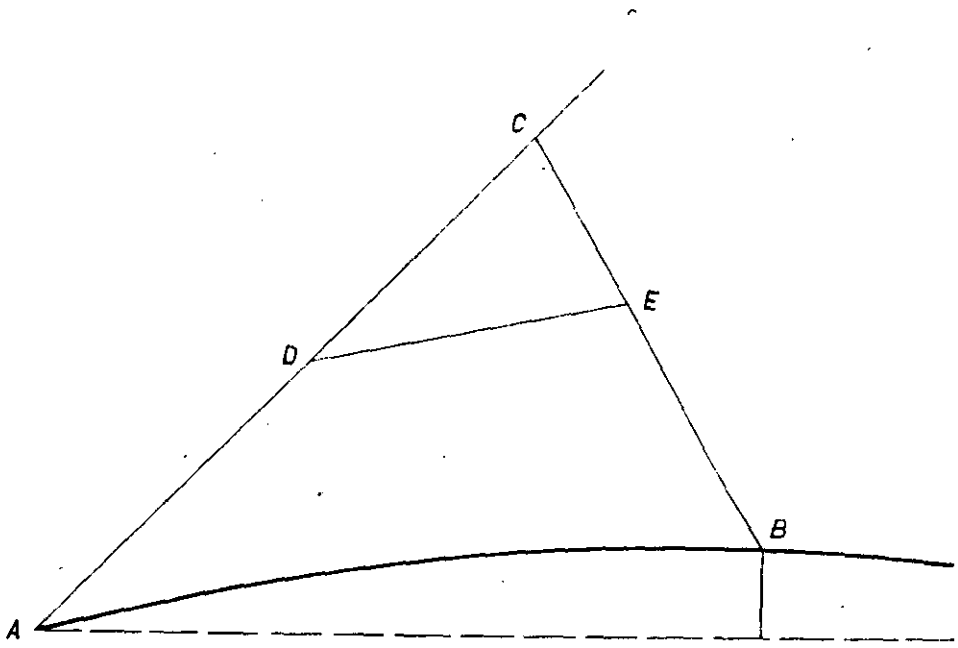

FIG. 8 THE APPROXIMATE POSITION OF THE STREAMLINE DE.

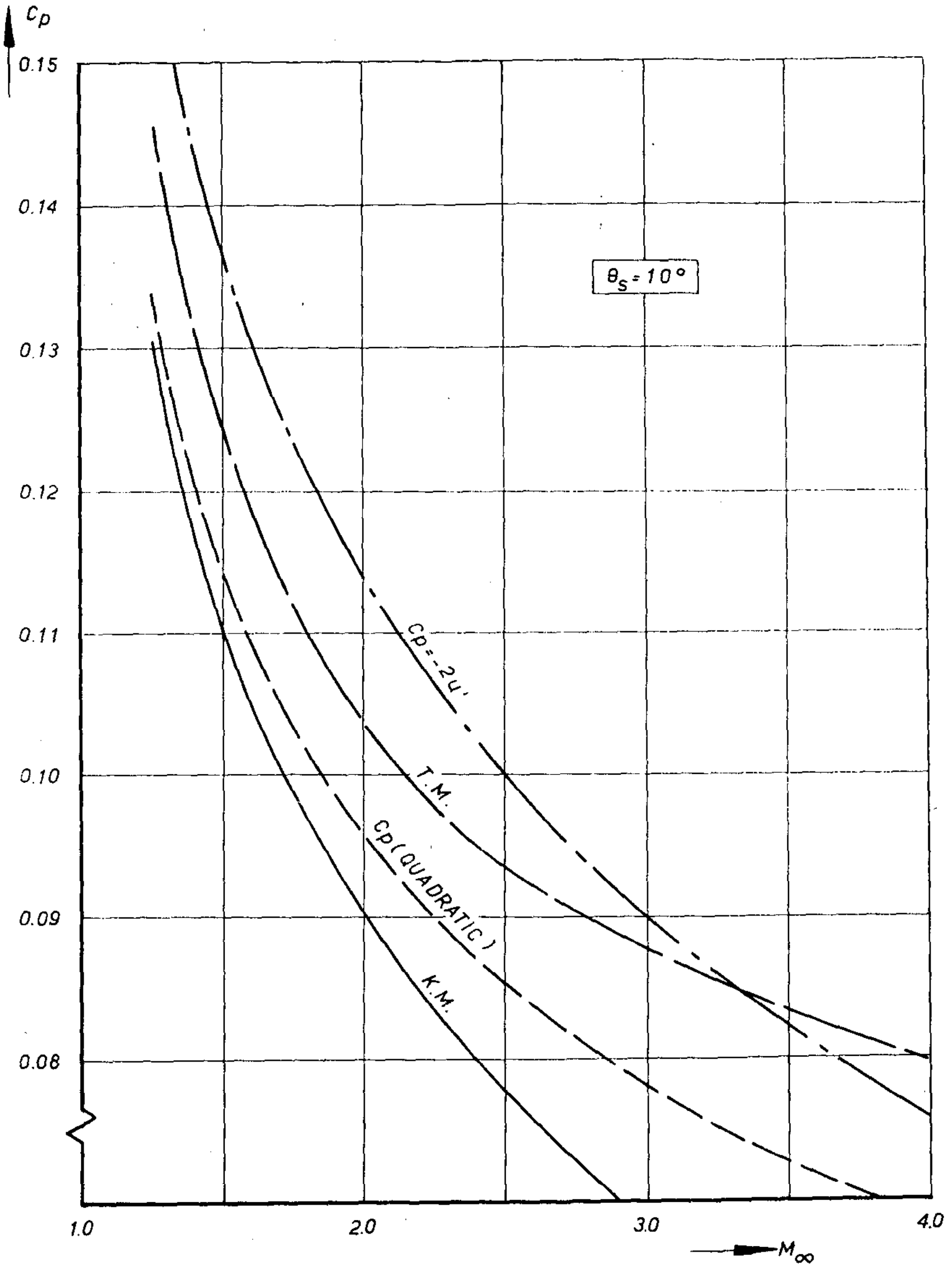

FIG. 9a C_p AS A FUNCTION OF M_∞ FOR $\theta_s = 10°$.

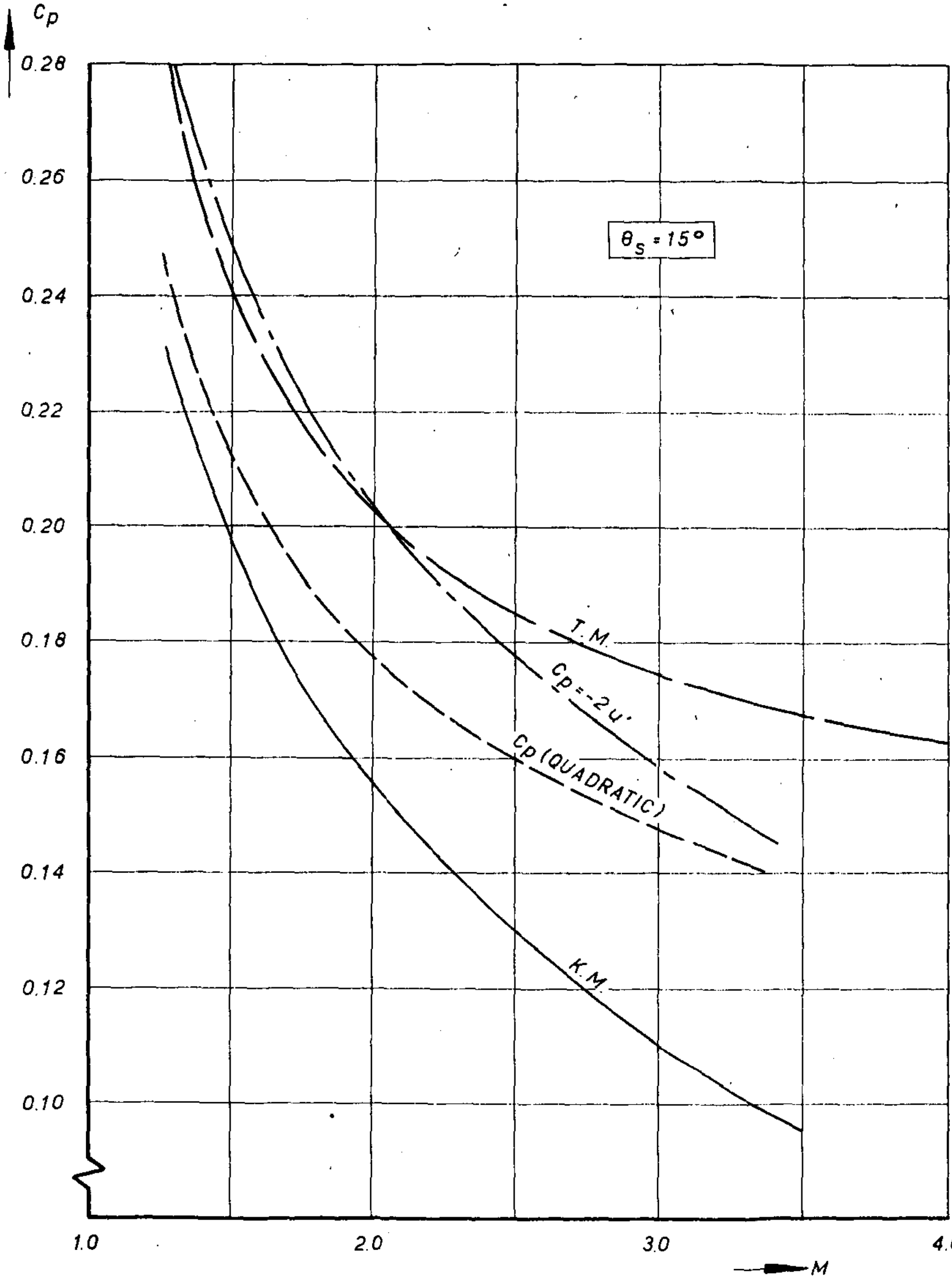

FIG. 9b C_p AS A FUNCTION OF M_∞ FOR $\theta_s = 15°$.

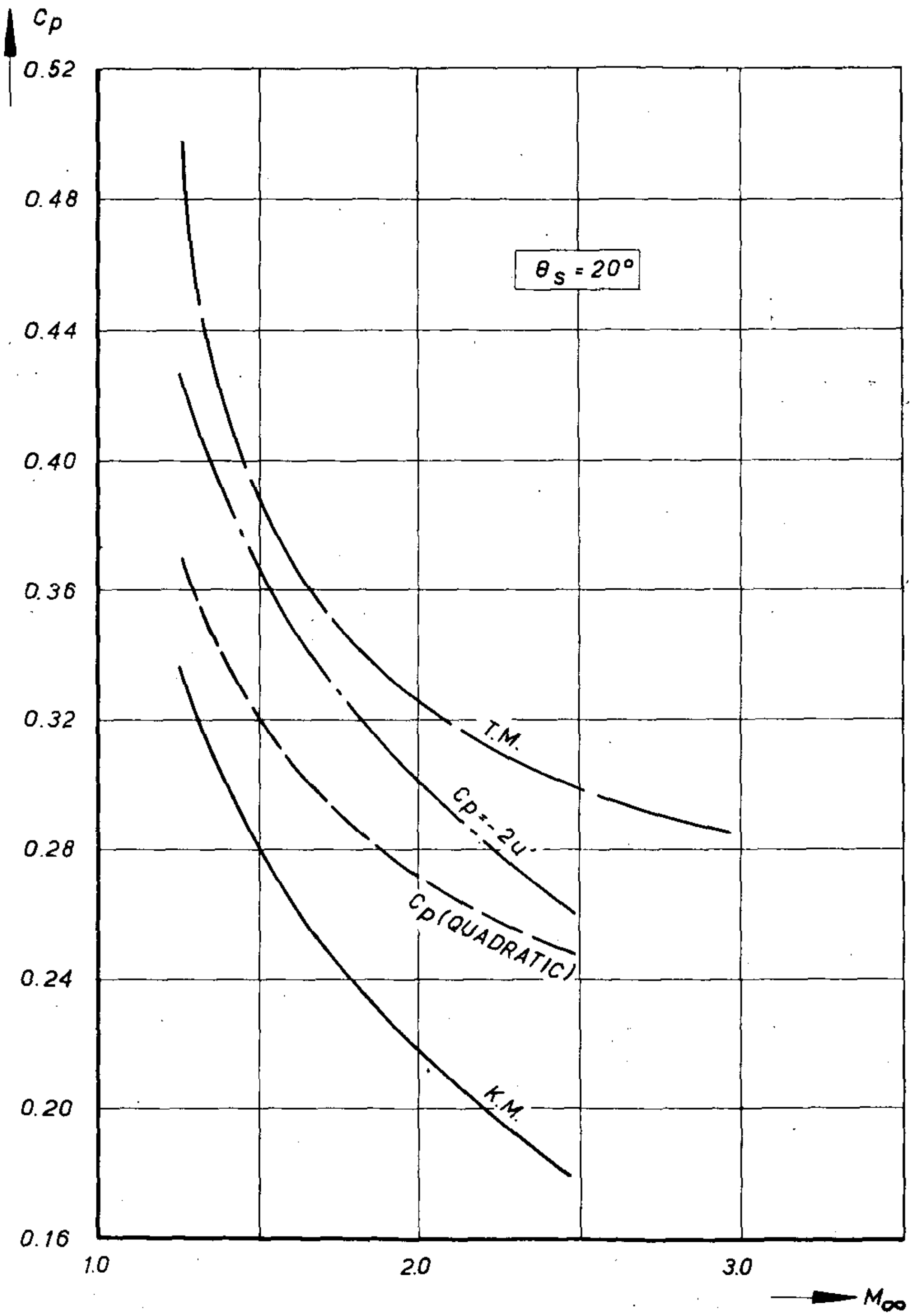

FIG. 9c C_p AS A FUNCTION OF M_∞ FOR $\theta_S = 20°$.

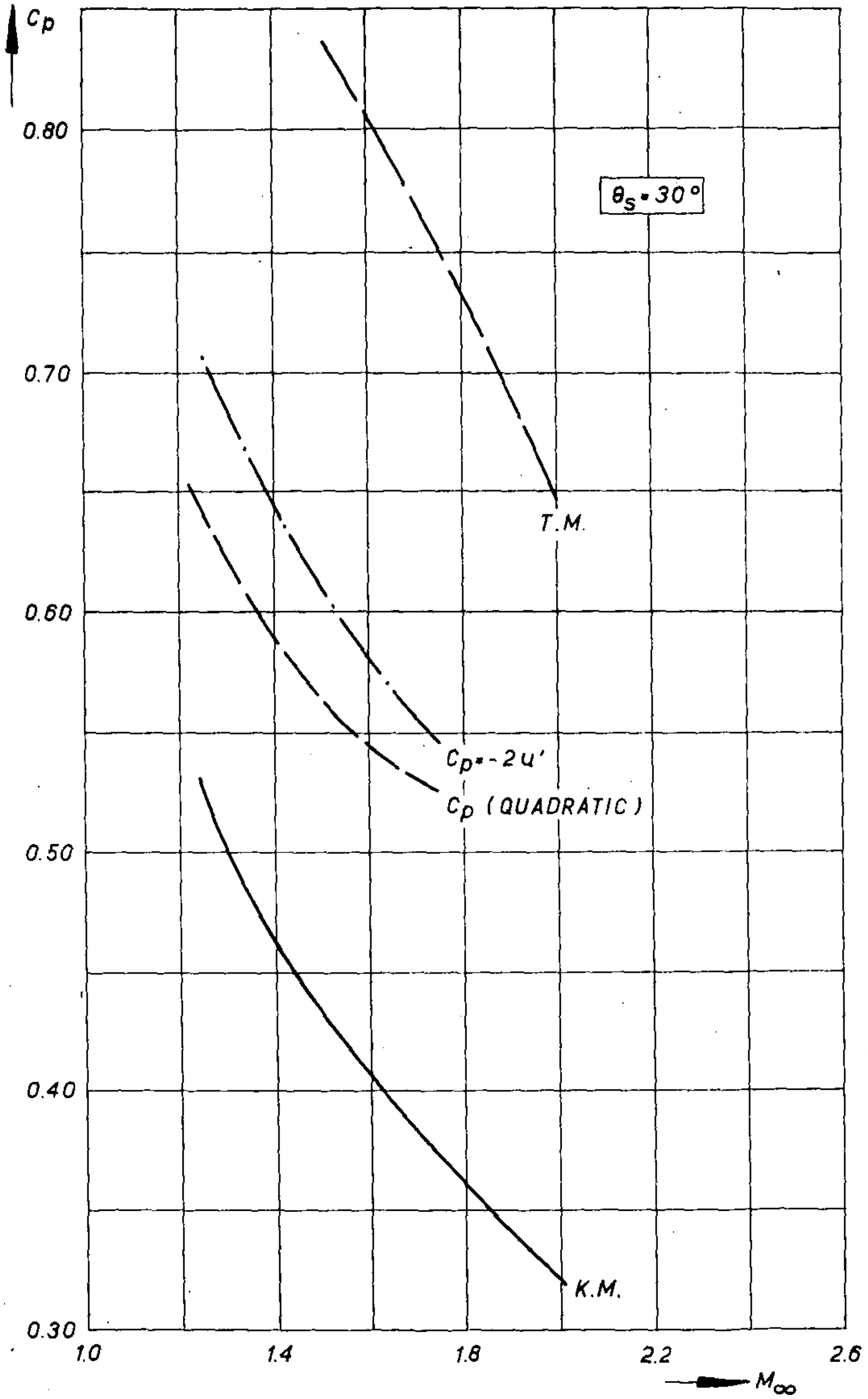

FIG.9d C_p AS A FUNCTION OF M_∞ FOR $\theta_S = 30°$.

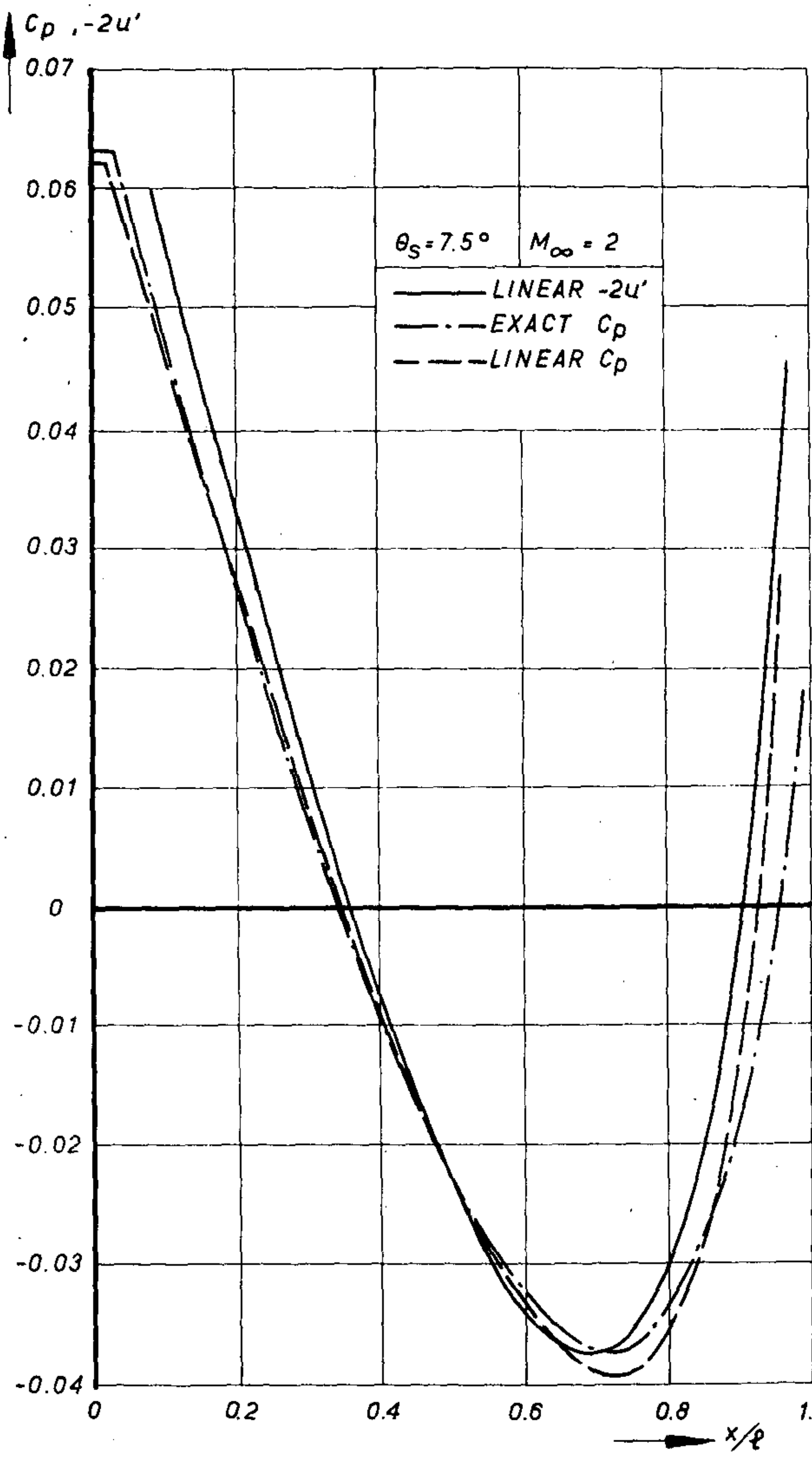

FIG.10a THE PRESSURE DISTRIBUTION ON THE BODY WITH $s = 13.7$ AND $M_\infty = 2$.

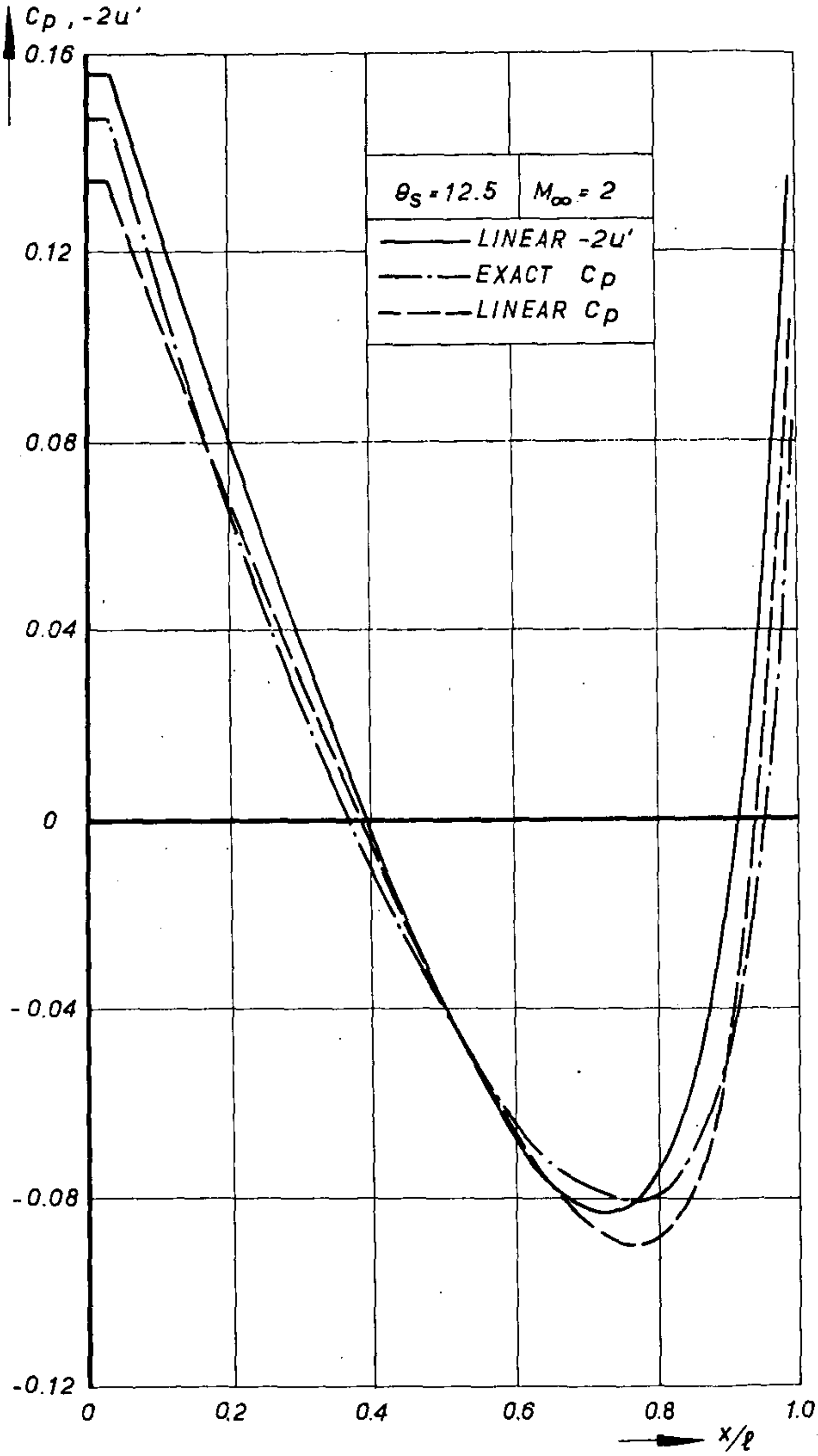

FIG. 10 b THE PRESSURE DISTRIBUTION ON THE BODY WITH $s = 8.4$ AND $M_\infty = 2$.

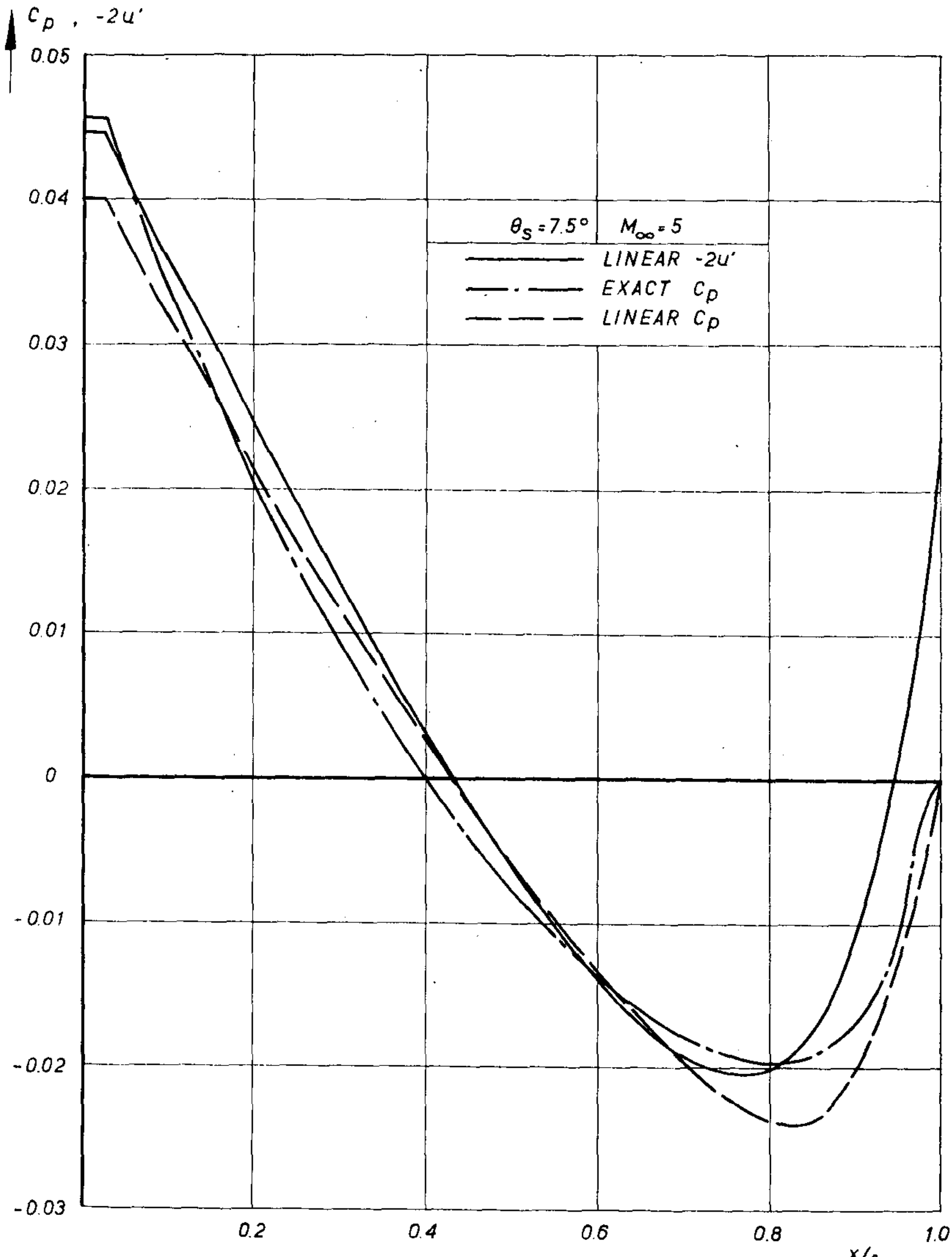

FIG.10c THE PRESSURE DISTRIBUTION ON THE BODY WITH $s = 13.7$ AND $M_\infty = 5$.

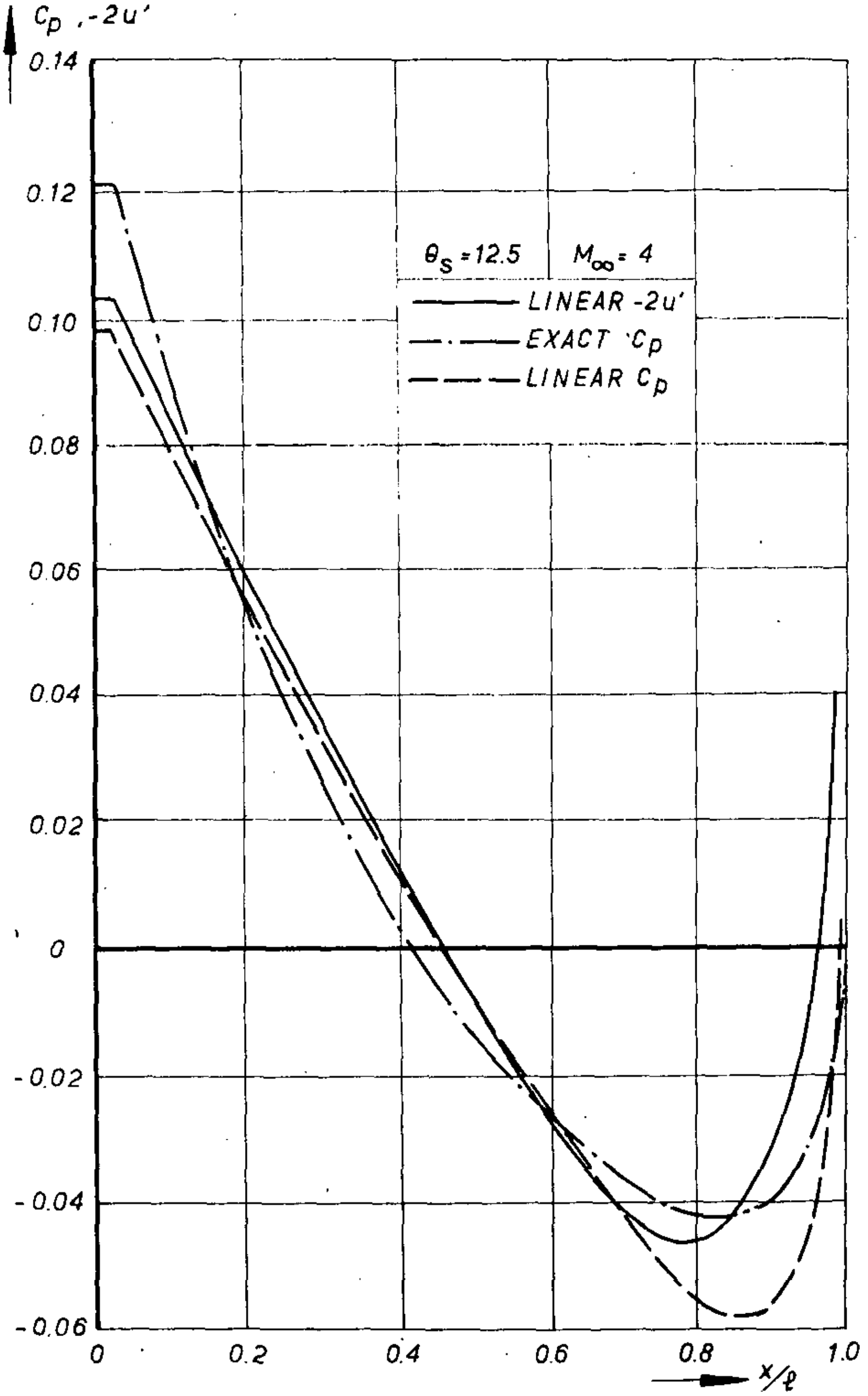

FIG. 10 d THE PRESSURE DISTRIBUTION ON THE BODY WITH $s = 8.4$ AND $M_\infty = 4$.

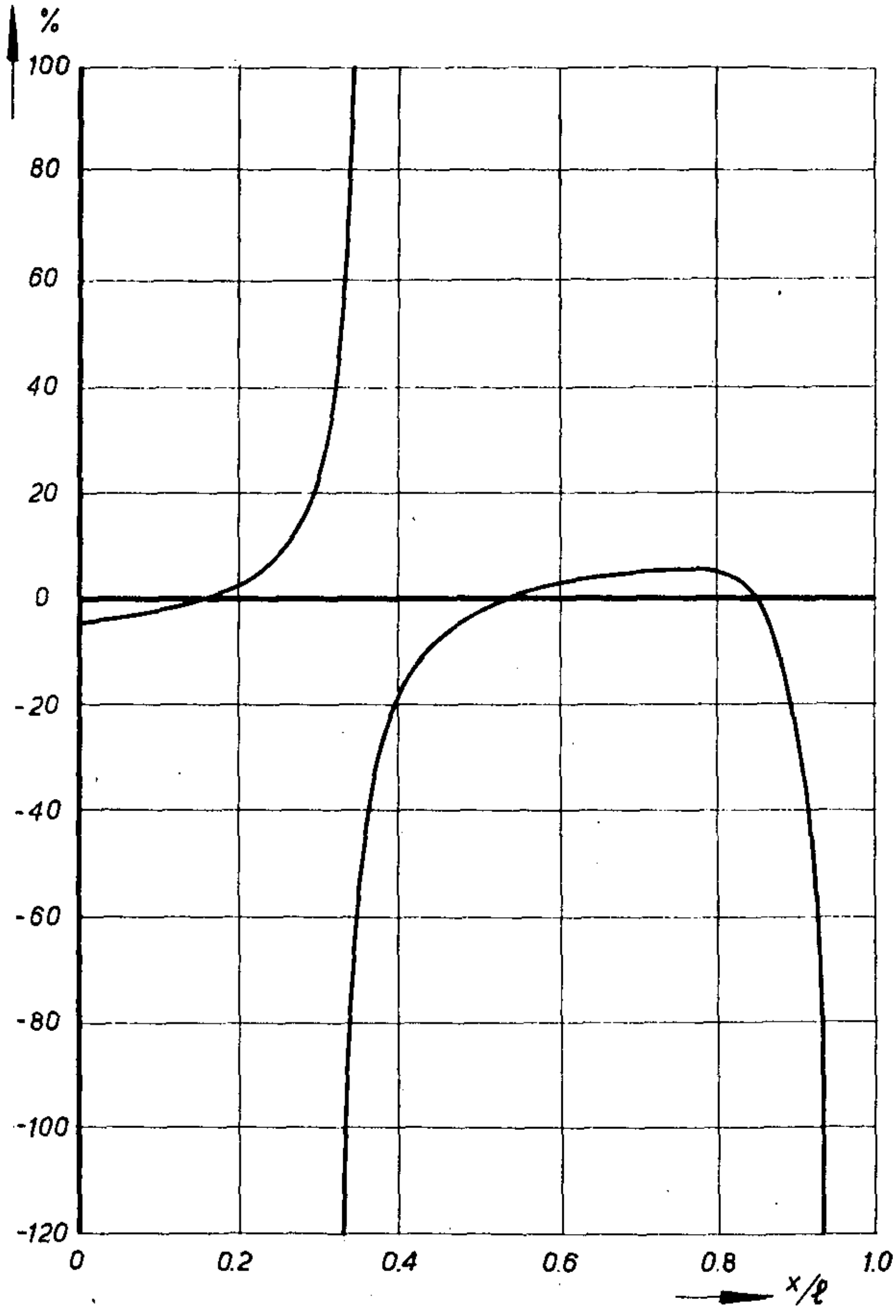

FIG. 11a THE PERCENTUAL DIFFERENCE BETWEEN THE EXACT AND THE LINEARIZED PRESSURE COEFFICIENT FOR THE BODY WITH $s=13.7$, $M_\infty=2$.

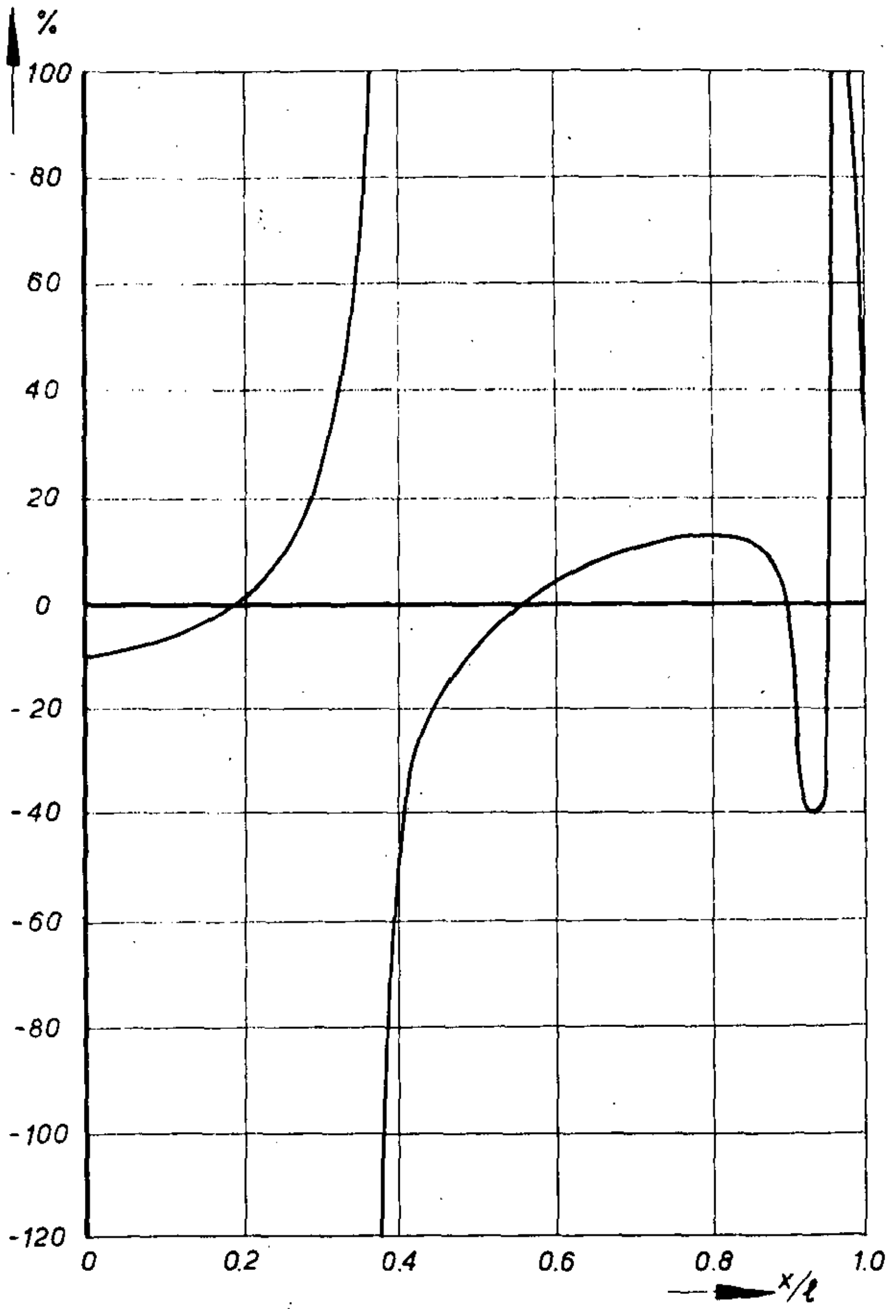

FIG. 11b THE PERCENTUAL DIFFERENCE BETWEEN THE EXACT AND THE LINEARIZED PRESSURE COEFFICIENT FOR THE BODY WITH $s = 8.4$, $M_\infty = 2$.

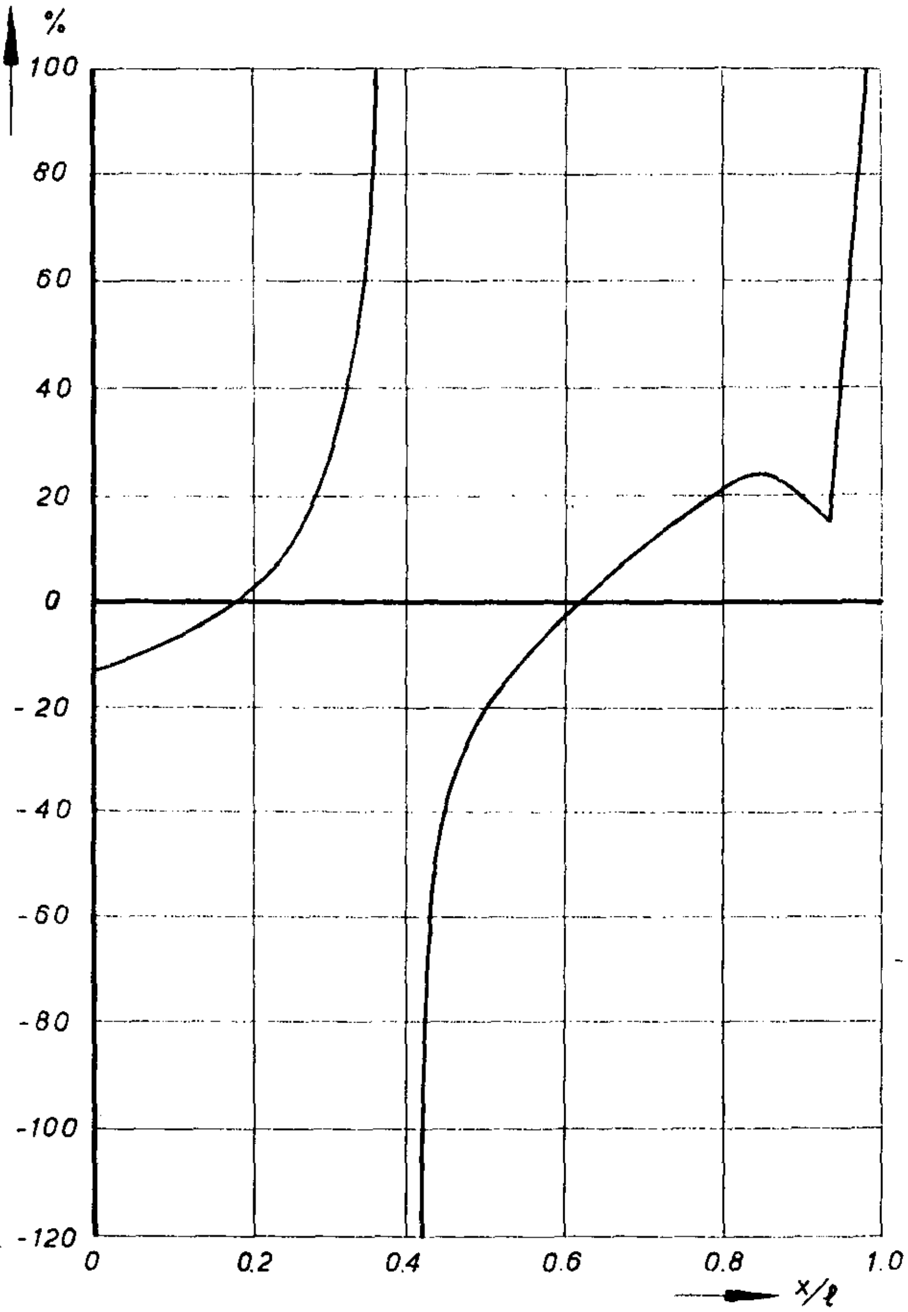

FIG.11c THE PERCENTUAL DIFFERENCE BETWEEN THE EXACT AND THE LINEARIZED PRESSURE COEFFICIENT FOR THE BODY WITH $s = 13.7$ AND $M_\infty = 5$.

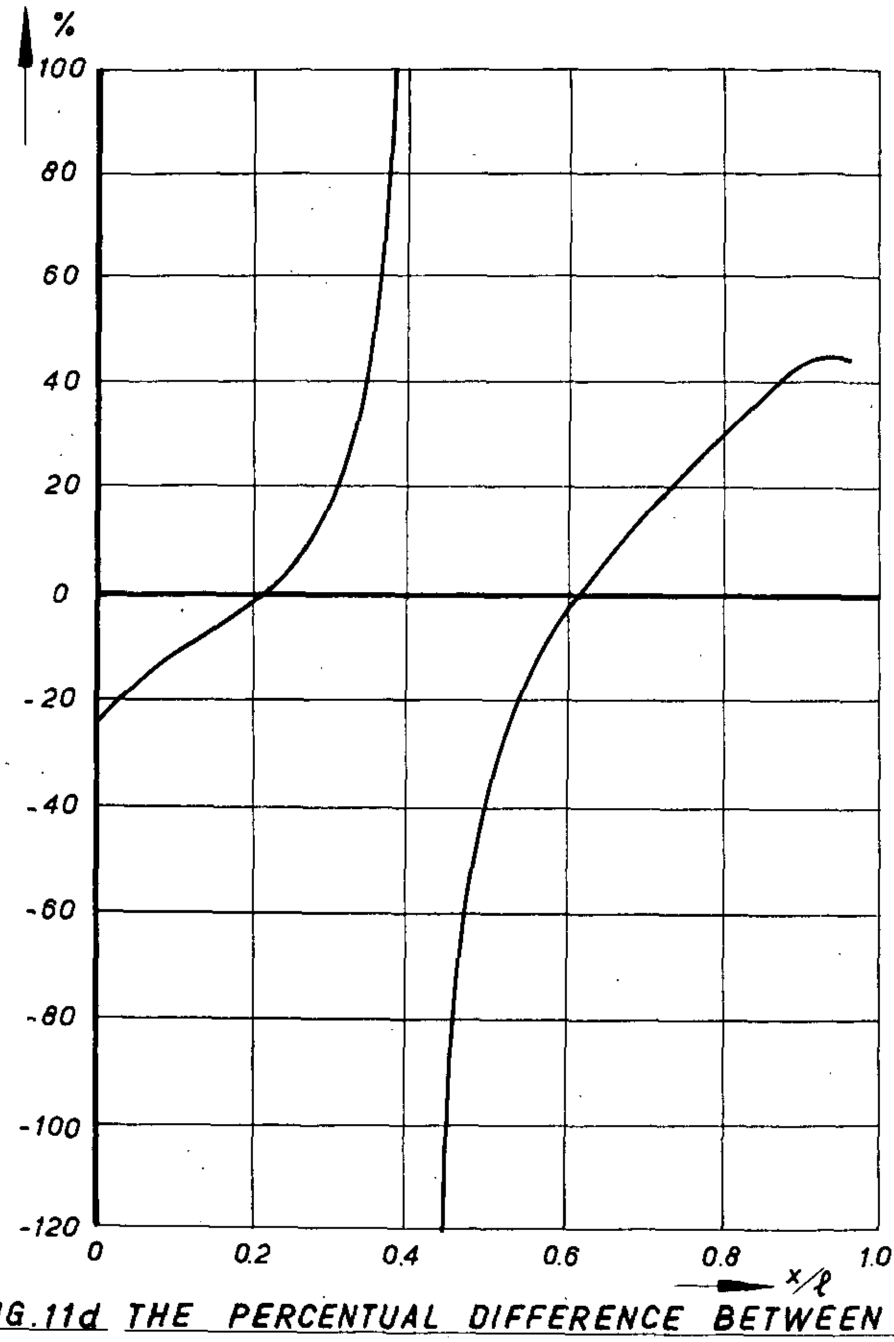

FIG. 11d THE PERCENTUAL DIFFERENCE BETWEEN THE EXACT AND THE LINEARIZED PRESSURE COEFFICIENT FOR THE BODY WITH $s = 8.4$ AND $M_\infty = 4$.

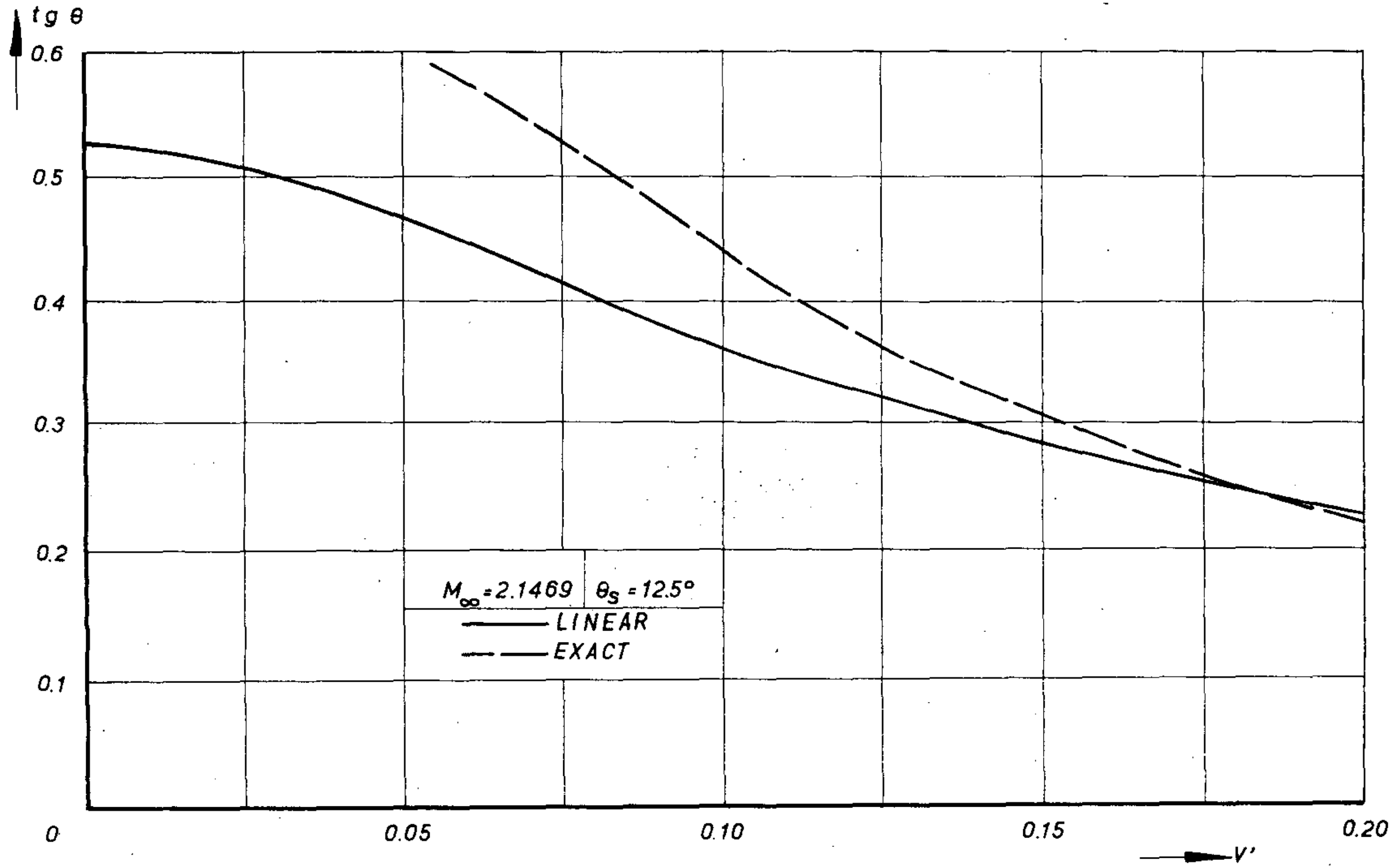

FIG. 12a COMPARISON OF THE FLOW FIELD FOR A CONE.

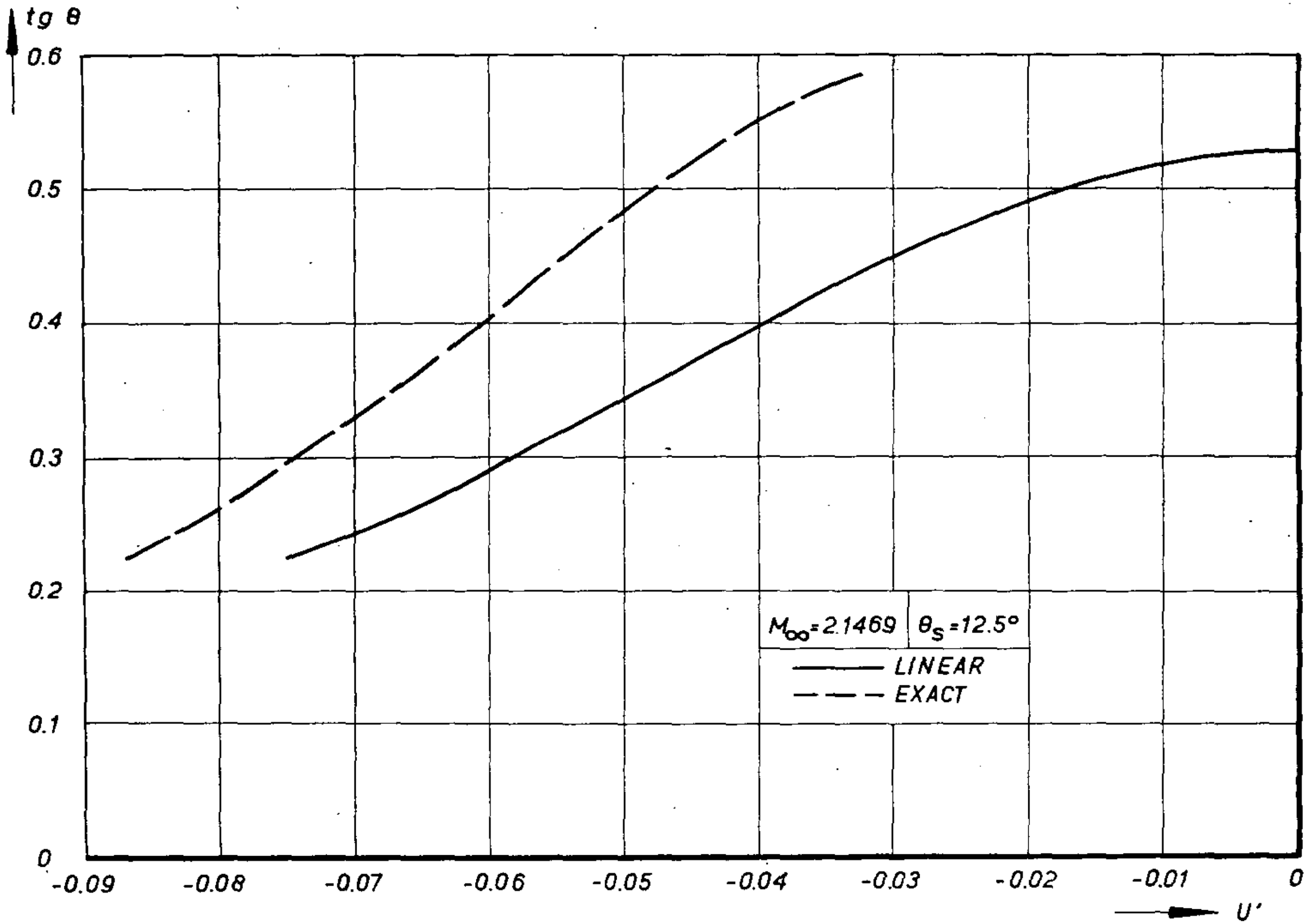

FIG.12b COMPARISON OF THE FLOW FIELD FOR A CONE.

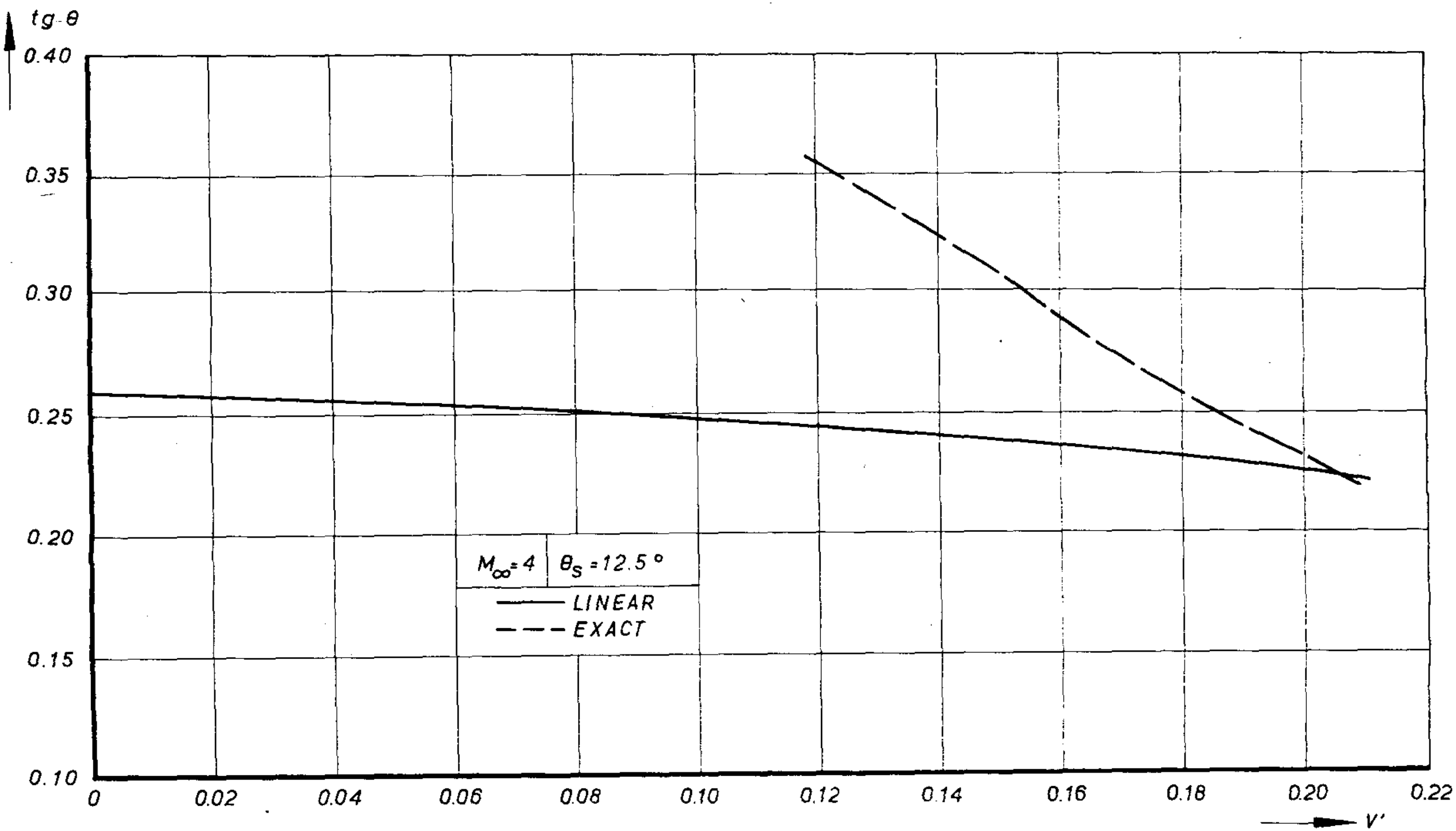

FIG. 12 c COMPARISON OF THE FLOW FIELD FOR A CONE.

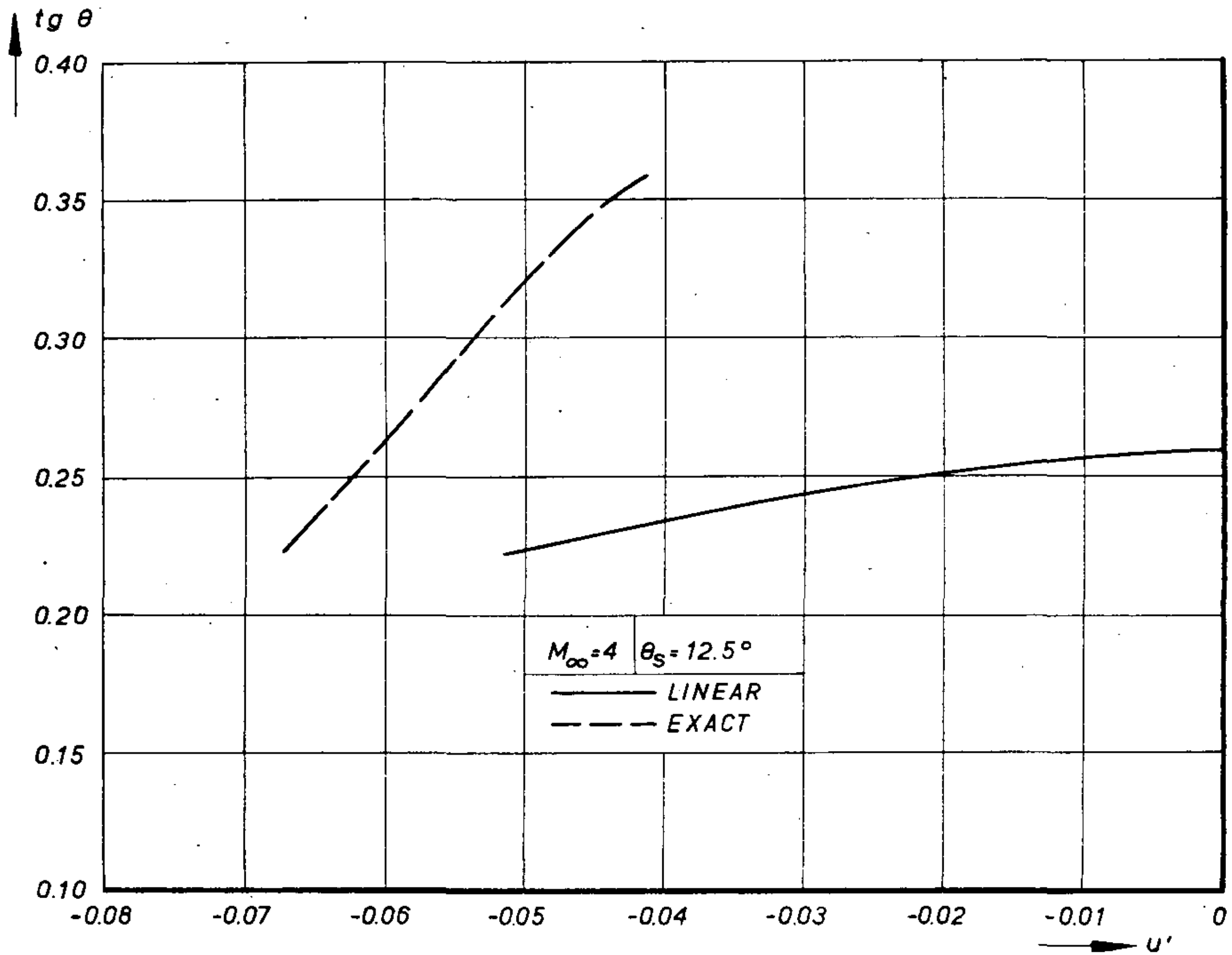

FIG.12d COMPARISON OF THE FLOW FIELD FOR A CONE.

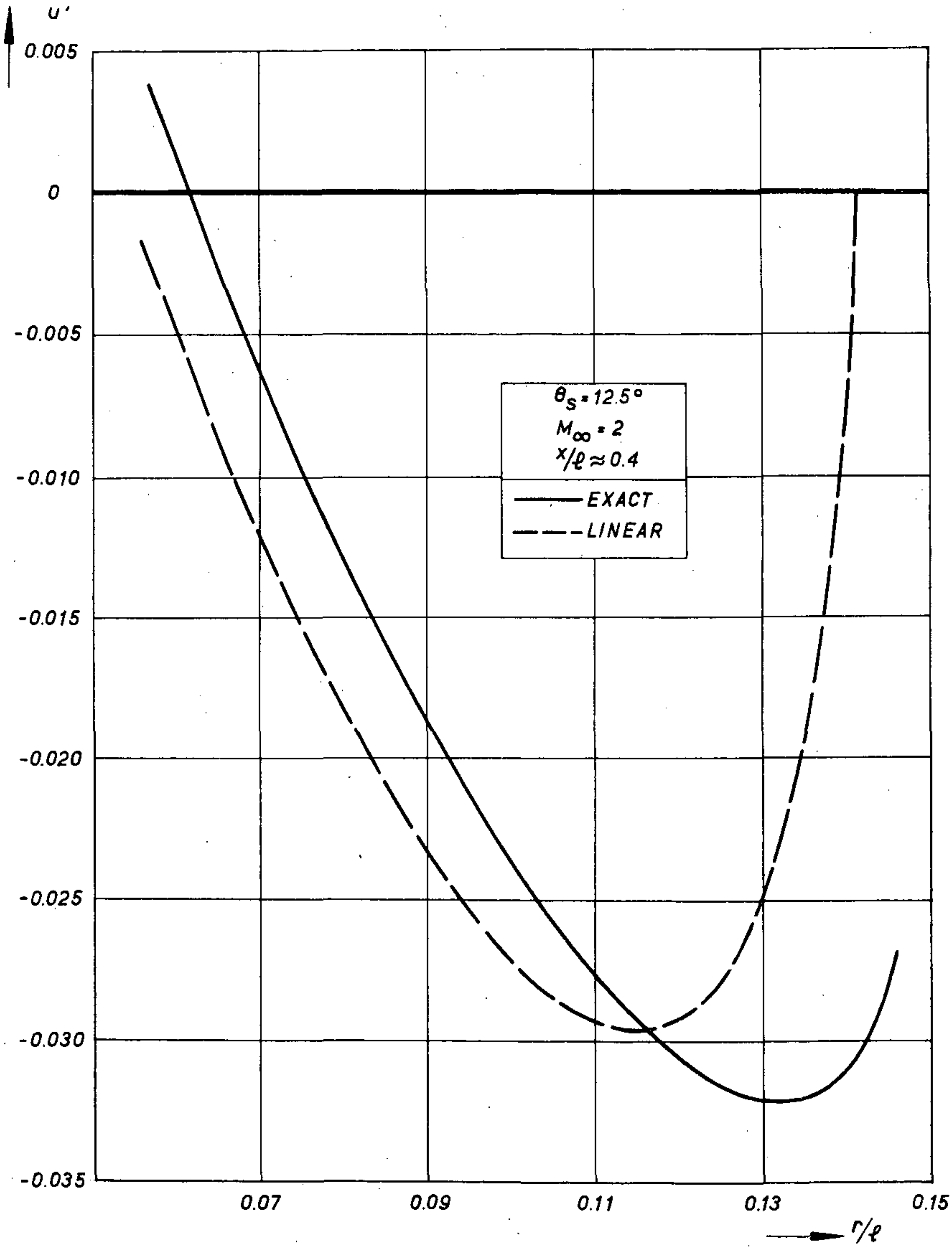

FIG. 13a COMPARISON OF THE FLOW FIELD.

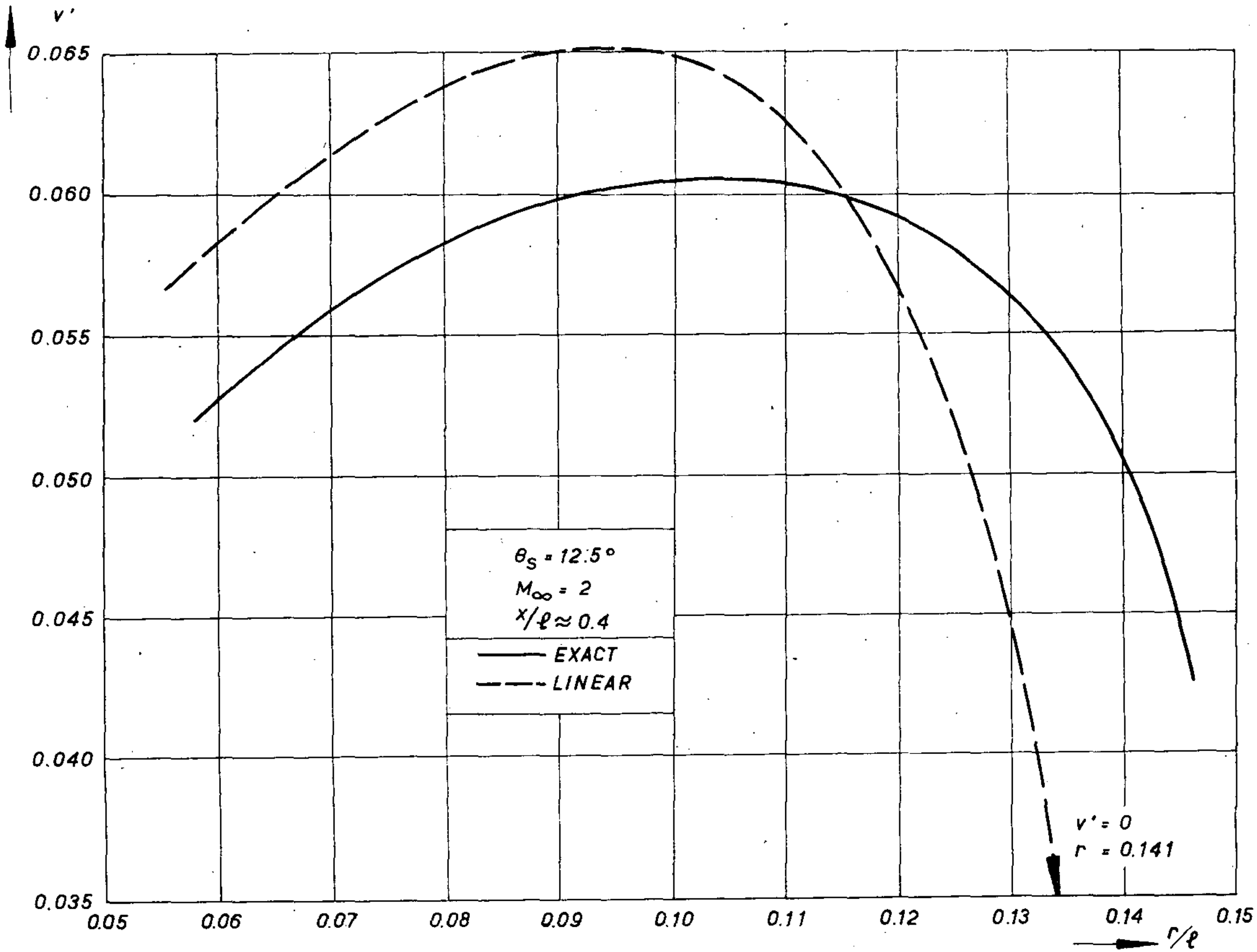

FIG. 13 b COMPARISON OF THE FLOW FIELD.

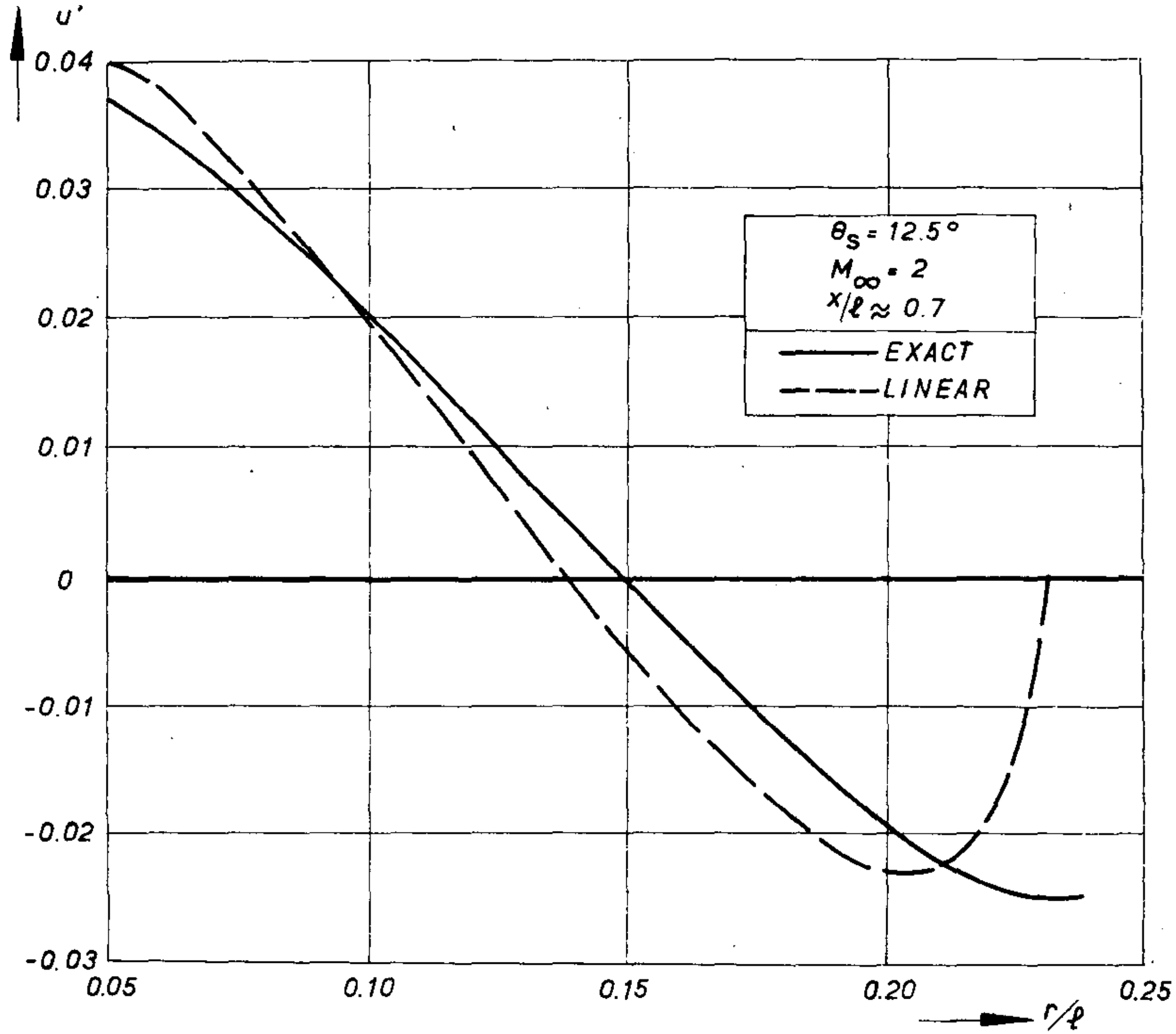

FIG. 13c COMPARISON OF THE FLOW FIELD.

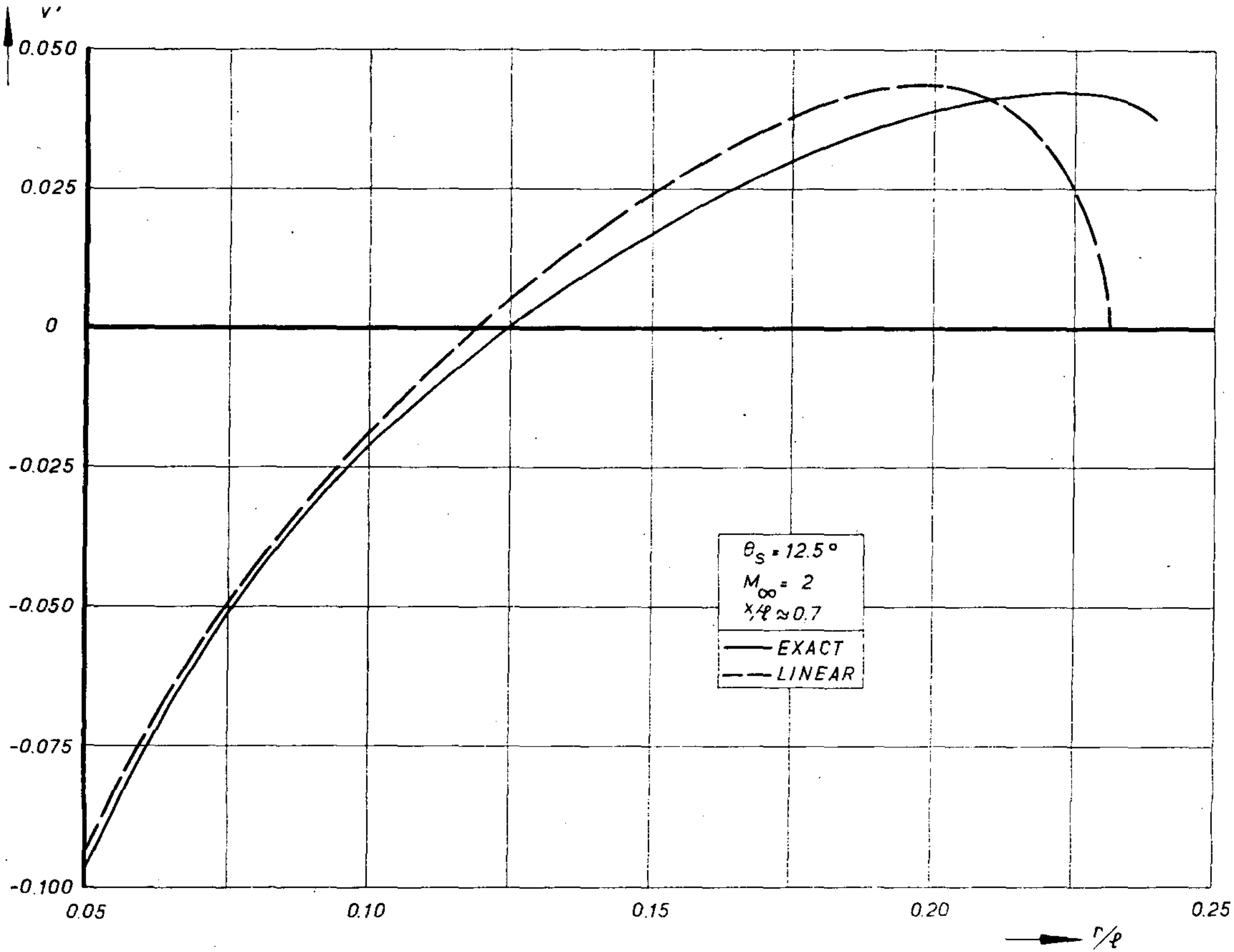

FIG. 13d COMPARISON OF THE FLOW FIELD.

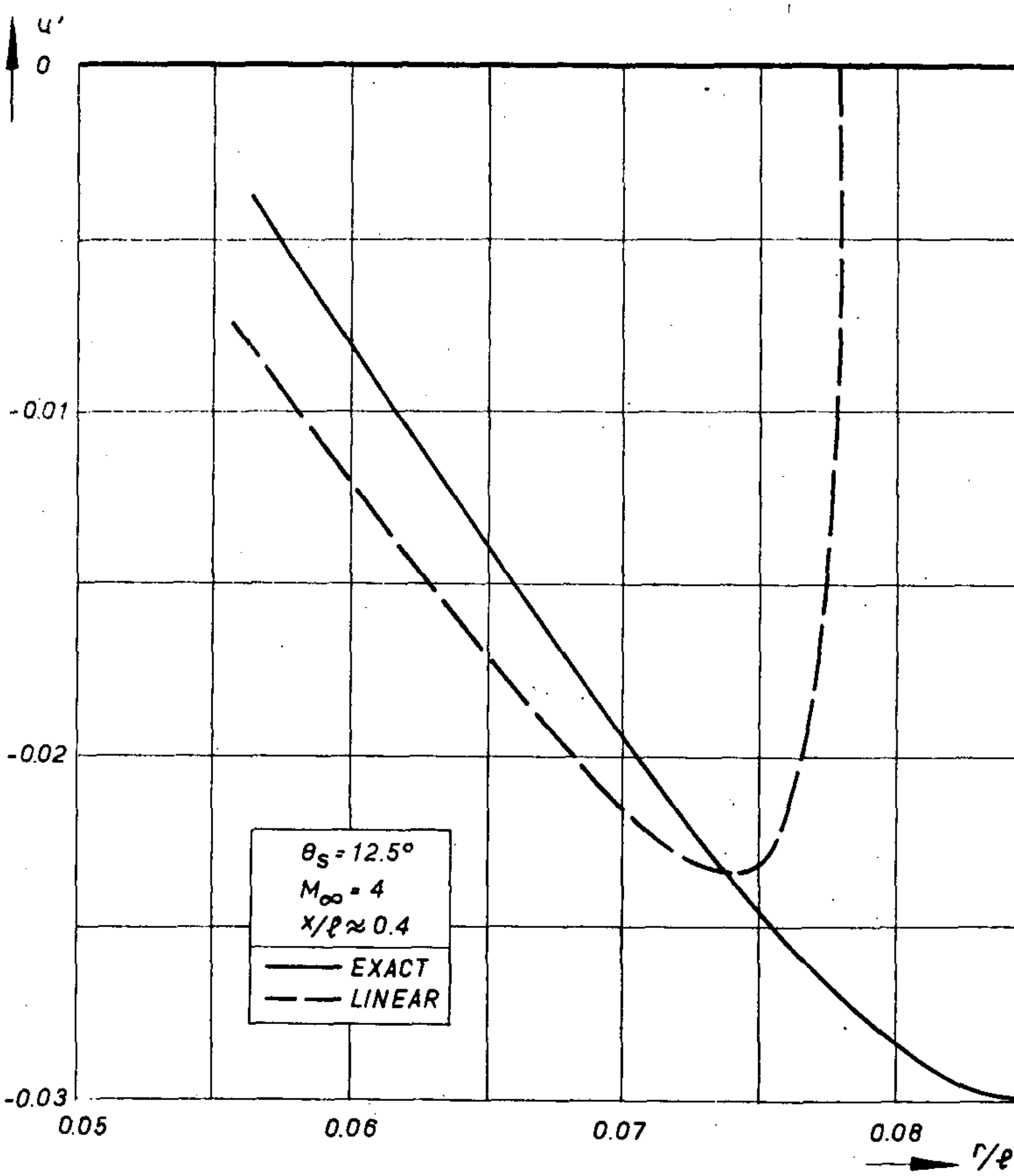

FIG. 14 a COMPARISON OF THE FLOW FIELD.

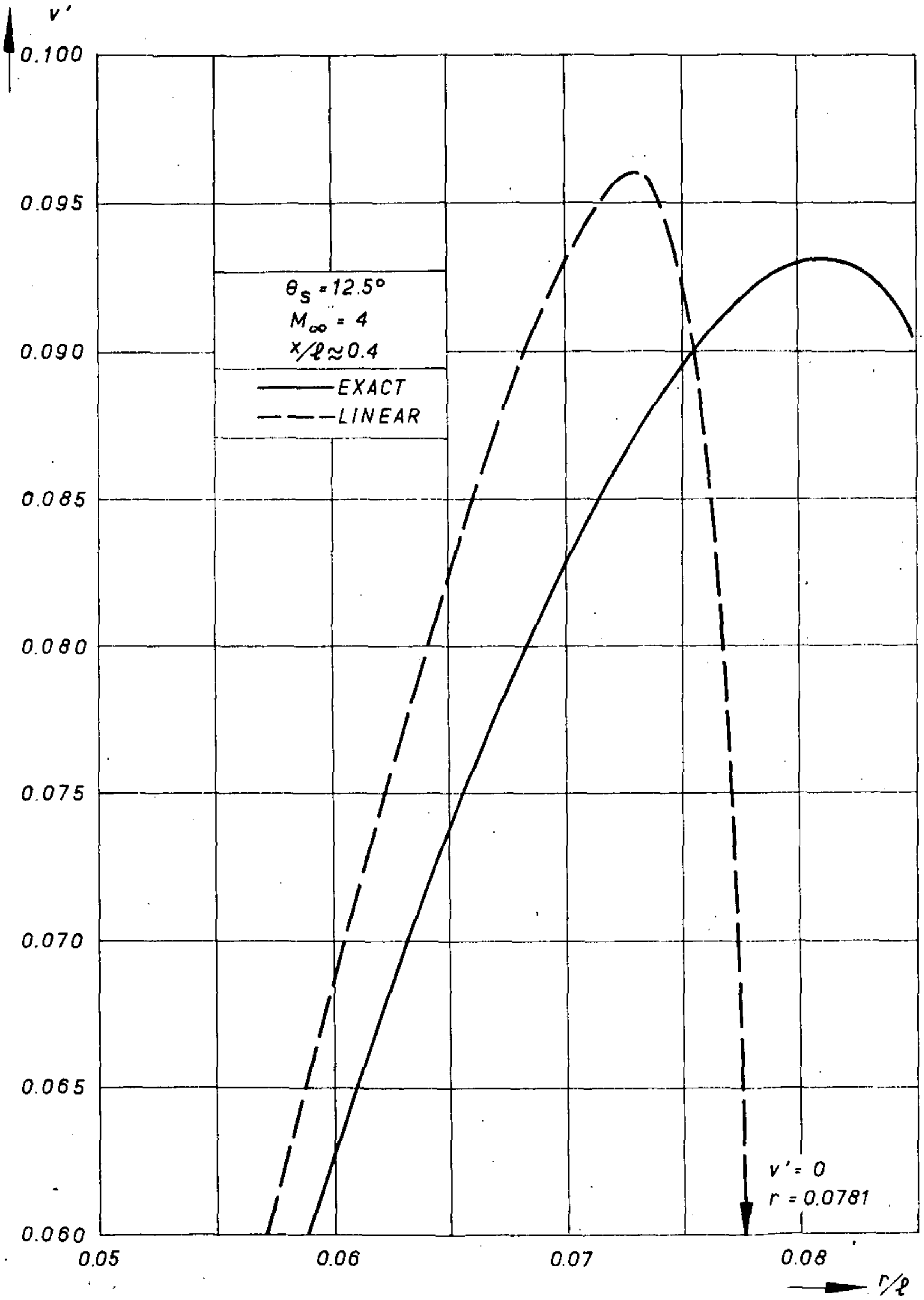

FIG. 14 b COMPARISON OF THE FLOW FIELD.

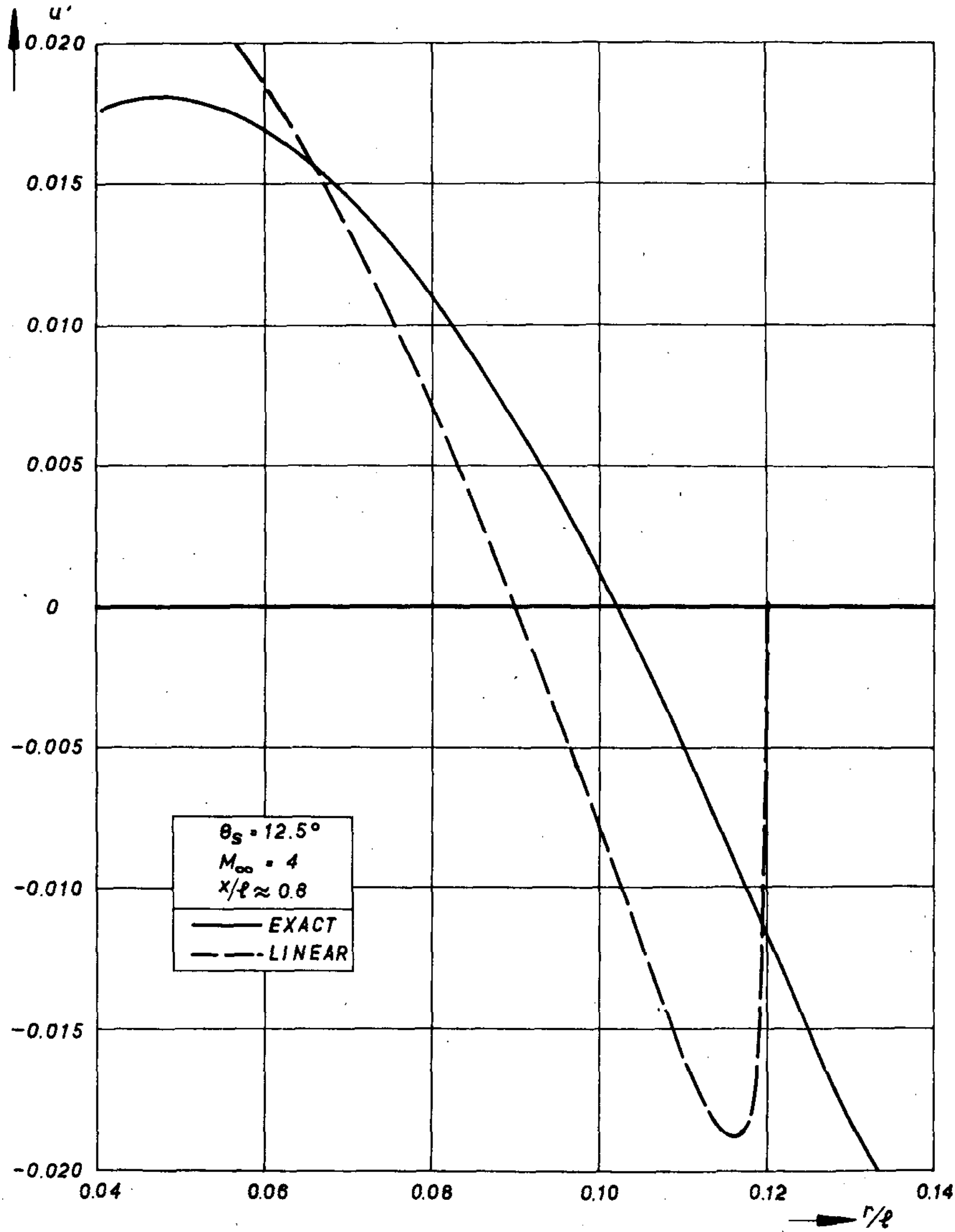

FIG. 14c COMPARISON OF THE FLOW FIELD.

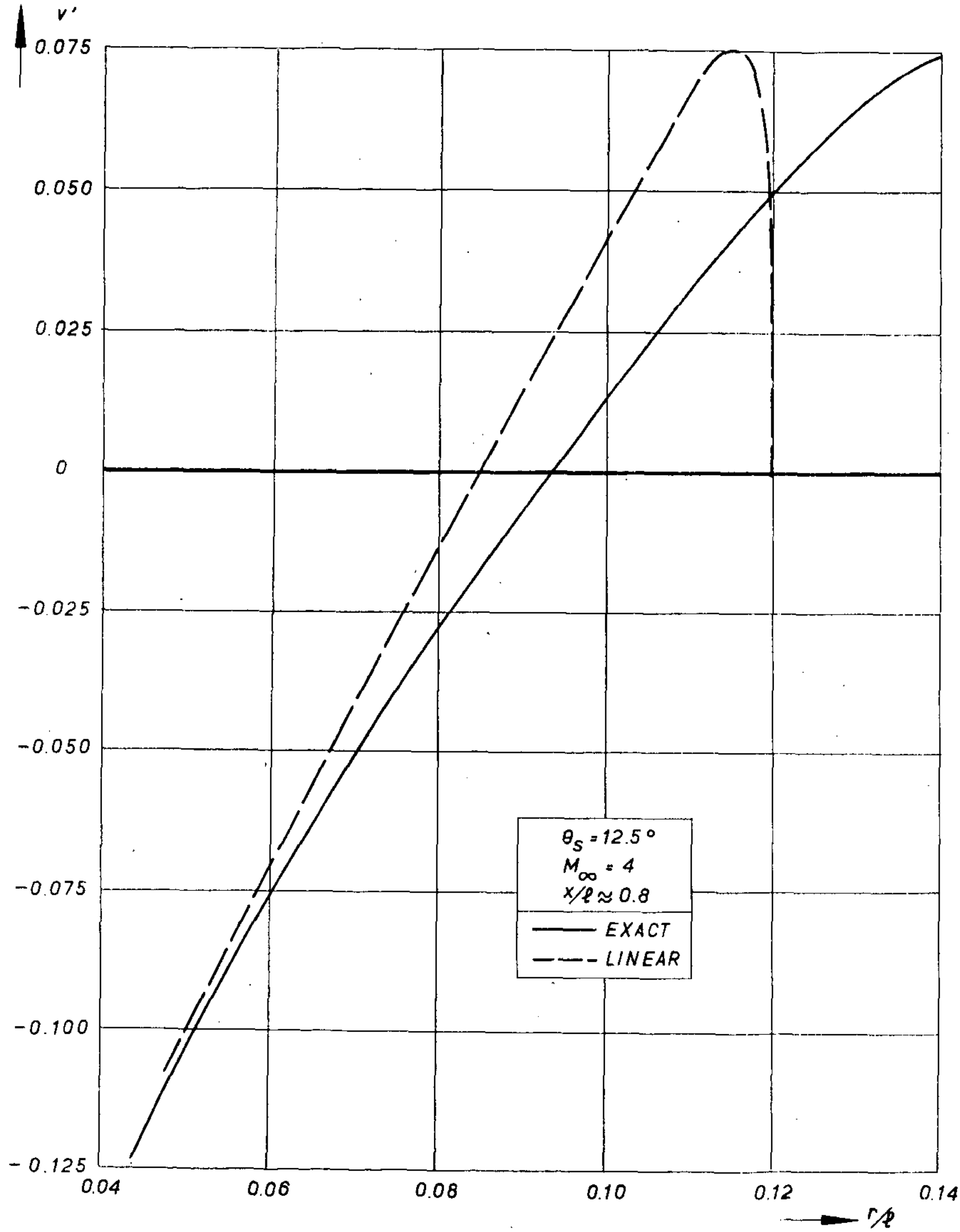

FIG. 14d COMPARISON OF THE FLOW FIELD.

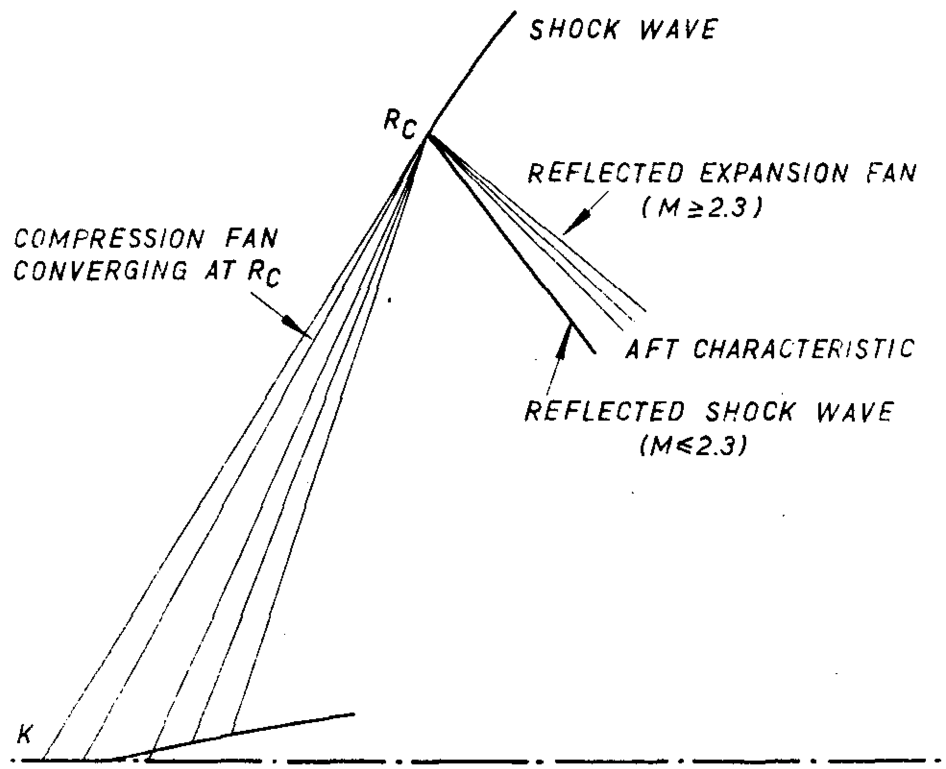

FIG. 15 FLOW PHENOMENA OCCURING AT THE NOSE OF THE BODY.

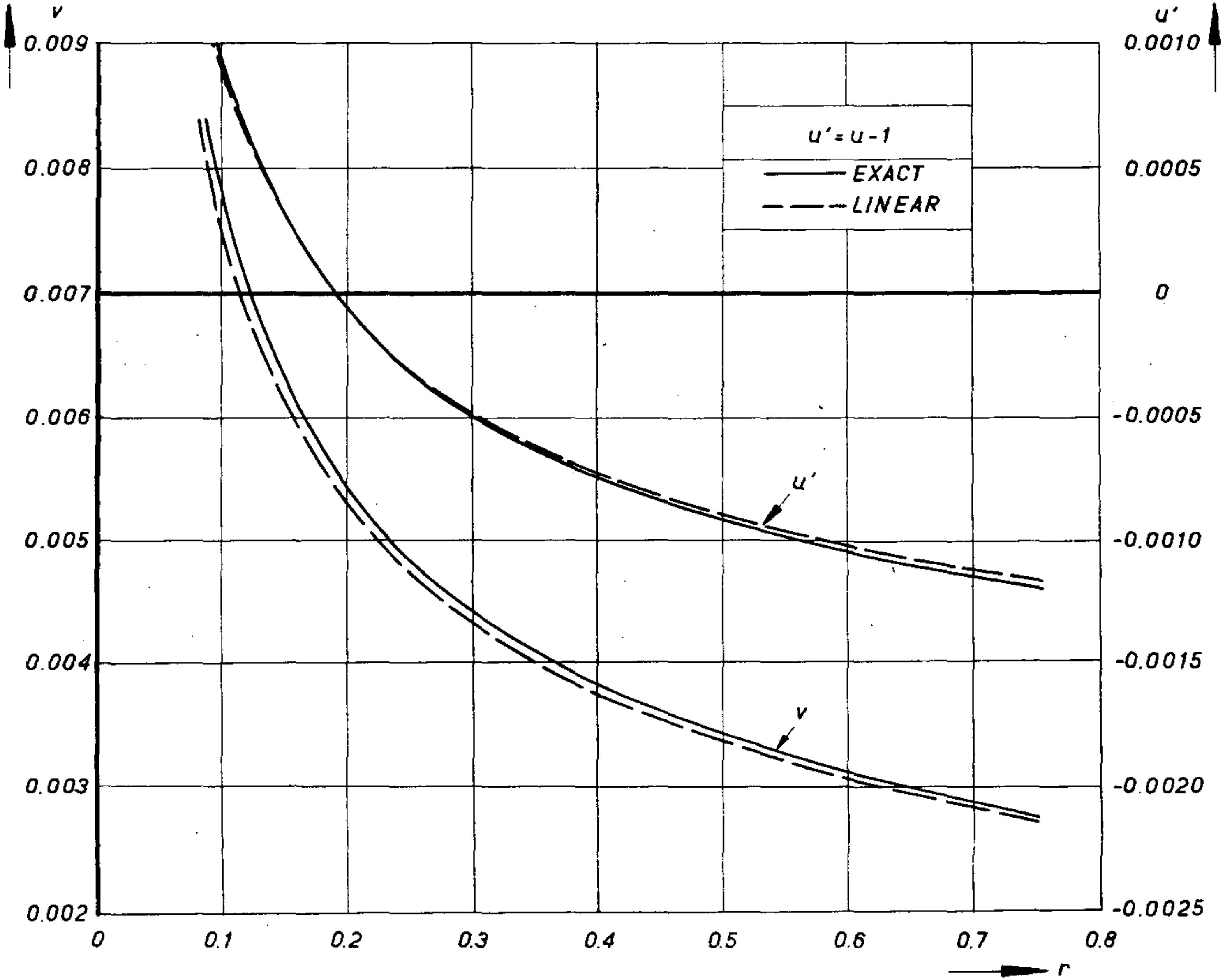

FIG. 16 a COMPARISON BETWEEN THE VELOCITY DISTRIBUTIONS AS DERIVED BY USING LINEAR- AND EXACT THEORY FOR $M_\infty = 2.5$.

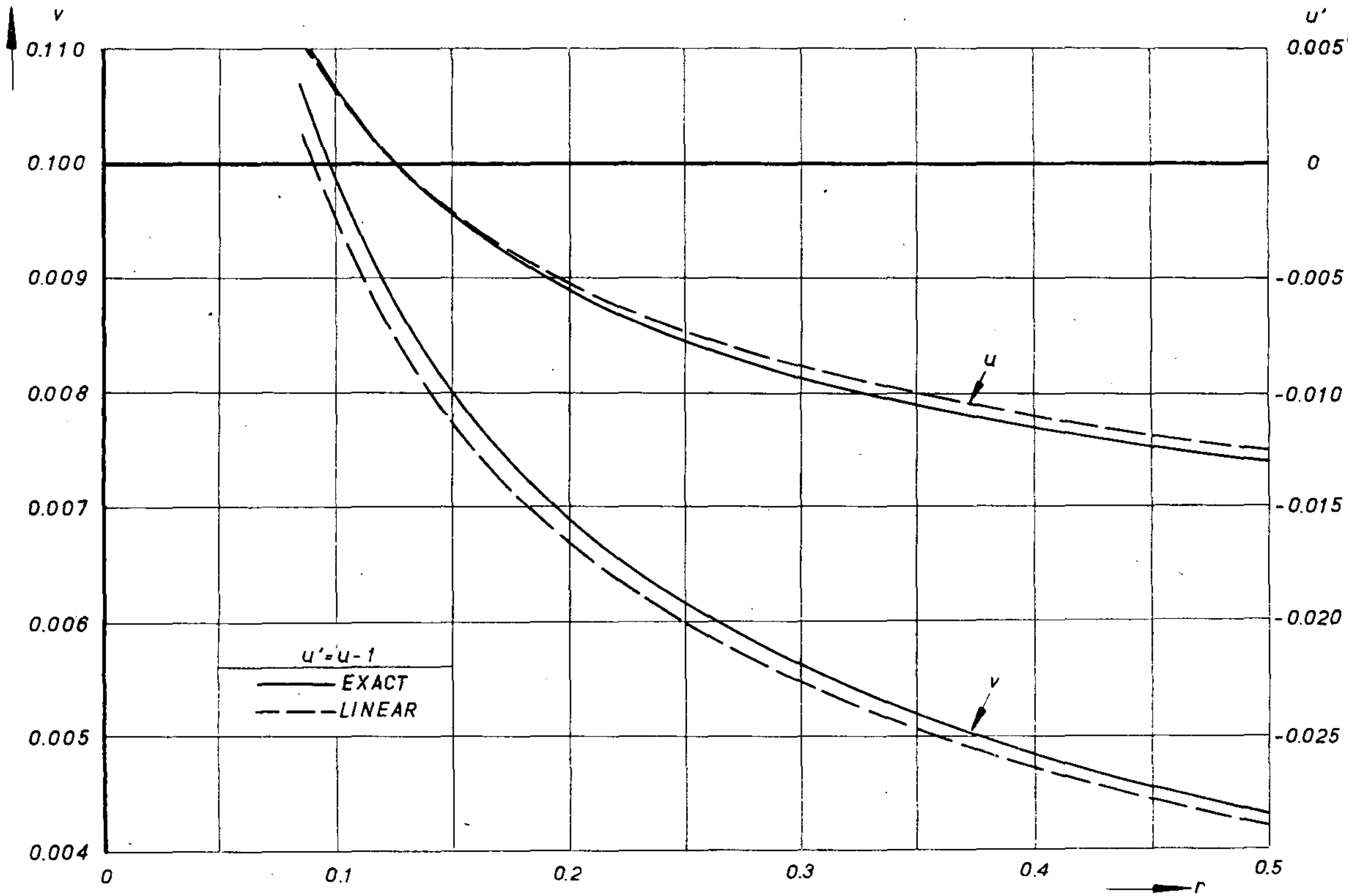

FIG. 16b COMPARISON BETWEEN THE VELOCITY DISTRIBUTIONS AS DERIVED BY USING LINEAR- AND EXACT THEORY FOR $M_\infty = 3.5$.

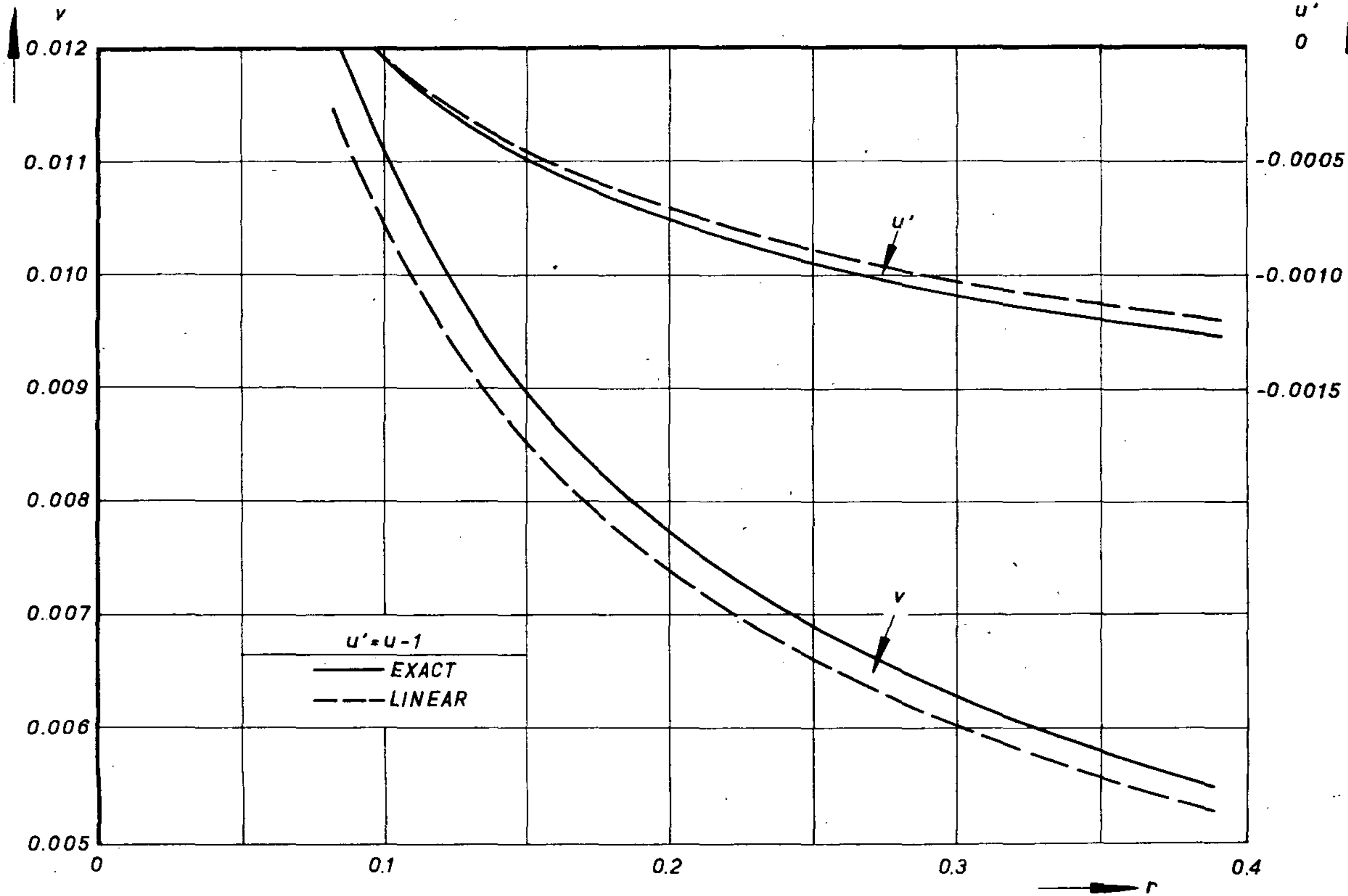

FIG. 16c COMPARISON BETWEEN THE VELOCITY DISTRIBUTIONS AS DERIVED BY USING LINEAR- AND EXACT THEORY FOR $M_{\infty} = 4.5$.

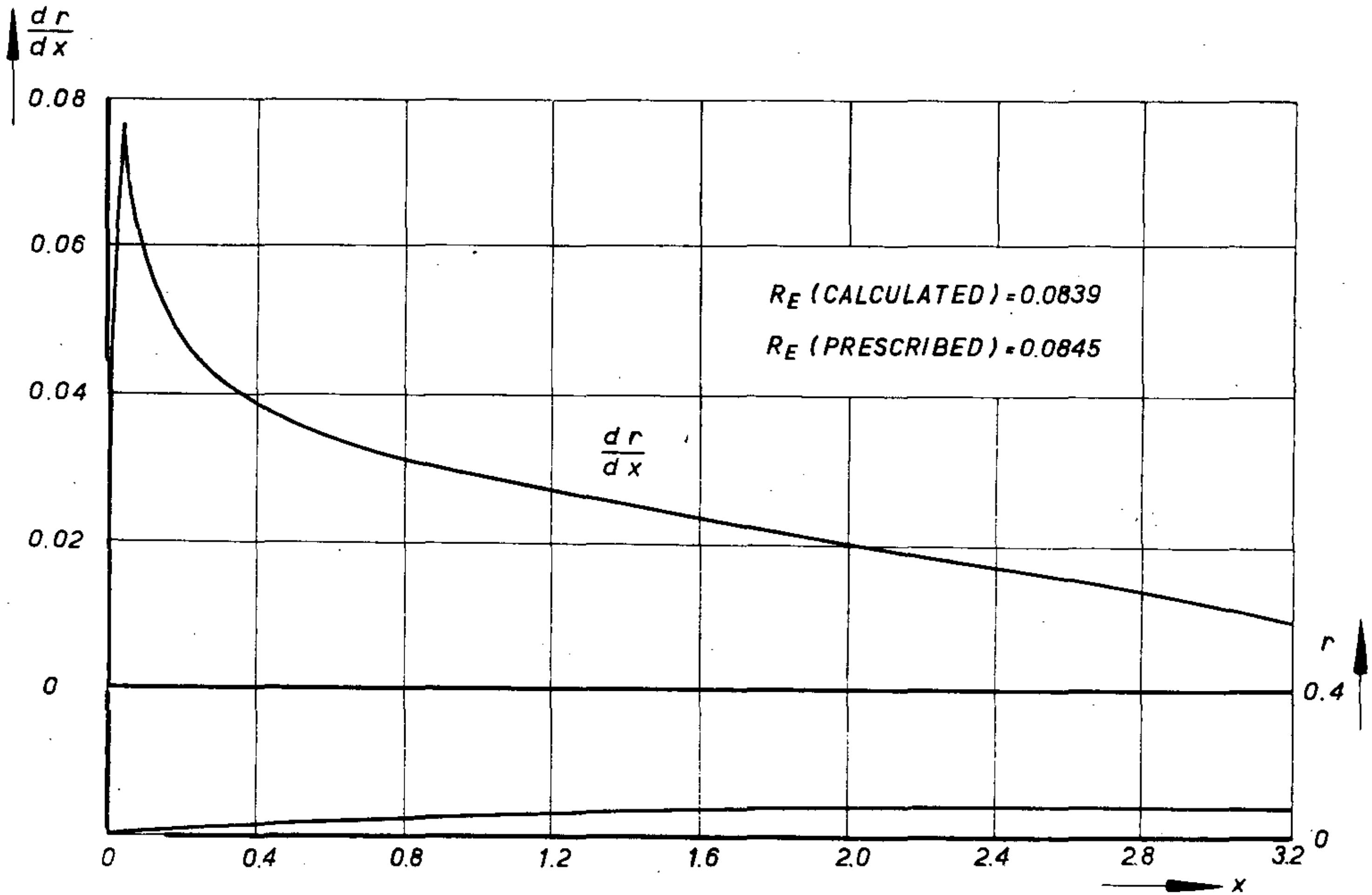

FIG. 17a THE SHAPE AND THE SLOPE OF AN OPTIMUM BODY FOR $M_\infty = 2.5$.

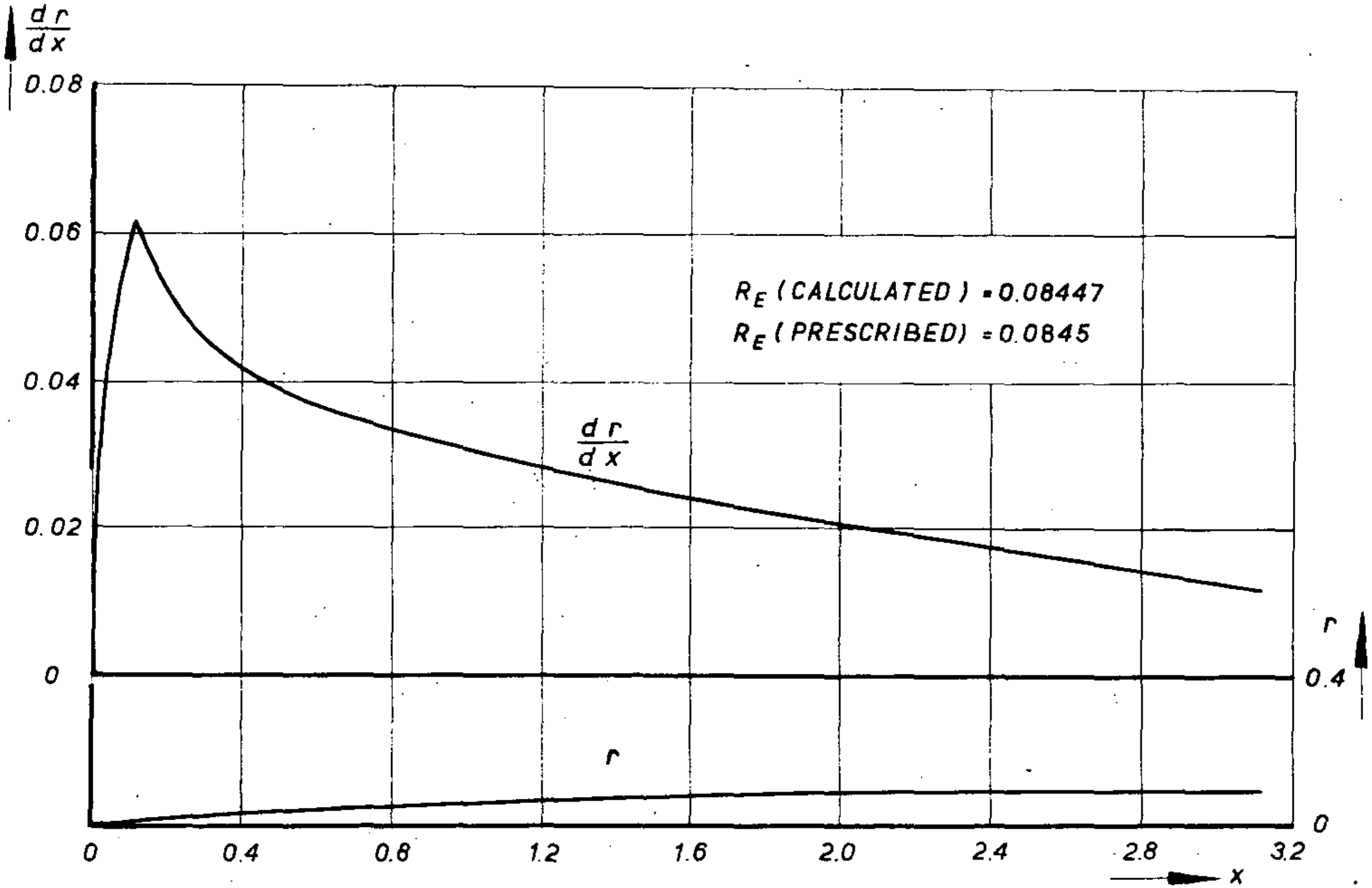

FIG.17b THE SHAPE AND THE SLOPE OF AN OPTIMUM BODY FOR $M_\infty = 4.5$.

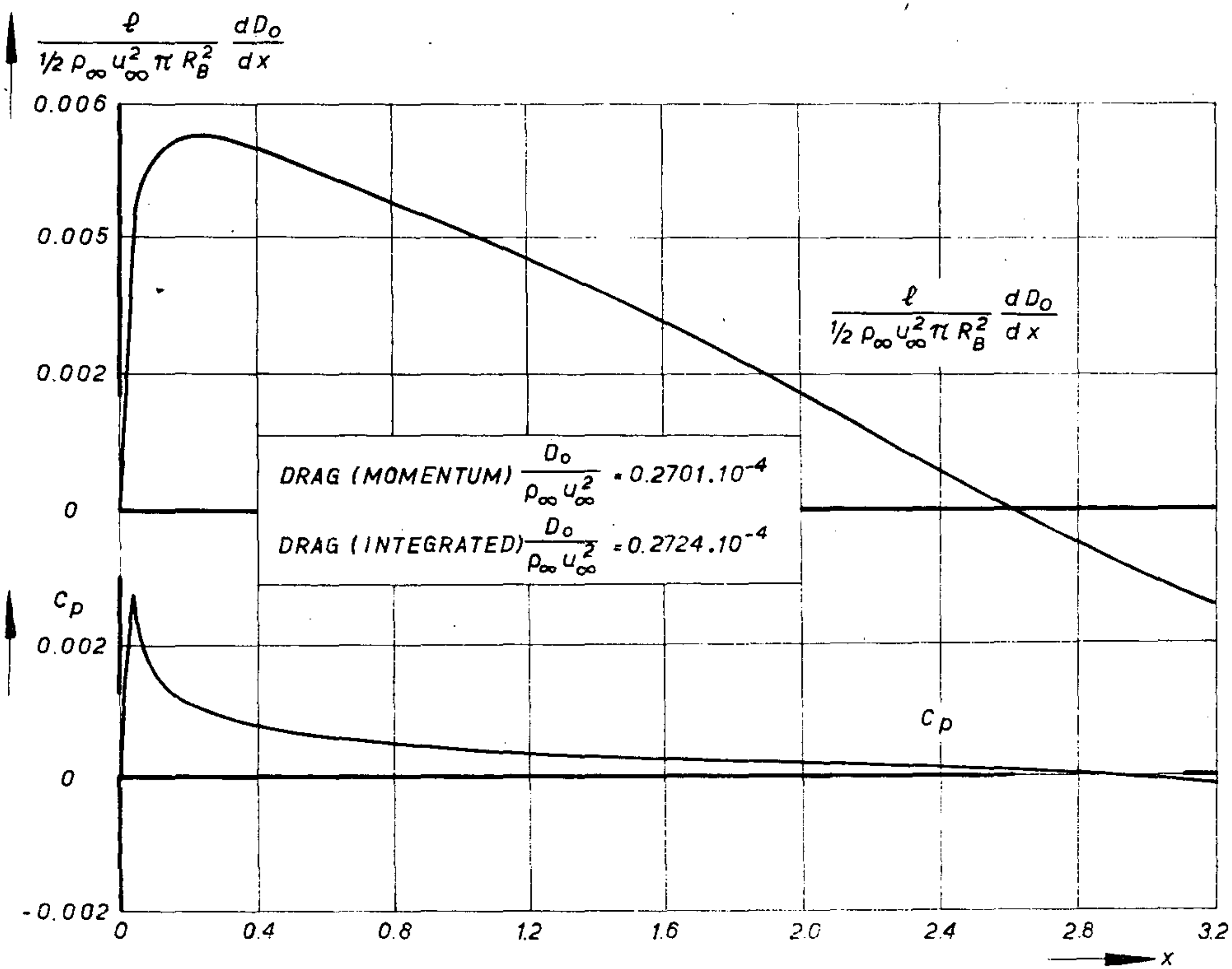

FIG. 18a THE PRESSURE COEFFICIENT AND THE DISTRIBUTION OF THE DRAG FOR $M_\infty = 2.5$.

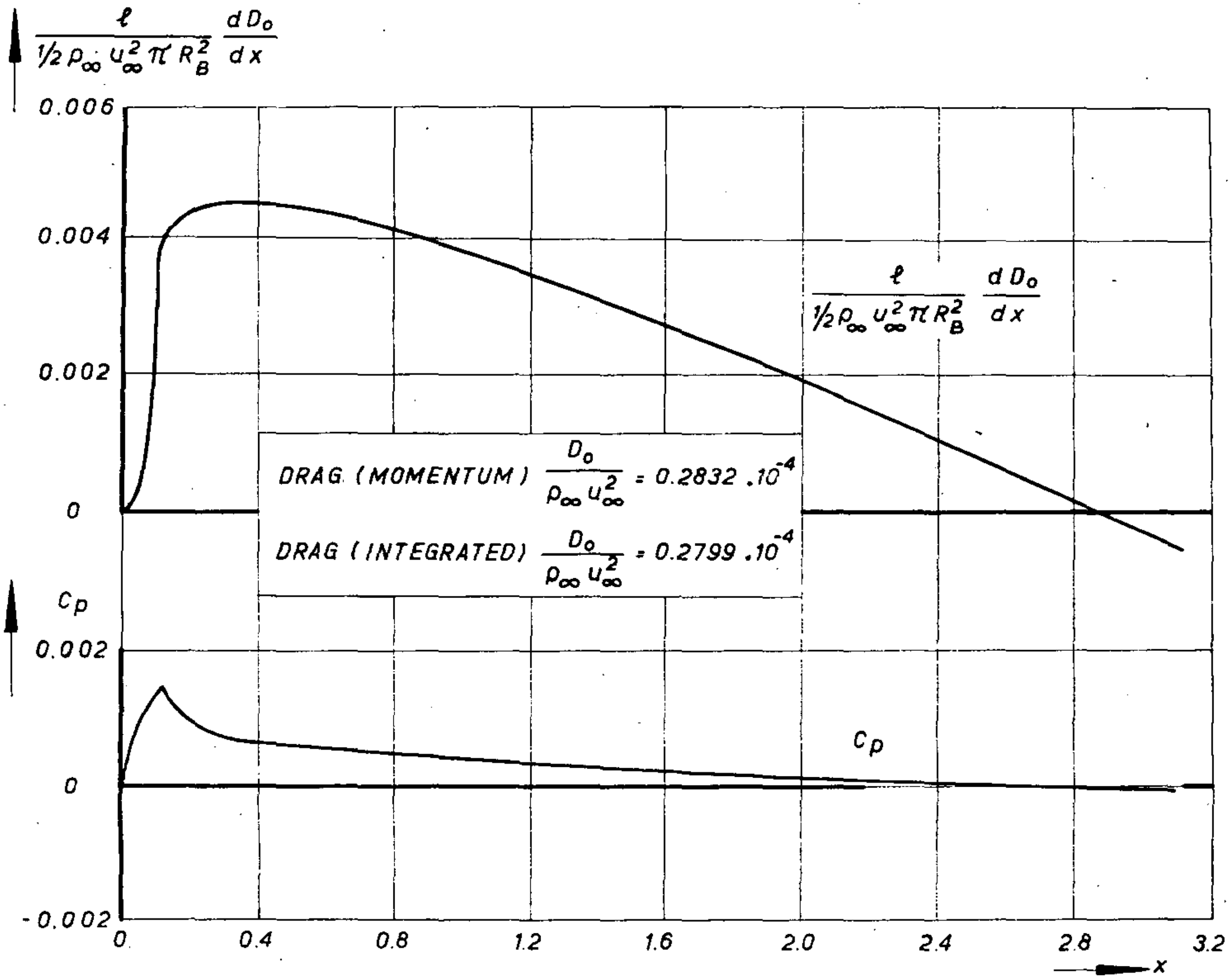

FIG. 18b THE PRESSURE COEFFICIENT AND THE DISTRIBUTION OF THE DRAG FOR $M_\infty = 4.5$.

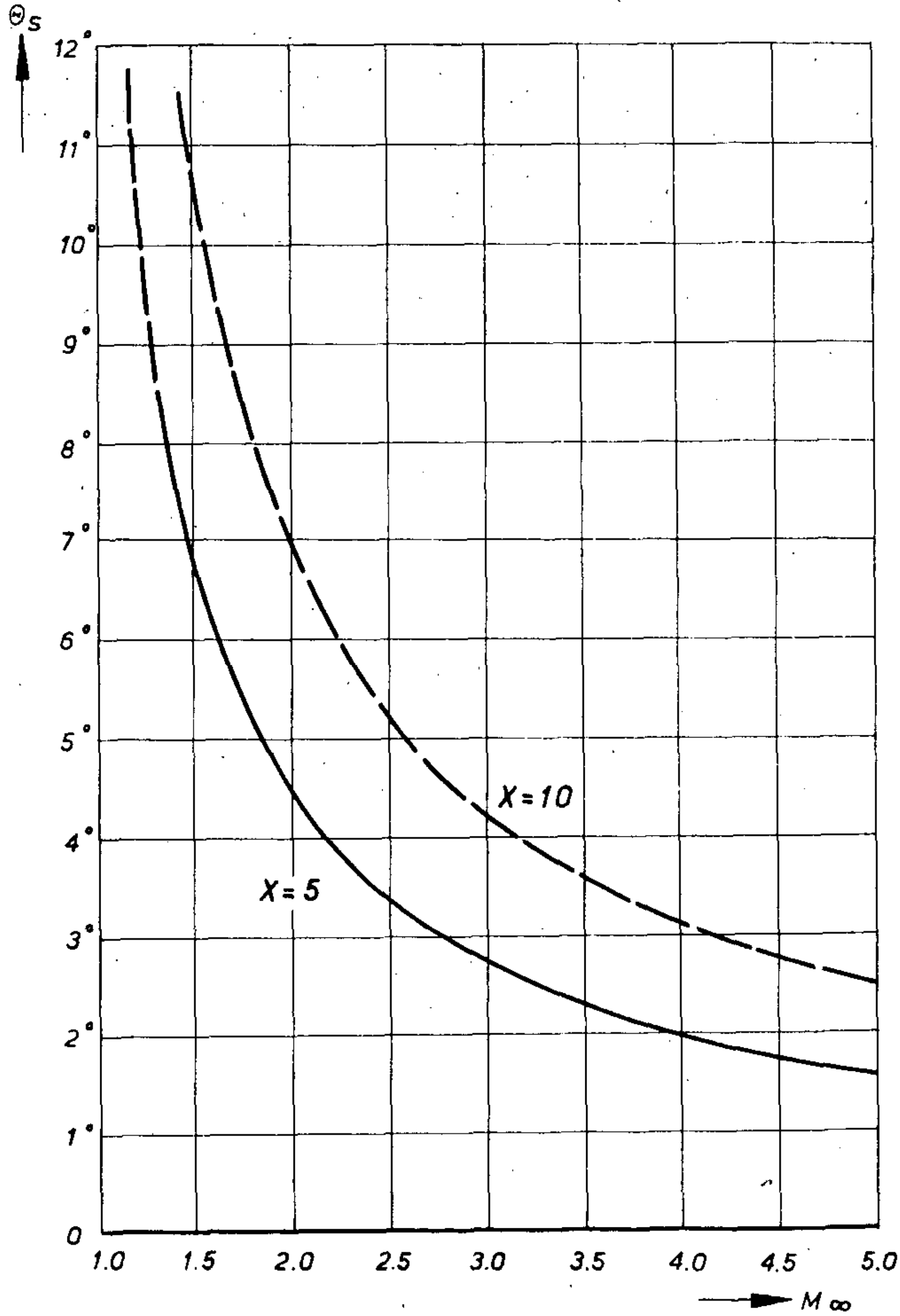

FIG. 19 LIMITS OF APPLICABILITY OF LINEARIZED THEORY FOR THE FLOW AROUND A CONE AT AN ANGLE OF ATTACK.

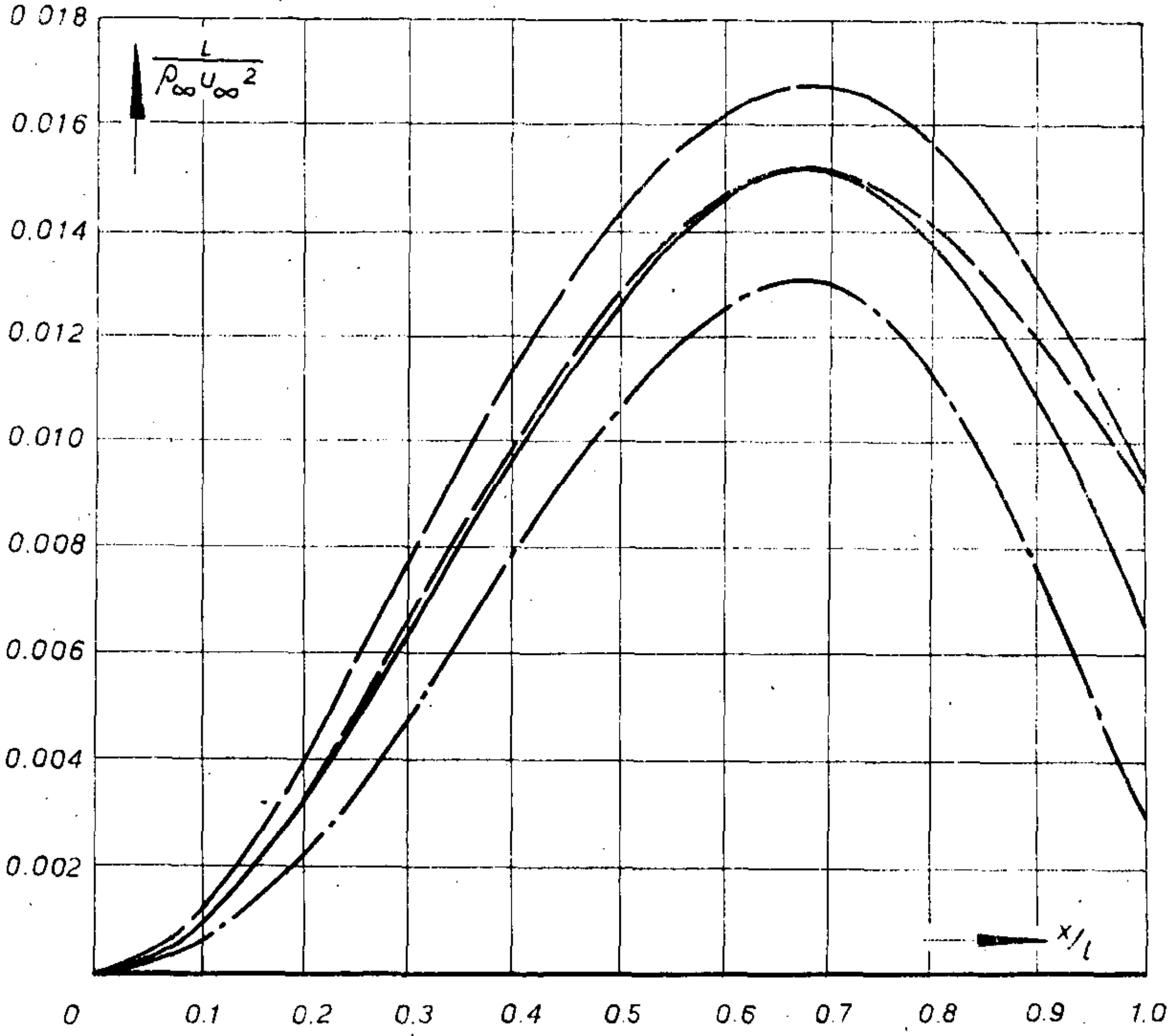

$= \int \pi \frac{r}{l} \left\{ u''(1-\beta_\infty^2 u') + v'v'' \right\} d\frac{x}{l}$

$= \int \pi \frac{r}{l} \; u'' \; d\frac{x}{l}$

ALONG THE FUSELAGE

$= \int \pi (\beta_\infty u'' - v'' + w'' + 2)(1-\beta_\infty^2 u' + \beta_\infty v') \frac{r}{l} d\frac{r}{l}$

$= \int \pi (\beta_\infty u'' - v'' + w'' + 2) \frac{r}{l} d\frac{r}{l}$

MOMENTUM EQUATION

$\vartheta_S = 12.5^\circ \quad M_\infty = 2.476$

FIG. 20 COMPARISON OF THE LIFT ON FUSELAGE SECTIONS AS DERIVED BY VARIOUS METHODS.

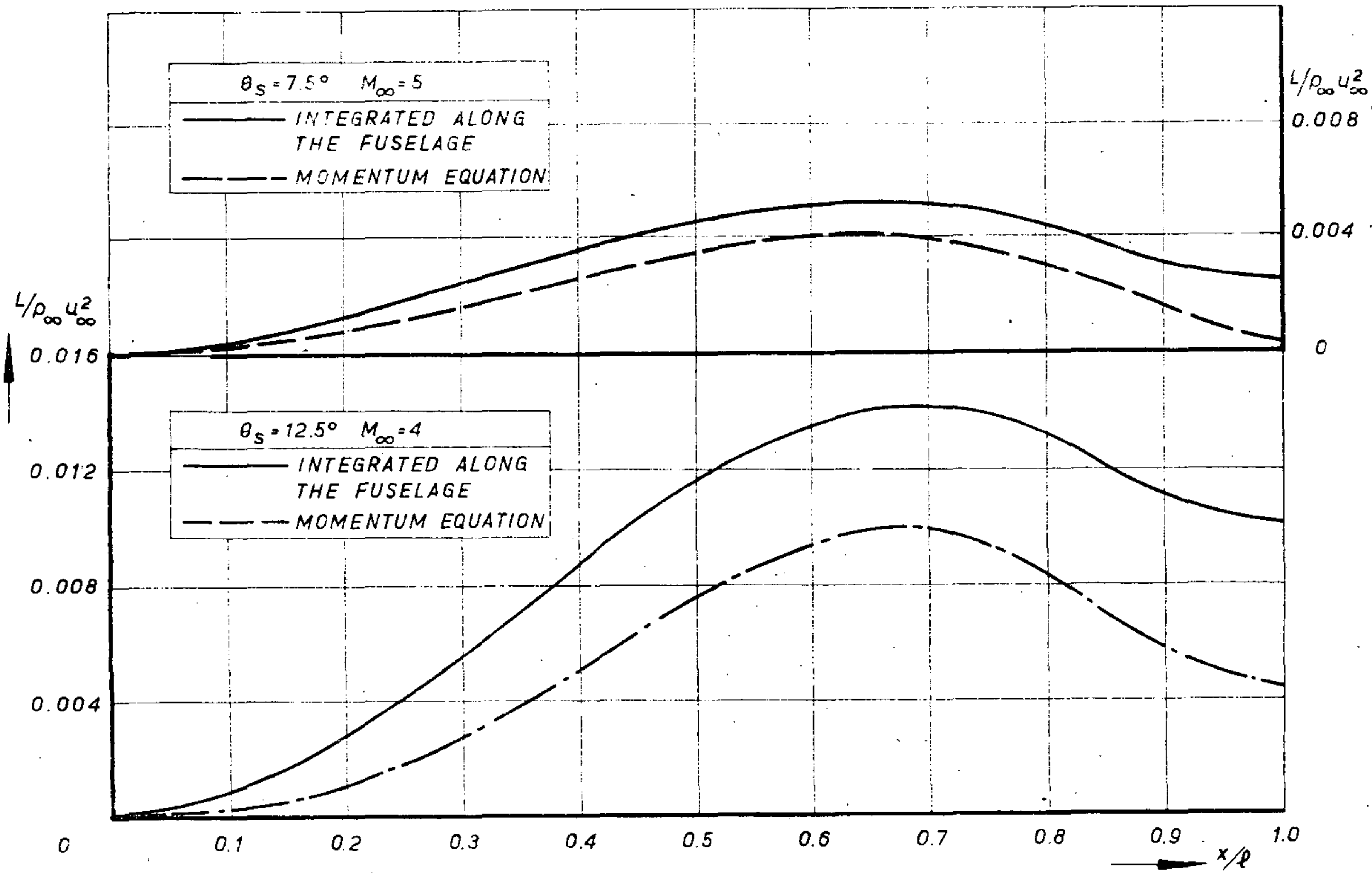

FIG. 21a THE LIFT ON THE CONFIGURATIONS.

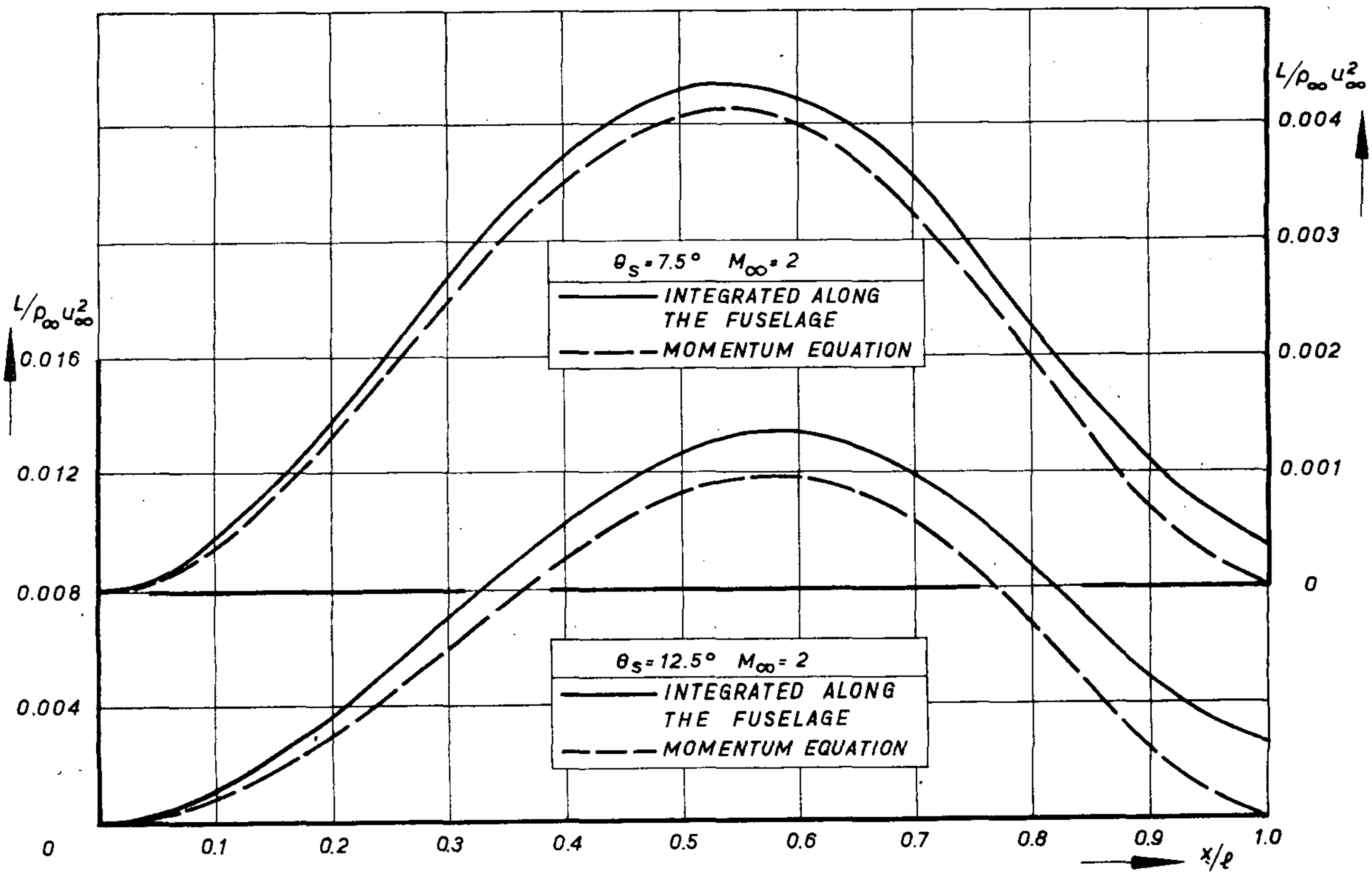

FIG. 21b THE LIFT ON THE CONFIGURATIONS.

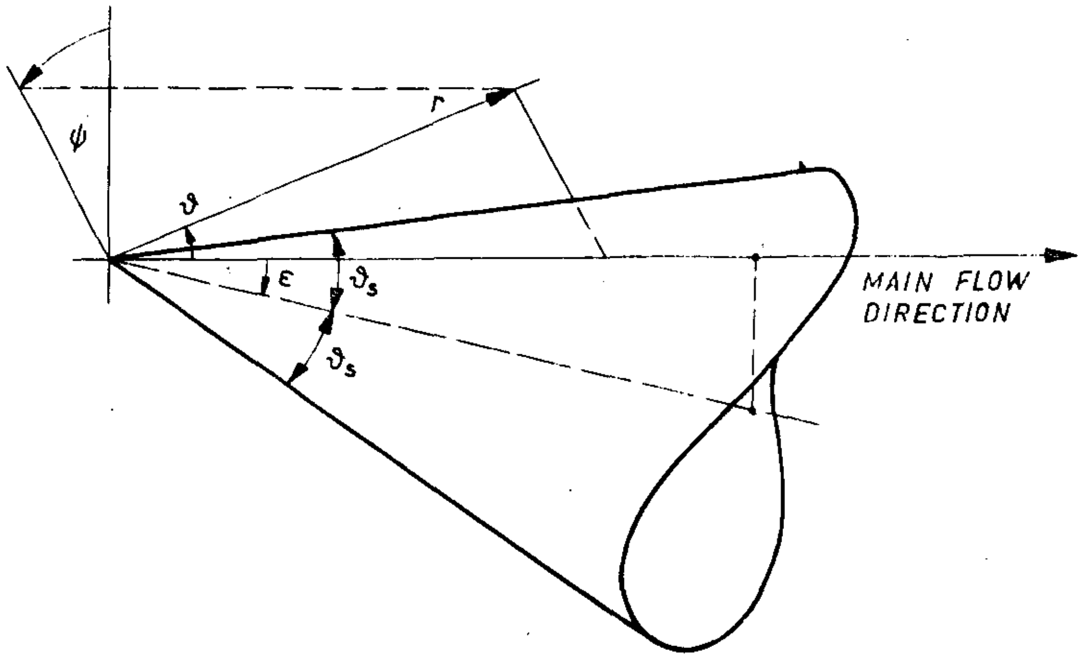

FIG.22 THE SPHERICAL COORDINATE SYSTEM USED TO STUDY THE FLOW FIELD AROUND A CONE INCLINED AT AN ANGLE ε.

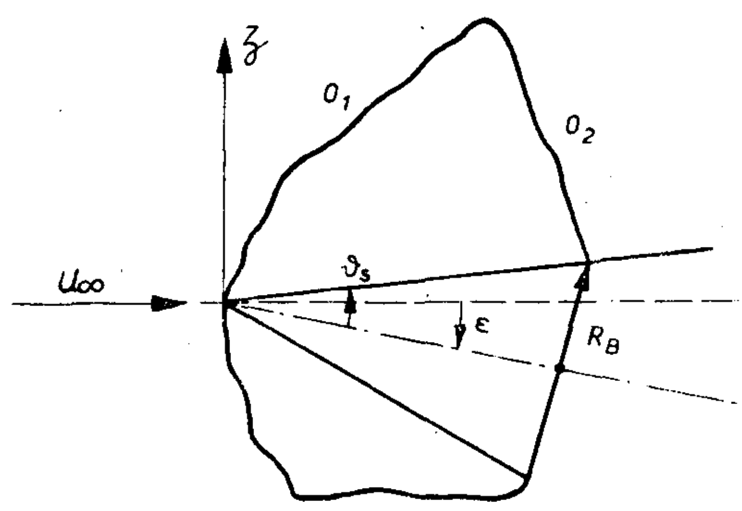

FIG.23 A CONE AT AN ANGLE OF ATTACK ε.

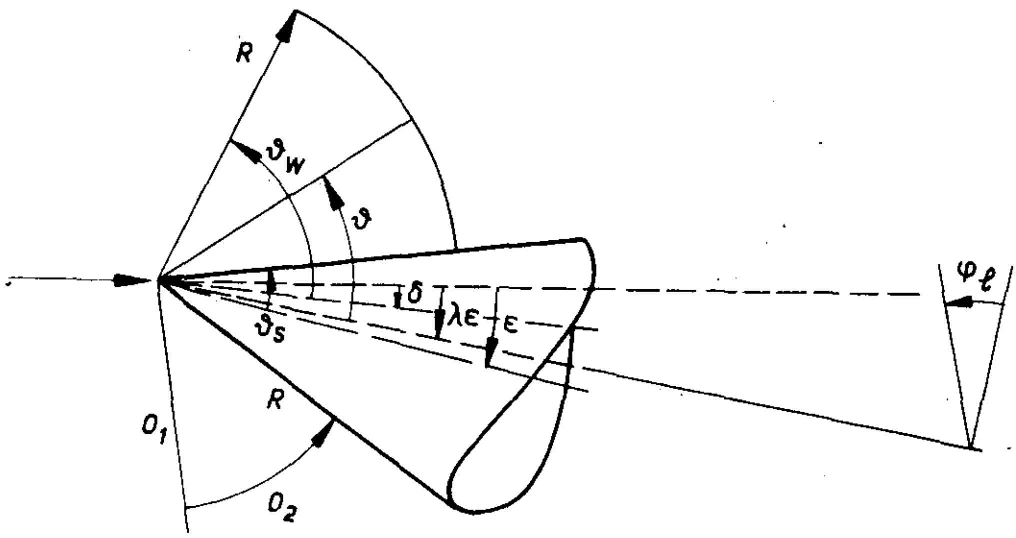

FIG. 24 LOCAL COORDINATE SYSTEMS USED IN THE REAL FLOW FIELD.

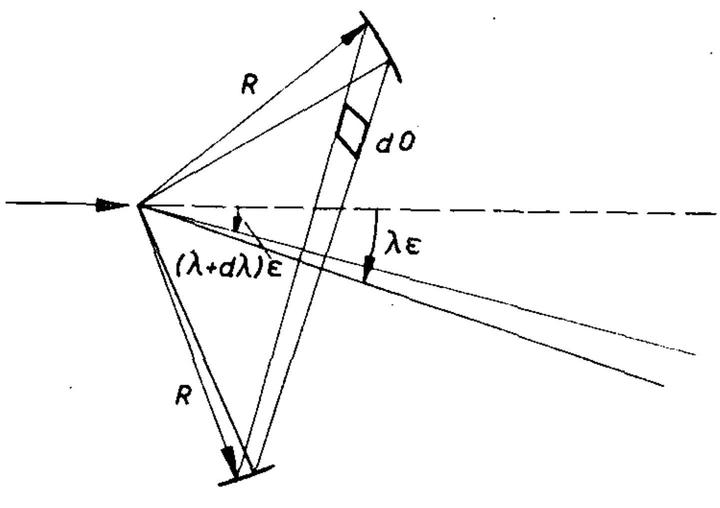

FIG. 25 DEFINITION OF A SURFACE ELEMENT OF THE SPHERE.

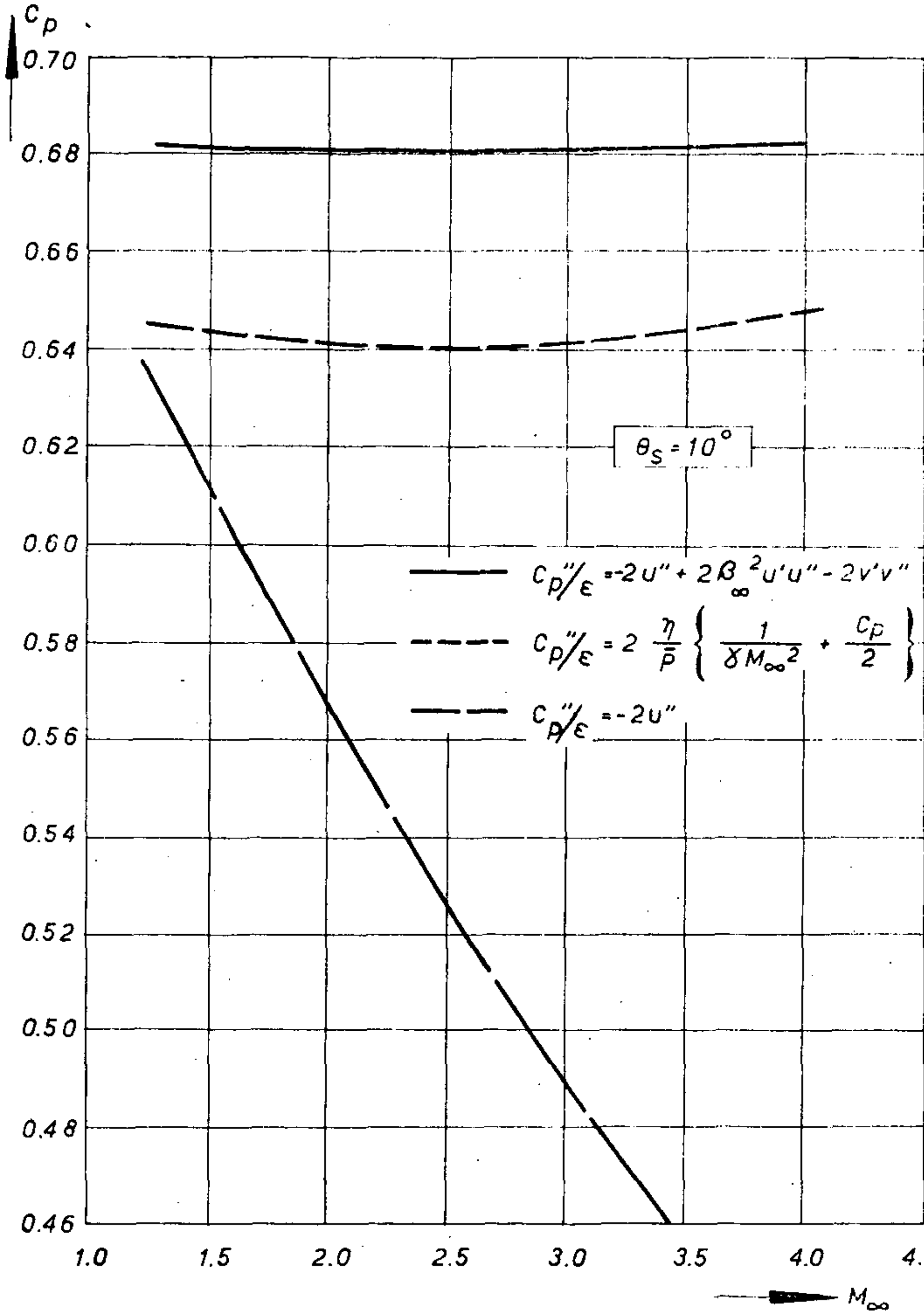

FIG. 26a COMPARISON OF THE LIFT COEFFICIENTS ON AN INCLINED CONE.

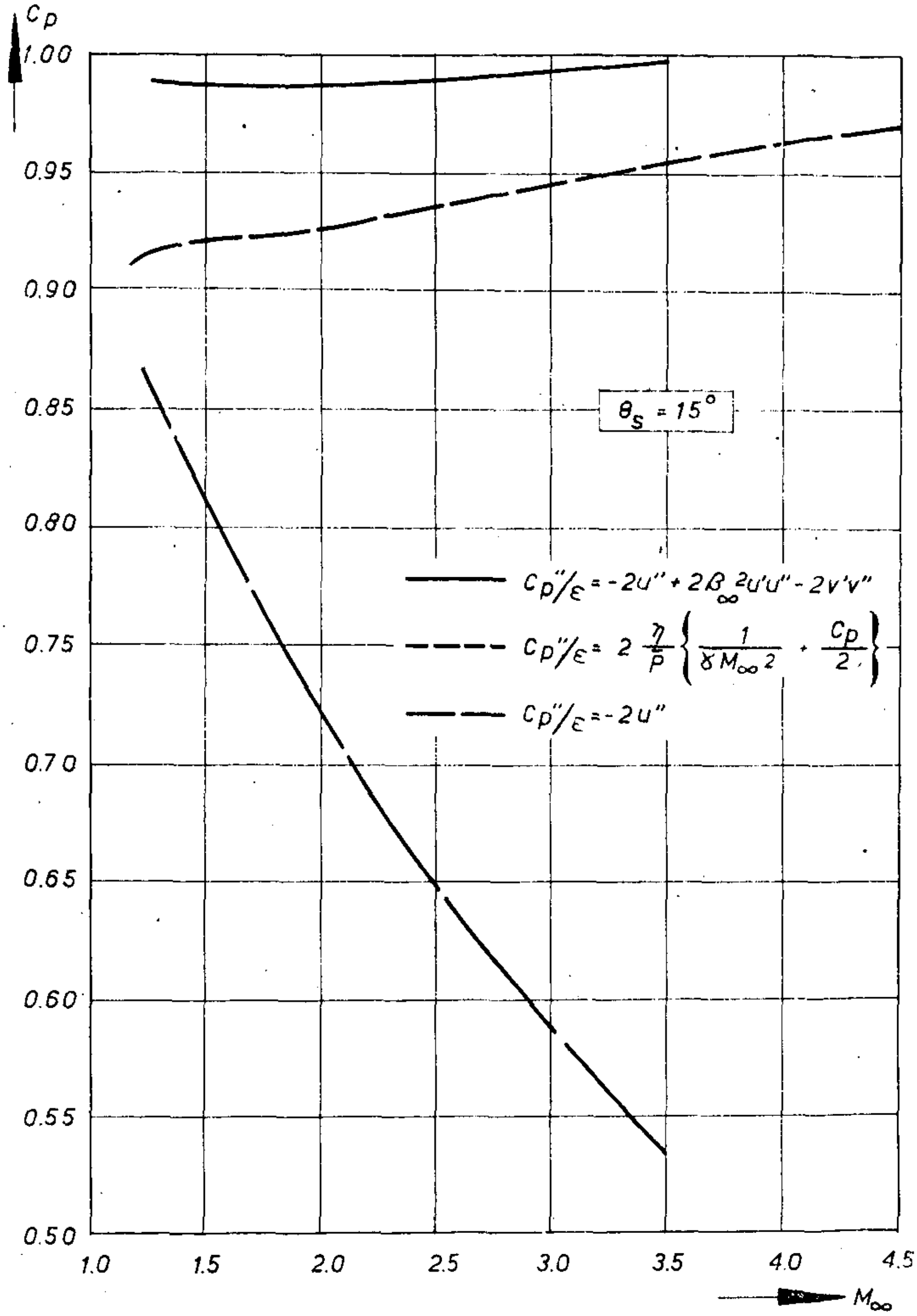

FIG. 26b COMPARISON OF THE LIFT COEFFICIENTS ON AN INCLINED CONE.

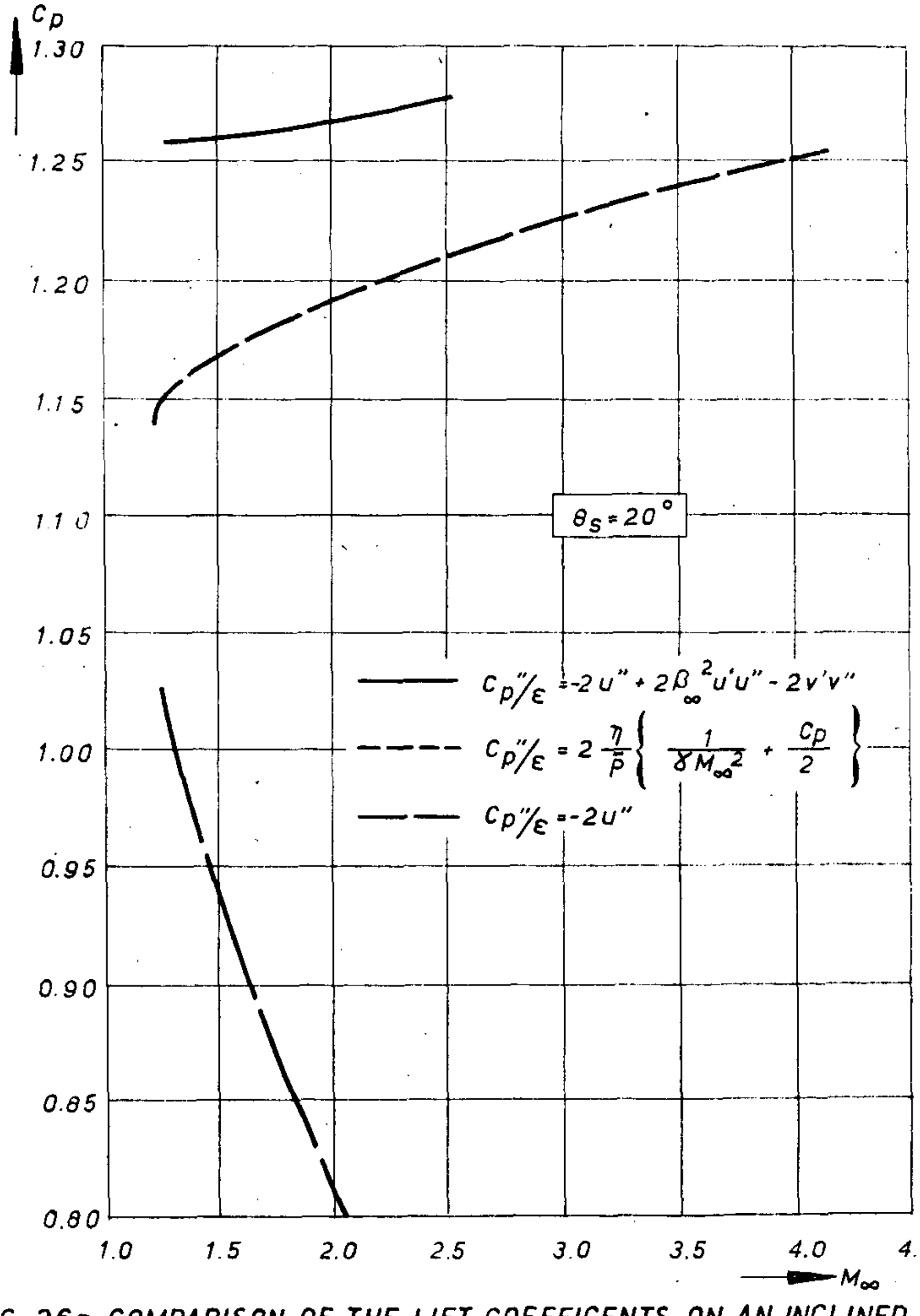

FIG. 26c COMPARISON OF THE LIFT COEFFICENTS ON AN INCLINED CONE.

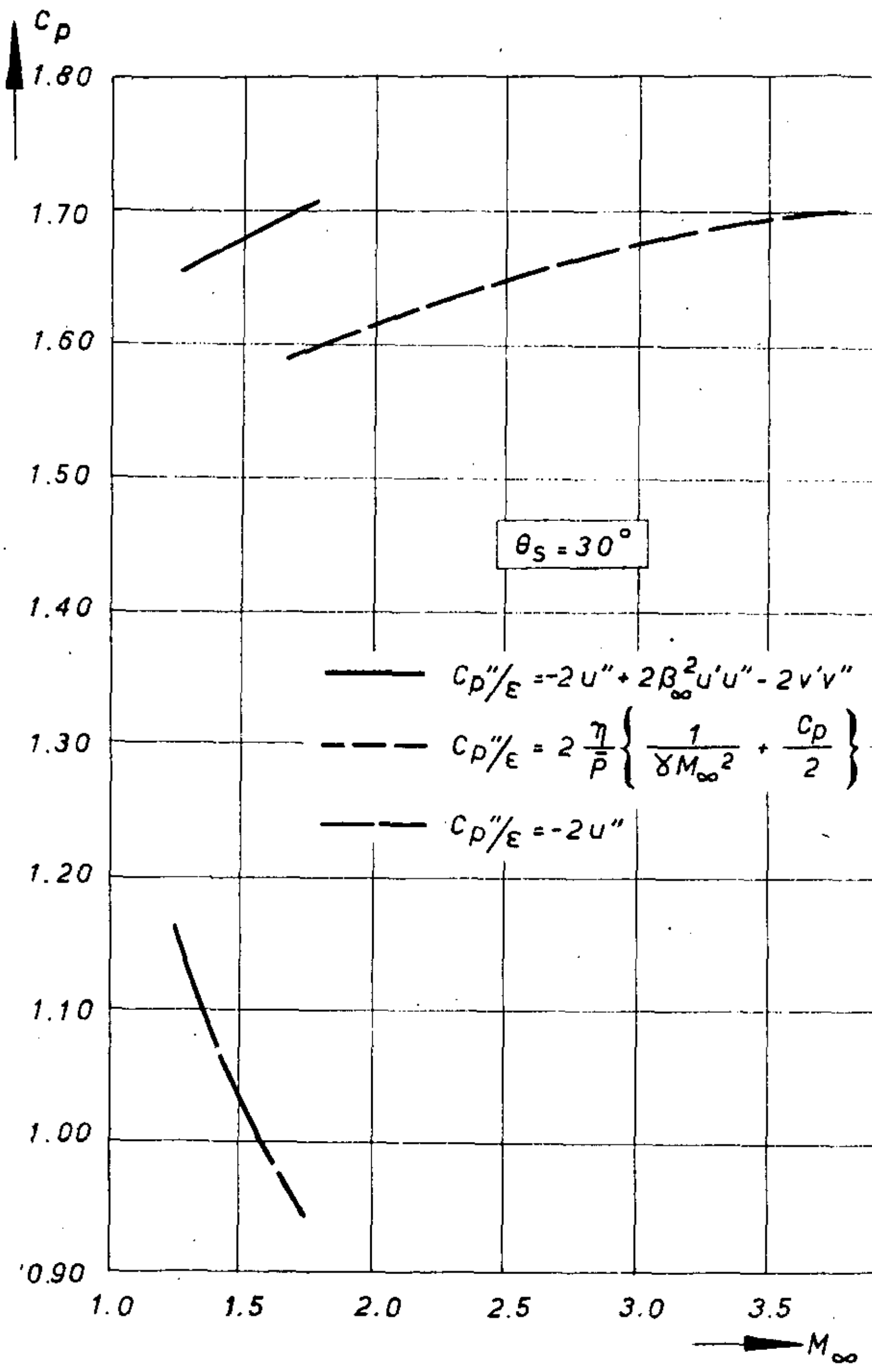

FIG. 26d COMPARISON OF THE LIFT COEFFICIENTS ON AN INCLINED CONE.

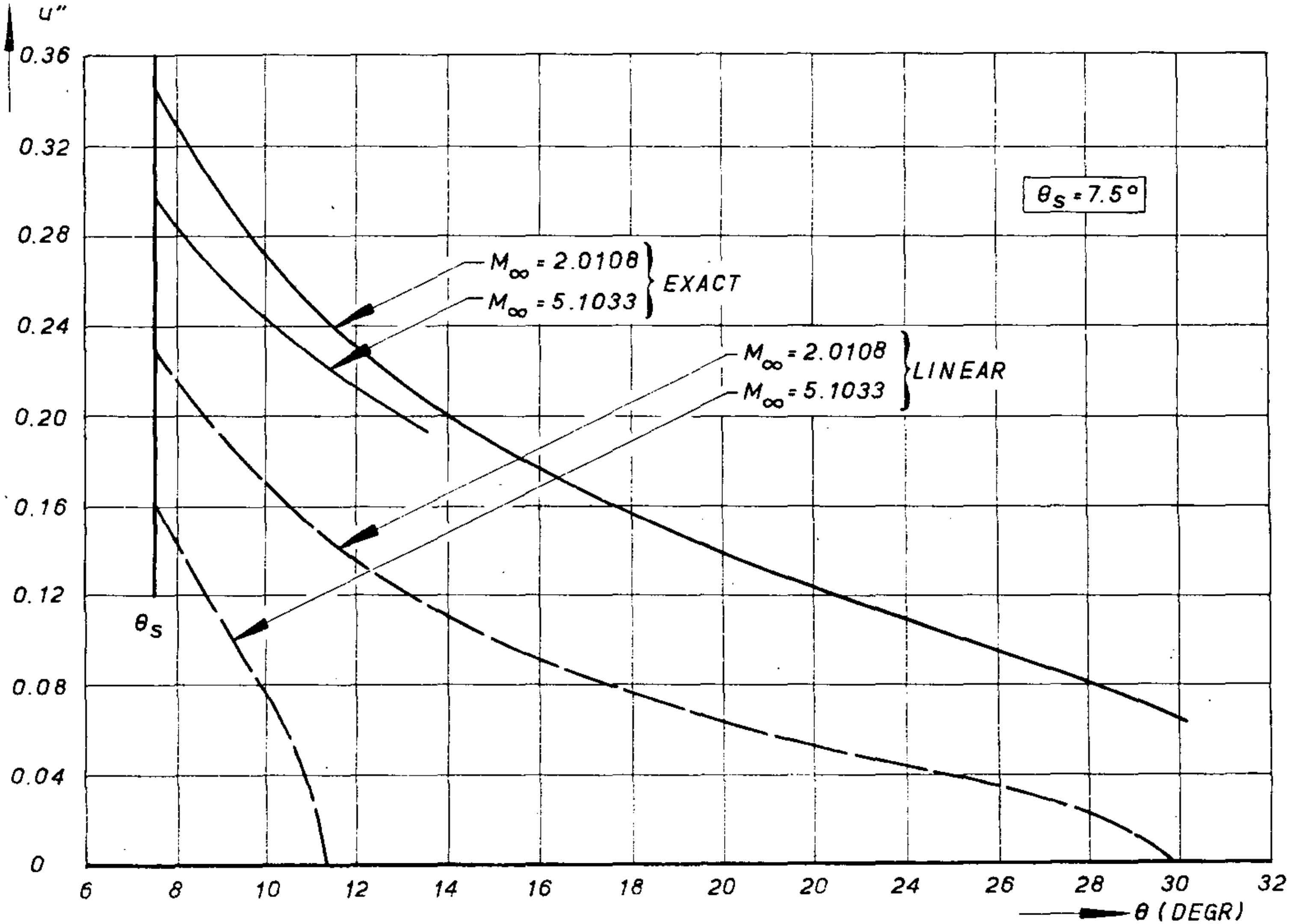

FIG. 27 a COMPARISON OF THE FLOW FIELD FOR A CONE WITH $\theta_S = 7.5°$.

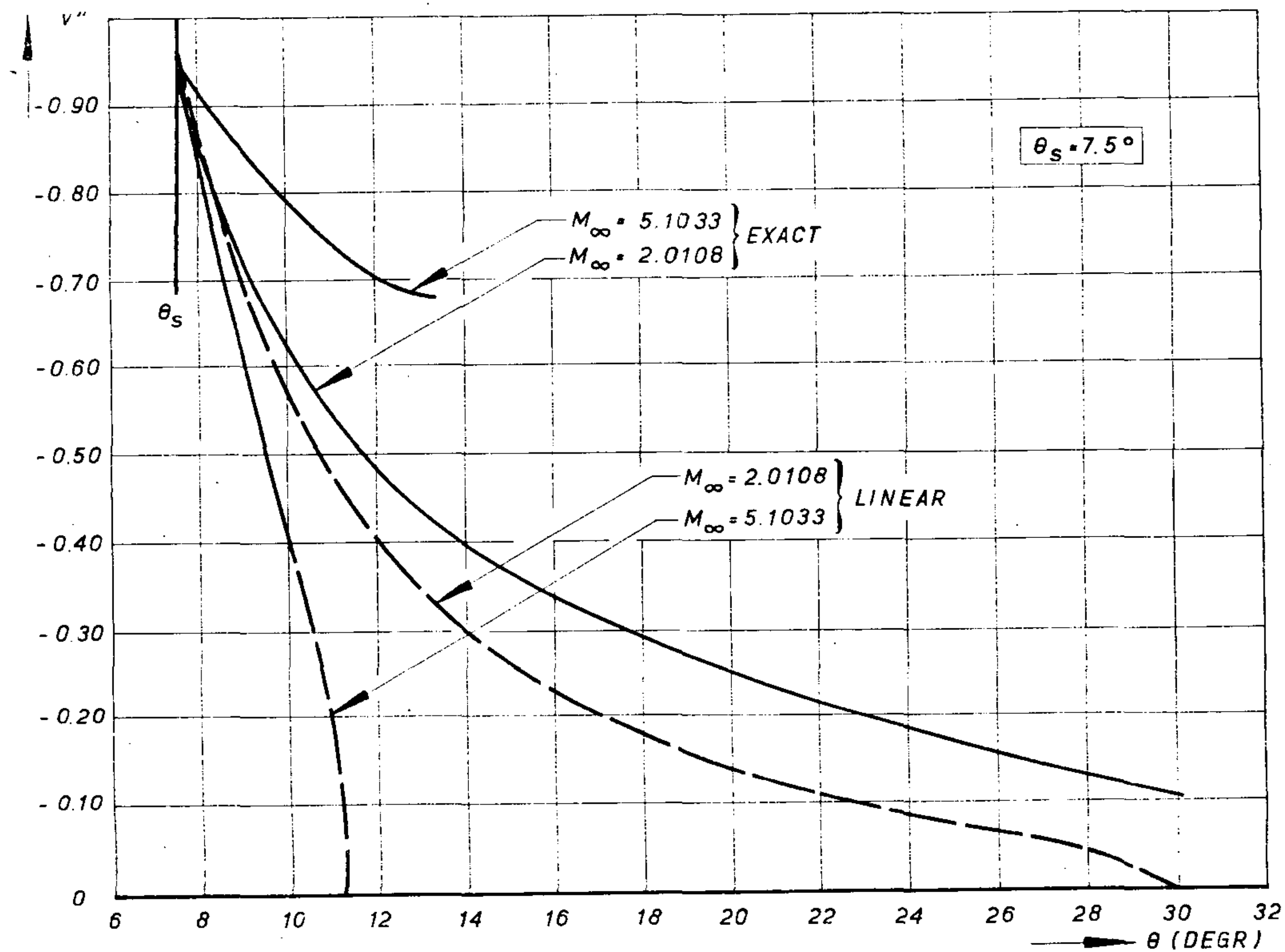

FIG. 27 b COMPARISON OF THE FLOW FIELD FOR A CONE WITH $\theta_S = 7.5$.

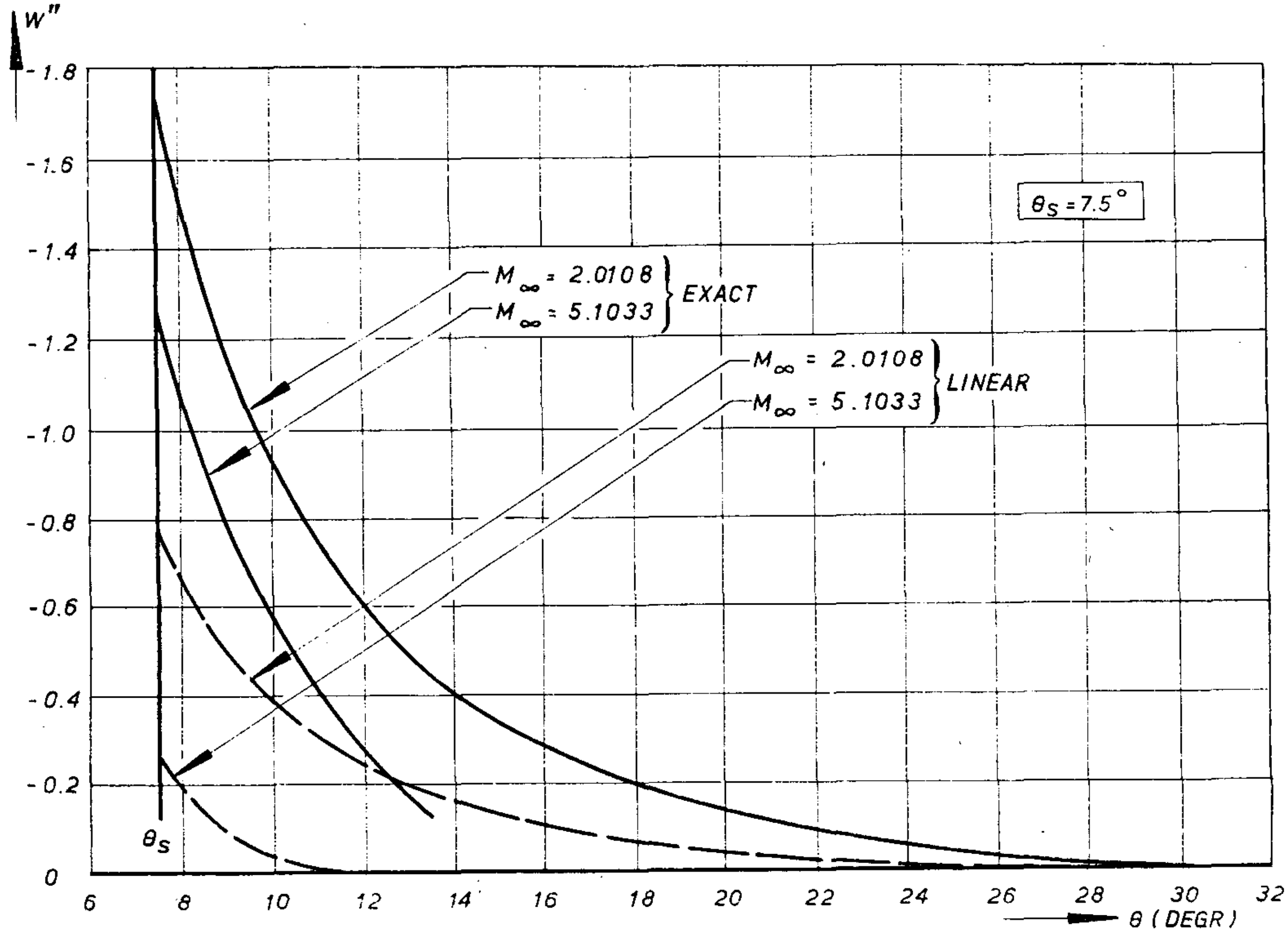

FIG.27c COMPARISON OF THE FLOW FIELD FOR A CONE WITH $\theta_S = 7.5^\circ$.

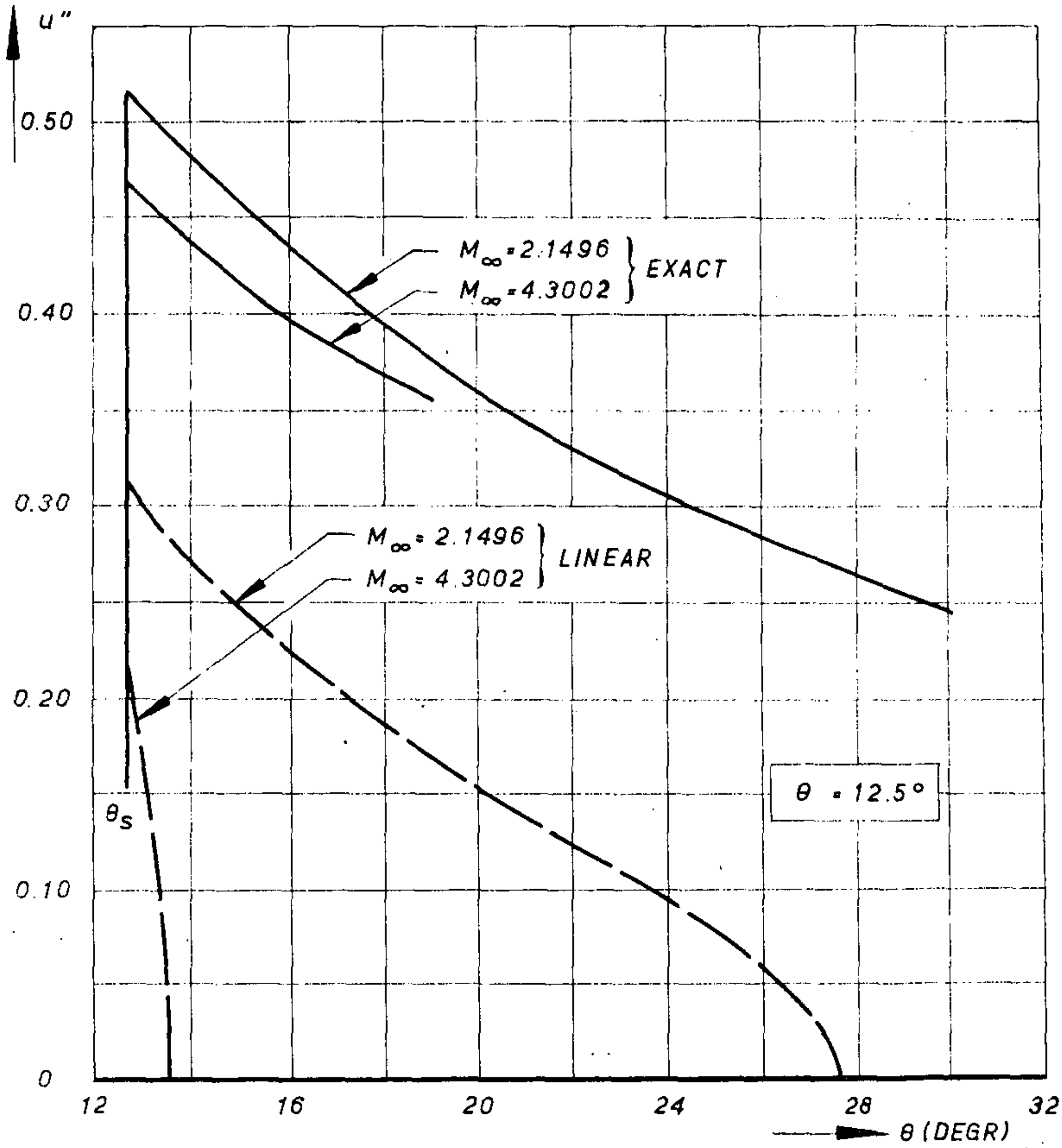

FIG. 28a COMPARISON OF THE FLOW FIELD FOR A CONE WITH $\theta_S = 12.5°$.

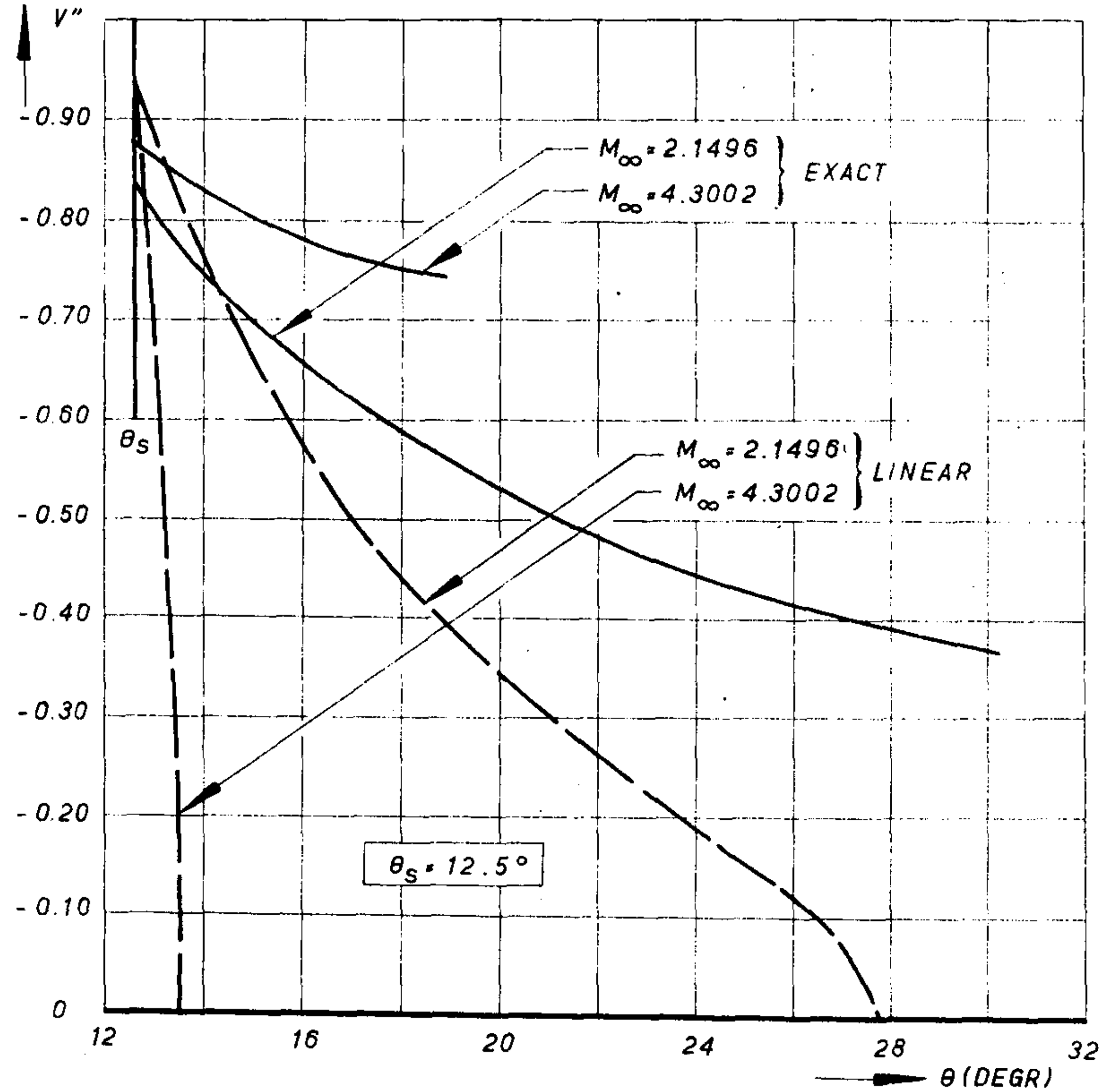

FIG. 28b COMPARISON OF THE FLOW FIELD FOR A CONE WITH $\theta_S = 12.5°$.

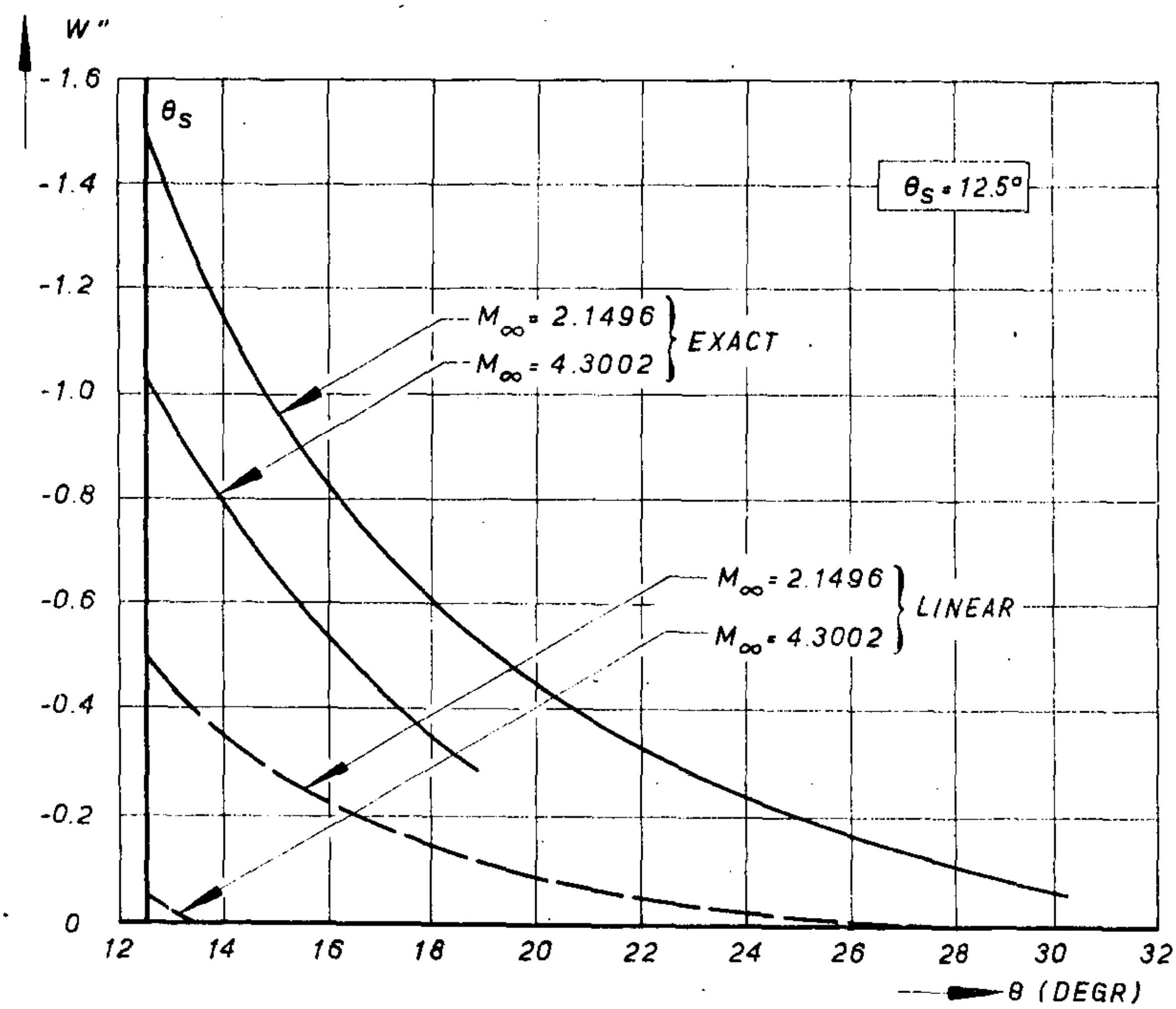

FIG. 28c COMPARISON OF THE FLOW FIELD FOR A CONE WITH $\theta_S = 12.5°$.

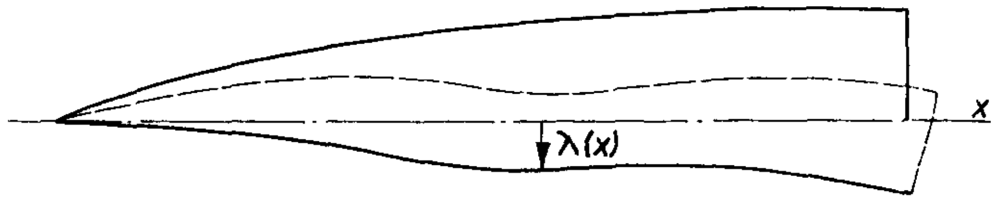

FIG.29 THE AXIALLY-SYMMETRIC CONFIGURATION AND THE DEFORMATION $\lambda(x)$.

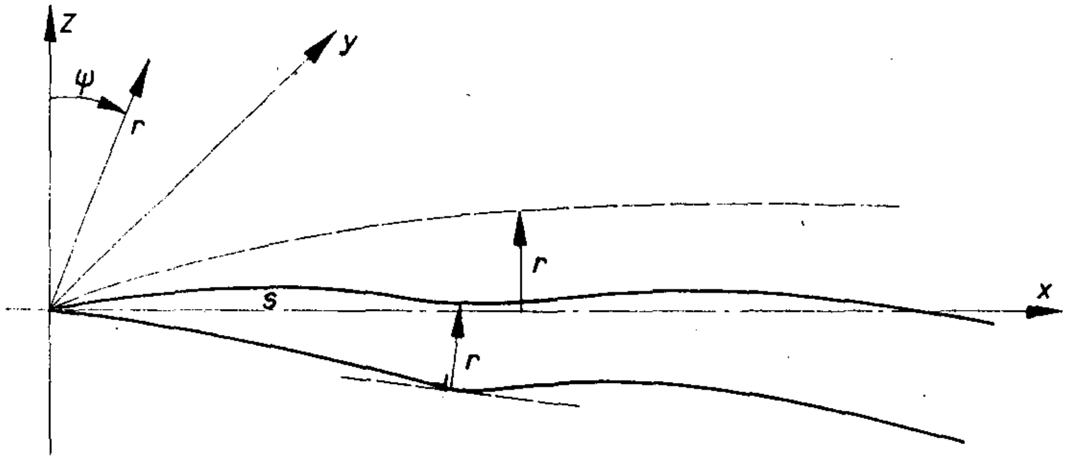

FIG. 30 THE CORRESPONDENCE BETWEEN THE AXIALLY-SYMMETRIC AND THE QUASIAXIALLY-SYMMETRIC SHAPE.

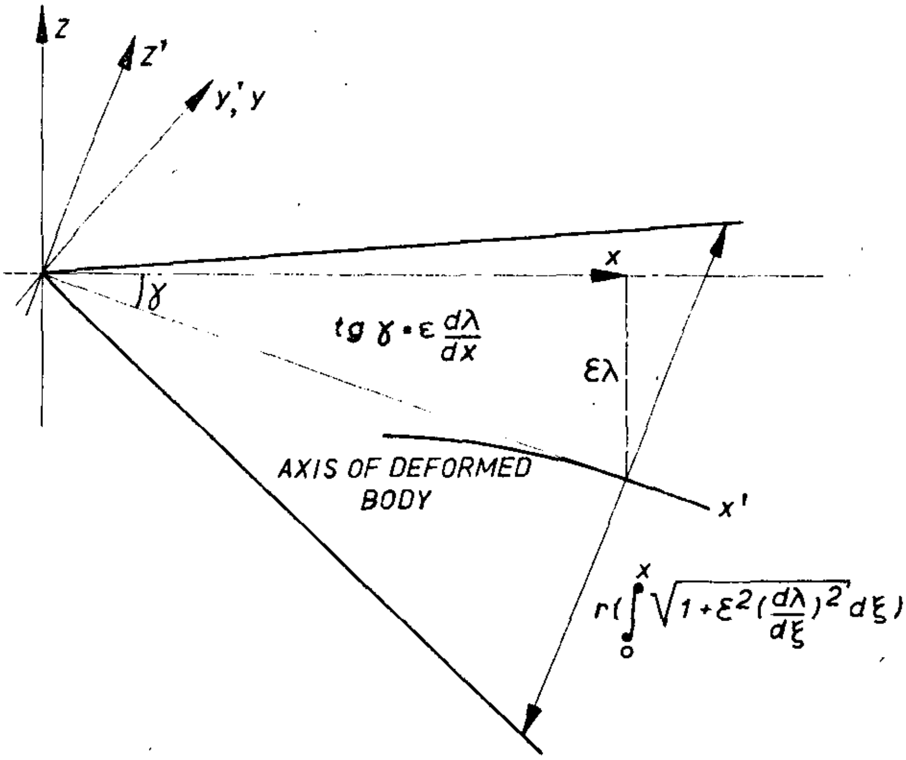

FIG.31 THE GEOMETRY OF THE CIRCLE AT THE POINT x OF THE DEFORMED BODY.

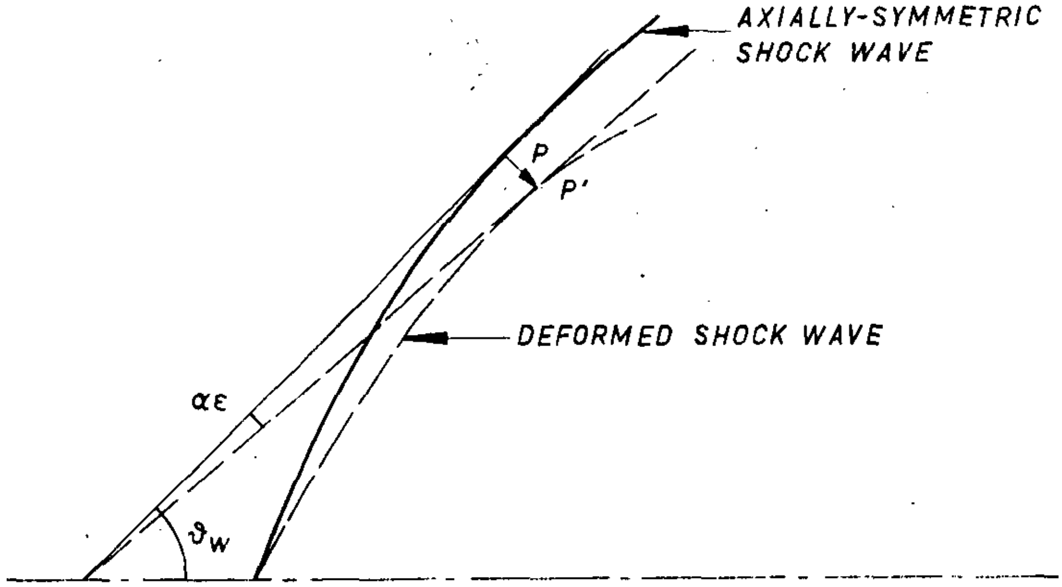

FIG.32 THE SHAPE OF THE DEFORMED SHOCK WAVE.

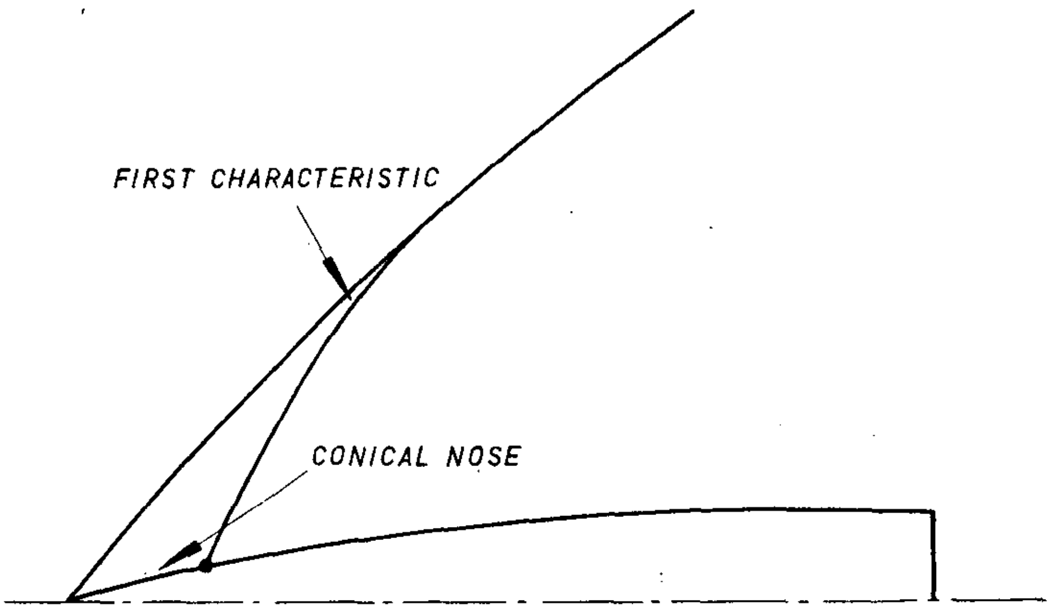

FIG.33 THE BODY CONSIDERED WITH THE FIRST CHARACTERISTIC.

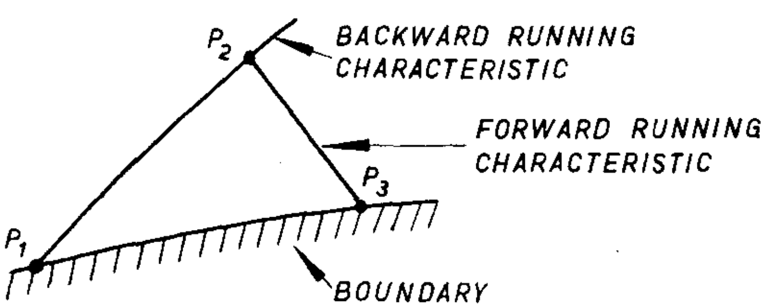

FIG.34 THE BOUNDARY POINT P_3.

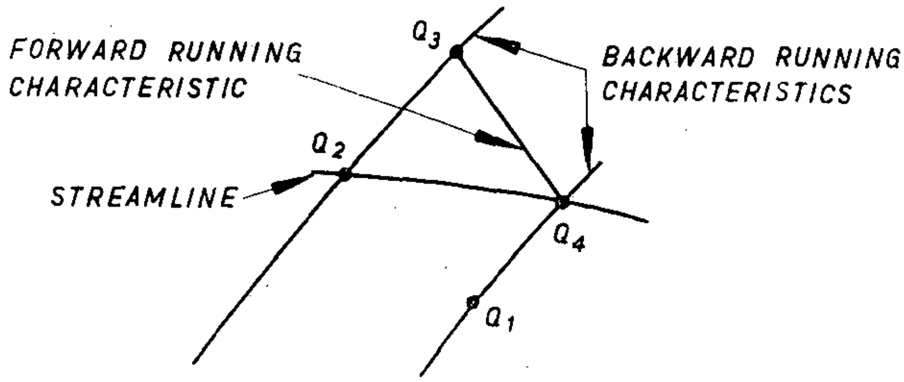

FIG. 35 THE FIELD POINT Q_4.

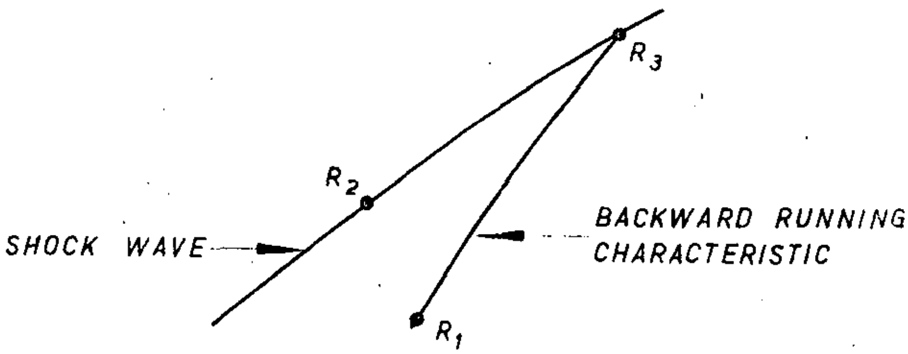

FIG. 36 THE POINT R_2 AT THE SHOCK WAVE.

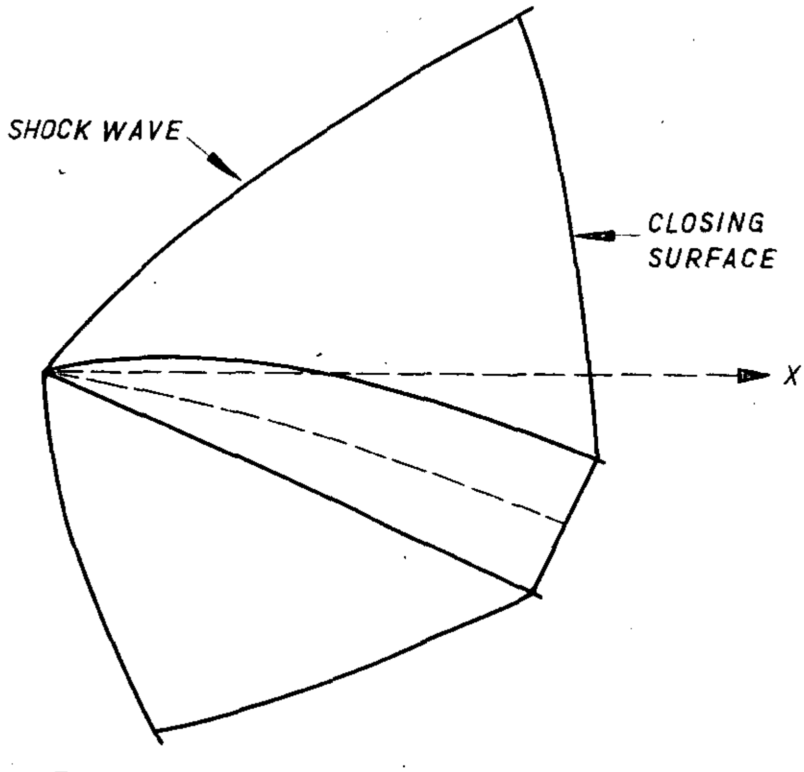

FIG. 37 THE CONTROL SURFACE USED TO CALCULATE THE LIFT.

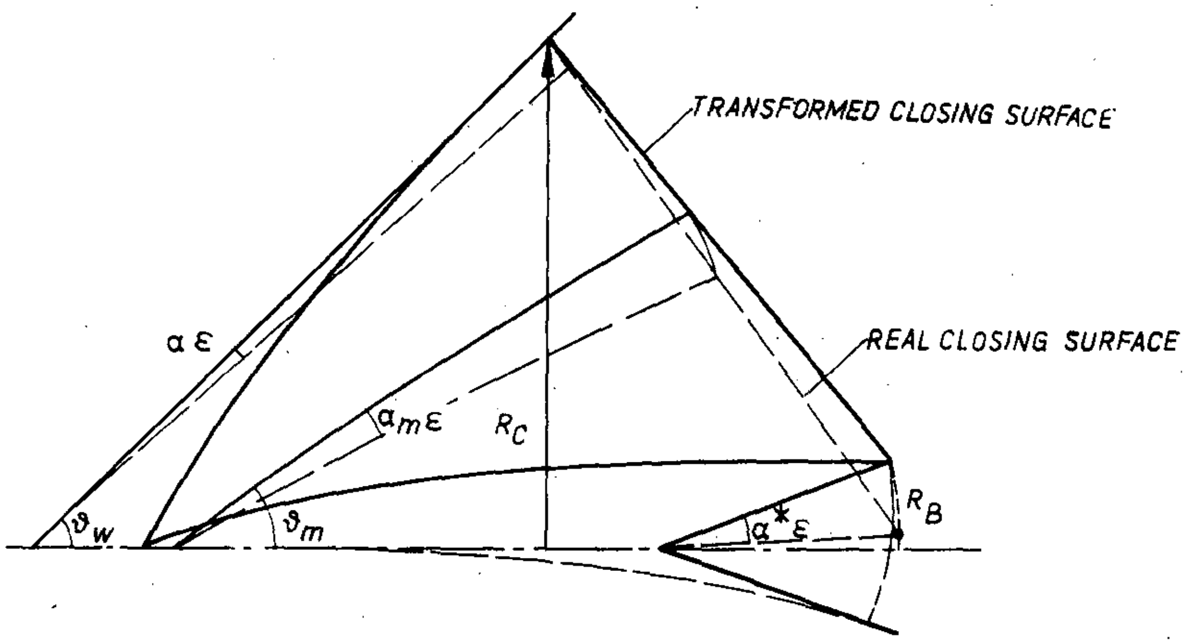

FIG. 38 THE CONNECTION BETWEEN THE REAL AND THE TRANSFORMED CLOSING SURFACE.